

**Production of Plastic Injection Moulding Tools using Selective  
Laser Sintering and High Speed Machining**

by

**Ismet Priana Ilyas**

Submitted in accordance with the requirements for the degree of  
Doctor of Philosophy

**The University of Leeds  
School of Mechanical Engineering**

**August, 2007**

The candidate confirms that the work submitted is his own and that appropriate credit has been given where reference has been made to the work of others.

This copy has been supplied on the understanding that it is copyright material and that no quotation from the thesis may be published without proper acknowledgement.

---

## **Acknowledgements**

My greatest appreciation to my supervisors, Professor K. W. Dalgarno and Professor T. H. C. Childs, for their supervision and valuable guidance throughout the research works and the preparation of the thesis.

I am deeply grateful to Dr. Chris M. Taylor for the much appreciated assistance and valuable discussion during the industrial project. Also many thanks to a group of professionals from the industrial collaborative partners for providing a valuable knowledge and industrial experience. Among them are Mr. Nick Brooks (RAPRA Technology ltd.); Mr. Brian Laurence and Paul Clark (Seaquist Closures Lt.); Mr. Brian Hawkshaw (DELICAM Uk Tooling Services); Mr. Stephen Clark (Trisport ltd.); and Ms. Sarah Leech (Unilever Research Laboratory).

I am grateful to Mr. Andrew Marsden and Raymond Taylor (Keyworth Institute), and Mr. Alan G. Heald and Adrian (Measurement Laboratory) from the School of Mechanical Engineering for their assistances.

Finally, a special thank you must go to my parents and family. Also, thanks to Abifa for the special moments together. And last, but definitely not the least, I would like to express my sincere gratitude to my beloved wife, Transmissia, for the unconditional support and patience.

---

## Abstract

Global manufacturing trend and competition challenge every industry to seek new manufacturing methods to improve their business processes and speed up the product development cycle [Conolly, 2004a and Knights, 2001]. Among the candidates, layer manufacturing (LM) technologies appear to be a potential solution [Plam, 2002, and Grimm, 2004]. Recent LM technologies have led to a demanding application for developing production tools to manufacture parts, known as rapid tooling (RT). Selective laser sintering (SLS) is one of the leading LM systems available today in RT to manufacture injection mould (core/cavity) inserts [Kruth, 1998, Chua, 1999, Dormal, 1999, and Grenda, 2005]. However, the current capabilities of the SLS in producing metal parts have not yet fulfil the requirements of the injection mould inserts, especially in dimensional accuracy and surface finish quality [Francis, 2002 and Dalgarno, 2001a].

The aim of this research is to use indirect SLS and high speed machining (HSM) in developing production-quality plastic injection moulding (core/cavity) inserts. The idea is that the indirect SLS process is utilised to build a near-net-shape inserts, while HSM is then utilised to finish the inserts to production specifications. Benchmark studies have been carried out to characterise the capabilities of both SLS and HSM with reference to the typical requirements of injection mould inserts. Utilising the study results, new developments of the mould inserts have been implemented on three major industrial case studies. Their performances have been evaluated and measured by comparing them with its respective original inserts. Furthermore, a set of design rules has been derived from best practices of the case studies, and have been validated by developing a new design for each case studies inserts.

The results have demonstrated that the indirect SLS process has a capability in manufacturing a near-net shape of the insert which requires further related finishing to achieve final production specifications. The insert performances in some case studies have indicated significant improvements in process productivity and energy consumption as well as economic benefits to using the inserts. Regarding the

---

significant considerations in realising the design, a recommendation on further strategic design rules and manufacturing process are highlighted so that the development of the insert using the selected approach can be more effective and efficient. Moreover, a utilisation of computer analysis software and further durability trial is also highlighted in order to predict and evaluate the optimum overall performance.

## Contents

<b>Acknowledgements</b>	i
<b>Abstract</b>	ii
<b>Contents</b>	iv
<b>Figures</b>	viii
<b>Tables</b>	xiv
<b>Chapter 1. Introduction</b>	1
1.1. Background	1
1.2. Research Aim and Objectives	3
1.3. Organisation of the Thesis	3
<b>Chapter 2. Literature Review</b>	5
2.1. Introduction to Plastic Injection Moulding (PIM)	5
2.1.1. Basic Process	5
2.1.2. Construction and Functions of Plastic Injection Mould	7
2.1.3. Injection Mould Design and Manufacturing Procedures	9
2.1.3.1. Mould Requirements	9
2.1.3.2. Basic Mould Design Process	17
2.1.3.3. Mould Manufacturing Procedures	44
2.2. Layer Manufacturing (LM) Technology	50
2.2.1. Basic Process	51
2.2.2. Development of LM Systems	52
2.2.2.1. Liquid-Based Systems	52
2.2.2.2. Solid-Based Systems	53
2.2.2.3. Powder-Based Systems	55
2.2.3. Layer Manufacture of Metal Parts	57
2.2.3.1. Indirect Metal Parts Manufacture	57
2.2.3.2. Direct Metal Parts Manufacture	58
2.2.3.3. Other Technologies	61
2.2.3.4. Comparison of Metal Processes	61
2.3. The application of LM Systems	62

2.3.1. Rapid Prototyping (RP)	62
2.3.2. Rapid Tooling (RT)	63
2.3.2.1. Introduction to Metallic RT Techniques	63
2.3.2.2. Review of Indirect SLS/LS Metallic Tooling	64
2.3.2.3. Limitations from Current Research and Potential for Improvements	65
2.3.3. Rapid Manufacturing (RM)	66
2.4. Summary of Literature Review	67
2.5. Aim of the Research Works	68
<b>Chapter 3. Benchmark Studies</b>	70
3.1. Introduction	70
3.2. Part Design and Manufacture	70
3.2.1. Green Part Development	71
3.2.2. Metal Part Development	73
3.3. Equipment	74
3.4. Benchmark Studies of Indirect SLS Process	77
3.4.1. Dimensional Accuracy and Surface Flatness	77
3.4.1.1. Model Development	77
3.4.1.2. Measurement	78
3.4.1.3. Results	80
3.4.1.4. Building Limitations	94
3.4.2. Surface Flatness	96
3.4.3. Surface Finish	102
3.4.3.1. Model Development	102
3.4.3.2. Model Measurements	104
3.4.3.3. Results	105
3.4.4. Surface Hardness	110
3.4.5. Material Porosity	111
3.5. Discussion and Summary	111
<b>Chapter 4. Case Studies</b>	114
4.1. Introduction	114
4.2. Case Study 1: 50 mm Snap-On Tube Top	116
4.2.1. Product Evaluation	116
4.2.2. Insert Design	117

4.2.3. Inserts Manufacture	123
4.2.4. Moulding Trial	126
4.2.4.1. Procedure and Measurements	126
4.2.4.2. Results	128
4.2.5. Production/Durability Trial	130
4.2.6. Cost Analysis	133
4.3. Case Study 2: Receptacle Spoke	135
4.3.1. Product Evaluation	135
4.3.2. Insert Design	136
4.3.3. Insert Manufacture	137
4.3.4. Moulding Trial	140
4.3.4.1. Procedure and Measurements	141
4.3.4.2. Results	142
4.3.5. Cost Analysis	143
4.4. Case Study 3: Cassio 200 ml Bottle Top	146
4.4.1. Product Evaluation	146
4.4.2. Insert Design	146
4.4.3. Insert Manufacture	152
4.4.4. Moulding Trial	155
4.4.4.1. Procedure and Measurements	156
4.4.4.2. Results	156
4.4.5. Cost Analysis	157
4.5. Summary	159
<b>Chapter 5. Design Rules Application</b>	161
5.1. Issues Arising	161
5.1.1. Design of the Inserts	161
5.1.1.1. Geometry	162
5.1.1.2. Additional Material	162
5.1.1.3. Powder Removal	162
5.1.2. Manufacturing the Net Shape Inserts	163
5.2. Design Rules	163
5.2.1. Product Design Review	163
5.2.1.1. Product Use/Function	164

5.2.1.2. Product Geometry	164
5.2.2. Tool Insert Design and Manufacture	166
5.2.2.1. Design of Net Shape Inserts	166
5.2.2.2. Design of Near-Net Shape Inserts	168
5.2.2.3. Manufacture of Inserts	172
5.3. Design Rules Application	173
5.4. Case Study (CS) 1: 50 mm Snap-On Tube Top	173
5.4.1. Product Review	173
5.4.2. Inserts Design	174
5.4.2.1. Net shape Inserts	174
5.4.2.2. Near-Net Shape Inserts	181
5.4.3. Inserts Manufacture	185
5.4.4. Discussion	187
5.5. Case Study (CS) 2: Receptacle Spoke	188
5.5.1. Product Evaluation	188
5.5.2. Insert Design	188
5.5.2.1. Net Shape Inserts	188
5.5.2.2. Near-Net Shape Inserts	192
5.5.3. Insert Manufacture	193
5.5.4. Discussion	194
5.6. Case Study (CS) 3: Cassio 200 ml Bottle Top	194
5.6.1. Product Review	194
5.6.2. Inserts Design	195
5.6.2.1. Net shape Inserts	195
5.6.2.2. Near-Net Shape Inserts	197
5.6.3. Inserts Manufacture	199
5.6.4. Discussion	201
5.7. Summary	201
<b>Chapter 6. Conclusions And Recommendations</b>	<b>203</b>
<b>References</b>	<b>206</b>



## Figures

Figure 2-1. Cycle Sequence in PIM Process	6
Figure 2-2. Basic Elements and Structures	6
Figure 2-3. Schematic Lay-out of Injection Mould	8
Figure 2-4. Temperature-Time Diagram during Moulding Cycle	12
Figure 2-5. Cooling Channel Layout	15
Figure 2-6. A Mould Design Procedure	18
Figure 2-7. Runner Systems	21
Figure 2-8. Sprue Dimensions	22
Figure 2-9. Design of Sprue-Pullers	23
Figure 2-10. Gate Cross-Section and Position at the Runners	24
Figure 2-11. Nomogram for Cooling Time Calculation	28
Figure 2-12. Effective Thermal Diffusivity for Crystalline Plastic	28
Figure 2-13. Heat Flow in an Injection Moulding	29
Figure 2-14. Specific Enthalphy	31
Figure 2-15. Flow-rate of Coolant (Water)	32
Figure 2-16. Cooling Channel Diameter and Coefficient Heat Transfer	33
Figure 2 17. Coefficient of Heat Transfer (coolant: Water)	35
Figure 2 18. Thermal Reactions (Steady Conduction)	35
Figure 2-19. Computation of Heat-Transfer Data	36
Figure 2-20. Cooling Channel Layout	36
Figure 2-21. Distance between Cavity Wall and Cooling Channels	37
Figure 2-22. Feasible Cooling Layout	38
Figure 2-23. Distribution of Heat Flow	38
Figure 2-24. Typical Pin Ejection System	42
Figure 2-25. Type of the Stripper Ejector System	42
Figure 2-26. Down-Time for Mould Changes in Injection Moulding Machines	44
Figure 2-27. Hobbing Mould Inserts	46
Figure 2-28. Basic Principle of EDM	48
Figure 2-29. Basic Movements during Planetary Erosion	48
Figure 2-30. Basic Process of LM	51

Figure 2-31. Classification of LM Systems	52
Figure 2-32. Stereolithography Apparatus (SLA)	53
Figure 2-33. Fused Deposition Modelling	54
Figure 2-34. Contour and Raster	54
Figure 2-35. Laminated Object Modelling	54
Figure 2-36. Multi-Jet Modelling	55
Figure 2-37. Selective Laser Sintering	56
Figure 2-38. Heat Treatment Cycle	58
Figure 3-1. The Main Route of Model Development	71
Figure 3-2. File Format Conversion	71
Figure 3-3. Feature Size due to Laser Beam Offset	73
Figure 3-4. Furnace Cycle	74
Figure 3-5. Vanguard SLS System	75
Figure 3-6. Carbolite Furnace	75
Figure 3-7. Coordinate Measuring Machine	76
Figure 3-8. Surface Profiler	76
Figure 3-9. Hardness Testing Machine	76
Figure 3-10. 3D CAD Solid Model	77
Figure 3-11. Green Part	78
Figure 3-12. Metal Model	78
Figure 3-13. Benchmark Model on CMM	79
Figure 3-14. Individual Features of the Model	79
Figure 3-15. Average Linear Errors	91
Figure 3-16. Average Radial Error	92
Figure 3-17. Ave. Absolute Linear Error: Internal vs. External Dimension	93
Figure 3-18. Ave. Relative Linear Error: Internal vs. External Dimension	93
Figure 3-19. Ave. Absolute and Relative Error: Internal vs. External Diameter	94
Figure 3-20. Incomplete Features	94
Figure 3-21. Sinking Marks on the Model	95
Figure 3-22. Different Absolute Error in Z Direction	96
Figure 3-23. 3D CAD Solid Models	97
Figure 3-24. Green Part Models	97
Figure 3-25. Metal Part Models	98

Figure 3-26. Thickness Measuring Points	99
Figure 3-27. Flatness Measuring Points	99
Figure 3-28. Schematic of the Measurements	99
Figure 3-29. Groups of Measuring Points	100
Figure 3-30. Average Absolute and Relative Error of Thickness	101
Figure 3-31. Surface Gap Profiles of the Benchmark Models	102
Figure 3-32. SLS Metal Plate for Surface Roughness and Hardness	103
Figure 3-33. Schematic Diagram of an Optical Profiler	104
Figure 3-34. Average Surface Roughness Ra	105
Figure 3-35. As Infiltrated	106
Figure 3-36. As Machined	106
Figure 3-37. As Polished (area 1)	107
Figure 3-38. As Polished (area 2)	107
Figure 3-39. As Polished (area 3)	108
Figure 3-40. As Polished (area 4)	108
Figure 3-41. As Polished (area 5)	109
Figure 3-42. As Polished (area 6)	109
Figure 3-43. Average Surface Roughness Summary	110
Figure 3-44. 3D CAD Solid Model	111
Figure 3-45. 3D Metal Model	111
Figure 4-1. Development Procedures	115
Figure 4-2. 50 mm Snap-On Tube Top	116
Figure 4-3. Small Features	117
Figure 4-4. Existing CS1 Inserts	118
Figure 4-5. The Design of the New CS1 Inserts	119
Figure 4-6. Cooling Channels: Existing vs. New Mould Inserts	120
Figure 4-7. Conformal Cooling Channels	120
Figure 4-8. O-Ring Seals	121
Figure 4-9. Split Approach of the new CS1 Top Insert	122
Figure 4-10. The Green Part of the New Inserts	123
Figure 4-11. SLS Metal Part of the New CS1 Inserts	124
Figure 4-12. Manufacturing Operations of the Top Insert	124
Figure 4-13. Manufacturing Operation of the Bottom Inserts	124

Figure 4-14. Polishing Colour Code of the Inserts	125
Figure 4-15. Finished Mould Inserts	126
Figure 4-16. Example of Readings	127
Figure 4-17. CS1 Product Quality	128
Figure 4-18. Feature Measurements	129
Figure 4-19. Power Consumption at 20% Cycle Time Reduction	130
Figure 4-20. Dimensions of the Inserts	131
Figure 4-21. Diameter 'O' on the Product	132
Figure 4-22. Surface Finish Area	132
Figure 4-23. Failed Products at 11.3s Cycle Time	133
Figure 4-24. CS1 Product Costs Analysis	135
Figure 4-25. Receptacle Spoke	136
Figure 4-26. CS2 Inserts	137
Figure 4-27. The New CS2 Cooling Channels Geometry	137
Figure 4-28. Near-Net Shape Design of the New CS2 Inserts	138
Figure 4-29. Colour Code of Turning and Grinding Operation	139
Figure 4-30. Colour Code of HSM and EDM Operations	139
Figure 4-31. Undersized Inserts	140
Figure 4-32. Mould halves and Inserts Arrangement	140
Figure 4-33. CS2 Product Quality	142
Figure 4-34. Energy Measurement	142
Figure 4-35. CS2 Product Measurements	143
Figure 4-36. CS2 Product Cost Analysis	145
Figure 4-37. A Cassio 200ml Tube Top	146
Figure 4-38. Existing CS3 Inserts	147
Figure 4-39. Surface Temperature Scales	148
Figure 4-40. Cooling Efficiency	149
Figure 4-41. Existing vs. New CS3 Cooling Systems	150
Figure 4-42. New Surface Temperatures	151
Figure 4-43. New Cooling Efficiency	151
Figure 4-44. Wireframe of the CS3 Near-Net Shape Inserts	152
Figure 4-45. Green Parts of the New CS3 Inserts	153
Figure 4-46. Finished CS3 Inserts	153

Figure 4-47. Machining Operation of the New CS3 Inserts	154
Figure 4-48. Polish Finishing of the New CS3 Inserts	155
Figure 4-49. CS3 Product Quality	156
Figure 4-50. CS3 Product Measurements	157
Figure 4-51. CS3 Product Cost Analysis	159
Figure 5-1. Cut-Out Volume Selection	170
Figure 5-2. Design Specification of the Cut-Out Volume	171
Figure 5-3. Design and Specifications of Guiding Features	171
Figure 5-4. Groove Construction for Epoxy/Sealing Sealing	172
Figure 5-5. Product Orientation Relative to Parting Line	174
Figure 5-6. Sketch and Cut Section of a New CS1 Design	175
Figure 5-7. Conformal Cooling Channels Layout of a New CS1 Inserts	176
Figure 5-8. Design of New CS1 Conformal Cooling Channel	177
Figure 5-9. Net Shape Design of the New CS1 Inserts	182
Figure 5-10. Near-Net Shape Design of CS1 Inserts	183
Figure 5-11. Cut-Out Volume of the CS1 Inserts	185
Figure 5-12. Manufacturing Colour Code of the CS1 Inserts	186
Figure 5-13. Polishing Colour Code of the CS1 Inserts	187
Figure 5-14. Receptacle Spoke	188
Figure 5-15. Outline of the New CS2 Inserts	189
Figure 5 16. New CS2 Inserts	190
Figure 5-17. The New CS2 Cooling Channels Geometry	191
Figure 5-18. Near-Net Shape Design of the New CS2 Inserts	193
Figure 5-19. Colour Code of Turning and Grinding Operation	194
Figure 5-20. Product Orientation Relative to Parting Line	195
Figure 5-21. New CS3 Inserts	195
Figure 5-22. Design of New CS3 Conformal Cooling Channel	196
Figure 5-23. Net Shape vs. Near-Net Shape of the new CS3 Inserts	198
Figure 5-24. 'Cut-Off Volume' of the Inserts	199
Figure 5-25. Manufacturing Colour Code of the new CS3 Inserts	200
Figure 5-26. Polishing Colour Code of the new CS3 Inserts	200

## Tables

Table 2-1. Advantages and Disadvantages of PIM	6
Table 2-2. Design Steps	14
Table 2-3. Shrinkage Factors of Thermoplastics	19
Table 2-4. Functions and Demands of Runner Systems	21
Table 2-5. Factors Affecting a Runner System	22
Table 2-6. Factors Affecting Design and Size of the Runners	23
Table 2-7. Functions of the Runners	23
Table 2-8. Factors Determining Gate Location, Design, and Size	24
Table 2-9. Recommended Vent Depths	25
Table 2-10. Equations for Cooling Time	26
Table 2-11. Material data	29
Table 2-12. Parameters for Release Forces	41
Table 2-13. Comparison of LM technologies to Produce Metal Parts	62
Table 2-14. SLS Metal Materials	65
Table 2-15. Overview of Current RT Developments	66
Table 3-1. LaserForm™ ST-100 Material Properties	72
Table 3-2. Process Parameters	73
Table 3-3. Identifications of the Model Features	80
Table 3-4a. Feature 1	81
Table 3-4b. Feature 2	82
Table 3-4c. Feature 3	83
Table 3-4d. Feature 4	84
Table 3-4e. Feature 5	85
Table 3-4f. Feature 6	86
Table 3-4g. Feature 7	87
Table 3-4h. Feature 8	88
Table 3-4i. Feature 9	89
Table 3-4j. Feature 10	90
Table 3-5. Proportion Weight of Bronze Ingots	98
Table 3-6. Thickness Measurements	100

Table 3-7. Flatness Measurements	101
Table 3-8. The Hardness Measurement Results	110
Table 4-1. Performance Parameter and Data/Information Required	116
Table 4-2. CS1 Material and Process Parameters	126
Table 4-3. CS1 Manufacturing and Moulding Comparison	133
Table 4-4. CS1 Product Cost Analysis	134
Table 4-5. CS2 Material and Process Parameters	141
Table 4-6. CS2 Manufacturing and Moulding Comparison	144
Table 4-7. CS2 Product Cost Analysis	144
Table 4-8. Moulding Parameters	148
Table 4-9. Comparison Effects on Surface Temperature	152
Table 4-10. Material and Process Parameters	155
Table 4-11. Cooling and Cycle Time Reductions	156
Table 4-12. CS3 Manufacturing and Moulding Comparison	158
Table 4-13. CS3 Product Cost vs. Expected Insert Durability	158
Table 5-1. List of Standard Surface Finish ISO 1302:2002	166
Table 5-2. Design Stages	173
Table 5-3. Results of Design Estimations and Evaluations for CS2	192
Table 5-4. Results of Design Estimations and Evaluations for CS3	197
Table 6-1. Summary of Indirect SLS Capabilities	203
Table 6-2. Inserts Performances	204

## Chapter 1

# **Introduction**



## Chapter 1. Introduction

### 1.1. Background

Currently, global manufacturing trends and competition challenges every industry to seek new and innovative manufacturing methods that can improve their business processes and speed up the development cycle of new products to compete more effectively [Conolly, 2004a and Knights, 2001]. Among the candidates, solid freeform fabrication (SFF) or layer manufacturing (LM) appears to be a potential manufacturing solution that offers the required characteristics to develop more competitive products [Palm, 2002]. The technologies have enabled LM systems to rapidly manufacture free-form or complex-geometry 3D parts directly from 3D CAD solid models without tooling, which allow to reduce design and manufacturing lead-time and cost, design error, tooling cost on short-run parts, and time to production and market [Grimm, 2004 and Conolly, 2004b].

Recent advancements in LM technology have led to its application not only use for rapid prototyping (RP) but also for developing production tool to manufacture parts, which rapid tooling (RT) is known [Kruth, 1998, and Levy, 2002]. Moreover, industry has also driven LM technological development and implementation toward a new concept of rapid manufacturing (RM), which is the use of LM systems to manufacture directly functional or finished products [Kochan, 1999, and Hopkinson, 2006]. Along with advanced developments in materials, recent technology developments have enabled the implementation of LM systems to be more reliable in developing production tool inserts such as for plastic injection mould [AMRCC, 2004 and Grenda, 2004].

There are many SFF/LM systems available today that are widely used, using different methods and materials, to manufacture finished/final parts [Kruth, 1998, Chua, 1999, Dormal, 1999, and Grenda, 2005]. Among them is selective laser sintering (SLS), which was one of the first LM systems to offer metal parts. Basically, there are two main approaches in metal SLS: direct and indirect [Karapatis, 1998, Hopkinson, 2001, and Dalgarno, 2003]. The direct approach enables SLS to develop 3D solid-dense metal parts directly without the furnace

cycle. Even though some use a single alloy metal powder, most of the direct approaches utilise a mixture of high and low melting point metal powder as an input. In this case, the laser sinters and melts the lower melting metal to form a matrix around the higher melting metal to develop 3D solid-dense metal parts. On the other hand, the indirect SLS approach uses coated metal powder materials which are heated by a CO<sub>2</sub> laser to develop first a 3D solid green-part. This green-part is then sent to a furnace for debinding, sintering, and infiltration process to develop a 3D fully-dense metal part. Despite significant development of the systems as well as improvements in metal powders, the current quality of the metal parts produced by both approaches still falls short of the demands of precision engineering application, and can also have limited mechanical properties [Venuvinod, 2004 and Dalgarno, 2003].

To date, machining processes such as milling, turning, grinding and electrical discharge machining (EDM), or their combinations are still the dominant methods in manufacturing plastic injection moulding tools. With significant growth of computer aided technology and developments in high-speed machining (HSM), tooling development has become more automated and faster than before. Tooling development is however still considered as the most expensive portion in the product development cycle due to the substantial length of time taken and the significant related costs required in the process [Urbanski, 2000 and Coremant, 2004].

LM systems utilize *additive* process in manufacturing parts. The successive layers of material are added and bonded to each other to build up the designed parts from scratch. This provides more design ‘freedom’ and offers advantages in manufacturing complex geometry parts rapidly and without any tooling, which potentially could reduce manufacturing lead-time and costs. Furthermore, the current research and development of RT solution has shown that the involvement of the LM system in tooling development has proved to be cost-effective and time-efficient approach, which can be utilised to provide an economical tool for plastic injection moulds [Rosochowski, 2000 and Pham, 2003].

Referring to their advantages and disadvantages, a combination of manufacturing principles between LM systems and conventional machining processes is a potential alternative RT solution in developing a high-quality insert

mould tools for production. Therefore, the use of the LM systems in this research work is to develop “near-net shape” insert tools, while machining methods such as EDM and HSM are utilised to resolve LM limitations in finishing and achieving the quality required.

## **1.2. Research Aim and Objectives**

The main aim of this research is to use indirect SLS and HSM/EDM in developing production-quality plastic injection moulding inserts (cores and cavities). To achieve this, the following objectives were established:

- To assess the technological capabilities of both SLS and HSM/EDM with reference to the typical requirements of injection mould tools.
- To investigate, using industrial case studies, how both SLS and HSM/EDM can be employed in the manufacture of injection mould tools.
- To evaluate and measure, through the case studies, the performance of the tools produced using SLS and HSM.
- To develop a set of design rules for injection mould tools to be produced using SLS and HSM/EDM, based on best practice as derived from the case studies.

It is expected that the results and outcomes of the research not only provide a potential manufacturing solution but also provide benefits and profits to the mould maker and injection moulder as end users.

## **1.3. Organisation of the Thesis**

The next following chapters of the thesis are organized as follows:

- Chapter 2. Literature Review: It highlights important information and review related literature in the research area to support the research work. It starts with a general introduction of plastic injection mould (PIM). Then, general information on current LM technologies is detailed in terms of system developments, basic processes, and major applications. Previous work regarding to the specific applications of the LM technologies in PIM are reviewed as well as technology future trends or

directions. At the end of the chapter the findings are summarized and the aim of this PhD research work is developed with reference to previous work.

- Chapter 3. Benchmark Studies: The chapter discusses two groups of benchmark studies which have been carried out to assess the technology capabilities of the indirect SLS and HSM processes based on the requirements and specifications for production quality mould inserts.
- Chapter 4. Case Studies: The design, manufacture and use of core and cavity inserts produced using indirect SLS with EDM/HSM finishing is described in this chapter, with the performance of the inserts compared to that of conventional inserts
- Chapter 5. Design Rules Application: This chapter takes the evaluation of the tool performance from the previous chapter, and proposes a set of design rules which may be used in the development of tooling inserts to be manufactured using the combined indirect SLS-HSM approach.
- Chapter 6. Conclusions and Recommendations: This chapter outlines the principal results and findings from the research work, and then identifies areas that should be consider for further research.

---

## Chapter 2

# Literature Review

## Chapter 2. Literature Review

The objective of this chapter is to provide information and review related references/literatures which underpins the research work. Section 2.1 provides a general introduction to plastic injection moulding (PIM), including the principles of moulding processes, design requirements and procedures. Section 2.2 overviews general information of layer manufacturing (LM) technologies available today with reference to basic processes, system development, and major applications. The hardware characteristics, manufacturing principles, and material developments of selective laser sintering (SLS) technologies are discussed in detail. Section 2.3 focuses on recent application of LM technologies in PIM as well as the LM technology future trends and directions. Section 2.4 summarises this chapter and section 2.5 outlines the aims of this research.

### 2.1. Introduction to Plastic Injection Moulding (PIM)

This section discusses the basic process of plastic injection moulding, describes the construction, function, and requirements of an injection mould, and reviews design and manufacturing procedures in developing injection moulds.

#### 2.1.1. Basic Process

Plastic injection moulding (PIM) is a major manufacturing method in the plastic industry. PIM is basically a repetitive and cyclical process in which melted plastic at high pressure is injected into a mould cavity, cooled and held under pressure until it can be ejected, duplicating the shape of the mould cavity [Rubin, 1972, Gastrow, 1993, and Jack, 2001]. Figure 2-1 shows the basic sequence of operations which occur in a moulding cycle: (a) heating and injecting, (b) moulding, and (c) ejecting [Rosato, 2000]. To overview the benefits of the PIM, Table 2-1 presents the advantages and disadvantages of PIM [Menges, 2001 and Rosato, 2000].

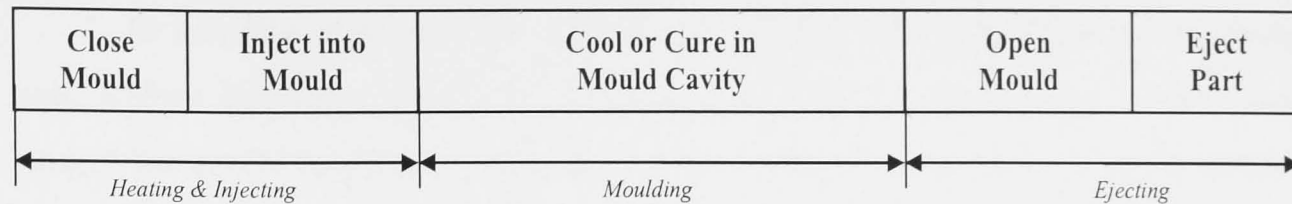


Figure 2-1. Cycle Sequence in PIM Process [Rosato, 2000]

Table 2-1. Advantages and Disadvantages of PIM [Rosato, 2000]

Advantages	Disadvantages
<ul style="list-style-type: none"> <li>• high reproducibility</li> <li>• low product cost for large volume production</li> <li>• high tolerances</li> <li>• wide range of plastic materials can be used</li> <li>• minimal scrap losses</li> <li>• no (very little) finishing required</li> </ul>	<ul style="list-style-type: none"> <li>• running costs may be high</li> <li>• parts must be designed with moulding consideration</li> <li>• expensive equipment investment</li> </ul>

Within the first heating and injecting sequence, the basic operation is to melt the raw plastic material so that it can be injected. The raw material in the form of plastic pellets is fed through a hopper into a plasticizing unit for melting. This unit consists of a single-screw extruder in which the screw reciprocates coaxially against an actuated cylinder. The heated barrel (Figure 2-2) and continually rotating screw plasticizes the pellets to form molten plastic that is then transported forward by the rotation. During this plasticizing operation, the injection nozzle is closed. Therefore, the melted plastic is pushed forward to the front of the screw. As a result, the screw is pushed to the right against the resistance of the barrel, which is called the back pressure.

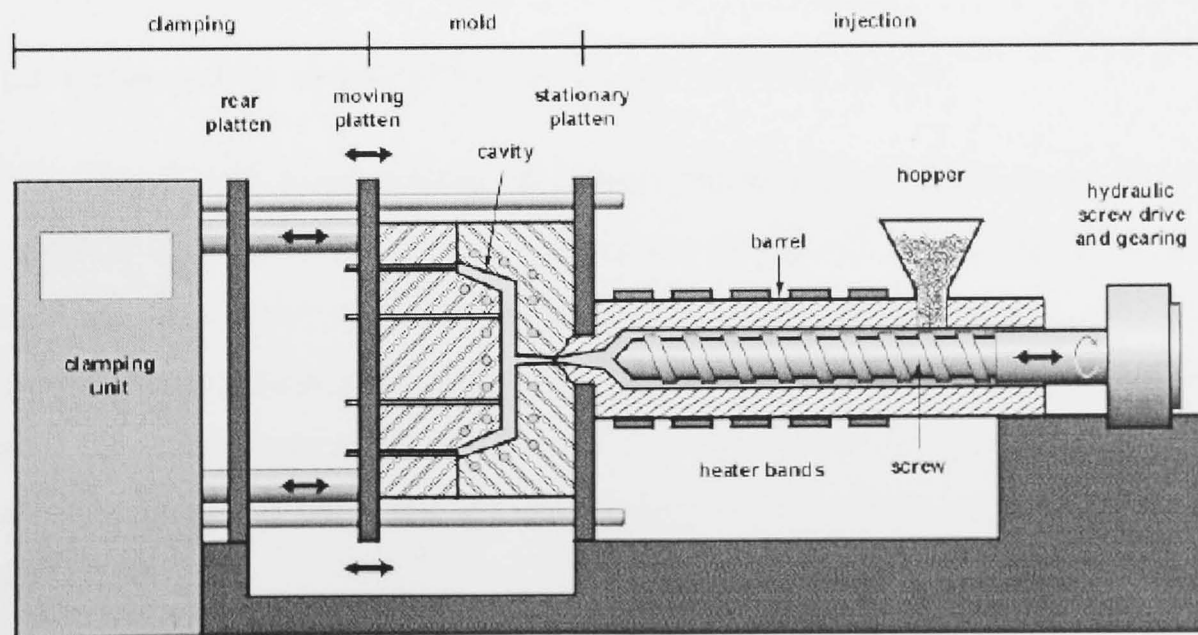


Figure 2-2. Basic Elements and Structures [Colton, 2004]

In this first sequence, the mould at the start is closed by machine clamping unit. Before injecting melted plastic into the mould, the plasticizing unit crosses against the mould to press the injection nozzle against a sprue bushing on the mould. As this happens, the nozzle simultaneously opens and the molten plastic is injected into the mould cavity. The pressure builds up as the melting plastic is injected into the cavity mould. This occurrence is counteracted by pressing the clamping unit against the mould with as much clamping force as possible to prevent 'flashing' of melting plastic.

In the second sequence, moulding, the filled melting plastic is cured and/or cooled to allow solidification inside the mould cavity. It is important to note that the volume of melting plastic inside the cavity usually changes during this sequence. It is necessary to maintain the connection between the mould and plasticizing unit until the process is complete, which is indicated by solidification of melting plastic at the gate. The connection is broken by screwing back the plasticizing unit, and closing the injection nozzle. Cutting the connection of the nozzle causes thermal isolation between the mould and the plasticizing unit. Since the plasticizing process requires a certain amount of time, as soon as the nozzle is detached and closed, the plasticizing unit starts rotating, drawing in more material and melting it and moving it forward.

Once the moulded part has solidified and reaches to the extent that it can retain its shape without external support, the third (ejecting) sequence is started. The clamping unit opens the mould and the moulded plastic is ejected from the cavity by ejectors. As this sequence is completed, the cycle then repeats.

### **2.1.2. Construction and Functions of Plastic Injection Mould**

The mould is a complex, expensive investment, and the most important element in PIM [Avery, 1998, and Gastrow, 1993]. Two basic functions of the mould are: to convey a desired shape to the melted plastic, and to solidify the moulded plastic products. To overview a typical design of a plastic injection mould, Figure 2-3 shows basic schematic lay-out of a typical injection mould and views six main functions that build up the construction of the mould [Menges, 2000; and Rosato, 2000].



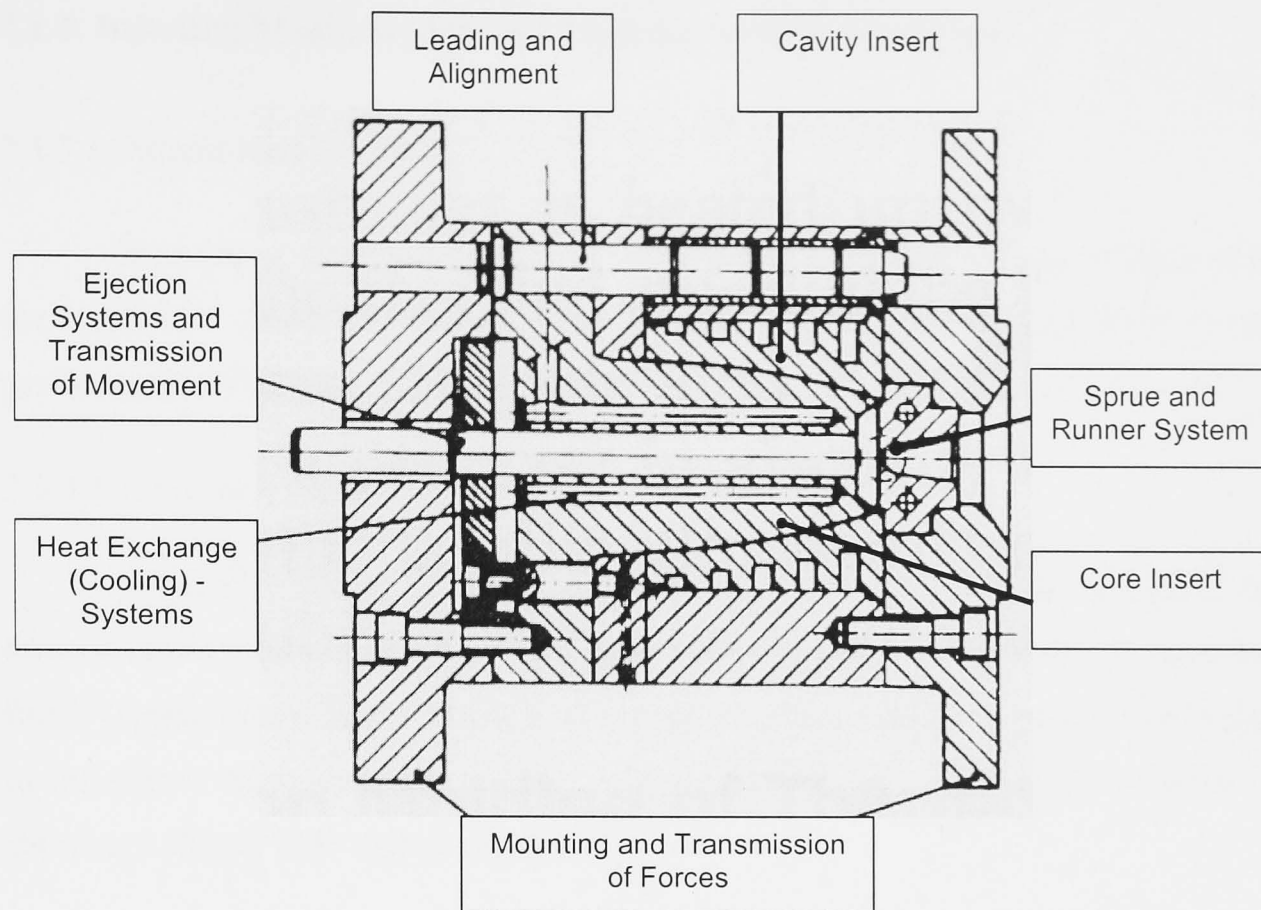


Figure 2-3. Schematic Lay-out of Injection Mould [Menges, 2000]

Clearly, the core and cavity inserts which form mould cavity are the most important features of a mould [Avery, 1998, and Gosden, 1983]. To facilitate and transport the flow of melted plastic into the mould cavity, the sprue and runner systems are constructed. The sprue, which is located in the stationary half of the mould, is a passage for injecting melted plastic from plasticizing unit into a mould. Thus, the runner systems are the channels or flow path that transports the melted plastic into the mould cavity. The heat exchange (cooling) system is constructed to remove effectively the heat from melted plastic inside the cavity in order to produce high quality parts [EFUNDA, 2002, and Engelman, 2001].

The ejection system and transmission of movement accommodates the mechanism to eject the solidified parts from the mould cavity. Since, the mould itself mostly is separated into at least two (moving and fixed) halves, and contains a number of moving parts such as the ejector system, the leading and alignment function are constructed to ensure that important parts, especially the core and cavity, are matched up and function properly and consistently for long production runs [Rosato, 2000, Fu, 2001, and Rubin, 1972].

### 2.1.3. Injection Mould Design and Manufacturing Procedures

#### 2.1.3.1. Mould Requirements

In practice, the requirements of an injection mould are heavily influenced by the customer expectation toward the quality of the product as well as the performance of the mould [Rees, 1995].

##### 2.1.3.1.1. Accuracy and Finish.

Generally, the customer expects that parts produced from a mould are dimensionally accurate within requested tolerances and comply with the specified finish (appearance). Therefore, it is important to understand and consider shrinkage of the plastic material used in order to accommodate allowable cavity oversize for shrinkage [Rees, 1995 and Menges, 2000].

##### 2.1.3.1.2. Mould Performance.

As an expensive investment, the development of a mould is in anticipation of it having a useful lifetime [Avery, 1998]. When considering the reliability of its operation and life expectancy as well as product quality and cost, mould performance is not only a measure of its productivity but it is also a measure of comparison with other moulds. The productivity of a mould usually relates to the ability of the mould to produce a certain number of products during a given time-frame. To gain more understanding, the mould productivity depends on factors which are discussed below [Menges, 2000, Chen, 1999, and Fu, 2001].

##### 2.1.3.1.2.1. Number of Cavities

Usually, the type of mould and the number of cavities are decided by customer requirements. The designers are therefore required to understand the actual requirements and to be aware of the reasons for selecting certain designs and sizes of the moulds. The following overviews the types of moulds based on their development purposes [Rees, 1995, and Rosato, 2000].

- Experimental purposes (before launching a new product): a single cavity mould is usually required to produce prototype(s). Therefore, it is very important to notice that this type of mould is usually required as soon as

possible, and should cost little.

- Engineering purposes (test): the mould is usually designed as an initial production run for producing a limited number ('zero' series) of a new product. A single cavity for this type of mould is usually sufficient. However, multi-cavity (2 to 4) moulds at low cost are preferable in order to provide a better evaluation of mould performance to predict the long-term production run.
- Production purposes: the main concern in determining the required number of cavities for this type is that the mould should be designed at the lowest investment and able to deliver desired product at the lowest possible cost.

Concerning moulds for production, the decision to determine the number of cavities should consider the followings important factors [Menges, 2000]:

- Projected/required product quantity
- Product accuracy or tolerance
- Product cost
- Product material
- Product geometry and dimension
- Injection moulding machine

The purpose of evaluating and deciding number of cavities is to ensure the economics of production as well as to guarantee the quality of the product; the more cavities the more complex and expensive the mould. However, a mould with more cavities could be profitable for long production runs [Chen, 1999, and Menges, 2000]. From the moulder's point of view, the number of cavities generally can be determined as follows [Rosato, 2000]:

- The maximum theoretical number of cavities ( $N_1$ ) is the ratio of shot weight ( $S_v$ ) and the moulding weight ( $M_v$ ), including sprue and runners.

$$N_1 = \frac{S_v}{M_v} \dots (2-1)$$

This formula assumes about 80% utilization of the whole maximum shot size. However, it is not a recommended practice for the reasons of uniform molten plastic and adequate cushion for holding pressure.

- The number of cavities for thin-wall parts ( $N_2$ ) can furthermore be

determined by plasticizing rate ( $R$ ) of the machine, the estimated number of shots per minute ( $Z$ ) and the moulding volume ( $M_v$ ).

$$N_2 = \frac{R}{Z \times M_v} \dots (2-2)$$

This number of cavities should be checked for thin-walled parts with large shot size, using the following empirical rule:  $0.4 N_1 \leq N_2 \leq 0.8 N_1$

Other factors that can affect the number of cavities are space restrictions, such as mould cavity location and layout. One of the most important aspects in multi-cavity mould design is that the cavities should be arranged properly around the sprue and receive uniform/balance pressure [Rubin, 1972]. Therefore, the distance from the sprue, and an adequate and proportional runner system, including gate dimensions, need to be considered carefully. A well designed cavity arrangement will provide better product quality [Rosato, 2000].

#### 2.1.3.1.2.2. Quality of Cooling

A cooling system constructed inside the mould cavity is an essential element. The efficiency of this cooling system in transferring the heat from melting plastic defines the economical performance of the mould and improves the product quality: the more efficient the cooling system inside the mould, the lower the cycle time and the higher the productivity [Menges, 2000, Sachs, 2000, and Xu, 2001]. Considering the moulding process, a certain amount of heat is added to the plastic during plasticizing to change its state from granulate to a viscous fluid which can be injected to a mould. This amount of heat must be therefore taken away, by the cooling system, in order to allow moulded plastic to be ejected from the mould. Figure 2-4 shows the temperature profile of the mould cavity wall during the process [Rees, 1995]. The profile illustrates that the heat is actually extracted from the mould during the entire moulding cycle, not only during the cooling time.

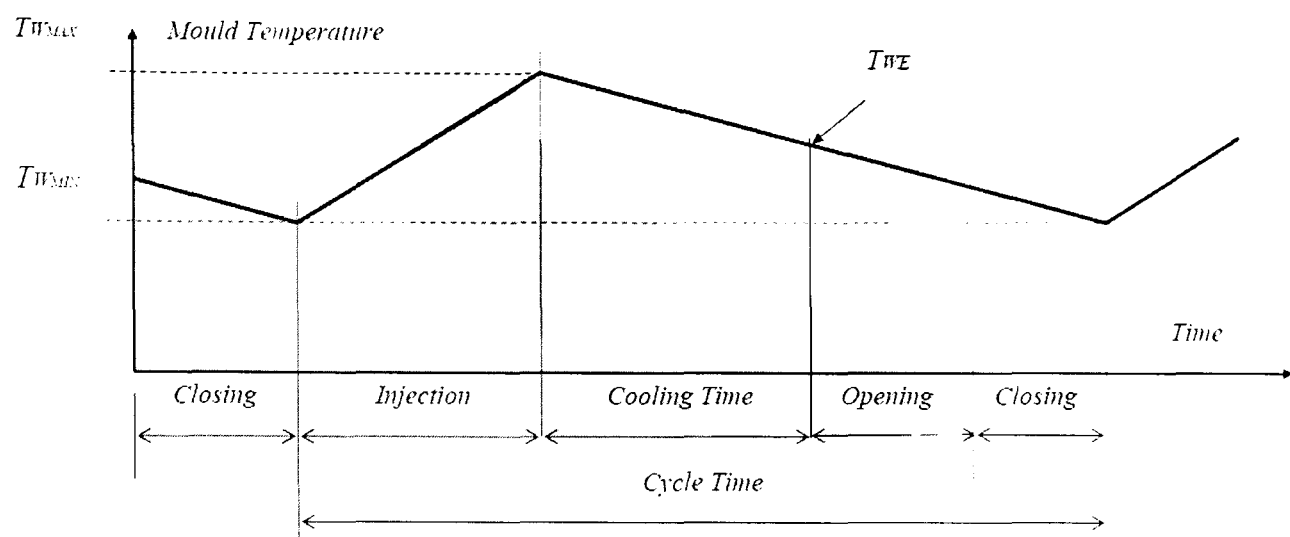


Figure 2-4. Temperature-Time Diagram during Moulding Cycle [Rees, 1995]

As the coolant enters the mould before injection, the mould temperature gradually drops to coolant temperature ( $T_{W_{MIN}}$ ). It then remains at this point until melted plastic material is injected. Once the injection process is started and the melting plastic injected, the mould temperature starts to rise gradually as the coolant continues to flow and removes the heat. As the injection process completed, the temperature of the mould starts to drop gradually from its maximum value ( $T_{W_{MAX}}$ ) as no more heat is added and the coolant continues to remove the heat from the mould. This temperature drop occurs until the next cycle begins [Menges, 2000 and Zollner, 1997].

From the above, it becomes clear that the major amount of heat is exchanged during the cooling time, where an efficient cooling system can improve the total moulding cycle time to ensure the desired temperature of the cavity wall [Menges, 2000]. Therefore, it is necessary to understand and take special consideration on the following essential factors that may affect the cooling condition [Rosato, 2000]:

- Pressure difference: The pressure difference between coolant supply and return lines needs to be consider in order to determine the required pressure for the coolant. The geometry and dimension of cooling channels, type of coolant, and coolant pumping capacity are the factors that are particularly important to consider.
- Temperature difference: There are three basic temperature differences that need to be considered in the mould: plastic temperature between injections, coolant temperature between entering and leaving the mould, and temperature between plastic and coolant.

- Cooling channel geometry and dimension: The quantity/flow-rate of coolant is proportional to the cross-sectional area of the cooling lines: the larger the area, the more coolant flows. Therefore, the cross section should be designed properly to deliver adequate quantity and provide evenly distributed coolant to remove the heat from the mould. Based on the rules developed previously by Dalgarno et al. [Dalgarno, 2001], the parameters (diameter, length, geometrical complexity and location) employed in designing the new cooling channels are identified that a channel diameter of at least 8 mm is preferred although the minimum diameter that can be manufactured is 5 mm. To determine the location and to avoid stress concentration in the insert, it is also suggested that a proper distance between the cavity surfaces and cooling channel centre line and between adjacent channels is at least equal to a channel diameter.
- Condition of cooling channels: The resistance against coolant flow is linearly proportional to the length of the cooling lines. Changes in direction create flow resistance and reduce the coolant flow. Also, contaminations and deposits inside the channels affect the cooling efficiency. They reduce the cross section area of the channels which eventually reduces the flow of coolant. Furthermore, the heat conductivity of the contaminations is usually much lower so that they can reduce the rate of heat transfer from the plastic to the coolant.
- Coolant flow condition: During cooling turbulent flow conditions (Reynolds number,  $Re > 2300$ ) should always be maintained because, at this flow condition, the coolant removes the heat from the cavity wall effectively which improves the heat exchange process.
- Design of the products: Design considerations in the desired products such as uneven wall-thickness influence the efficiency level of the cooling system.
- Type of coolant: the heat transfer coefficient of the coolant used affects the heat exchange condition.

To plan and establish an efficient cooling system, Menges as well as Zollner [Menges, 2000 and Zollner, 1997] proposes the essential steps as outlined in Table 2-2. Section 2.1.3.2.4. will explain these steps in more detail.

Table 2-2. Design Steps [Menges, 2000 and Zollner, 1997]

Design Steps	Criteria
1. Cooling time calculation	Minimum cooling time to reach ejecting temperature
2. Heat flow balance	Required heat flow through coolant
3. Flow rate of coolant	Uniform temperature along cooling channels
4. Diameter of cooling channels	Turbulent flow
5. Position of cooling channels	Uniform heat flow
6. Pressure drop calculation	Selection of optimum cooling system

### 2.1.3.1.2.3. Mould Strength and Durability

A properly designed, well built and maintained mould should last for its designated service life because production failure due to an improperly designed mould is very costly [Menges, 2000]. Therefore, the next consideration regarding to mould productivity is the strength and durability. Concerning this, the following outline the factors that could influence the mould strength and durability [Rees, 1995]:

- mould material selection,
- heat treatment, and
- manufacturing process

Mostly, these factors are interrelated so that they should be considered at all times in designing the mould. The following describes the most important areas that need to be considered in mould design [Rees, 1995]:

- Stiffness and Strength

A mould is designed and expected to provide reliable and fully repeatable function under extremely high pressures during the moulding process. Accordingly, there are several problems related with the stress generated by these applied pressures if the cavity wall is not designed adequately.

Basically, the cavity will stretch or enlarge or deform somewhat, no matter how thick the walls are. However, it will return to its original shape after the injection pressure is released if the loads applied are below the yield point of the cavity material. Moreover, a mould is subjected to fluctuated pressures as it is injected at every moulding cycle. This fluctuated pressure creates the worst condition in a mould when considering the effect of material fatigue [Rees, 1995].

- Compressive Strength

Injection pressure causes compressive stresses on the cavity. If features such as cooling channels or screw holes are built extremely close to the surface, the cavity will constantly deform or deflect at these weak spots and build up fatigue stress after a number of moulding cycles.

The cooling channels should be located as close as possible to the cavity surface in order to effectively remove the heat from the molten plastic in the shortest time. However, the strength needs to be considered in order to set a minimum distance between cooling channels and the cavity surface. To determine the allowable distance  $d$  in Figure 2-5., Rao [Rao, 1991] developed a model to predict mould stress and deflection based on the following rectangular model as follow:

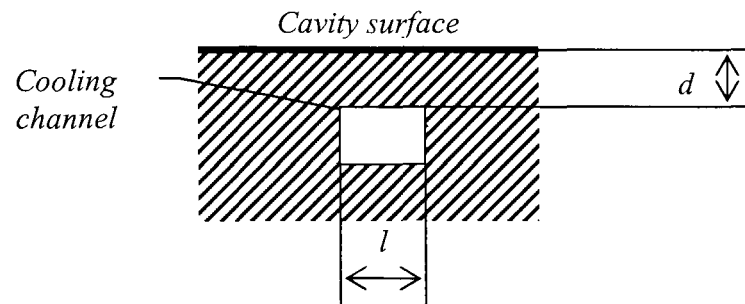


Figure 2-5. Cooling Channel Layout

- maximum tensile stress ( $\sigma_{max}$ ):

$$\sigma_{max} = \frac{0.5 \cdot P \cdot l^2}{d^2} \dots\dots(2-3)$$

- maximum shear stress ( $\tau_{max}$ ):

$$\tau_{max} = \frac{0.75 \cdot P \cdot l}{d} \dots\dots(2-4)$$

- maximum surface deflection ( $f_{max}$ ):

$$f_{max} = \frac{P \cdot l^2}{d} \left( \frac{d^2}{32 \cdot E \cdot d^2} + \frac{0.15}{G} \right) \dots\dots(2-5)$$

where,

- $P$  = Injection pressure
- $D$  = Cooling channel diameter
- $d$  = Distance from cooling channel to mould surface
- $E$  = Young's modulus of the mould material
- $G$  = Shear modulus of the mould material



Based on this model, the conditions where  $f \leq f_{max}$ ;  $\sigma \leq \sigma_{max}$ ;  $\tau \leq \tau_{max}$  have to be fulfilled in order to achieve a minimum distance  $d$ . Moreover, Rao mentioned that this model can also be employed to determine minimum distance of the channels with circular cross-section.

#### 2.1.3.1.2.4. Costs

In order to measure the impact and evaluate the economical performance of the mould, the cost of the product should be analyzed and taken into account [Chen, 1999]. A number of factors that basically affect the product cost can be broken into the following elements [Rees, 1995]:

- plastic material,
- utilities,
- direct human resources,
- injection mould,
- injection machine,
- maintenance, and
- overhead.

Concerning this, a simple model to analyse comparative product cost has been developed by Dalgarno [Dalgarno, 2001]. In the model, the above cost elements are simplified into the total costs that directly relate to the development of the cavity and core inserts. Described below is the model for the evaluation of the total cost required [Dalgarno, 2001]:

- Total cost ( $C_T$ ): the sum of three essential dependent costs, the cost of tooling ( $C_{to}$ ), the cost of moulding ( $C_m$ ), and the cost of tool changes ( $C_{tc}$ )

$$C_T = C_{to} + C_m + C_{tc} \dots (2-6)$$

- Cost of tooling ( $C_{to}$ ): the total cost in manufacturing the number of cavity and core inserts required ( $N_t$ ). This cost is obtained as follows:

$$C_{to} = N_t \cdot c_t \dots (2-7)$$

where,

$c_t$  = cost required in manufacturing a set of cavity and core insert.

- Cost of moulding ( $C_m$ ): the total cost required for moulding process. It is determined based on the cost rate which relates to direct human resources

( $C_{hr}$ ), running machines and utilities ( $C_{mt}$ ), and the total time required ( $t_T$ ) to produce the expected number of parts ( $N_m$ ). Where, the total time  $t_T$  is obtained based on the moulding cycle time ( $t_c$ ).

$$C_m = (C_{hr} + C_{mt}) \cdot t_T \quad \dots(2-8)$$

$$C_m = \frac{(C_{hr} + C_{mt}) \cdot t_c \cdot N_m}{3600}$$

- Cost of tool changes ( $C_{tc}$ ): the total cost required in changing a set of cavity and core insert during moulding. It is then obtained based on a total set of cavity and core inserts required ( $N_t$ ), the cost rate of direct human resource involved ( $C_{hr}$ ) and of running the machine ( $C_{mt}$ ), and the total time required to change the inserts ( $t_{tc}$ ) from/to the machine.

$$C_{tc} = (N_t - 1) \cdot (C_{hr} + C_{mt}) \cdot t_{tc} \quad \dots(2-9)$$

- Cost of Product ( $C_p$ ): the cost of the moulded part. It is obtained by dividing the total cost  $C_T$  with the total number of product required/expected ( $N_m$ )

$$C_p = \frac{C_T}{N_m}$$

or  $\dots(2-10)$

$$C_p = \frac{C_{to} + C_m + C_{tc}}{N_m}$$

As noted,  $C_p$  is not a “real” overall cost. The calculation of the  $C_p$  considers only cost elements which are directly related to the cavity/core inserts.

### 2.1.3.2. Basic Mould Design Process

A mould design process is one of the most crucial steps in producing plastic parts. Therefore, having a systematic design procedure is very important because a mould and its operation require to comply with pre-determined conditions [Rosato, 2000]. Figure 2-6 shows the basic interrelated stages in mould design procedures [Menges, 2000].

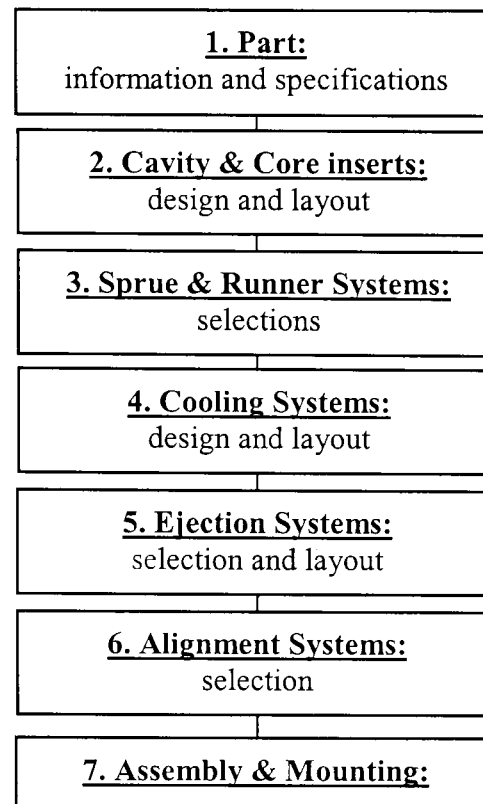


Figure 2-6. A Mould Design Procedure [Menges, 2000]

#### 2.1.3.2.1. 1st Stage: Part information and specifications

Before designing a new mould, the first stage starts with gathering information and specifications which are relevant to the plastic part to be moulded. Therefore, evaluating the function and usage of the desired product is necessary [Rosato, 2000]. These activities include identifying the importance of certain aspects and critical areas of products such as required geometry, dimensions, tolerances, finish quality, fit with other parts, location of gate and ejectors. In evaluating product geometry, wall thickness, “heavy” sections and thin passages are other important features that need to be considered carefully because these are undesirable features for moulding which affect the filling process and cause distortion on the products [Rees, 1995].

Furthermore, understanding the important characteristics of part materials also crucial. Described below is the material characteristics which are considered to directly affect the design of the cavity and core inserts [Rees, 1995 and Bryce, 1998]:

##### 2.1.3.2.1.1. Material viscosity:

This material characteristic has a big influence in the constructions of runner and gating systems, ventilations, and also affects the physical properties of the

plastic parts. In mould design, the viscosity is usually employed to determine: the pressure required to inject the material into the mould; the geometry and dimensions of the runner and gate systems to allow the material flow easily into the mould; and the depth of vents for removal of trapped air in the mould cavity [Bryce, 1998].

#### 2.1.3.2.1.2. Material thermal properties:

The efficiency of plastic materials in absorbing and dissipating heat will influence the cooling efficiency during moulding. To some degree, plastic materials are heat sensitive when they are exposed to high temperatures over a length of time. Therefore, it is required to understand the relation between the moulding temperatures (the highest and lowest temperatures at which the material could be injected safely) and the elapsed time before degradation starts at these temperatures. For example, a very heat sensitive plastic materials are normally moulded at low temperature with a short elapsed time. In contrast, low heat sensitive materials are moulded at high temperature with a long elapsed time, which makes the design of mould cooling system more important [Rees, 1995].

#### 2.1.3.2.1.3. Material shrinkage:

Another significant characteristic to be considered in injection moulding is material shrinkage. Every plastic material has a shrinkage factor assigned to it in order to determine adequate dimensions of cavity inserts in producing a desired finish size of the part after being removed from the mould. To simplify the estimation of shrinkage for dimensioning the mould cavity, the following Table 2-3 lists shrinkage factors of some thermoplastics [Menges, 2000].

Table 2-3. Shrinkage Factors of Thermoplastics [Menges, 2000]

Material	Shrinkage (%)	Material	Shrinkage (%)
Nylon 6	1 – 1.5	Polycarbonate	0.8
Nylon 6-GR	0.5	Polyoxymethylene (Acetal)	2
Nylon 6/6	1 – 2	Polyvinyl Chloride, rigid	0.5 – 0.7
Nylon 6/6-GR	0.5	Polyvinyl chloride, soft	1 – 3
Low-density polyethylene	1.5 – 3	Acrylonitrile-butadine-styrene	0.4 – 0.6
High-density polyethylene	2 – 3	Polypropylene	1.2 – 2
Polystyrene	0.5 – 0.7	Cellulose acetate	0.5
Styrene-acrylonitrile	0.4 – 0.6	Cellulose acetate butyrate	0.5
Polymethyl methacrylate (Acrylic)	0.3 – 0.6	Cellulose propionate	0.5

In practice, predicting accurate shrinkage for dimensioning a mould cavity is not a simple task due to the many factors that have to be considered to achieve the final shrinkage result. Changes in one feature of a product design could cause different shrinkage to occur in other features. Different temperature in the mould also produce different shrinkage in the moulded part. Therefore, it is recommended to have as much information and advice as possible from experienced moulders, mould-makers, and material suppliers in predicting accurate shrinkage [Bryce, 1998].

#### 2.1.3.2.2. 2nd Stage: Cavity and core inserts design and layout

The following are the factors that will be decided in designing both cavity and core inserts [Menges, 2000]:

- Geometry/dimensions/tolerances
- Parting lines
- Surface finish
- Material specifications
- Number of cavity inserts
- Layout of cavity inserts

The selected product's design will provide the information regarding to the location where the surface of both cavity and core inserts touches (parting line). The product's position relative to the parting line defines the design required, including its geometry, material specifications, and surface finish quality. By having related information about injection machine (i.e. plasticizing rate, clamping force, shot capacity, injection pressure, and mounting plate), and production (i.e. number of part required), the mould size can be determined.

In determining the mould size, an economic number of cavities is a crucial factor. As mentioned previously, equations (2-1) and (2-2) can be used to estimate the maximum number of cavities required. However, Rosato suggests that considering the economical number of cavities is more important. The following equation (2-11) can be used to estimate the most economical number of cavities [Rosato, 2000];

$$N = \sqrt{\frac{N_p \cdot C_{mt} \cdot t_c}{M_{eff} \cdot 3600 \cdot C_e}} \dots(2-11)$$

where,

- $N_p$  = number of part required
- $C_{mt}$  = Cost of machine rate
- $t_c$  = Cycle time
- $M_{eff}$  = Mould machine efficiency (~ 80%)
- $C_e$  = Estimated cost per-cavity

With the number of cavities decided, the layout of the cavity inserts inside the mould can then be arranged so that an estimation of the mould dimensions relative to the cavity insert dimensions can be determined [Rosato, 2000].

### 2.1.3.2.3. 3rd Stage: Sprue and runner systems selection

As mentioned previously, the runner system accommodates and transports the molten plastic travelling from the machine to the mould cavity. Its construction, geometry and connection with the moulded part affect significantly the filling process and the product quality [Bryce, 1998]. Figure 2-7 illustrates a typical runner system which is generally composed of sprue, runner, and gate [Menges, 2000]. Table 2-4 lists functions of and demands on the runner systems. To construct runner systems, Table 2-5 furthermore lists the factors that are to be considered [Menges 2000].

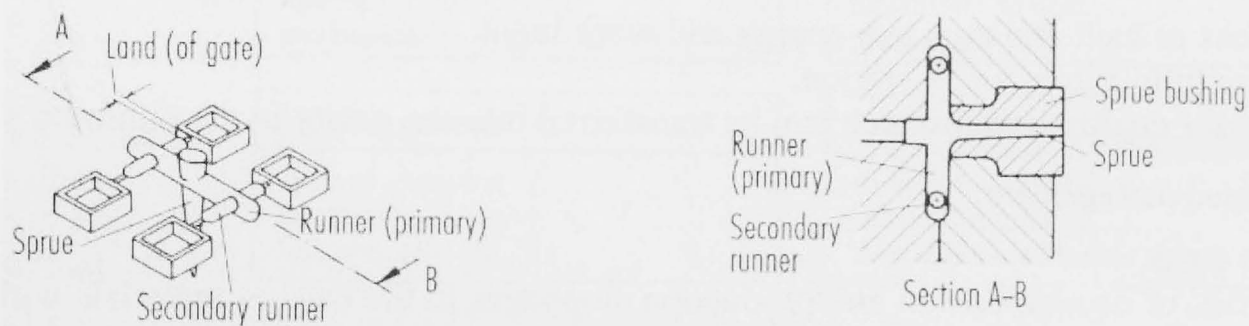


Figure 2-7. Runner Systems [Menges, 2000]

Table 2-4. Functions and Demands of Runner Systems [Menges, 2000]

Functions	Demands
<ul style="list-style-type: none"> <li>• Cavity filling with a minimum weld lines</li> <li>• Minimum flow restrictions</li> <li>• Minimum total weight</li> <li>• Ease of ejection</li> <li>• Not affect part appearance</li> </ul>	<ul style="list-style-type: none"> <li>• Minimum losses in pressure, temperature and material</li> <li>• Balanced cooling time and holding pressure</li> <li>• Not affect cycle time</li> <li>• Locate gate at the thickest section of moulded part</li> <li>• Gate location and design prevent jetting</li> </ul>

Table 2-5. Factors Affecting a Runner System [Menges, 2000]

Moulded Part	Geometry; Volume; Wall thickness; Quality requirements (Dimensional; Appearance; Function)
Part Material	Viscosity; Chemical composition; Filler; Freezing time; Softening range and temperature; Sensitivity of heat; Shrinkage
Injection Mould	Ejection systems; Runner systems temperature
Moulding Machines	Type of clamping; Injection pressure and rate

Technically, the molten plastic enters the mould via sprue bushing. In order to fulfil its proper functions, the following sprue bushing properties are required:

- wear resistance
- flexural fatigue strength
- minimum mark on the moulded part
- a leak proof connection between injection nozzle and mould.

Figure 2-8 shows the application of rules to the dimensions of the sprue that ensure desired quality and reliable operations.

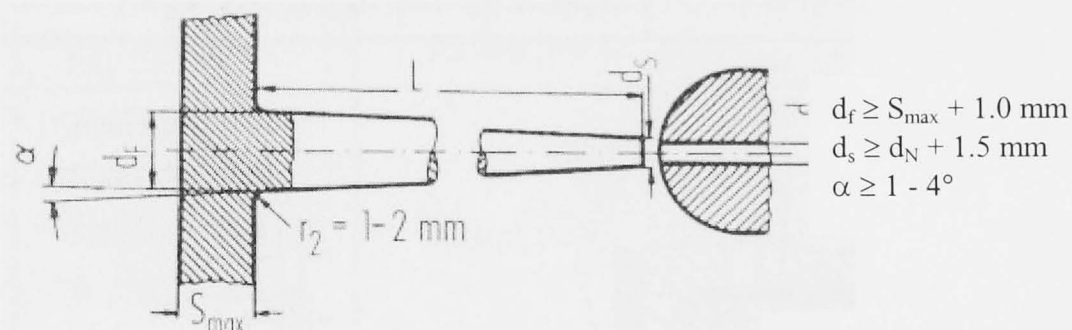


Figure 2-8. Sprue Dimensions [Menges, 2000]

The sprue in single cavity moulds is pulled from the orifice and then ejected by the moulded part. In multi cavity moulds, the sprue however serves only to feed the molten plastic material to the runner. Therefore, special injection support is required. Generally, a sprue-puller (Figure 2-9), which acts as an undercut that grips the sprue, is constructed opposite the sprue.

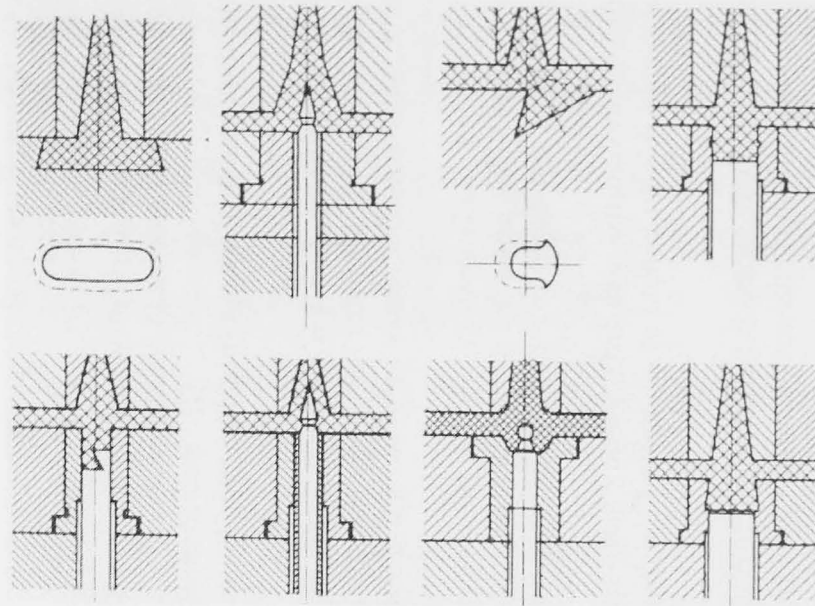


Figure 2-9. Design of Sprue-Pullers [Menges, 2000]

Runners connect the sprue with mould cavity through the gate. The following Table 2-6 and Table 2-7 summarize the factors affecting a design of the runner and its functions [Menges, 2000].

Table 2-6. Factors Affecting Design and Size of the Runners

<ul style="list-style-type: none"> <li>• Part volume</li> <li>• Wall thickness</li> <li>• Plastic material</li> <li>• Length of flow path</li> <li>• Resistance to flow</li> <li>• Surface/Volume ratio</li> </ul>	<ul style="list-style-type: none"> <li>• Heat losses</li> <li>• Losses from friction</li> <li>• Cooling time</li> <li>• Amount of scrap</li> <li>• Cost of manufacturing</li> <li>• Mould type</li> </ul>
--	---

Table 2-7. Functions of the Runners

<ul style="list-style-type: none"> <li>• Conveying molten plastic rapidly and unrestricted into mould cavity in the shortest way and with a minimum of heat and pressure loss</li> </ul>
<ul style="list-style-type: none"> <li>• Molten plastic must enter mould cavities at all gate at the same time under the same pressure and with the same temperature</li> </ul>
<ul style="list-style-type: none"> <li>• To save material, cross section should be kept small although a larger cross section may be more favourable for optimum cavity filling and maintaining adequate holding pressure. Larger cross section may increase cooling time</li> </ul>
<ul style="list-style-type: none"> <li>• The surface over volume ratio should be kept as small as feasible</li> </ul>

Furthermore, the gate connects the mould cavity with runner. Gate size and location are basically determined by considering the following requirements [Menges, 2000]:

- the gate should be as small as possible so that molten material is heated but not damaged by shear
- the gate should be easy to eject



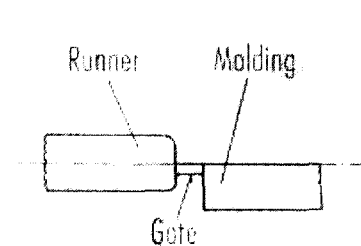
- the gate should allow automatic separation of the runner from the moulded part, without leaving significant marks on the moulded part.

Table 2-8 represents the factors which affect the size, location, and design of gates. Whilst, Figure 2-10 summarizes some considerations in selecting the geometry and locating the gates on the moulded part [Menges, 2000].

Table 2-8. Factors Determining Gate Location, Design, and Size

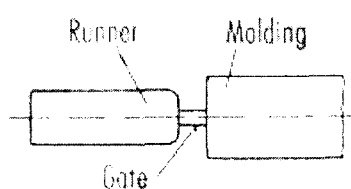
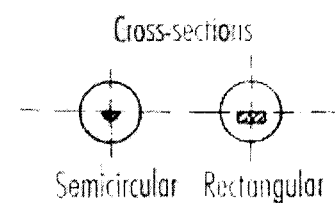
Moulded Part	Geometry; Wall thickness; Loading direction; Quality requirements (Dimensional; Appearance; Function); Flow length/wall thickness ratio
Part Material	Viscosity; Temperature; Flow characteristics; Filler; Shrinkage
Generalities	Distortions; Weld lines; Ease of Ejection; Separation from moulded part; Costs

### Characteristics



#### Eccentric gate:

- the eccentric position of the gate facilitates machining
- ease of ejection and separation moulded part
- gate orifice aligned to a wall prevents jetting



#### Centric Gate:

- small surface to volume ratio of circular cross section reduces heat loss and friction
- machining operation in both mould halves required.
- centric position renders separation more difficult and may require post-processing
- gate promotes jetting

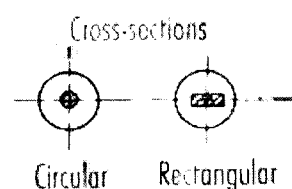


Figure 2-10. Gate Cross-Section and Position at the Runners [Menges, 2000]

Concerning the best moulding result, the gate is recommended to be located at the thickest cross-section to avoid sink marks on the moulded part due to low holding pressure and premature cooling of the gate area [Bryce, 1998]. Also, the location of the gate orientates the flow direction of the molten plastic entering the mould cavity, which may affect the physical properties of the moulded part. Therefore, understanding in advance the type of loading and the direction of the

principal stress applied in the moulded part before designing the mould is recommended [Menges, 2000].

Any air and processing gases inside mould cavity during the injection process must be vacated. Gases can prevent complete filling, and may become very hot from compression and burn up the moulded part. To avoid this happening, mould ventilation is required. In most mould design, it is not necessary to have a special design for the ventilation because there are certain features of the mould that can accommodate sufficient possibilities for the air and gases to escape from the mould. For example, the air can escape along the ejector pins or at the parting line as long as it has sufficient surface roughness [Bryce, 1998 and Menges, 2000].

If ventilation is required, its geometry and location need to be considered. Table 2-9 shows recommended vents depths based on the viscosity of the plastic material and the location of the vents. In practice, it is recommended that at least 30% of the perimeter of the mould cavity parting line should be the vented [Bryce, 1998].

Table 2-9. Recommended Vent Depts [Bryce, 1998]

<b>Material</b>	<b>Cavity (mm)</b>	<b>Runner (mm)</b>
ABS	0.05	0.10
Acetal	0.017	0.038
Acrylic	0.05	0.10
Cellulose acetate	0.025	0.05
Cellulose acetate butyrate	0.025	0.05
Ionomer	0.017	0.038
Nylon 6/6	0.0127	0.025
Polycarbonate	0.05	0.10
Polyethylene	0.025	0.05
Polypropylene	0.025	0.05
Polyphenylene oxide	0.05	0.10
Polyphenylene sulfide	0.0127	0.025
Polysulfone	0.025	0.05
Polystyrene	0.025	0.05
Rigid PVC	0.05	0.10

#### 2.1.3.2.4. 4th Stage: Cooling systems design and layout

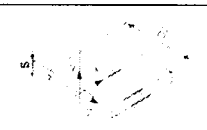
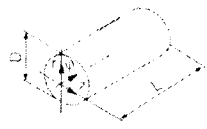
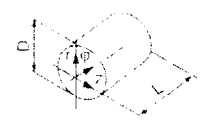
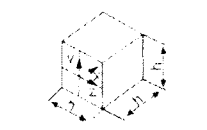
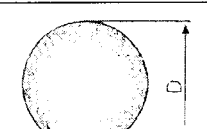
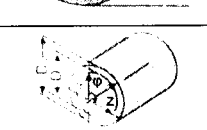
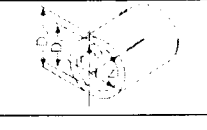
After the molten plastic is injected into the mould cavity, it is allowed to

remain there under pressure until it is cooled down and solidified enough to be ejected from the mould. Concerning its quality and performance in removing heat from mould cavity as mentioned section 2.1.3.1. , the followings describe in detail guidelines which can be employed in designing efficient cooling system.

- Step1: Calculating the Cooling Time

The cooling time calculation is basically focused on the required time to cool down a plastic part from melt to ejection temperature. For practical reasons, this required cooling time is determined based on the longest calculated time for different section of the plastic part. A sufficient calculation of the longest cooling time usually occurs at the critical (thickest) wall-thickness of the plastic part. Table 2-10 outlines equations for a variety of configurations for different geometry that can be used for this purpose [Menges, 2000 and Zollner, 1997].

Table 2-10. Equations for Cooling Time [Menges, 2000]

Geometry	Condition	Equation
	Plate $\dot{Q}_x = 0$ $\dot{Q}_y = 0$	$t_c = \frac{s^2}{\pi^2 \cdot a} \cdot \ln\left(\frac{8}{\pi^2} \cdot \frac{T_M - \bar{T}_w}{\bar{T}_E - \bar{T}_w}\right)$ $t_c = \frac{s^2}{\pi^2 \cdot a} \cdot \ln\left(\frac{4}{\pi} \cdot \frac{T_M - \bar{T}_w}{\bar{T}_E - \bar{T}_w}\right)$
	Cylinder $\dot{Q}_\varphi = 0$ $\dot{Q}_z = 0$ $L \gg D$	$t_c = \frac{D^2}{23.14 \cdot a} \cdot \ln\left(0.692 \cdot \frac{T_M - \bar{T}_w}{\bar{T}_E - \bar{T}_w}\right)$ $t_c = \frac{D^2}{23.14 \cdot a} \cdot \ln\left(1.602 \cdot \frac{T_M - \bar{T}_w}{\bar{T}_E - \bar{T}_w}\right)$
	Cylinder $\dot{Q}_\varphi = 0$ $L = d$	$t_c = \frac{1}{\left(\frac{23.14}{D^2} + \frac{\pi^2}{L}\right) \cdot a} \cdot \ln\left(0.561 \cdot \frac{T_M - \bar{T}_w}{\bar{T}_E - \bar{T}_w}\right)$ $t_c = \frac{1}{\left(\frac{23.14}{D^2} + \frac{\pi^2}{L}\right) \cdot a} \cdot \ln\left(2.04 \cdot \frac{T_M - \bar{T}_w}{\bar{T}_E - \bar{T}_w}\right)$
	Cube	$t_c = \frac{h^2}{3 \cdot \pi^2 \cdot a} \cdot \ln\left(0.533 \cdot \frac{T_M - \bar{T}_w}{\bar{T}_E - \bar{T}_w}\right)$ $t_c = \frac{h^2}{3 \cdot \pi^2 \cdot a} \cdot \ln\left(2.064 \cdot \frac{T_M - \bar{T}_w}{\bar{T}_E - \bar{T}_w}\right)$
	Sphere	$t_c = \frac{D^2}{4 \cdot \pi^2 \cdot a} \cdot \ln\left(2 \cdot \frac{T_M - \bar{T}_w}{\bar{T}_E - \bar{T}_w}\right)$
	Hollow cylinder $\dot{Q}_\varphi, \dot{Q}_z = 0$ $r \ll D/2$ $\dot{Q}_r = 0$	same as plate with $s = D_a - 0$ ,
	Hollow cylinder $\dot{Q}_\varphi, \dot{Q}_z = 0$	same as plate with $s = (D_a - D_i) / 2$

Moreover, a major heat exchange between injected plastic and coolant takes places during the cooling time through thermal conduction. Because the nature of plastic part sections is mainly two-dimensional and the heat transfer is in one-direction only, a one-dimensional calculation is sufficient to compute heat flow. In

the case of one-dimensional heat flow, the Fourier differential equation can be reduced to:

$$\frac{\partial T}{\partial t} = a \frac{\partial^2 T}{\partial x^2} \dots (2-12)$$

with,

$$a = \frac{k}{\rho \cdot c_p} \dots (2-13)$$

where,

$T$	= Temperature
$t$	= Time
$x$	= Distance
$a$	= Thermal diffusivity
$k$	= Thermal conductivity
$\rho$	= Density
$c_p$	= Specific heat capacity

With assumptions that the melt temperature in the cavity is constant immediately after injection, the temperature of cavity wall rises rapidly and remains constant, then the following equation is a compilation of a solution for one dimensional heat exchange with respect to the cooling time  $t_c$  [Menges, 2001].

$$t_c = \frac{s^2}{\pi^2 \cdot a} \ln \left( \frac{8}{\pi^2} \cdot \frac{T_M - T_W}{\bar{T}_E - T_W} \right) \dots (2-14)$$

where,

$s$	= wall thickness
$\bar{T}_E$	= Average of ejection temperature
$T_W$	= Cavity-wall temperature
$T_M$	= Melt temperature

With the effective thermal diffusivity  $a_{eff}$  (a mean value of the thermal diffusivity  $a$ ), Figure 2-11 presents nomograms which are developed for simple and quick calculation to determine the cooling time of plate-shaped and cylindrical plastic parts [Zollner, 1997]. The cooling time  $t_c$  is plotted against the cavity-wall temperature  $T_W$  for a number of constant average ejection temperatures  $\bar{T}_E$ , various wall thicknesses  $s$ , and cooling rate  $\bar{\theta}$ .

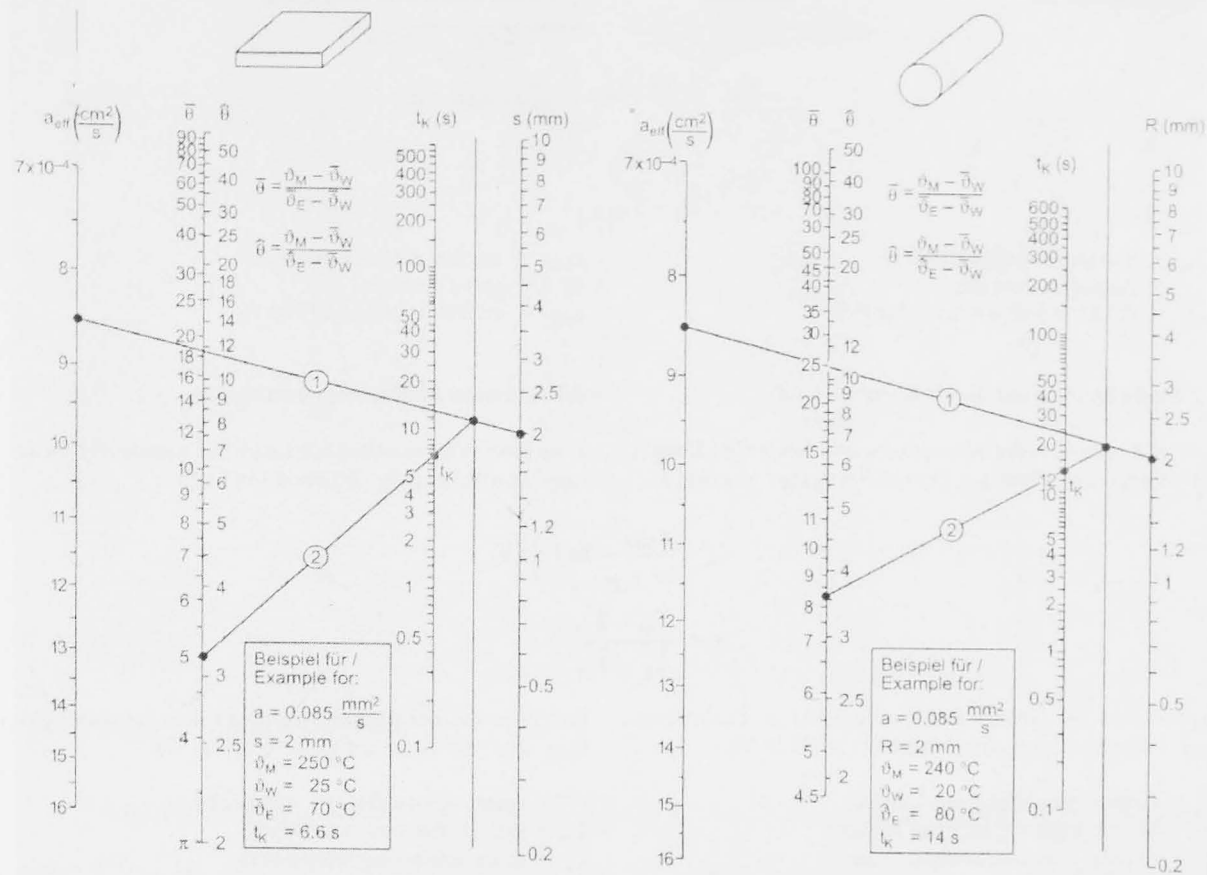


Figure 2-11. Nomogram for Cooling Time Calculation [Menges, 2000]

Note:  $\vartheta_M = T_M$  ;  $\bar{\vartheta}_W = \bar{T}_W$  ;  $\bar{\vartheta}_E = \bar{T}_E$  ;  $t_k = t_c$

The effective thermal diffusivity  $a_{eff}$  of several important crystalline plastics is presented in Figure 2-12 [Zollner, 1997].

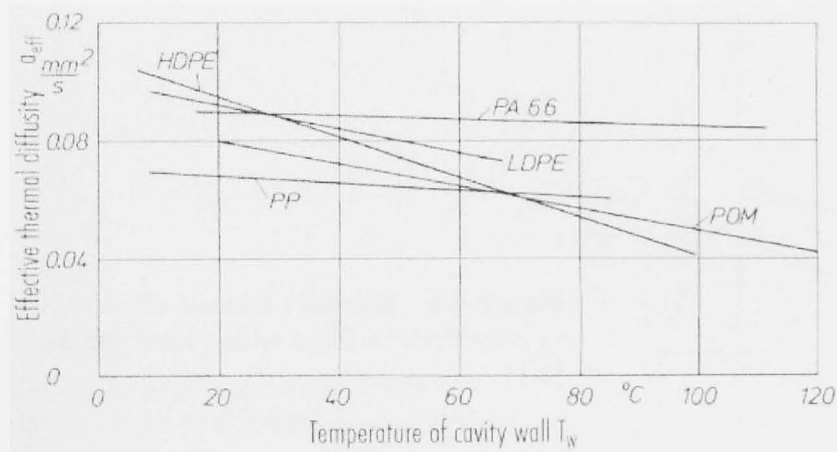


Figure 2-12. Effective Thermal Diffusivity for Crystalline Plastic [Menges, 2000]

The dimensionless cooling rate  $\bar{\theta}$  is obtained by:

$$\bar{\theta} = \frac{T_M - \bar{T}_W}{\bar{T}_E - \bar{T}_W} \dots (2-15)$$

Table 2-11 lists reference data of melt  $T_M$ , average mould wall  $\bar{T}_W$  and average ejection temperature  $\bar{T}_E$  as well as the average density between melt and ejection temperature for common plastic materials.

Table 2-11. Material data [Menges, 2000]

Material	Melt temperature (°C)	Wall temperature (°C)	Demolding temperature (°C)	Average density (g/cm <sup>3</sup> )
ABS	200–270	50–80	60–100	1.03
HDPE	200–300	40–60	60–110	0.82
LDPE	170–245	20–60	50–90	0.79
PA 6	235–275	60–95	70–110	1.05
PA 6.6	260–300	60–90	80–140	1.05
PBTP	230–270	30–90	80–140	1.05
PC	270–320	85–120	90–140	1.14
PMMA	180–260	10–80	70–110	1.14
POM	190–230	40–120	90–150	1.3
PP	200–300	20–100	60–100	0.83
PS	160–280	10–80	60–100	1.01
PVC rigid	150–210	20–70	60–100	1.35
PVC soft	120–190	20–55	60–100	1.23
SAN	200–270	40–80	60–110	1.05

- Step 2: Heat Balance

Understanding basic principles of heat exchange in a mould in advance is crucial in order to plan an efficient cooling system [Menges, 2000]. Heat basically flows from higher to lower temperature. Inside a mould, the heat from plastic flows into the mould, and then from the mould into the coolant and very small amount into the air and other mould plates (Figure 2-13).

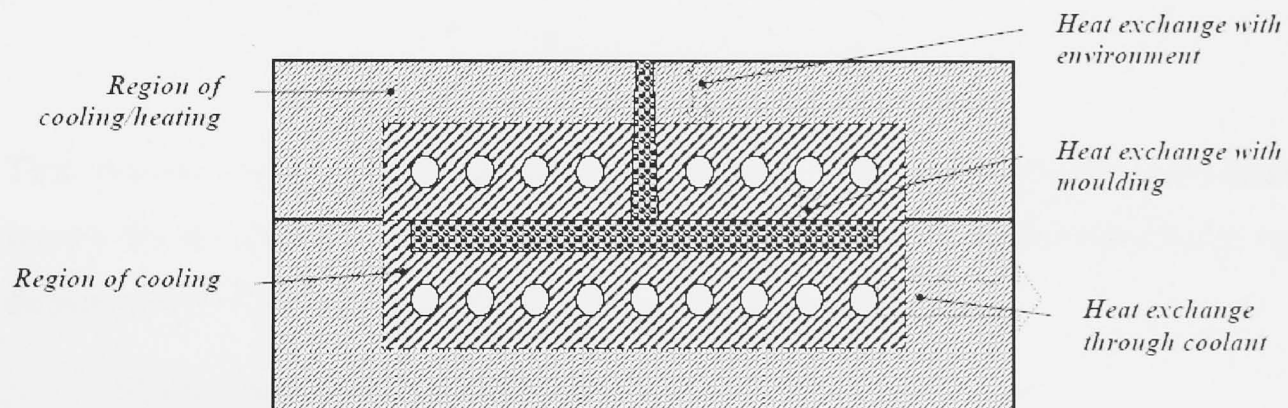


Figure 2-13. Heat Flow in an Injection Moulding [adopted from Menges, 2000]

Figure 2-13 shows that the mould material transfers the heat conductively from the plastic to the cooling lines, which then will be carried away by the coolant. As shown previously in Figure 2-4, the contact temperature between injected plastic and cavity wall is basically the maximum mould temperature  $T_{W_{MAX}}$  established during moulding cycle. This  $T_{W_{MAX}}$  according to Zollner is a function of the heat permeativity  $b$  of the mould and plastic material, which can be estimated by the following equation:

$$T_{WMAX} = \frac{b_W \cdot T_{WMIN} + b_M \cdot T_M}{b_W + b_M} \dots(2-16)$$

where,

$$b = \sqrt{\rho \cdot \lambda \cdot c} \dots(2-17)$$

- $T_{WE}$  = Mould ejected temperature  
 $T_{WMAX}$  = Mould temperature maximum  
 $T_{WMIN}$  = Mould temperature minimum  
 $b$  = Heat permeativity  
 $b_W$  = Heat permeativity of mould material  
 $b_M$  = Heat permeativity of plastic material  
 $\rho$  = density  
 $\lambda$  =thermal conductivity  
 $c$  =specific heat capacity

To sufficiently determine an accurate cooling time and necessary heat exchange capacity, the average of both maximum and minimum mould temperature  $\bar{T}_W$  in equation (2-18) can be used [Zollner, 1997].

$$\bar{T}_W = \frac{T_{WMAX} + T_{WMIN}}{2} \dots(2-18)$$

This average mould temperature will act as a heat sink for the plastic and a heat source for the mould. Therefore, the resulting heat quantity in the mould can be determined as follows [Menges, 2000]:

Heat quantity from the molten plastic:

$$\dot{Q}_M = \Delta h \cdot A_M \cdot s \cdot \rho \dots(2-19)$$

Hence, the heat quantity from the molten plastic into each mould half per cycle:

$$\dot{Q}_M = \frac{\Delta h \cdot A_M \cdot s \cdot \rho}{2 \cdot t_c} \dots(2-20)$$

where,

- $\dot{Q}_M$  = Heat quantity from molten plastic  
 $\Delta h$  = Enthalpy difference (Figure 2-14)  
 $A_M$  = Surface area of plastic part  
 $s$  = Wall thickness

$\rho$  = Density of plastic

$t_c$  = Cycle time

with,

$$t_c = t_C + t_n$$

$$t_C = C_C \cdot s^2$$

$$t_n = t_o + t_{cl} + t_e$$

$t_o$  = Opening time

$t_{cl}$  = Closing time

$t_e$  = Ejecting time

$C_C$  = Coefficient of thermal diffusivity = 2 to 3 (s/mm<sup>2</sup>)

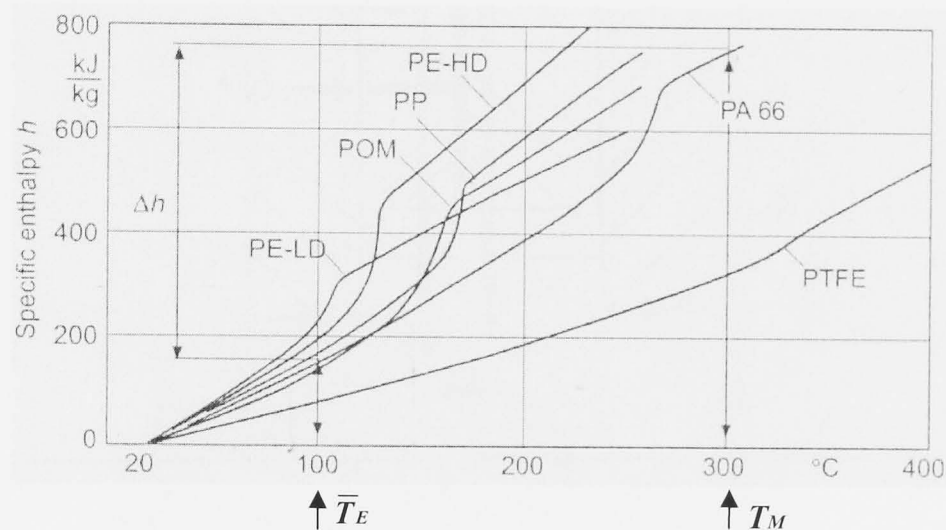


Figure 2-14. Specific Enthalpy [Zollner, 1997]

Heat density flow or specific heat flow  $\dot{q}$  from molten plastic is obtained by [Menges, 2000]:

$$\dot{q} = \frac{\Delta h \cdot s \cdot \rho}{t_c} \dots (2-21)$$

To a first estimation, the period of time during which no plastic is inside the cavity  $t_n$  can be ignored. By ignoring it, equation (2-21) can then be simplified as follows:

$$\dot{q} = \frac{\Delta h \cdot \rho}{C_C \cdot s} \dots (2-22)$$

Within the usual range of processing temperatures, the specific heat flow according to Menges depends only on the material and the wall thickness  $s$ .

- Step 3: Coolant Flow Rate

Therefore, the specific heat flow  $\dot{q}$  is the central parameter in determining coolant flow rate (see Figure 2-15). Multiplying  $\dot{q}$  by the corresponding surface



area of the plastic part  $A_M$  produces the amount of heat that needs to be removed by coolant during one moulding cycle. Therefore, the required coolant flow rate  $\dot{V}_C$  is determined by the temperature difference of coolant  $\Delta T_C$  [Menges, 2000]. It is recommended that  $\Delta T_C$  should not exceed 3 to 5 °C in order to ensure uniform cooling.

$$\dot{V}_C = \frac{\dot{q} \cdot A_M}{\rho_c \cdot c_c \cdot \Delta T_C} \dots(2-23)$$

where,

$\rho_c$  = Density of coolant

$c_c$  = Specific heat of coolant

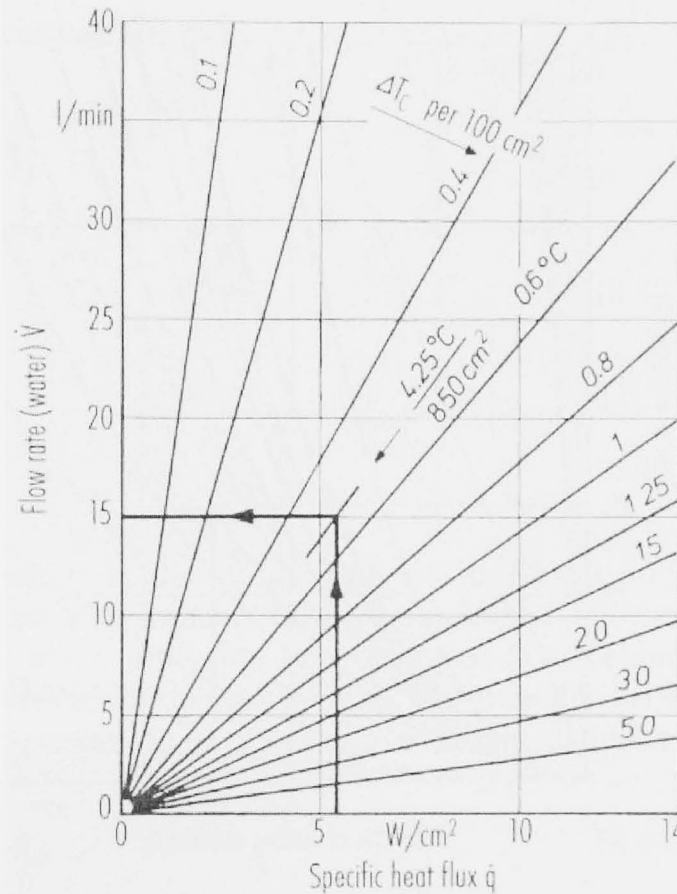


Figure 2-15. Flow-rate of Coolant (Water) [Menges, 2000]

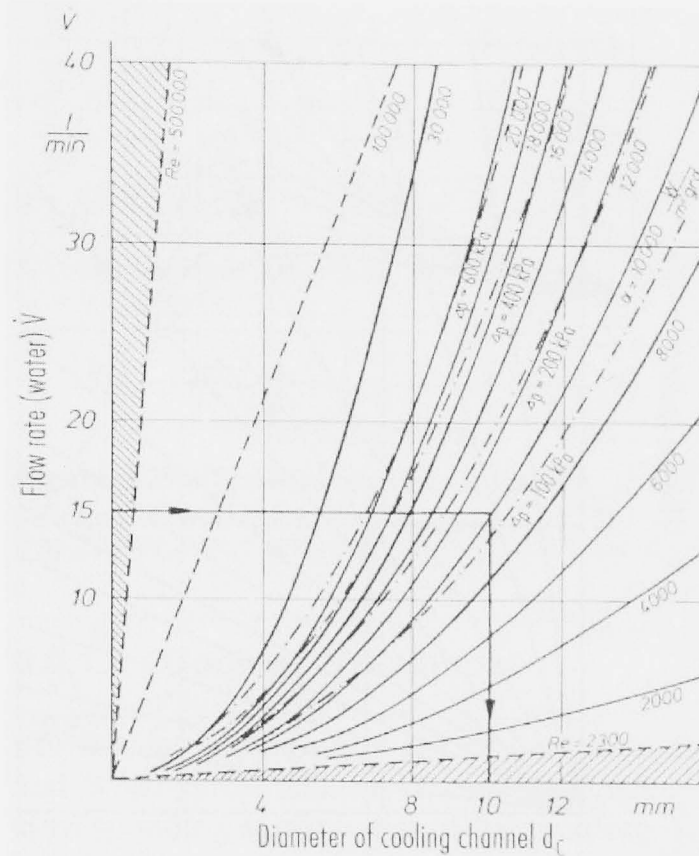
- Step 4: Cooling Channel Diameter

Adequate diameter of cooling channels ensures the necessary coolant flow rate. The following equation (2-24) and Figure 2-16 can be used to determine cooling channels diameter  $d_c$  and coefficient of heat transfer [Menges, 2000].

$$d_c = \sqrt[4]{\frac{\rho_c \cdot V_c^2 \cdot 16}{\Delta p \cdot 2 \cdot \pi^2 \cdot 3600} \cdot \left( f_c \cdot \frac{L_c}{d_c} + n_c \cdot K_c \right)} \dots(2-24)$$

where,

- $f_c$  = Friction factor in pipes  
 $L_c$  = Channels length  
 $d_c$  = Diameter of cooling channels  
 $n_c$  = Number of turns  
 $K_c$  = Resistance coefficient  
 $V_c$  = Coolant flow rate  
 $\Delta p$  = Pressure drop/loss



$$\alpha = \frac{k_c}{d_h} \cdot \{0.0235 \cdot [Re^{0.8} - 230] \cdot [1.8 \cdot Pr^{0.3} - 0.8]\} \cdot K_f \dots (2-26)$$

where,

$d_h$  = Hydraulic diameter

$k_c$  = Coolant thermal conductivity

$K_f$  = Correction factor

$$Re = \frac{4 \cdot \dot{V}}{\pi \cdot v \cdot d_h}$$

$$Pr = \frac{v \cdot \rho \cdot c_p}{k_c}$$

The equation for the heat transfer coefficient  $\alpha$  applies to the range of turbulent flow ( $Re > 2300$ ), which results in the maximum cooling diameter (2-27).

$$d_c < \frac{4 \cdot \dot{V}_c}{\pi \cdot 2300 \cdot v_c} \dots (2-27)$$

With the channel diameter determined, the coefficient of heat transfer  $\alpha$  can be calculated with the flow rate of the coolant for  $2300 < Re < 10^6$ ,  $0.7 < Pr < 500$ , and  $L_C \gg d_c$ :

$$\alpha = \left( 0.037 \left( \frac{\dot{V}_c \cdot 4 \cdot 1000}{d_c \cdot \pi \cdot v_c \cdot 60} \right)^{0.75} - 180 \right) \cdot Pr^{0.42} \cdot \frac{k_c}{a_c} \dots (2-28)$$

where,

$v_c$  = Kinematic viscosity of coolant

$d_c$  = Cooling channel diameter

$Pr$  = Prandtl number

$k_c$  = Coolant thermal conductivity

$a_c$  = Coolant thermal diffusivity

The dependency of the coefficient of heat transfer  $\alpha$  on flow rates (expressed in Figure 2-16 by  $\Delta p$ ), temperature and channel diameter is presented (coolant: water) in Figure 2-17.

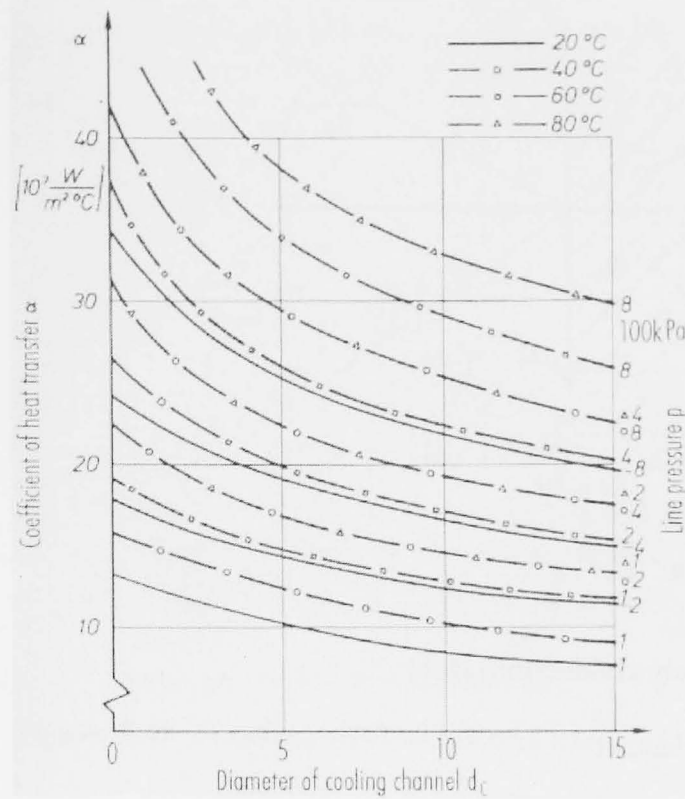


Figure 2-17. Coefficient of Heat Transfer (coolant: Water) [Menges, 2000]

- Step 5: Position of the Cooling Channels

The distance between two cooling channels inside a mould can be based on the relationship given in Figure 2-18. To determine the channel dimensions Figure 2-19 can be used [Menges, 2000].

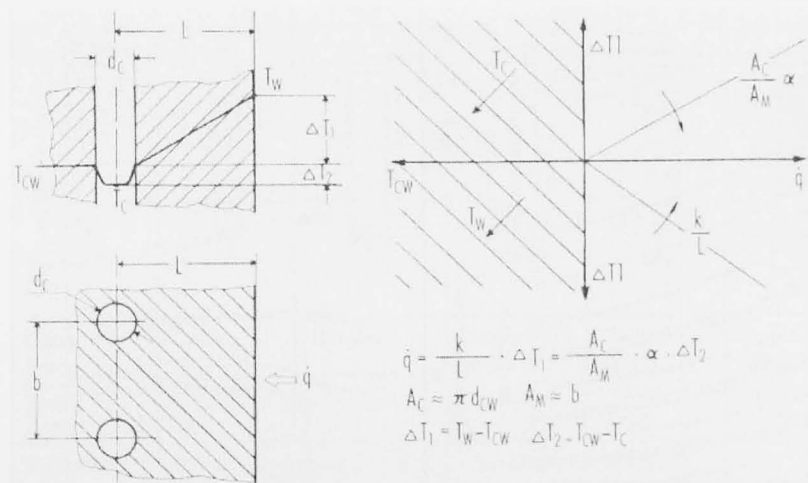


Figure 2-18. Thermal Reactions (Steady Conduction) [Menges, 2000]

where,

- $d_{cw}$  = Diameter of cooling channel
- $A_c$  = Surface of cooling channel
- $A_M$  = Surface of moulding (part)
- $k$  = Thermal conductivity of mold material

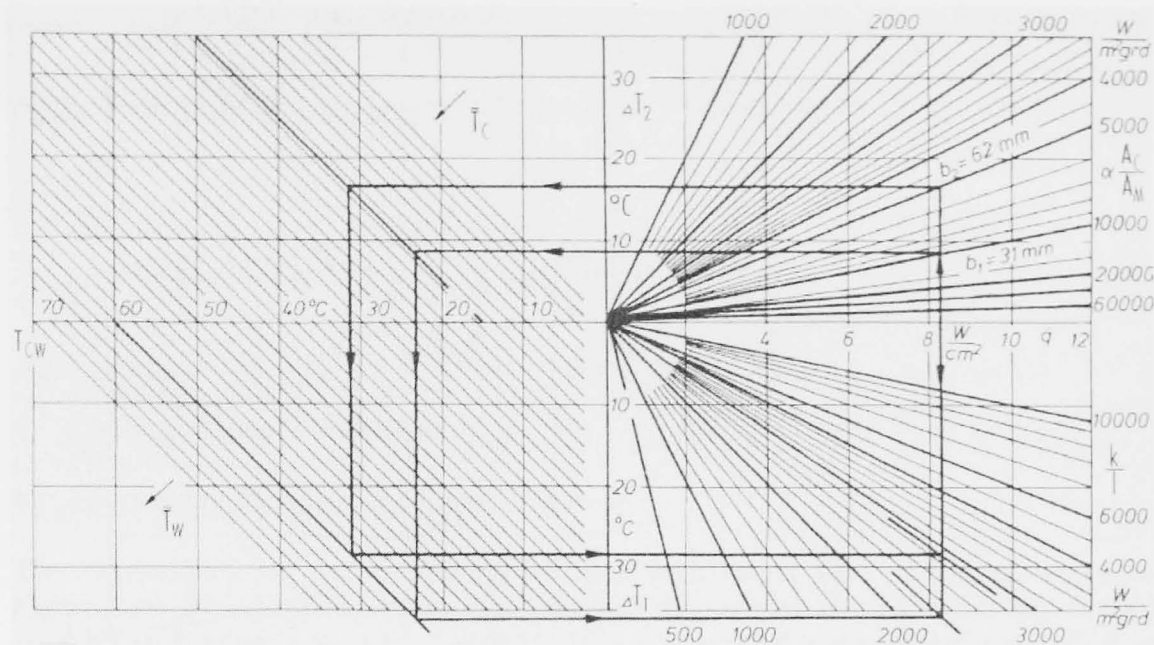


Figure 2-19. Computation of Heat-Transfer Data [Menges, 2000]

where,

$$\dot{q} = \frac{k_w}{L} \cdot \Delta T_1 \quad \dots(2-29)$$

$$\Delta T_1 = \bar{T}_W - T_{CW}$$

$\bar{T}_W$  = Average cavity wall temperature

$T_{CW}$  = Cooling channel wall temperature

The ratio  $A_C/A_M$  is presented with Figure 2-20 as a function of the distance of the channels between each other  $b$  and their diameters  $d_C$  [Menges, 2000].

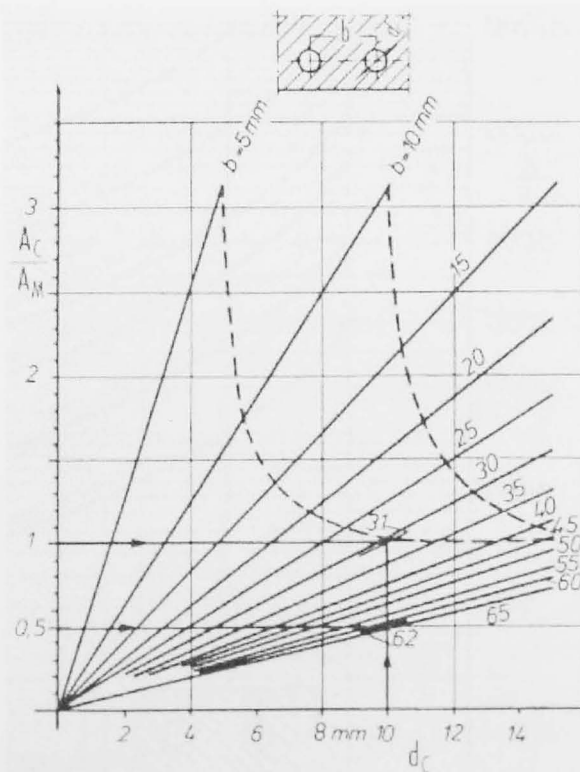


Figure 2-20. Cooling Channel Layout [Menges, 2000]

The same specific heat flow is transferred into the coolant through convection. This produces, depending on the coefficient of heat transfer, temperature difference  $\Delta T_2$ .

$$\dot{q} = \alpha \cdot \Delta T_2$$

$$\Delta T_2 = T_{CW} - T_C \quad \dots(2-30)$$

$T_C$  = Coolant temperature

The ratio between the areas of the cooling channels wall  $A_{CW}$  and the corresponding plastic part surface  $A_M$  affects the specific heat flow  $\dot{q}$  in the same way as  $\alpha$  the coefficient of heat transfer. Hence,

$$\dot{q} = \frac{A_{CW}}{A_M} \cdot \alpha \cdot \Delta T_2 \quad \dots(2-31)$$

The specific heat flow  $\dot{q}$  transferred by thermal conduction and convection must be equal, and temperature differences  $\Delta T_1$  and  $\Delta T_2$  have the temperature of the cooling channel wall  $T_{CW}$  as a common parameter. With the exception of the interdependent  $\dot{q}$  and  $\bar{T}_W$ , all other parameters can be subjectively varied so that a sufficient solution can be determined [Zollner, 1997].

There is a functional correlation between the cooling channels L and b in Figure 2-18, if the specific heat flow  $\dot{q}$  is constant. If the range validity of b is 2 to 5dc, Figure 2-21 shows that the distance L can be determined from the thermal conductance  $kM/l$  with the thermal conductivity of mould  $kM$  [Menges, 2000].

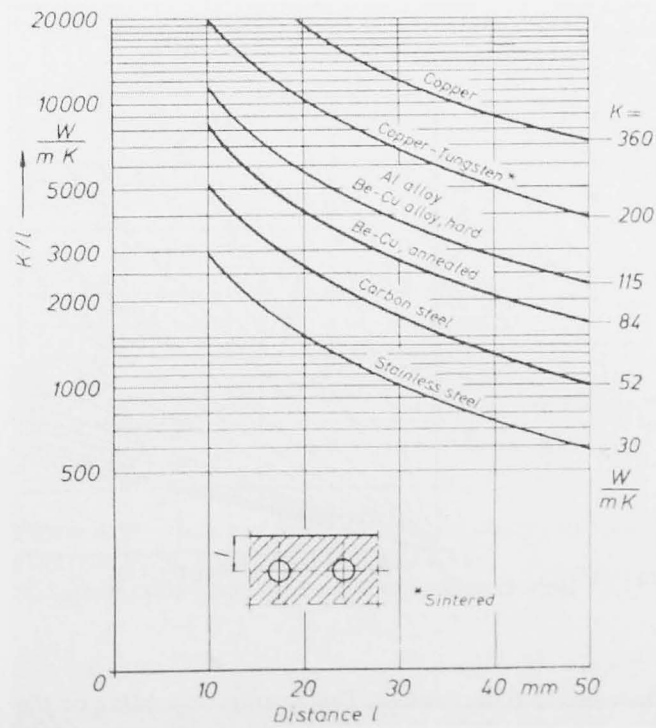


Figure 2-21. Distance between Cavity Wall and Cooling Channels

To provide uniform cooling during the moulding process, there are different combinations of  $l$  and  $b$  that can produce the same temperature difference: many cooling lines ( $< b$ ) require a large distance ( $> l$ ), and few cooling lines ( $> b$ ) require a small distance ( $< l$ ). These two distance parameters are equivalent in term of thermal efficiency. However, the uniformity of cooling is different and smaller in the second case. To provide uniform surface temperature at the plastic part, a relatively small cooling error  $j$  is recommended [Zollner, 1997]. This error  $j$  is defined by the heat flow differences, and can be used to measure the cooling uniformity (Figure 2-22 and Figure 2-23) [Menges, 2000].

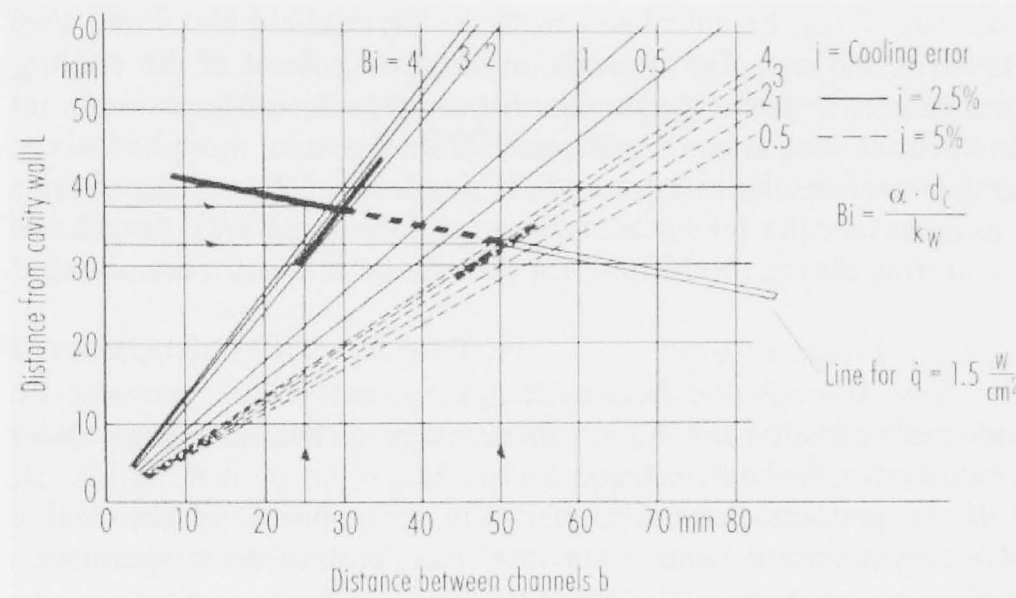


Figure 2-22. Feasible Cooling Layout [Menges, 2000]

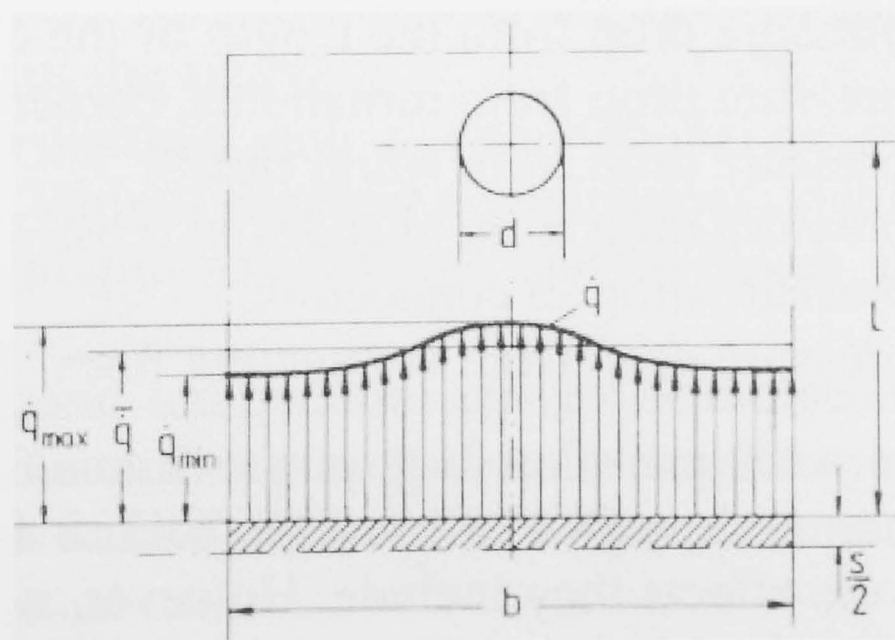


Figure 2-23. Distribution of Heat Flow [Menges, 2000]

$$j = 2.4 \cdot Bi^{0.22} \cdot \left(\frac{b}{l}\right)^{2.8 \cdot k} \dots (2-32)$$

$j$  = Cooling error (%)

$Bi$  = Biot number =  $\frac{\alpha \cdot d_c}{k_M}$

$k$  =  $|\ln(b/l)|$

To avoid inhomogeneous properties of the plastic part, it is recommended that the maximum cooling error  $j$  for crystalline plastic should be 2.5 – 5%, and 5 – 10% for amorphous plastic [Menges, 2000].

The distance  $b$  increases from the predetermined ratio of cooling channel to plastic part area ( $A_C/A_M$ ), which establishes the line of equal cooling efficiency. This line of equal cooling efficiency offers a number of cooling layout alternatives for avoiding other mould components such as bolts and ejector pins [Zollner, 1997].

- Step 6: Pressure Drop

In accordance with the heat flow, the temperature of coolant entering and leaving the mould changes.

$$\begin{aligned} \dot{Q}_C &= \dot{V} \cdot \rho \cdot c_p \cdot \Delta T \dots (2-33) \\ \Delta T &= T_{in} - T_{out} \end{aligned}$$

In practice, it is recommended that the average temperature difference  $\Delta T$  should not exceed a maximum of 3 to 5 °C to ensure a uniform heat exchange over the entire cooling channel [Zollner, 1997]. A required minimum flow rate  $\dot{V}$  can be calculated from the maximum permissible temperature difference. However, the flow rate also depends on the layout of the cooling elements. In a ‘series’ layout, the temperature difference applies to the total heat flow from all segments. Whilst, a ‘parallel’ layout applies temperature difference to each segment because this particular layout produces a lower flow rate and smaller pressure drop [Menges, 2000]. In the case that the pressure drop is higher than the cooling capacity, then the necessary flow rate and permissible temperature difference between coolant entering and leaving cannot be achieved, which consequently produces non-uniform cooling, and an in-homogeneous and distorted plastic part. The total pressure in the cooling channels may be dropped by the following conditions [Rees, 1995]:

- The length of cooling channels



- The resistances (corners, elbows, etc.)
- Spiral flow
- Connecting lines

From the total pressure drop and the heat flow to the coolant, equation (2 -34) can in practice be used to estimate the capacity of the cooling system:

$$P = \Delta p \cdot \dot{V} + |\dot{Q}_c| \dots (2-34)$$

where,

$P$  = Pumping capacity

$\Delta p$  = Pressure drop/loss

$\dot{V}$  = Volumetric flow

$\dot{Q}_c$  = Coolant heat efficiency

#### 2.1.3.2.5. 5th Stage: Ejection systems selection and layout

After the moulded part is cooled down and solidified, the next feature which has to be considered is the systems to remove or eject the part from the mould. Basically, it would be ideal if moulded parts could be freely removed from the mould by gravity. However, part design (i.e. undercuts), adhesion, and internal stresses, which retain the moulded part in place, are some of the common reasons why an ejection system is needed.

When considering the number, location, and type of the ejectors, it is important to know the release forces. Usually, these can be determined after the part design is established and the position of the part inside the mould is also known. The following are two kinds of release forces that can be considered [Menges, 2000]:

- Loosening forces: generated by the shrinking of parts onto the core, and thin ribs with little taper.
- Pushing forces: generated by too little taper of a core, and the friction between moulded plastic and the core.

Furthermore, Table 2-12 shows groups of parameters which affect the release forces in injection moulding [Rosato, 2000].

Table 2-12. Parameters for Release Forces

Mould	Part	Processes
<ul style="list-style-type: none"> <li>• Rigidity (design)</li> <li>• Cooling</li> <li>• Material: <ul style="list-style-type: none"> <li>+ Thermal Characteristics</li> <li>+ Surface finish (frictions)</li> </ul> </li> </ul>	<ul style="list-style-type: none"> <li>• Geometry (i.e. wall thickness, cross section, undercuts)</li> <li>• Projected area</li> <li>• Material: <ul style="list-style-type: none"> <li>+ Friction</li> <li>+ Modulus of elasticity</li> <li>+ Thermal characteristics</li> <li>+ Shrinkage</li> </ul> </li> </ul>	<ul style="list-style-type: none"> <li>• Build up pressure</li> <li>• Moulding temperature</li> <li>• Melt temperature</li> <li>• Time of ejection</li> <li>• Contact temperature</li> <li>• Ejection rate</li> </ul>

Generally, the ejection system is a mechanism that is actuated mechanically by utilizing the mould opening stroke or movement of the injection moulding machine, which causes the ejection system to be moved toward the parting line to eject the moulded part. In most cases, the moulded part shrinks onto a core in the moving half of the mould. This is the reason why most of the ejection systems are constructed and arranged inside the moving half [Menges, 2000 and Bryce, 1998].

The moulded part is normally ejected using a set of ejector pins. In constructing the ejector pins, it is required to consider length, location, and diameter. To keep the pins from penetrating the moulded part during ejection, its diameter should be as large as possible so that the ejection pressure is distributed over a large area. A large pin diameter also minimizes distortion of the part during the ejection process [Bryce, 1998].

Ejector pins [Figure 2-24] are usually assembled together with ejector bar (plate), retainer, and return pins (mechanism). This entire assembly is then located inside an ejector housing, which is mounted on the moving half. In most cases, the ejector system is equipped with return pins and sprue puller. The function of the return pins is basically to bring the ejector system back to its original position in preparation for the next cycle. In constructing the ejector pins, determining appropriate length is crucial. The pins are expected to perfectly align with the cavity bottom surface to prevent significant marks on the moulded part [Bryce, 1998 and Menges, 2000].

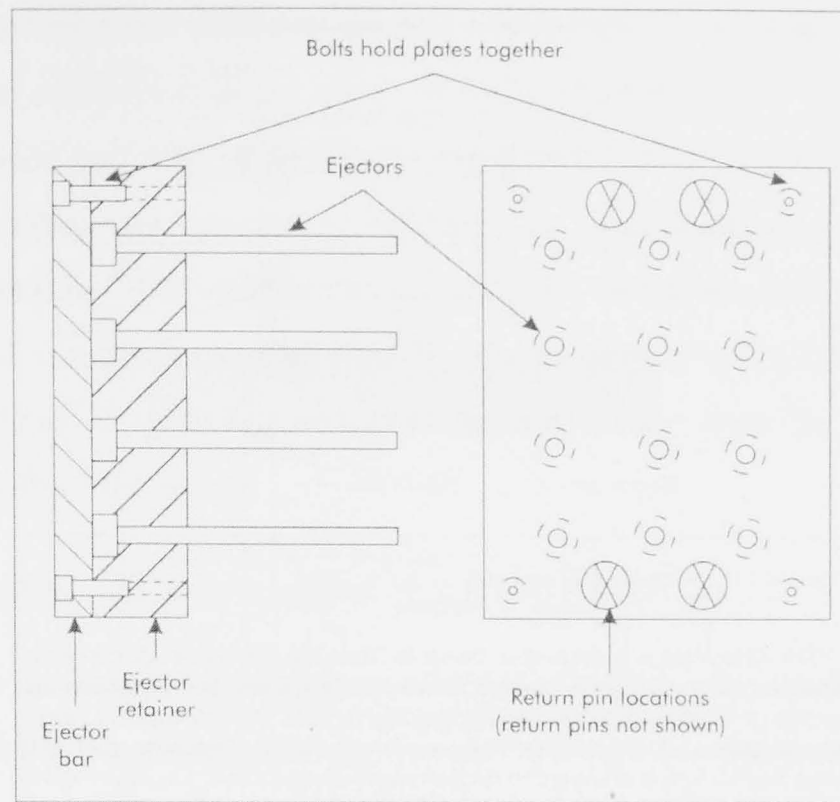


Figure 2-24. Typical Pin Ejection System [Bryce, 1998]

There are situations where standard ejector pins cannot be used as the pin diameter would be too small, or there is limited (or no) space to locate the pins. In these situation, stripper ejector systems can be considered. Figure 2-25 shows two types of the stripper systems: (a) plate and (b) sleeve.

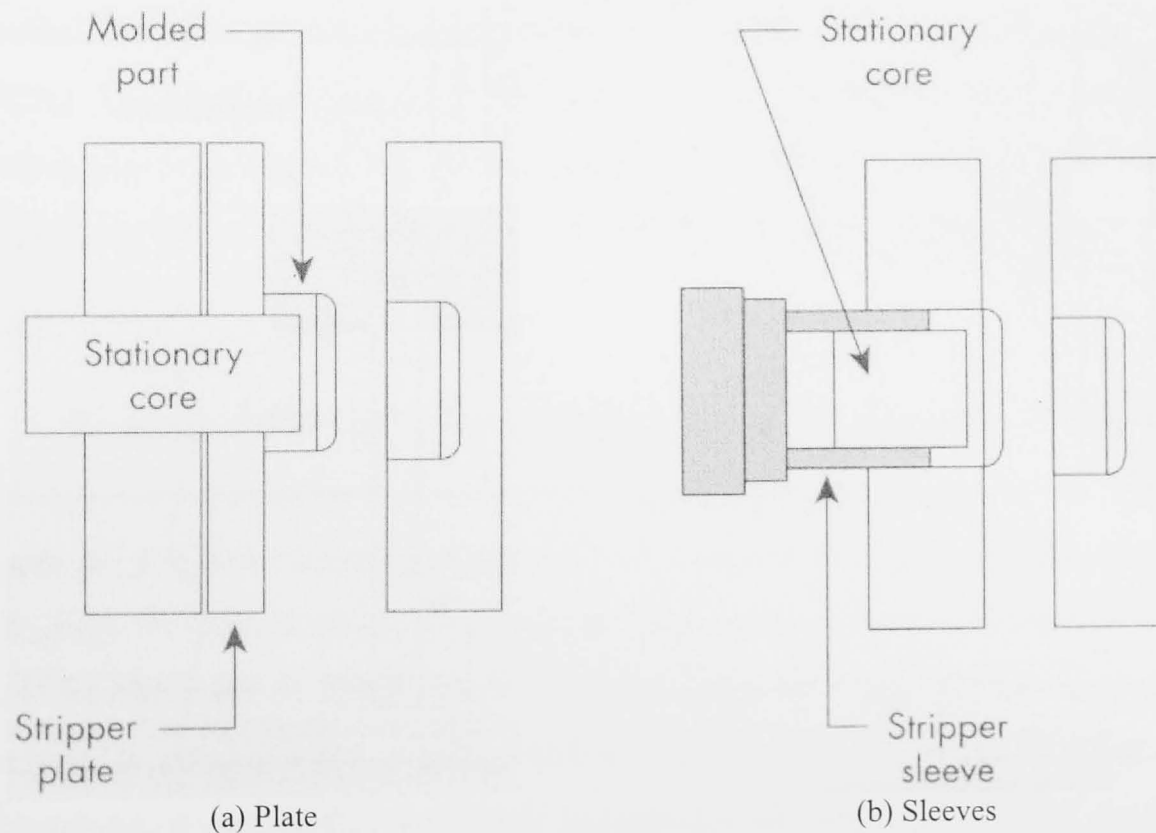


Figure 2-25. Type of the Stripper Ejector System

While ejector pins and stripper ejection are two most commonly used systems for removing a moulded part from the mould, other ejection systems such as

split cavity concept, three-plate system, and compressed air ejection may be required if the two most common systems cannot be used. The split cavity is commonly used for deep moulded part with or without external undercuts or sidewall openings. The three-plate systems are commonly equipped in three-plate mould which allow automatic separating of the part from runner system during the ejection process. The compressed air ejection is usually used to remove deep-draw parts or parts that by design are difficult to push. The air forces the plastic away from the core and allows it to fall freely from the mould.

#### 2.1.3.2.6. 6th Stage: Alignment system design and layout

As all the mould components assembled, the next consideration is a precise alignment among the components as well as between the mould and the injection moulding machine. The mould needs to be guided in such a way so that both cavity and core inserts are accurately aligned and both mould halves are closed tightly. A common method used to align mould halves is standard shouldered leader pins and corresponding bushings. The core and cavity must also be aligned properly and locked in place in order to locate accurately during injection process. To ensure proper fit and sealing of the nozzle to the mould, the alignment of mould to the injection machine is accomplished primarily through a locating ring and sprue bushing. The structural integrity of the plates and tie bars as well as the parallelism between plates provides an alignment mechanism to ensure proper mould location and position during the moulding process [Menges, 2000 and Bryce, 1998]

#### 2.1.3.2.7. 7th Stage: Mould mounting

As mentioned above, the moulds are mounted and clamped to the machined plate and connected to power and water supply lines. Depending on the size and weight of the mould and the number of connections, placing and mounting (changing) the mould leads to shutdown times (typical values shown in Figure 2-26). In the case of small batch size and frequent changes, this down times considerably affect the productivity and the cost. To place and mount the mould into the machine, it is therefore necessary to consider equipping the mould with such components or features that can quickly: detach and fasten the mould at the machine plate; disconnect and connect the supply lines, and bring the mould into the clamping unit or take it out [Menges, 2000].

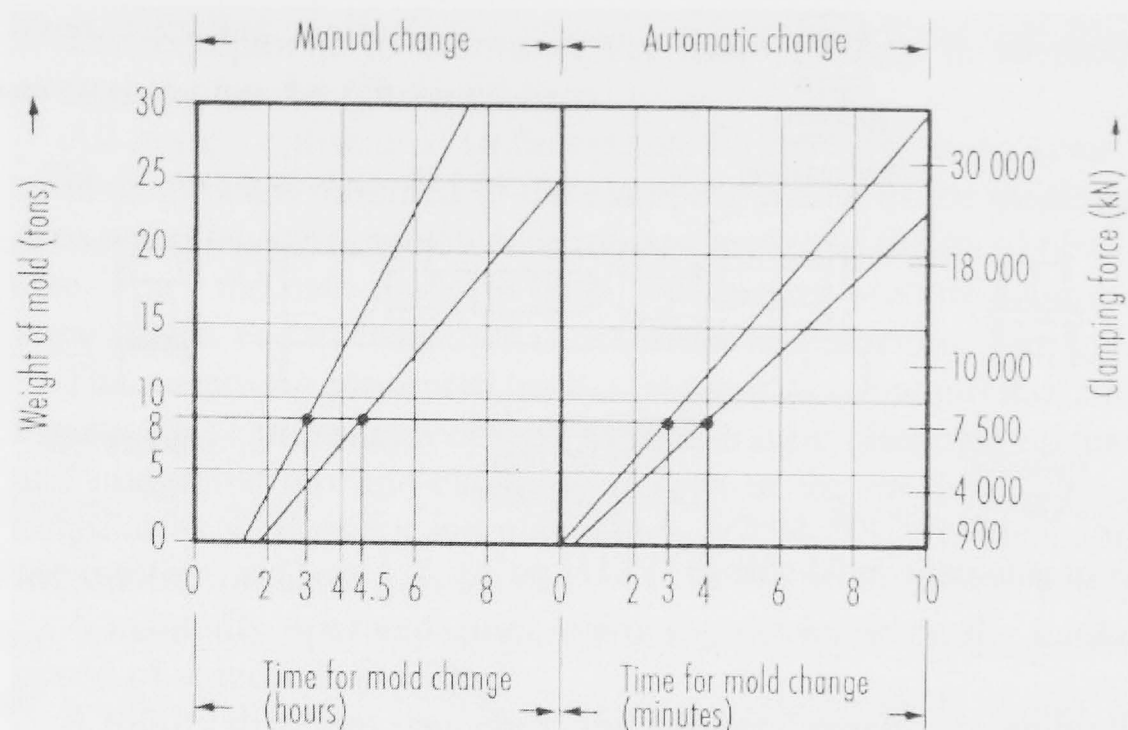


Figure 2-26. Down-Time for Mould Changes in Injection Moulding Machines [Menges, 2000]

### 2.1.3.3. Mould Manufacturing Procedures

There are many ways to develop a complete mould. Some mould components are standard and available to purchase in either a finished or semi-finished state. But the main mould components (cavity and core inserts) are manufactured according to a particular part design. To manufacture cavity and core inserts, the standard methods widely employed includes milling, surface grinding, cylindrical grinding, turning, and drilling. Moreover, advanced manufacturing technologies such as high-speed machining (HSM) and electrical discharged machining (EDM) have also been used in order to produce accurate and precise inserts [Rees, 1995, Menges, 2000 and Bryce, 1998].

In conventional procedures for manufacturing the cavity and core inserts, the primary stage of the constituent activities is to make the inserts the approximate size and then to square and size the inserts. If hardened material is assigned for the inserts, this activity is carried out while the material is in soft or annealed stage. Although in this primarily stage it appears that not much progress in being made on the inserts, squaring and sizing the inserts is one of the most important activities in mould manufacture. Therefore, the utilization of available standard oversized blocks is considered to save the time. The next important activity is to construct the cooling channels inside the inserts. Drilling is normally used for this operation. In general, the construction of the cooling channels is to have only one inlet and one outlet in

each insert. Therefore, the remaining channels is then blocked using brass or steel plugs to direct coolant flow [Rosato, 2000].

The following discuss the predominant group of manufacturing technologies that commonly employed in developing the cavity and core inserts.

#### 2.1.3.3.1. Casting

Developing mould inserts by casting has certain advantages in some applications. The reasons are that the casting process offers suitable materials for more applications, no limit concerning geometry, and no extensive machining is required. Another important advantage of this process is that cooling channels can be cast internally in some materials. Sand casting and precision casting are two predominant methods employed in manufacturing the mould inserts. The selection of the methods basically depends on the dimensions, tolerances, and surface quality [Rosato, 2000 and Menges, 2000].

Precision casting is employed for developing high reproducibility mould inserts. The techniques are suitable for fine contours and high surface quality. A number of different types of this casting method are available that each of them is vary in the sequence of processes, the moulding material, and the binder employed. This method requires a negative pattern that already contains the shrinkage allowance and forms the basis for producing a ceramic casting mould. After the mould has been produced, it is baked for several hours. Post-treatment of precision cast parts is generally limited to the mounting and matting surfaces, as well as all regions that comprise the mould parting surface.

#### 2.1.3.3.2. Hobbing

Hobbing is employed for manufacturing accurate hollow moulds. There are two type of this method available: cold and hot hobbing. Described below is the cold hobbing method which is more common.

Cold hobbing is a method for manufacturing mould inserts without removing material. In this method, a hardened and polished hob, which forms a negative pattern, is forced into blank mould inserts. The method is limited by the maximum permissible pressure on the hob and the yield strength of the inserts. During the process, the rim of the blank is pulled in, which is then to be machined off

afterwards and considered in order to determine the hobbing depth required. Figure 2-27.a shows the relationship among hob travel, usable depth and indentation. And, Figure 2-27.b show an example of hobbing mould inserts.

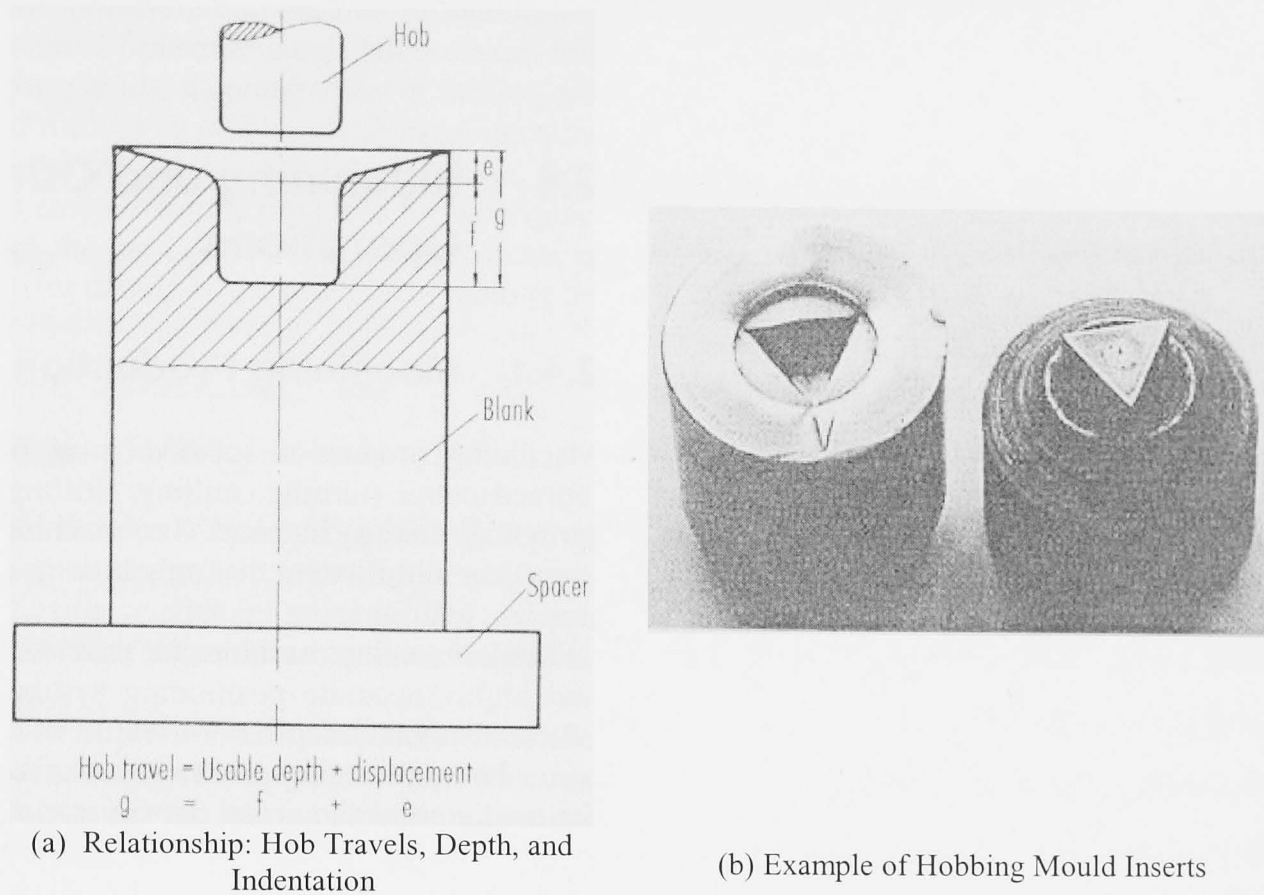


Figure 2-27. Hobbing Mould Inserts [Menges, 2000]

For hobbing, the surface quality of both hob and blank is very important in order to provide the smoothness of the material flow, and prevent sticking and welding. For this reason, lubrication is used. Besides the surface quality of hob and blank, the dimensions of the blank are also important to get the desired flow of material. It is recommended that the original height of the blank should not be less than 1.5 to 2.5 times the diameter of the hob. The diameter of the blank, which corresponds to the size of the opening in the cavity retainer plate, should be double the diameter of the hob [Menges, 2000].

Cold hobbing, which is generally used for low cavities with less height, offers several advantages. The positive pattern of the hob can be manufacture more economically compared to a negative pattern. With the same hob, several mould inserts can be manufacture repeatedly in a short time. Moreover, a better surface quality and durability of the mould inserts can be obtained because there is no cutting material involved in this hobbing process. However, mechanical properties of the hob and blank and the size of the cavity are limitation that need to be considering in employing the method.

#### 2.1.3.3.3. Machining Operations

Machining operations can be divided into three groups which are classified according to their method of operations, and they are discussed below.

##### 2.1.3.3.3.1. Milling

Milling has long been used as a method of generating inserts, and modern machines are well equipped for the task. They are equipped with multi-axial computer numerical control (CNC) and highly accurate positioning systems which improve the accuracy and the efficiency of the process. Heat-treated inserts are able to be machined to final strength by this type of machine [Urbanski, 2000 and Coremant, 2004]. High Speed Machining (HSM) is characterized by high cutting speed and high spindle speeds (up to 20,000 rpm), and a low depth of cut and its technical capability to machine materials with hardness values of up to 62 HRC. With these capabilities, HSM in some cases is able to shorten a manufacturing lead-time in producing the inserts. In addition, good surface quality can be achieved by HSM, which allows for significant time reduction in manual post-processing. In the production of injection moulds, a combination of milling and spark-erosive machining (described below) is often performed, especially for complex geometry, small internal radii and deep grooves/cavities. Furthermore, a crucial advantage of involving spark-erosive machining in producing the injection mould inserts is that materials of any hardness can be processed. For this, it is advisable that the amount of milling should be maximized on account of higher metal removal capabilities [Fallboumer, 1996, Urbanski, 2000 and Jenga, 2001].

##### 2.1.3.3.3.2. Electric-Discharge Machining Processes

EDM is a process which employs successive electric discharge in a dielectric fluid as a principle of material removal [Manufacturing Advisor Services (MAS), 2004]. An electrode is required in this procedure as a tool to produce the desired geometry. With consecutive impulses, a small amount of mould and electrode material is heated up to the melting temperature and blasted from the working area by electrical and mechanical forces. Through the use of appropriate process parameters, greater amount of material removal at the mould can be obtained than at the electrode. The removal process basically generates craters on both electrode and



mould. The size of the craters depends on the spark energy. Generally, high impulse energy is employed for roughing. The debris is flushed out of the spark gap and deposited in the container [Charmilles, 2004]. Figure 2-28 illustrates the underlying principle of EDM.

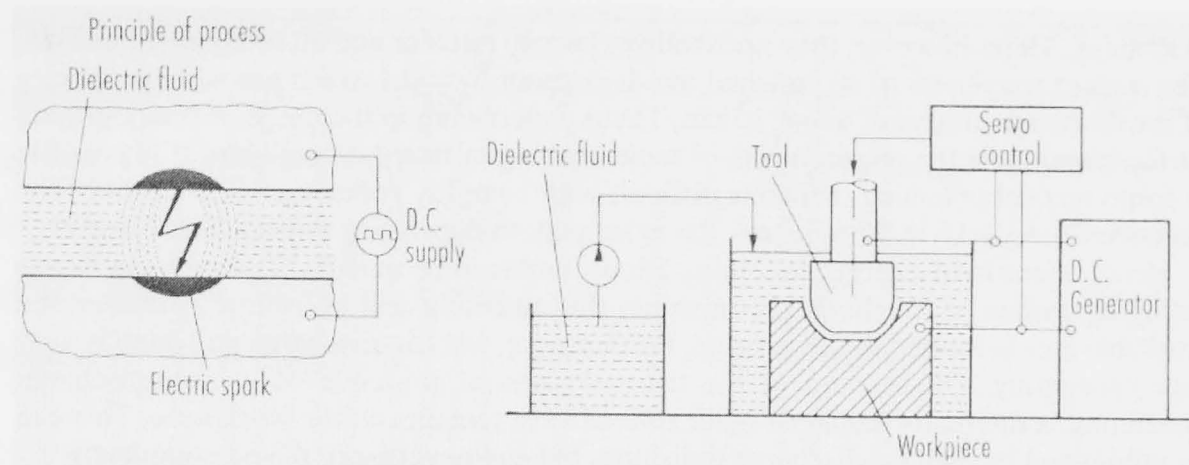


Figure 2-28. Basic Principle of EDM [Menges, 2000]

In vertical eroding, the configuration is dimensionally determined by the shape and dimensions of the electrode, and the machining of undercuts is not feasible. The introduction of planetary EDM has now extended the possibilities of the erosion techniques. Planetary EDM is also known as the 3D or multi-space EDM features a combination of three relative motions between work-piece and electrode: vertical, eccentric and orbital (Figure 2-29). It is able to form undercuts in a cavity. It is possible to completely machine a mould with only one electrode through compensation of the undersized electrode [Menges, 2000].

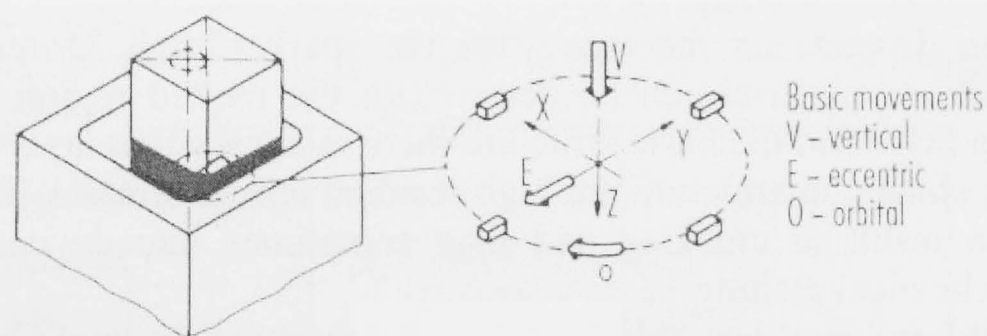


Figure 2-29. Basic Movements during Planetary Erosion [Menges, 2000]

Basically, all good electrical conductor and thermal conductivity materials can be employed as electrodes. A high melting point of these materials is required to prevent rapid wear of the electrodes, for example graphite and copper electrodes for steel and tungsten-copper electrodes for hard metals. In general, the electrodes are made by turning, milling or grinding, depending on the configuration, required accuracy and material used.

In spark erosion, the structure of the surface is changed by heat. The high spark temperature melts the cavity surface and decomposes simultaneously the high molecular hydrocarbons of the dielectric fluid into their components. The released carbon diffuses into the steel surface and produces very hard layers with carbide-forming elements. The thickness depends on the energy of the spark. A concentration of the electrode material can be detected in the melted region. Between the hardened top layer and the basic structure there is a transition layer. The consequences of this change in structure are high residual tensile stresses in the surface that can result in cracking and may sometimes impede necessary post-treatment [Charmilles, 2004].

#### 2.1.3.3.3. Surface Treatment (Finishing)

To achieve the final quality of the plastic part the condition of the mould cavity surfaces is crucial. This has a significant effect on the time and costs required for manufacturing the mould. Mirror-finish quality generally requires the greatest amount of polishing and facilitates ejection. In contrast, release properties (i.e. draft angle) in untreated cavity surfaces are the criterion governing the condition of featured cavity surfaces.

After the mould cavity has been machined, the surfaces have to be smoothed by grinding and polishing. To date, this operation is still mainly done manually. Coarse grinding produces a surface with a roughness of  $Ra < 1 \mu\text{m}$ , which can then be finished by a precision-grinding step or by polishing. Careful work and observance of some basic rules can yield a better surface quality after polishing. A disadvantage of manual finishing processes is that they are personnel intensive and do not guarantee reproducibility. Machine-assisted removals such as grinding, honing, and lapping have nonetheless been unable to provide a better process, and they have major technological restrictions in the case of complex 3D contours. Some of the fully automatic polishing processes presented below also exhibited considerable shortcomings so that they almost exclusively combined with manual polishing [Menges, 2000]:

- *Vibratory (slide) Grinding*: an alternative to the conventional rotary barrel process. Its disadvantage is recognized as abrasion of protruding edges.
- *Sand Blasting*: the most known and common procedures. The blasting

medium is a water-air mixture containing fine glass beads. The surface quality attained is not comparable to manual surfaces treatment. The procedure is suitable only for flat parts. Disadvantages are non-reproducible removal and relatively low dimensional stability.

- *Pressure Lapping*: a variant of sand blasting and also known as ‘extrude-honing’. It is limited to the opening treatments, especially for polishing profile-extrusion tools with lower cross section. The procedure uses a polishing compound that contains silicon carbide, boron carbide or diamond grits. The advantages of this procedure are less time required to set up and achieve average roughness (Ra) of 0.05  $\mu\text{m}$ .
- *Electrochemical Polishing*: the procedure is based on anodic metal machining, and works without contact which provides no mechanical loading. The advantages of this procedure are that high dimensional and moulding accuracies as well as a better surface properties can be achieved. However, defects like inclusions and pores in the material are exposed. Therefore, high purity material is recommended when employing this procedures.
- *Electric Discharge Polishing*: it is an extension of electric discharge machining and follows erosive fine finishing procedure. Therefore, erosion and polishing are done on the same machine. However, a low material removal rate results in a time consuming procedure.

## 2.2. Layer Manufacturing (LM) Technology

Layer Manufacturing (LM) is a set of advanced manufacturing technologies that have revolutionised product development and realisation since its first commercial introduction in the late 1980s [Jacobs, 2000, and Kulkarni, 2000]. LM is also referred to as Solid freeform fabrication (SFF) processes that have an ability to physically model freeform or complex-geometry parts taken directly from 3D CAD solid models without the use of tooling [Kruth, 1998 and Dalgarno, 2003]. Some of the common advantages of the LM include: (a) reduction in design phase cycle time and cost; (b) reduction in the potential for expensive design errors; (c) reduction in tooling costs on short-run parts; (d) reduction in time to production and market [Kochan, 1999 and Palm, 2004]. The following sections outline basic process, system development, and application of the LM technologies

### 2.2.1. Basic Process

A wide range of LM technologies have been developed, and every LM technology uses different methods and materials to produce a final part. Although the processes vary substantially, the same three common steps as illustrated in Figure 2-30 are always employed [Pham, 2001]. The first step starts with generating a 3D CAD solid model of the desired part as required input data. Within the CAD environment, a drawing format of the 3D CAD solid model is then converted into a stereolithography (STL) file format. Basically, the STL file format defines the part as a grouping of triangular facets, which describe the surfaces of the parts [Sherman, 2004]. This STL file format is then transferred electronically to the LM system

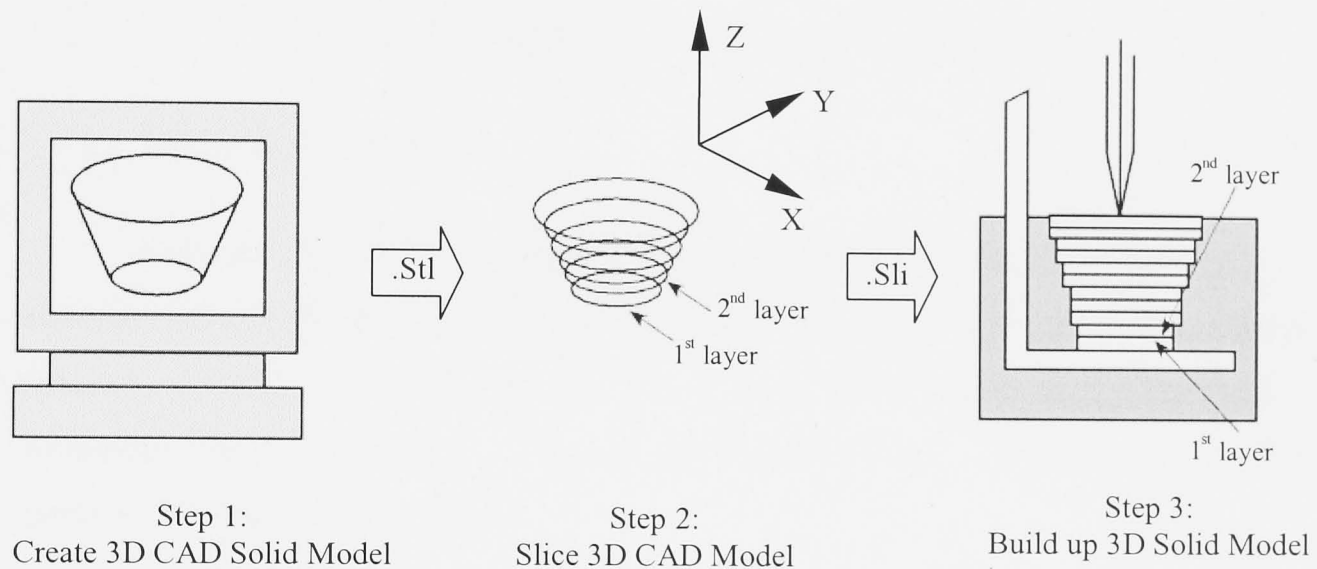


Figure 2-30. Basic Process of LM [Oki Electric, 1997]

In the second step, the LM system then reviews the STL format 3D model for various design criteria (part building requirements) and then sends it to the modelling system for slicing the STL 3D model into a stack of 2D cross-sectional layers in the Z direction. Thus, the third (final) step involves the actual development of the physical 3D solid parts. Based on the sliced layer, a laser or machine head traces and scans the profile of the part in the X and Y direction on a build platform to form the first layer. The build platform lowers in the Z direction one layer thickness and the next part layer is traced. Layers are added successively to build up the part from the bottom [Pham, 2004 and Oki Electric, 1997]. As the 3D solid part developed, it is then removed from the machine for any required post-processing.

### 2.2.2. Development of LM Systems

LM systems can be classified in a variety of ways. One classification scheme (Figure 2-31) developed by Kruth et. al. is defined based on the raw material used [Kruth, 1998 and Pham, 2001]. Based on this classification, the following review major commercial LM systems in terms of hardware, process and performance.

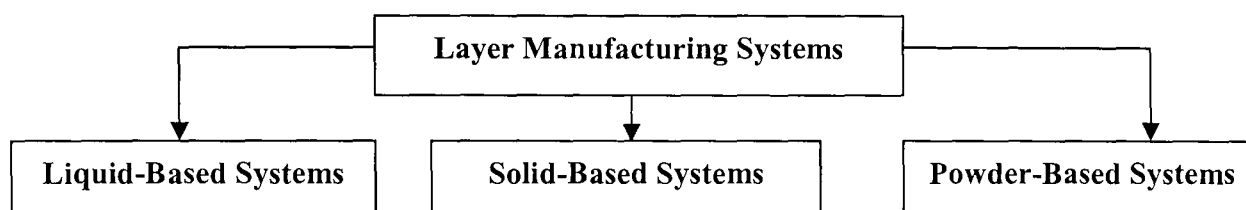


Figure 2-31. Classification of LM Systems [Kruth, 1998]

#### 2.2.2.1. Liquid-Based Systems

Basically, the building principle of liquid-based systems is to convert raw material (photosensitive polymer) in liquid-state into solid state through a curing process. A most common system in this classification is Stereolithography Apparatus (SLA), the pioneer of the LM system which was commercialised by 3D systems in 1988 [Wohler, 2002].

Stereolithography Apparatus (SLA) is a method of building a 3D solid part based from a photo-curable liquid resin (Figure 2-32). The surface layer of resin (min. 0.025mm) is cured selectively by ultraviolet (UV) laser beam according to the predefined path in the slicing model. Once one layer is complete, a new layer of liquid resin is flooded over it and the process repeated to build a complete part [Rosochowski, 2000].

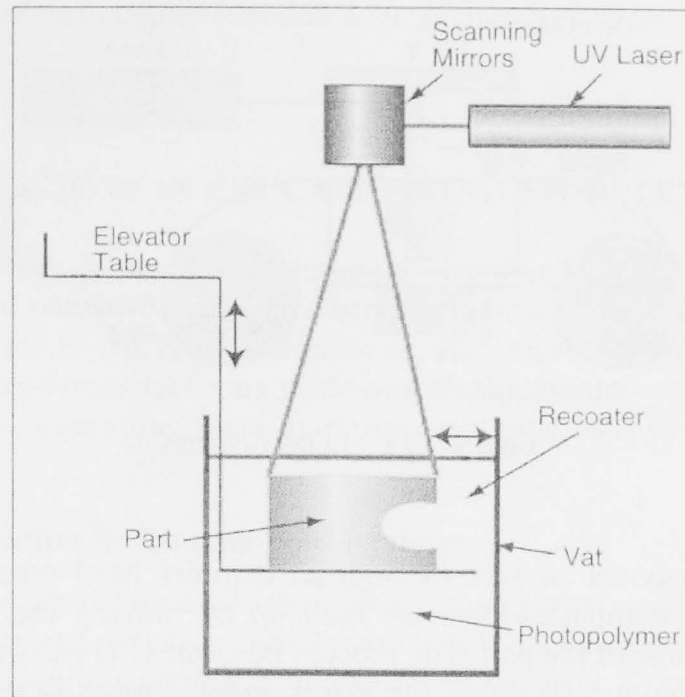


Figure 2-32. Stereolithography Apparatus (SLA) [Noorani, 2006]

#### 2.2.2.2. Solid-Based Systems

In this classification, the basic principle is that a 3D solid part is developed from solid raw (non-powder) material in various forms, including wire, roll, laminate or pallet. The most predominant LM systems in this classification are Fused Deposition Modelling (FDM), Laminated Object Modelling (LOM), and Multi-Jet Modelling (MJM) Systems

##### 2.2.2.2.1. Fused Deposition Modelling (FDM)

Fused Deposition Modelling (FDM) from Stratasys develops a 3D solid part by extruding a thin stream of plastic paste from a heated extrusion head (Figure 2-33). The plastic paste is laid across the X-Y plane to form a determined 2D layer. To build each layer, the extrusion head deposits the outline of the layer first and then fills each layer according to the raster dimension set-up (Figure 2-34). As each layer is built up, it fuses to previous one, developing a 3D solid part. Thermoplastic (ABS) is the common plastic material used [Pham, 2001].

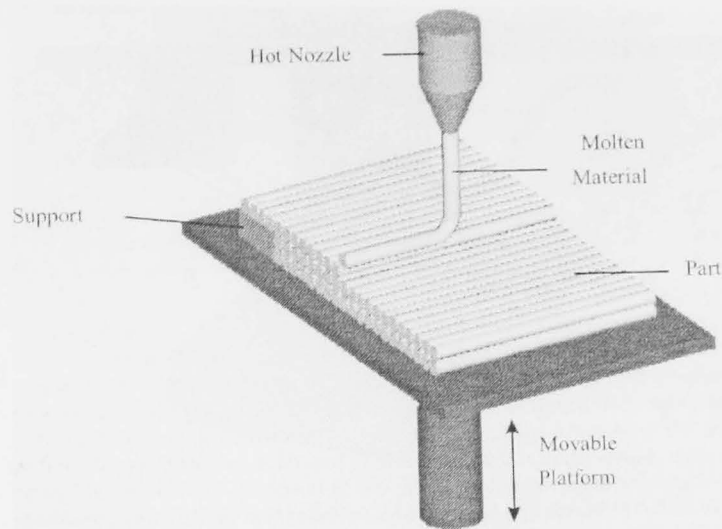


Figure 2-33. Fused Deposition Modelling [Pham, 2001]

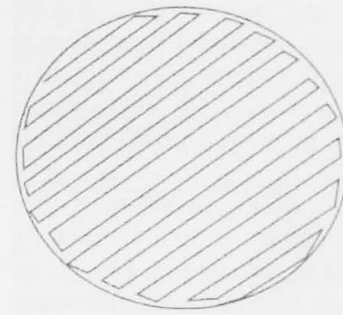


Figure 2-34. Countour and Raster [Bryce, 1998]

#### 2.2.2.2.2. Laminated Object Modelling (LOM)

Laminated Object Modelling (LOM) from Helix develops a 3D solid part by stacking layers of paper cutting with a laser (Figure 2-35). The material is fed in sheet form. The cross sections cut from the sheets are then bonded into a solid block form using a thermal adhesive coating. The automatic process continues until all the cross sections of the desired part are developed. The excess material is then removed by hand [Rosochowski, 2000].

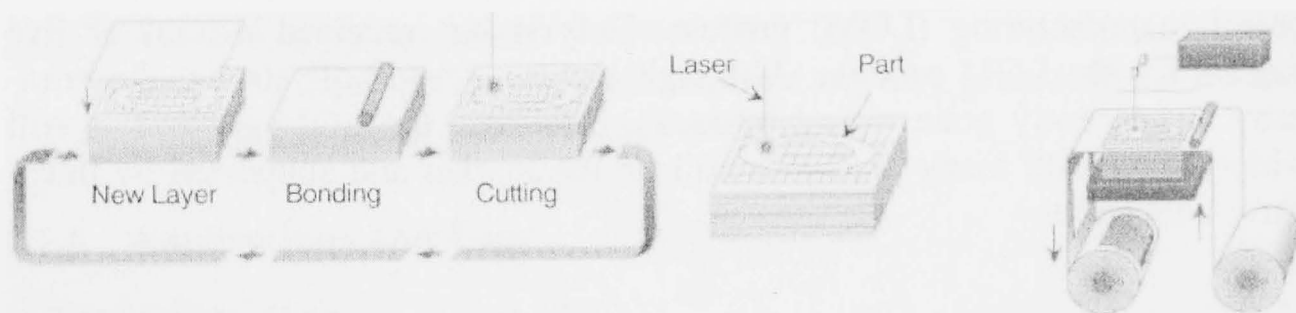


Figure 2-35. Laminated Object Modelling [Pham, 2001]

#### 2.2.2.2.3. Multi-Jet Modelling (MJM) Systems

The principle underlying the MJM system is similar to that employed in an ink-jet printer, but applied in three dimensions (Figure 2-36). The process starts by spraying tiny droplets of thermopolymer materials onto through a print head of linear array jets/spray nozzels. The print head movement is similar to a line printer, building 3D solid parts layer by layer. The parts is build on a movable platform that lowers after each layer is build [Pham, 2001].

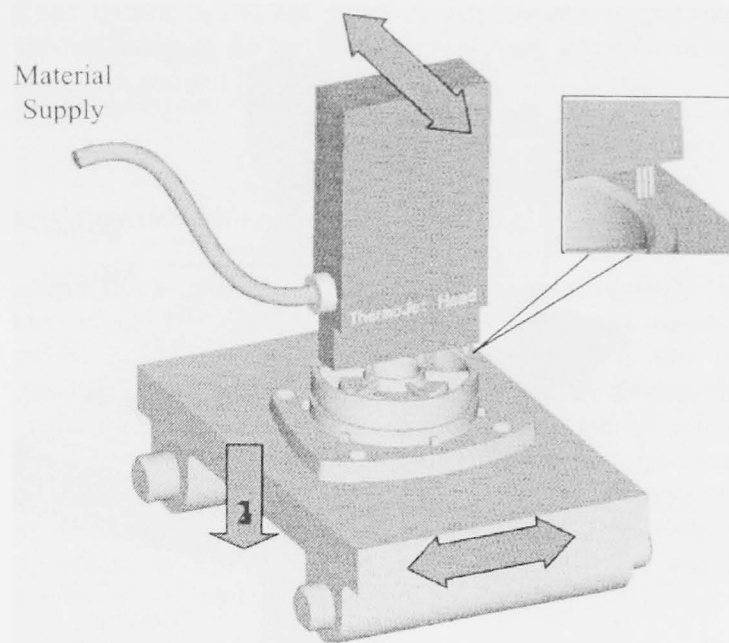


Figure 2-36. Multi-Jet Modelling [Pham, 2001]

### 2.2.2.3. Powder-Based Systems

While powder can be considered solid, a special classification for powder-based LM system is intentionally created. A wider variety of material such as polymers, metals and ceramics is available on current LM systems in this classification [Rosochowski, 2000 and Kruth, 2005]. Selective Laser Sintering (SLS), and Three Dimensional Printing (3DP) are the most predominant systems among them in this classification.

#### 2.2.2.3.1. Selective Laser Sintering (SLS)

Selective Laser Sintering (SLS) develops a 3D solid part based on laser fusing or sintering a layer of powdered raw material. First, a thin layer of powder is spread and deposited over the build platform. The powder is transferred from the powder feed container to the build cylinder (platform) through a counter rolling cylinder. The laser beam then selectively sinters the powder to a point of fusion/melting. As the process is repeated, layers of powder are deposited and sintered until the object is complete. Figure 2-37 shows a schematic process of the SLS. Un-sintered powder remains loose and utilizes as natural support for the next powder layer and object under fabrication.



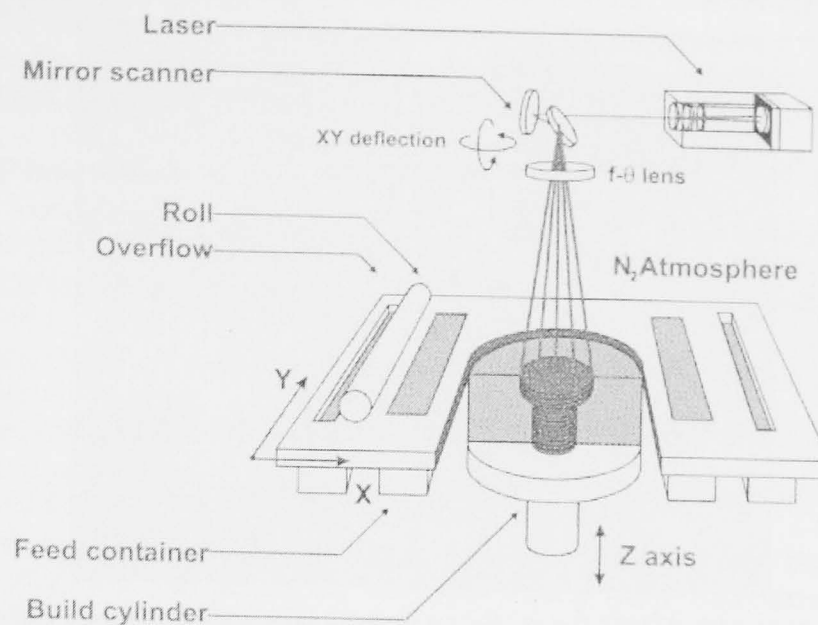


Figure 2-37. Selective Laser Sintering [Kruth, 2005]

During 1990s, DTM Corporation and EOS GmbH developed distinct SLS process for metal parts utilising polymer (resin) coated binder powder. In developing metal part, DTM apply SLS process to first produce green-parts. Then, the green-part is sent to a furnace for binding, sintering and bronze infiltrating process to produce fully dense metal parts. On the other hand, EOS develop a variation SLS process which able to produce metal parts without binder coating and subsequent post-processing, which is known a Direct Metal Laser Sintering (DMLS). The basic process of DMLS involves either melting or liquid phase sintering of a metal powder that mix different melting points [Hopkinson, 2006].

#### 2.2.2.3.2. Three Dimensional Printing (3DP)

The 3DP technology is invented at MIT. This LM technology uses ink-jet printing technology to build a 3D solid part. A thin layer of powder material is first spread over the surface of powder bed. Then, employing ink-jet printing technology, a binder material is sprayed and selectively bonds the powder particles to form the solid layer of the part. As the platform lowered, a fresh layer of powder is spread and deposited over the previous solid layer, and binder printed again. This layer by layer process is repeated until the part is developed completely [Noorani, 2006]. The 3DP steps of metal part development are similar to SLS. The 3DP process is first used to develop green-part. Post-processing (debinding, sintering and infiltrating) of the green-part is then followed in the furnace.

### 2.2.3. Layer Manufacture of Metal Parts

High demand on functional metal part and tooling has driven advanced development in metal materials for layer manufacture (LM) technology [Wohler 2006]. An original LM technology for producing durable metals parts is developed at the University of Texas at Austin, USA, in 1988 known as selective laser sintering (SLS). Substantial development of metal materials has been ongoing since the arrival of this SLS process into marketplace in 1992 by DTM Corporation (acquired by 3D Systems in 2001), which provide the opportunity and wider the possibility to develop rapid metal tooling for production. The first commercial SLS metal material introduced by DTM in 1993 known as RapidSteel™ (RS) which is steel/cooper based powder material. This RS material is then up dated by an improved material known commercially as LaserForm™ (LF) which is stainless steel 420 based powder material coated by polymer binder. Thus, other commercial metal material from competitors also introduced and developed, including Direct Metal Laser Sintering (DMLS) by Electro Optical Systems (EOS) GmbH, and Prometal 3D Printing by Extrude Hone.

Direct and indirect SLS are denominated as two distinct ways in developing metal parts using laser sintering process. In direct SLS, the development of intended metal part is generally by melting and consolidating a metal powder directly without debinding and infiltration process. On the other hand, the existing of the polymer binder in metal powder distinct the indirect SLS process in developing fully dense metal parts [Dalgarno et. al., 2003]. The following sections consider the principles of both direct and indirect SLS approaches, including its commercial technology development.

#### 2.2.3.1. Indirect Metal Parts Manufacture

##### 2.2.3.1.1. Indirect SLS

The principle of building process via indirect SLS is based on distinct approach of polymer binder on metal powder [Dalgarno, 2003, and Venuvinod, 2004]. In this approach, two stages of process are required to produce dense metal part. In the first stage, SLS system sinters metal powder with polymer binder in order to develop a green part directly from a 3D CAD solid model as explained in

section 2.2.2.2.3. In the second stage, after required post-processing, this green part is then debinded, sintered and metal infiltrated in a furnace cycle to produce a fully-dense metal part [3D Systems, 2003 and Dalgarno, 2003]. Figure 2-38 illustrates the heat treatment cycle during the process.

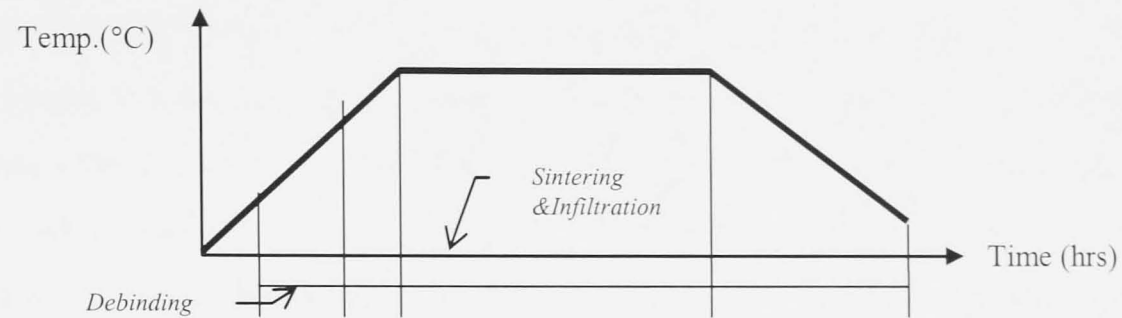


Figure 2-38. Heat Treatment Cycle

The process is started by increasing the temperature of the oven at a certain rate up to the infiltrant fusion/melting point. During this heating process, the polymer binder is vaporized (debinding), leaving only a porous metal skeleton. As the melting point is reached, the green part is then sintered and the infiltrant starts to infiltrate the green-part porous structure through capillary action to increase its density. At this stage, the temperature is held for about several hours for full sintering and infiltration. After this holding time, the temperature is lowered down at a certain rate and the part then cools at the natural rate of the oven.

#### 2.2.3.1.2. 3D printing (3DP)

ProMetal, USA, develops a LM system that employs MIT's licensed 3D printing (3DP) ink jet technology to jet a binder onto the surface metal powder. Layer by layer, the system builds a metal part. Thus, a furnace cycle burns out the binder and produces a fully dense metal part through infiltration. The available metal powders processed using this PM technology include steel alloys, copper alloy, tungsten alloy, and nickel alloy [ProMetal, 2006].

#### 2.2.3.2. Direct Metal Parts Manufacture

##### 2.2.3.2.1. Direct SLS

In the direct SLS approach, it is identified that there are two distinct metal powder mixtures used to develop fully dense metal parts: mixed metal powder mixtures and single metal powder mixture. For both mixtures, the key process in

direct SLS approach is characterized by melting and wetting or liquid flow mechanism which is known as liquid phase sintering (LPS) [Das et. al., 2000 and Venuvinod, 2004].

A mixed metal powder mixture is normally composed by low and high melting point metal mixture. This enable direct SLS process without the use of a polymer binder. In the process, laser sintering process firstly melts the low melting point metal mixtures (act as an infiltrant) and then flows it into the pores to wet and bind the solid particles of the higher melting point metal mixtures. As the temperature increases, continuous sintering process secondly homogenises both mixtures through diffusion and/or solutions. As a result, the infiltrant vaporizes leaving the pores and the higher melting point metal, which finally increase the density of the complete metal part [Klocke and Wagner, 2003].

In the case of single metal powder mixture, this LPS mechanism takes place due to the mixture surface melting and liquid flow. Factors that influence the LPS are a liquid solubility in solid and a solid solubility in liquid. When the liquid solubility is high, the transient liquid phase lead to the process sensitivity during heating. In contrast, the solid solubility promotes densification due to grain shrinkage which helps the rearrangement phase. A combination of low solid solubility with high liquid solubility promote swelling, which may be reduced by homogenous powder [Lu, 2001 and Santos, 2006].

Dalgarno et. al. [Dalgarno, 2003] has reported that the studies on direct SLS approach using single metal powder mixture mainly concern with pre-alloyed steel mixtures such as stainless steel and tool steels. Furthermore, most of the studies experimentally investigates the influence of the direct SLS process parameters. Das et. al. in their studies investigated the effects of combining direct SLS with hot isostatic pressing (HIP) in developing prototype of titanium alloy parts. The results shown that the parts were comparable to those produced by conventional processes [Das, 1998].

#### 2.2.3.2.2. Electron Beam Melting (EBM)

Electron Beam Melting (EBM) is developed by Arcam AB, Sweden. The EBM method produces metal parts directly from metal powder with characteristics of intended materials. As LM technologies, the EBM build the parts from 3D CAD

model and lays down successive layer of powdered material. To build a fully dense metal part, the EBM employs electron in vacuum to fuse the metal powder. The material is a pure alloy metal powder which does not require filler and additional heat treatment. Although the technology is able to build a 100% dense functional part directly, the surface finish is relatively poor, and post processing to enhance desired quality is required. The main materials now available to support the EBM technology include titanium, Ti16AlV, cobalt-chrome, and inconel [Larson, 2003 and Wohler, 2006].

#### 2.2.3.2.3. Direct Metal Laser Sintering (DMLS)

DMLS is the LM process for metal part that has been commercialised by EOS GmbH. The DMLS create a 3D solid parts directly from 3D CAD model, whereby layers of metal powder are applied to building platform and sequentially fused together by a scanning laser beam. There are two distinct steps in the process. First, a defined 2D cross-section of powder layer is levelled using levelling device. Second, the laser beam is subsequently moved across the powder layer according to defined cross-section, and then sintered the powder with a liquid phase. The subsequence of these two steps is repeated as a new powder layer added until the part is built completely [EOS, 2004].

#### 2.2.3.2.4. Selective Laser Melting (SLM)

SLM from MCP (Mining and Chemical Products Ltd.) is a direct LM process for metal based on a principle of melting a fine layer of metal powder using a laser beam. In each layer the laser beam generates the outline of a defined 2D cross-section from the expected part by melting the powder particles, before the building platform is lowered and coated with a new powder layer [MCP, 2004]

#### 2.2.3.2.5. Direct Laser Forming (DLF).

DLF is an LM technology developed by Trumpf, Germany. The DLF also build a metal part inside a powder bed similar to the manufacturing principle of SLM in MCP. The laser beam melts on the metal powder layer, Adjacent melting traces and stacked layers are welded together and the build platform is lowered by the set layer thickness. These steps are repeated until the entire component is complete [Trumpf, 2006].

### 2.2.3.3. Other Technologies

#### 2.2.3.3.1. Ultrasonic Consolidation (UC)

Ultrasonic Consolidation (UC) is developed by Solidica Inc., USA. Different from many other technology, the manufacturing principle of the UC is that the technology combines ultrasonic welding with high speed milling process to build a metal part through layered metal sheet bonding. In this process, a high frequency sound from ultrasonic technology is used to bond layer by layer metal sheets, and the high speed milling is then used to enhance the final quality of the part [Wohler, 2006].

#### 2.2.3.4. Comparison of Metal Processes

Since DTM corporation (now 3D Systems) and EOS have commercialised their LM systems for metal fabrication, a number of new technologies in this area is recently developed and commercialised. According to Wohler's Report 2006, the following Table 2-13 summarises the characteristics of the nine prominent LM technologies commercialised today which are expected to play a significant role in developing metallic parts [Wohler, 2006].

Table 2-13. Comparison of LM technologies to Produce Metal Parts [Wohler, 2006]

	SLS	DMLS	EBM	LC	SLM	SPLS	PM	UC	DLF
<b>Manufacturer</b>	3D Systems	EOS GmbH	Arcam AB	Concept Laser	MCP/F&S	Phenix Systems	ProMetal	Soidica	Trumpf
<b>Proces:</b>	Selective Laser Sintering	Laser Melting	Electron Beam Melting	Linear Laser Melting	Selective Laser Melting	Solid Phase Laser Sintering	Metal 3D Printing	Layered Metal Tape	Laser Melting
<b>Material</b>	Stainless steel-bronze; A6 tool steel	Stainless Steel, Cobalt-Chrome, Titanium, Ti16AV alloy	Titanium, Ti16AV, Cobalt-Chrome, and Inconel	Stainless steel, tool steel, Iron copper alloy, Chromium cobalt molybdenum, and Inconel. Titanium	Stainless steel, Tool steel, Titanium, Titanium alloy, Cobalt-Chrome	Stainless steel, tool steel, nickle, and ceramics	Tool steel, Inconel, Steel and Bronze, Aluminium, Gold	Aluminium Alloy Tape	Stainless Steel, Tool steel, Cobalt-Chrome, Titanium, Ti16AV, Inconel
<b>Density range (%)</b>	98 - 100	98 - 100	100	100	99 - 100	100	> 99	> 99.5	> 99.9
<b>Properties</b>	Comparable to conventional tool steel; high heat conductivity	Comparable to conventional tool steel (steel based) and Aluminium (bronze based)	same as conventional	same as conventional tool steel	Properties as pure base material used	similar to raw material	30 and 35 Rc (Steel & Bronze); 65 Rc (Tool Steel)	Same as conventional aluminium tools	Same as raw material
<b>Accuracy (mm)</b>	±0.115 - 0.250	±0.02 - 0.05	±0.3	±0.05	±0.05 /100	±0.05 /120	± 0.125	± 0.075	±0.3
<b>Surface Finish. (Ra µm)</b>	RMS 7.5 - 50	9 (as sintered); 3 (shot peening)	10 - 20	4.5-7 (after laser); 3 (after mcroblasting)	< 10	N/A (can be polished close to mirror finish)	6 - 10	15	15
<b>Max. Size (mm)</b>	200x250x125	250x250x200	200 x 200 x 200	350 x 300 x 280	250x250x250	dia. 250 x 300	1000 x 500 x 250	600x900x250	dia. 250; high 160
<b>GeometryLi mitation</b>	typical moulding limitation	min. wall thickness 0.3 mm	none	none	min. wall thickness 0.08 mm; 45° overhang (no support)	none	min. wall thickness 1.25 mm	N/A	min. wall thickness 0.3 mm

### 2.3. The application of LM Systems

Layer manufacturing systems have become an integral part of the computer-based design process. LM-generated parts are becoming widely used in many industries. With advanced development of the systems and material improvement, the LM system is now able to meet the requirement for a wide range of applications. The most common application of the LM technologies are classified for rapid prototyping (RP), rapid tooling (RT), and rapid manufacturing (RM), which are explained in detail below [AMRCC, 2004, Pham, 2001 and Folkestad, 2002].

#### 2.3.1. Rapid Prototyping (RP)

At the early stage of its development, a major application of the LM systems is able to meet the needs of industry for developing rapidly functional prototypes with material properties close to the production parts, which a term of rapid prototyping (RP) is mostly known. With this extended capability, LM systems can provide accurate and detailed parts that have many valuable uses to improve the product development cycle. Regardless to the material and process the LM parts are

made from, some of the significant uses as functional prototypes are as follows:

- a design verification and optimisation to qualify the form/fit/function of the intended parts and/or assemblies.
- concept visualisation to verify design details, acceptance and justification
- a means for communication with customer for design review, and for marketing for testing customer reaction.

Furthermore, advanced research and development toward the system, and significant improvement in material have brought the LM technologies to the next level of application.

### **2.3.2. Rapid Tooling (RT)**

#### 2.3.2.1. Introduction to Metallic RT Techniques

A much-anticipated application of the LM technology is that the LM can be embedded in rapidly developing quality tools (i.e. mould and dies) which meet required specifications for producing end products. This application is known as rapid tooling (RT), which potentially offers a faster tooling technique. Tooling is one of the slowest and most costly steps in the product development cycle due to its complex geometry and the requirement of high accuracy and tolerance [Karapatis, 1998, and Dalgarno, 2001a]. Moreover, it is also required that the tools must be durable, wear-resistant, and have surfaces with high finished quality. To speed up the process and meet the quality requirements, industry has currently incorporated advanced LM technologies with conventional practices in developing the tools [Pham, 2001].

As a range of methods has been researched and developed, the intended application of the RT techniques is initially to develop a type of tool known as 'prototype tool' to produce a prototype and a small volume of products for testing purposes as well as production set-up. Since the probabilities of the tool design changes are relatively high at product design phase, RT can be considered as a valuable technique to provide an effective and efficient solution for these purposes until the design of the product is proven and a permanent tool is completed.

As an RT ideal condition, many expect that the LM systems are also capable to directly develop 'mass-production tools' from 3D CAD data as the current LM



technology and material are significantly improved to meet specific application and material requirements for tooling [Pham, 2001 and Jacobs 2000]. A common feature of generative RT methods for direct production tools are characterized by manufacturing metal tools. As the predominant LM processes for metallic RT techniques has been discussed in section 2.2.3. , the following review specifically indirect SLS/LS metallic tooling, followed by over viewing limitations of the current researches and developments in this area.

### 2.3.2.2. Review of indirect SLS/LS Metallic Tooling

A manufacturing of metal tools by indirect selective laser sintering (SLS) is confirmed as one of the major development in rapid prototyping [Pham, 2003]. To understand more about the value of the indirect SLS process, the followings overview metal materials and processes used.

RapidSteel® (RS) and LaserForm™ (LF) are two prominent metal powder materials created exclusively by DTM for SLS. RapidSteel 1.0 and 2.0 are known as the first and second generation of polymer coated 316 stainless steel powder. A process of manufacturing a metal part using this material is through three phases process, which is known as RapidTool process [Steward, 1999, and King, 2003]. The first phase, the polymer melts and binds the steel powder to produce a ‘green’ part. In the second phase, the green part undergoes first furnace cycle for debinding and sintering the steel powder to produce ‘brown’ part. At the final phase, the brown part is then placed in a crucible for bronze infiltration at the second furnace cycle to produce fully dense metal part [Kruth, 1998]. Some of the benefits associated with RapidSteel are that it offers P20 steel hardness and durability, high thermal conductivity, and similar characteristics with tool steels [3D Systems, 2003].

Furthermore, DTM continuously improved their development through reducing the post-processing by introducing the third generation of RapidSteel™, called LaserForm™ (LF). LF ST-100 and ST-200 metal powder and the newest LF A6 steel are included in this new development. For ST-100, the final composition of the metal parts is about 40% bronze and 60% of 420 stainless steel, while in ST-200 the final composition is 46% bronze and 54% of 420 stainless steel. The tooling inserts and direct metal parts from both ST-100 and ST-200 will have similar characteristic to P20 Steel. The latest development of LF A6 steel furthermore offers

improvement in processing time and material characteristics which is similar to tool steel [3D Systems, 2003]. Unlike RapidSteel, a fully dense metal part of LF materials is produced through sintering and bronze infiltration process with single furnace cycle as described in section 2.2.3.1.1. . The metal part produced is suitable for machining, polish finishing, plating and coating. Thus, the metal part produced is ideal for creating durable prototype, functional part, and tooling insert due to its durability, characteristic which is similar to P20 steel, high thermal conductivity, and heat resistance [3D Systems, 2003]. The following Table 2-14 shows the properties of these metal-based powders.

Table 2-14. SLS Metal Materials [3D Systems, 2003]

Properties	P20 Steel (Ref.)	RS 1.0	RS 2.0	ST-100	ST-200	A6
Tensile Strength (MPa)	950	475	580	510	435	610
Yield Strength 0.2% (MPa)	751	255	413	305	250	470
Young Modulus (GPa)	210	210	263	137		138

Unfortunately, most of these materials have not yet complied with industrial standard in tooling development. Despite the significant improvements in materials characteristics as well as processes, concerns regarding the accuracy of the metal parts produced still remain a major problem with indirect SLS metal tooling [Dalgarno, 2001b, and Pham, 2000]. The post-processes of debinding, sintering, and infiltration cause considerable shrinkage of the material even though it creates a fully dense metal part with suitable mechanical properties for injection mould tools [Pham, 2003, and Levy, 2003]. Furthermore, an ability to be machined leads to another strong point of these metal materials

### 2.3.2.3. Limitations from Current Research and Potential for Improvements

A number of RT process which have the potential to produce production tooling has been researched and developed. These include the RT developments which are commercially available and under development or at early commercialisation stage. The following Table 2-15 overviews the strengths and weaknesses of the most predominant RT developments currently [Grenda, 2005]. From the table, it is indicated that each of these developments still presents at least two limitations from the following: accuracy, surface finish, durability, size, and geometry which may become most common technological problem of any LM/SFF technology.

Table 2-15. Overview of Current RT Developments [Grenda, 2005]

Method	Process	Suppliers	Strength	Weakness
<b>Indirect RT</b> (Commercially available)	<b>3D Keltool™</b>	3D Systems	Accurate; Relatively high volume	Part size
<b>Direct RT</b> (Commercially available)	<b>Direct AIM™</b>	3D Systems	Direct production of moulds	Rough materials; Process limitations.
	<b>Direct Metal Laser Sintering</b>	EOS GmbH	Able to generate complex conformal cooling; No burnout and infiltration cycle	Limited tool life; Lower pressures; Difficult to remove powder in conformal cooling channels
	<b>RapidTool™</b>	3D Systems	Good for Die casting and Injection mould	Requires burnout and infiltration cycle; may require finish machining; conformal cooling channels have limitations due to powder removal
	<b>DirectTool™</b>	EOS GmbH	No burnout and infiltration cycle; Accuracy; Surface finish is improving with new materials	May require finish machining; Difficult to remove powder in conformal cooling channels
<b>Indirect RT</b> (under Development or Early Commercialisation Stages)	<b>Polysteel™</b>	Dynamic Tooling	Able to generate complex conformal cooling; 90% steel; Stronger than epoxy ; No secondary machining and no metal inserts	Slow cycle times
	<b>RePliForm™</b>	RePliForm	Ability to scale to large sizes; Surface finish same as master; Complex parting lines possible	Might not be competitive for small parts; Difficult to repair or modify a mould; RP patterns are not as Accurate as CNC; Slow cycle times for ceramic backed versions of tools
	<b>Sprayform™</b>	Ford Global Technology	Large sizes; Surface finish; Able to generate complex conformal cooling; Actuators; Slides; Can be welded or repaired; Flexible applications	Deep slots may be difficult
<b>Direct RT</b> (under Development or Early Commercialisation Stages)	<b>STAT™</b>	Catalyst PDG	Tight tolerances; Lead time, Choice of resins and price	Tool durability
	<b>Directed Metal Deposition System</b>	Optomec	Fully dense H-13 tool steel; Possible to maintain; Multiple materials; Able to generate complex conformal cooling	Geometric limitations on overhangs; Requires finish machining
	<b>Direct Metal Deposition</b>	Precision Optical Manufacturing (POM)	Able to generate complex conformal cooling; Possible to maintain; Can be polished	Geometric limitations on overhangs; Requires finish machining
	<b>ProMetal™</b>	ProMetal Div of Extrudehone	60% steel / 40% bronze helps heat condition; Able to generate complex conformal cooling; Structural mass red technology for improved thermal isolation	Lots of finishing required

### 2.3.3. Rapid Manufacturing (RM)

A very recent application of the LM technologies is called rapid manufacturing (RM). According to Hopkinson, the RM is defined as a direct method to manufacture a functional or end product in which the LM technology is employed

[Hopkinson, 2006]. This means that parts made by the LM systems are intended to be used directly in many final application. Although current development of the LM systems as well as improvement in materials have able to lead the technology toward the RM direction, LM is still far away from conventional manufacturing techniques because LM technology has still not been designed for manufacturing due to a number of limitations on the LM part that need to be considered, including dimensional accuracy, surface quality, repeatability, and durability. Therefore, the generated LM part in many ways need to be post-processed such as infiltration, machining, polishing, painting, plating, etc. [Folkestad, 2002 and Pham, 2003].

Regardless to these limitation, the new application of LM offer significant potential for rapidly manufacturing functional parts. As an additive manufacturing process, LM technologies are able to develop any complex parts design without the requirement of tooling, which significantly impact many aspects of design and manufacturing process [Wang, 2002]. RM is suitable for low volume production and also offers great potential for mass-customization (ie. prostheses and implants) in biomedical industry [Pham, 2004].

Based on direct metal parts classification made by Levy [Levy et. al. 2003] and Greulich [Greulich, 1997], there are two main methods for RM: non-melting and melting process. SLS (partial melting), SLM (full melting) and 3D Laser Cladding (full melting) are some identified process included. SLM and 3D cladding are able to produce relatively high density parts. Heat treatment is required to reduce thermal residual stress or to optimize the microstructure of the parts. Moreover, machining and finishing processes also necessary in order to achieve the requirement of high quality surface finish.

#### **2.4. Summary of Literature Review**

On the basis of the literature survey, it can be concluded that:

- Plastic injection moulding remains an important manufacturing process in the manufacture of polymer components
- Core/cavity insert design and manufacture are key steps in the development of mould tools, and can have a significant impact on productivity through the placement of cooling channels.

- Layer manufacturing technologies have become integrated in current computer-based design and manufacturing process. They have evolved over the past two decades which allow for complex, one off parts to be produced in a range of materials, shorter time and less cost. However layer manufacture techniques cannot, in general, make precision parts.
- The use of layer manufacture in the production of injection mould core/cavities has shown promise, but finishing to the required quality level has been significant issue.
- Machining and polishing remain the most used process in finishing injection mould core/cavities, with high speed machining (HSM) increasingly used

In order to fully exploit the potential of layer manufacture, it is proposed that a hybrid approach to core and cavity manufacture be developed, utilising a layer manufacture system to develop a near-net shape core and cavity set, which will be finished using HSM and conventional finishing techniques to create a high productivity, production specification core and cavity set.

## **2.5. Aim of the Research Works**

The aim of the research outlined in this project is to examine the potential of the above approach, and outline rules for the development of the core/cavity designed using selected approach. The literature survey has demonstrated that the various metal layer manufacture systems have fairly similar capabilities, and the layer manufacture system used in this research was the 3D System indirect SLS approach, which being available at the University of Leeds.

Given the information which is presented in this chapter, opportunities to develop the production-quality plastic injection moulding tools using indirect SLS and HSM process have been identified. Therefore, it was intended to carry out a study which mainly focuses on the investigation of a total rapid tooling solutions (design-to-manufacture). Further verification would be done through a systematic works utilizing knowledge gained and/or practical experiences (experimental development) from both current researches and development in this area and real industrial case studies. In order to pursue the overall aim of the study, the following objectives were defined:

- **Benchmark Studies:** Investigating design considerations required for near-net shape insert by assessing the technological capabilities of both indirect SLS and HSM with reference to the requirements of injection mould core/cavity set
- **Industrial Case Studies:** Investigating how both indirect SLS and HSM can be employed in the manufacturing of the injection mould core/cavity set, and evaluating as well as measuring the performance of the core/cavity set produced using indirect SLS and HSM
- **Design Rules Development:** Developing a set of design rules for injection mould core/cavity set to be produced using indirect SLS and HSM, based on best practice as derived from the industrial case studies.

## Chapter 3

# **Benchmark Studies**

## Chapter 3. Benchmark Studies

### 3.1. Introduction

In understanding of the SLS technological capabilities, two main groups of benchmark studies on building process and material properties have been carried out. The first group of studies aims to allow the dimensional accuracy, surface flatness, and building limitations to be characterised and understood. Understanding the capabilities of indirect SLS building process is considered critical for designing and manufacturing mould inserts that are capable of being used in high tolerance and accuracy applications. Therefore, a series of measurements and capability investigations of the process are performed in order to understand how much machining allowance and what design manufacture rules should be considered in designing near-net shape mould inserts before machining processes.

The second group of benchmark studies characterizes surface finish, hardness, and a material porosity of indirect SLS metal parts in order to understand their physical properties. The machinability of the material is initially investigated. Following this, the roughness and hardness of the metal parts as infiltrated, machined, and polished are then assessed. Finally, the porosity measurement is performed in order to investigate how densely the material of the metal part is packed.

### 3.2. Part Design and Manufacture

Figure 3-1 shows the main route for developing an SLS metal part for each benchmark model via indirect SLS approach. The first physical step is to a green part, which is built directly in the SLS system based on data from 3D CAD solid models generated in a CAD system. Following this, as a second step, the green parts are then placed in a separate oven/furnace for post-processing (debinding/sintering and bronze infiltration) to create fully-dense metal parts. The following sections explain more detail about these two steps of the procedure.



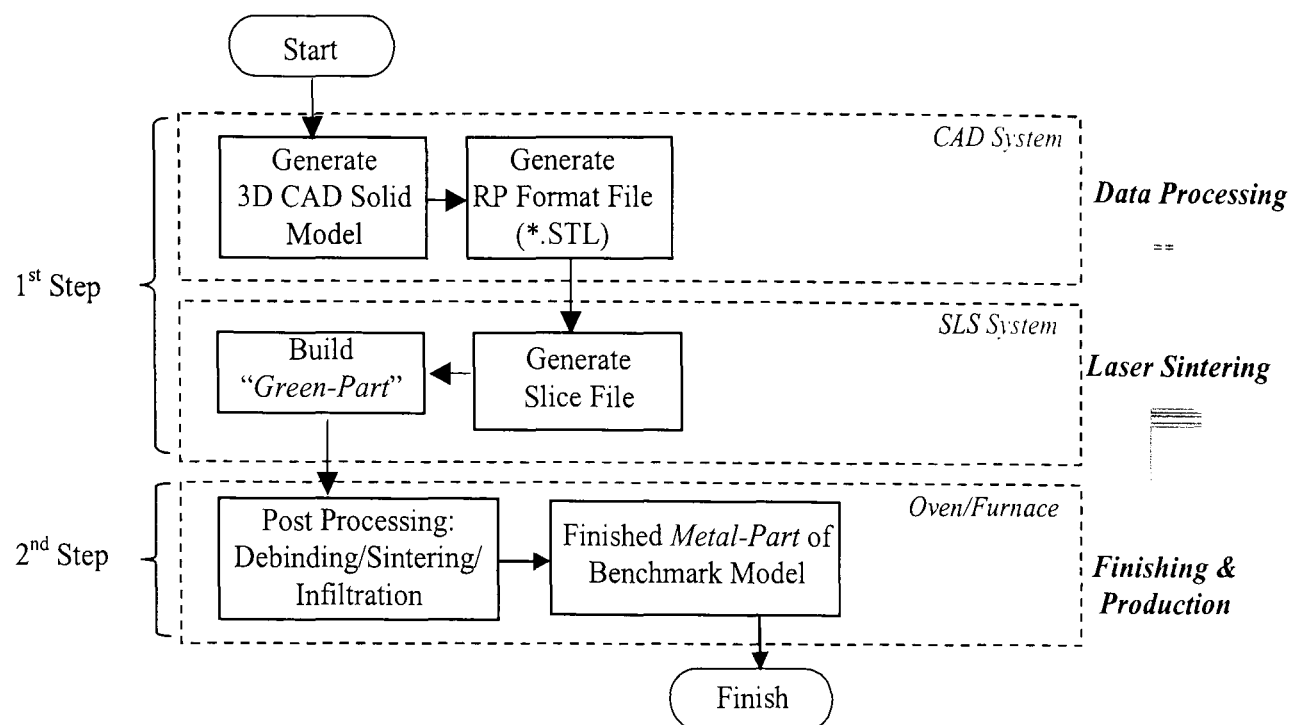


Figure 3-1. The Main Route of Model Development

### 3.2.1. Green Part Development

As mentioned above, the development of a green part requires a 3D solid model which is designed and generated using a CAD system. Within the CAD environment, the CAD solid model is then converted into an RP standard format input which is known as the STL file. Basically, the STL file approximates surfaces of a 3D CAD solid model with a collection of triangular facets, which presents a diamond-like approximation of the surface model. Figure 3-2 illustrates a conversion format from CAD to STL format model.

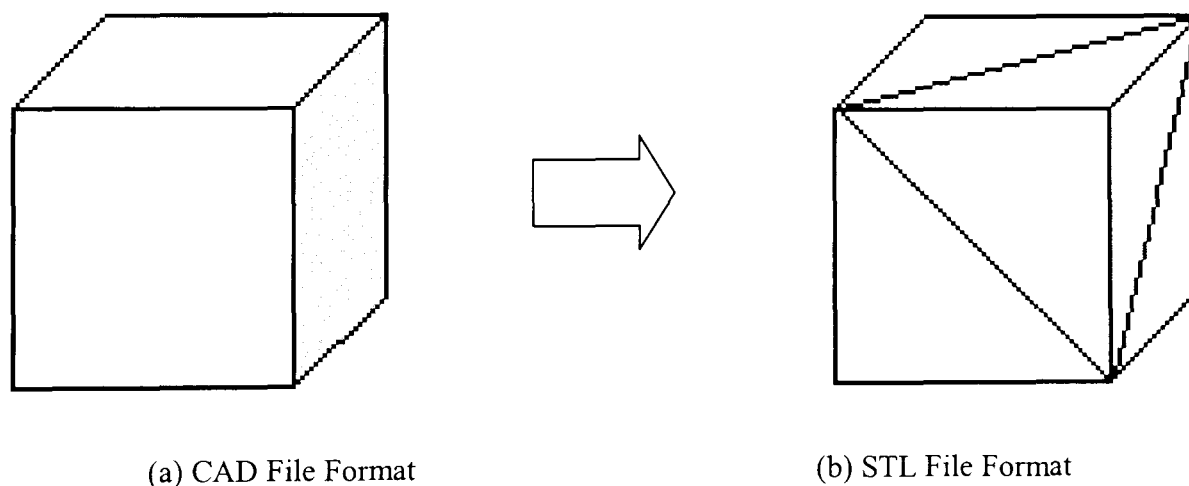


Figure 3-2. File Format Conversion

After this data processing, the STL file is then transferred to the SLS system for manufacture. As a building preparation, the STL model is first oriented relative

to the coordinate system. The SLS system then slices the STL model to generate successive 2D cross-sectional layers. Based on the geometry of each cross-sectional layer, as an input data, the SLS systems then starts building the green part by a laser beam scanning across a powder bed, as previously discussed in Chapter 2.

For all benchmark models, the *LaserForm™ ST-100* (ST-100) powder material has been used. Table 3-1 shows the typical properties of the ST-100 material. This powder is 420 stainless steel powder coated with polymer binder, which was developed exclusively for the SLS system by 3D Systems Inc. In the building process, the action of the laser causes the polymer to bond the steel particles together. The benefits provided of using ST-100 for mould inserts include its durability, characteristics similar to P20 steel, high thermal conductivity, and heat resistance [3D Systems, 2004].

Table 3-1. LaserForm™ ST-100 Material Properties [3D Systems, 2004]

Properties	Condition	Units	Test Method	Value
<b>1. POWDER PROPERTIES</b>				
Density	23°C	g/cm <sup>3</sup>	ASTM D792	7.7
<b>2. THERMAL PROPERTIES</b>				
Thermal Conductivity	100°C	W/m <sup>2</sup> K	ASTM E457	49
	200°C	W/m <sup>2</sup> K	ASTM E457	56
Coef. Thermal Expansion x 10 <sup>-6</sup>	51 - 150°C	m/m/°C	ASTM E837	12.4
<b>3. MECHANICAL PROPERTIES</b>				
Tensile -Yield Strength	(0.2%)	MPa	ASTM E8	305
Strength	-	MPa	ASTM E8	510
Elongation	-	%	ASTM E8	10
Young Modulus	-	GPa	ASTM E8	137
Compression -Yield Strength	(0.2%)	MPa	ASTM E9	317
Hardness	as infiltrated	HR <sub>B</sub>	ASTM E18	87
	as machined	HR <sub>B</sub>	ASTM E18	79

Table 3-2 shows the processing parameters that were set up to develop all the green parts of the benchmark models. The scaling factor and laser beam compensation (beam offset) are important parameters in determining the accuracy of the green part. The beam offset is equal to the radius of the laser beam. If the centre of the laser scans the required area then more material at the edge of the area will be sintered (see Figure 3-3). To compensate for this error, twice the beam offset (diameter of laser beam) has to be subtracted from the size of the features in X and

Y building direction. The scaling factor for model dimensions in the X and Y directions is to compensate for shrinkage in the furnace process.

Table 3-2. Process Parameters

<b>Absolute Facet Deviation (mm)</b>	0.15	
<b>Layer Thickness (mm)</b>	0.075 mm	
<b>Scaling Factor (X and Y)</b>	1.01 or 1%	
<b>Laser Beam Compensation :</b>	Fill (mm)	Outline (mm)
X-offset	0.289	0.289
Y-offset	0.299	0.279
Z-offset	0.000	0.000

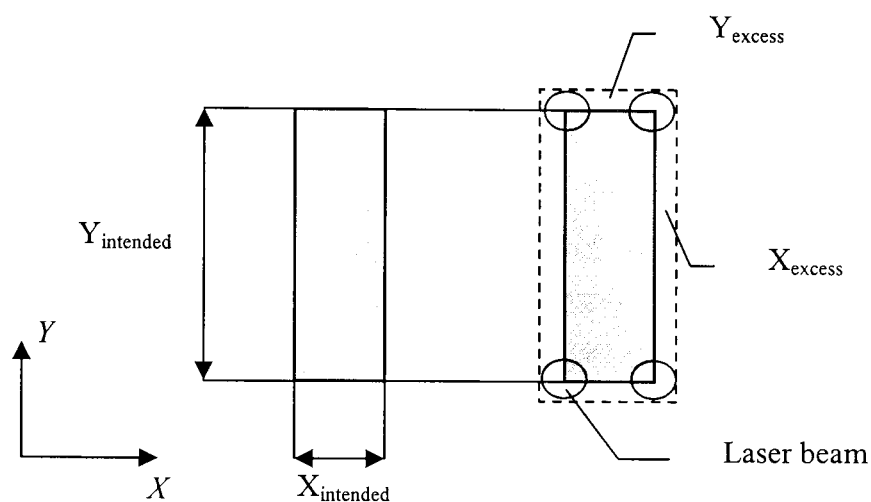


Figure 3-3. Feature Size due to Laser Beam Offset

### 3.2.2. Metal Part Development

After the green parts have been built and the loose (unprocessed) powder has been removed, the green parts are then transferred and placed in a crucible together with bronze (infiltrant) ingots for the furnace process. In this process, there are basically four stages: debinding, sintering, bronze infiltration, and cool down. Figure 3-4 illustrates the profile of the cycles during the infiltration process. At the beginning of the cycle, the temperature of the furnace is heated up to the melting point of bronze ( $1075^{\circ}\text{C}$ ) at a rate of  $110^{\circ}\text{C}/\text{hour}$ . As the temperature reaches approximately  $300^{\circ}\text{C}$ , the binder is burned off and vaporised, leaving only a porous metal skeleton (a process known as debinding). As the temperature increases to approximately  $1000^{\circ}\text{C}$ , sintering of the steel powder starts. Then, at a temperature of  $1075^{\circ}\text{C}$ , the bronze melts and is drawn into the porous structure through capillary

action, infiltrating the structure to increase its density. For full sintering and infiltration, the temperature is held for 4 hours. The furnace temperature is then reduced to 150 to 130°C at a rate of 130°C/hour, and the dense metal parts then cool at the natural rate of the furnace. Through this infiltration process, a fully dense metal with final composition of approximately 40% bronze and 60% 420 stainless steel is produced.

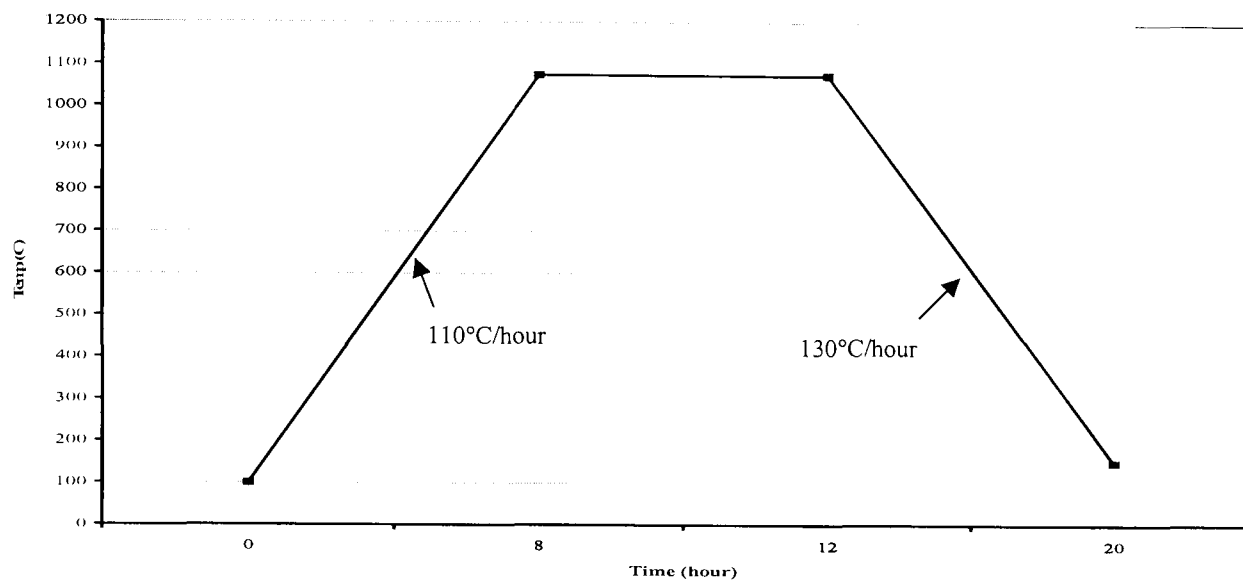


Figure 3-4. Furnace Cycle

### 3.3. Equipment

This section outlines and describes briefly the main equipment used for carrying out the benchmark studies.

Referring to the main processing route presented in Figure 3-1, the 3D CAD solid model as well as 3D STL model for the benchmark studies were designed and generated in IDEAS/SDRC CAD/CAM software package. For the development of the green parts, a Vanguard™ SLS System from 3D Systems Inc. (Figure 3-5) has been used. This machine uses a CO<sub>2</sub> laser, with a laser beam diameter or spot size of 0.4mm and maximum scan speed between 7,500 to 10,000 mm/s. The maximum build envelope for this machine is (W) 370 x (D) 320 x (H) 445 mm in size [3D Systems, 2004].



Figure 3-5. Vanguard SLS System

For the heat treatment, a Carbolite furnace (Figure 3-6) was used. This is a bottom loading elevator hearth furnace for debinding and sintering, with sand seal (zirconia). The furnace control allows a furnace cycle to be run via predefined program as required. The maximum operating temperature of this furnace is 1150°C, and a capacity of the usable chamber is 350 (height) x 500 (diameter) mm.

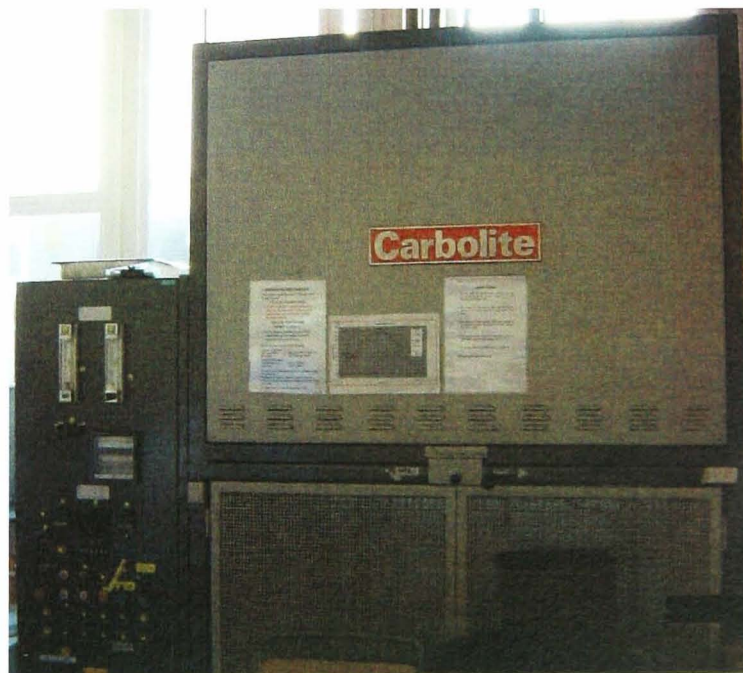


Figure 3-6. Carbolite Furnace

For the purpose of the measurements, three main measurement and testing facilities were used. For the dimensions of the models, the measurements are taken using KEMCO 400 3D coordinate measuring machine (CMM) (Figure 3-7). This

typical CMM can be manually or numerically operated (CNC program required), and has an accuracy of  $\pm 0.002$  mm for each axis. A WYKO<sup>®</sup> surface profiler (Figure 3-8), and INDENTEC hardness testing machine (Figure 3-9) have been used to characterise surface finish and hardness respectively. The technical information and set up specifications of these measuring equipments will be explained more in detail later.



Figure 3-7. Coordinate Measuring Machine



Figure 3-8. Surface Profiler



Figure 3-9. Hardness Testing Machine

### 3.4. Benchmark Studies of Indirect SLS Process

#### 3.4.1. Dimensional Accuracy and Surface Flatness

The following sections explain in detail the benchmark studies which are aimed to characterise (a) dimensional accuracy, (b) surface flatness, and (c) building limitations.

##### 3.4.1.1. Model Development

To investigate the dimensional accuracy, a series of linear and radial measurements are performed to assess and evaluate dimensional changes at the different stages of the process. For this purpose, a unique 3D CAD solid model as a benchmark model (Figure 3-10) was designed using IDEAS SDRC CAD/CAM software. As is required for the infiltration process, the model has additional features, called tabs, for the bronze ingot stands. The model was designed to have both internal and external dimensions in the X, Y and Z building directions. The smallest (0.5 mm) to the largest (30 mm) feature dimensions are created in all building directions.

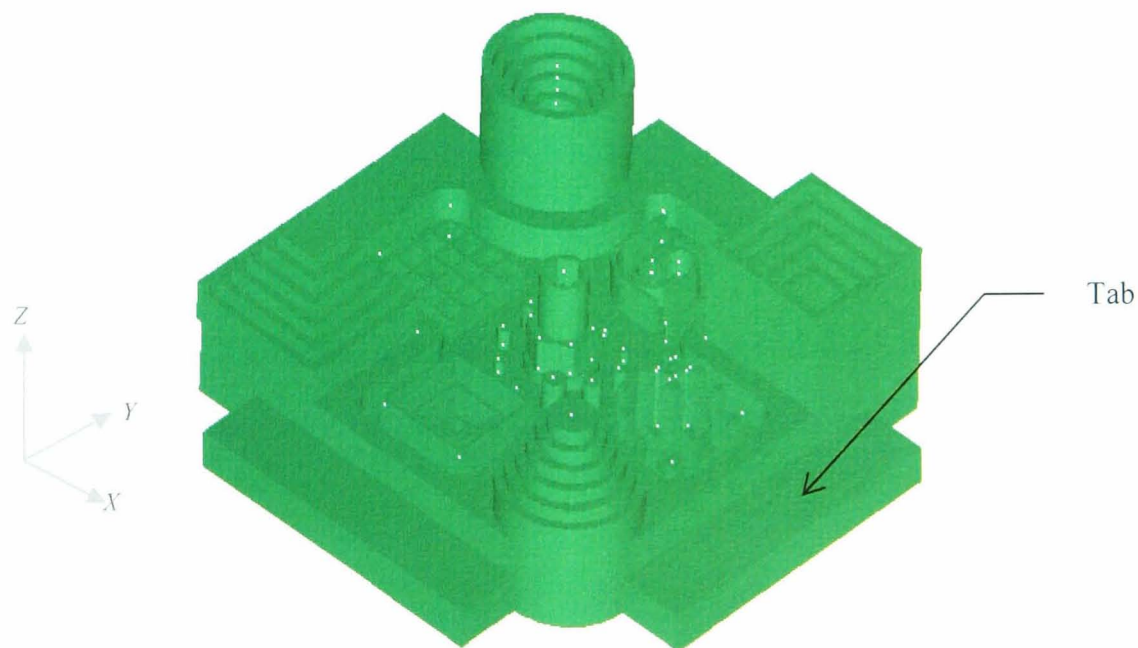


Figure 3-10. 3D CAD Solid Model

Following the route for model development shown in Figure 3-1, the 3D CAD model is firstly converted to STL model and then transferred to SLS systems for the development of a 3D green part model (Figure 3-11). In this green part

development, the set-up process parameters listed in Table 3-2 are employed. As the green part developed, it is then bronze infiltrated to develop a fully dense metal part (Figure 3-12). For this infiltration process, the required total weight of the bronze ingots is proportion to approximately 72% of the total weight of the green part.

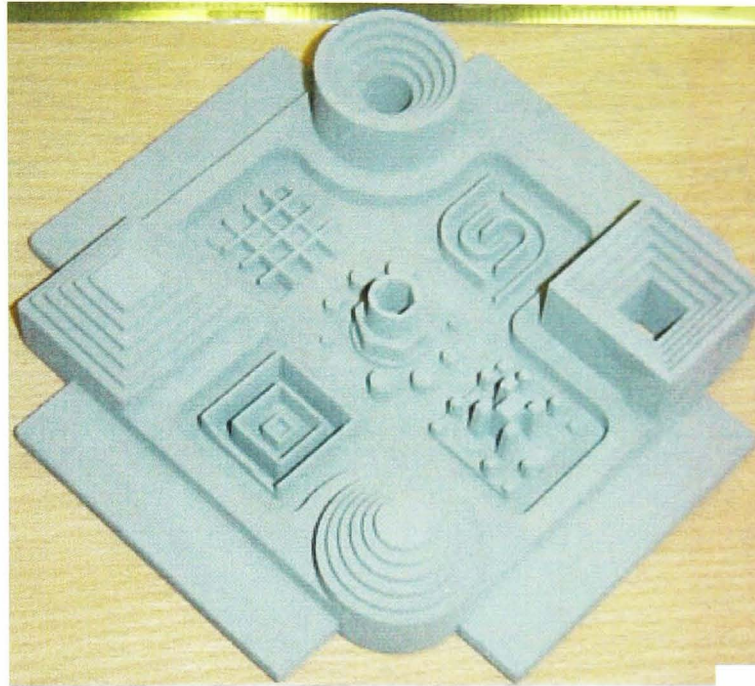


Figure 3-11. Green Part

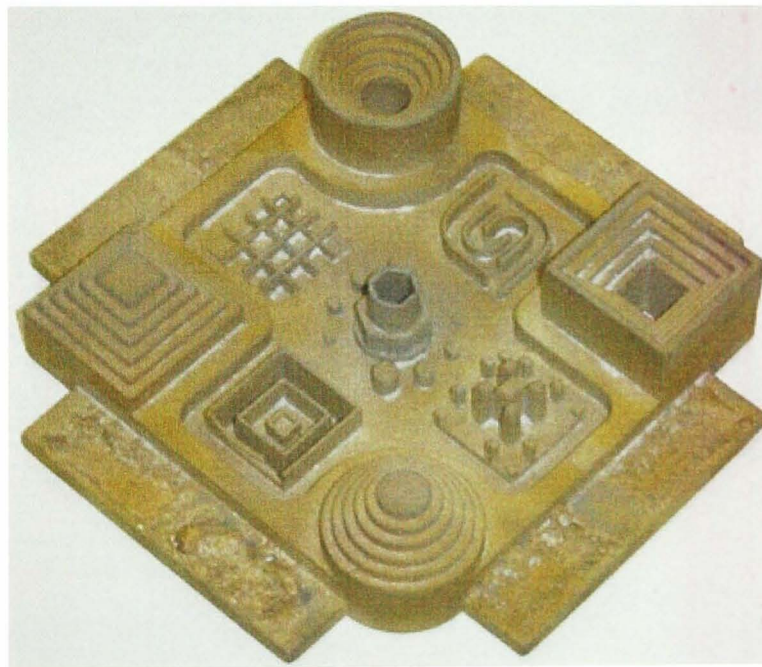


Figure 3-12. Metal Model

#### 3.4.1.2. Measurement

To assess any dimensional changes, the metal model was then measured on a KEMCO 400 CMM utilising a Renishaw PH1 probe with a spherical stylus of 2 mm diameter (Figure 3-13). The geometrical features of the model were measured individually because it was quite difficult to determine a common or reference



datum plane on the model for all features. Therefore, ten individual features of the model were defined as shown in Figure 3-14. Whilst, Table 3-3 details the identifications, method and target measurements of each features.

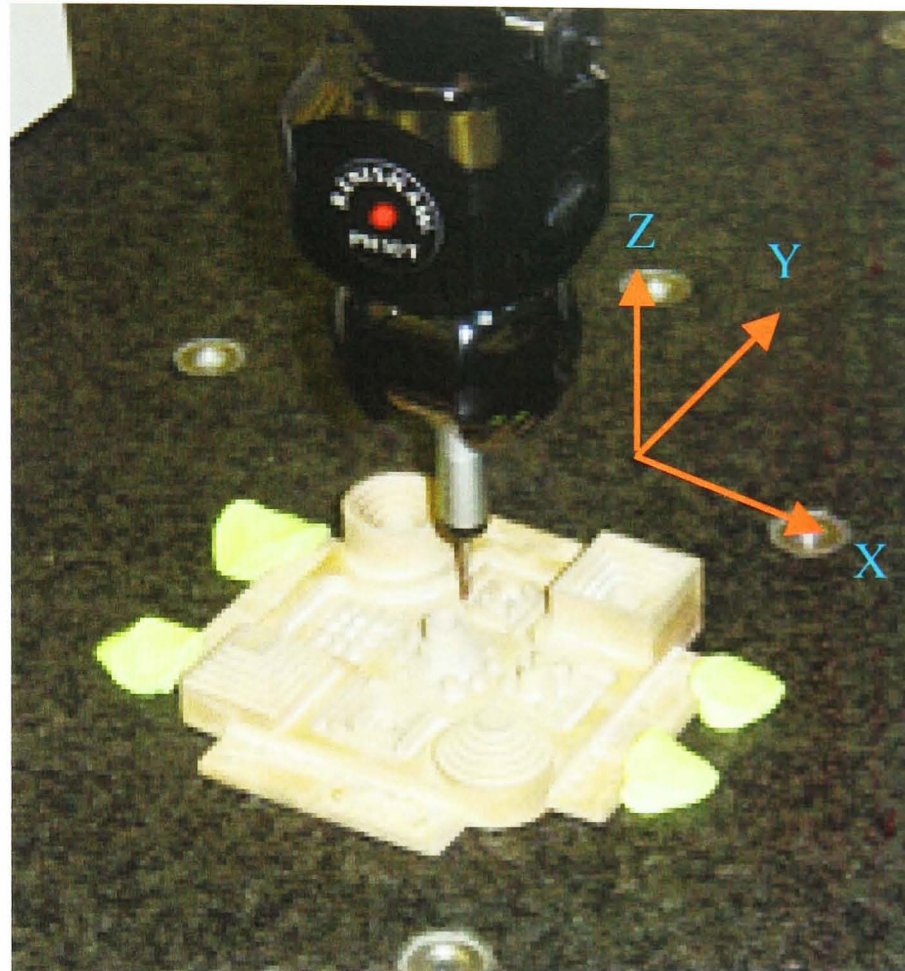


Figure 3-13. Benchmark Model on CMM

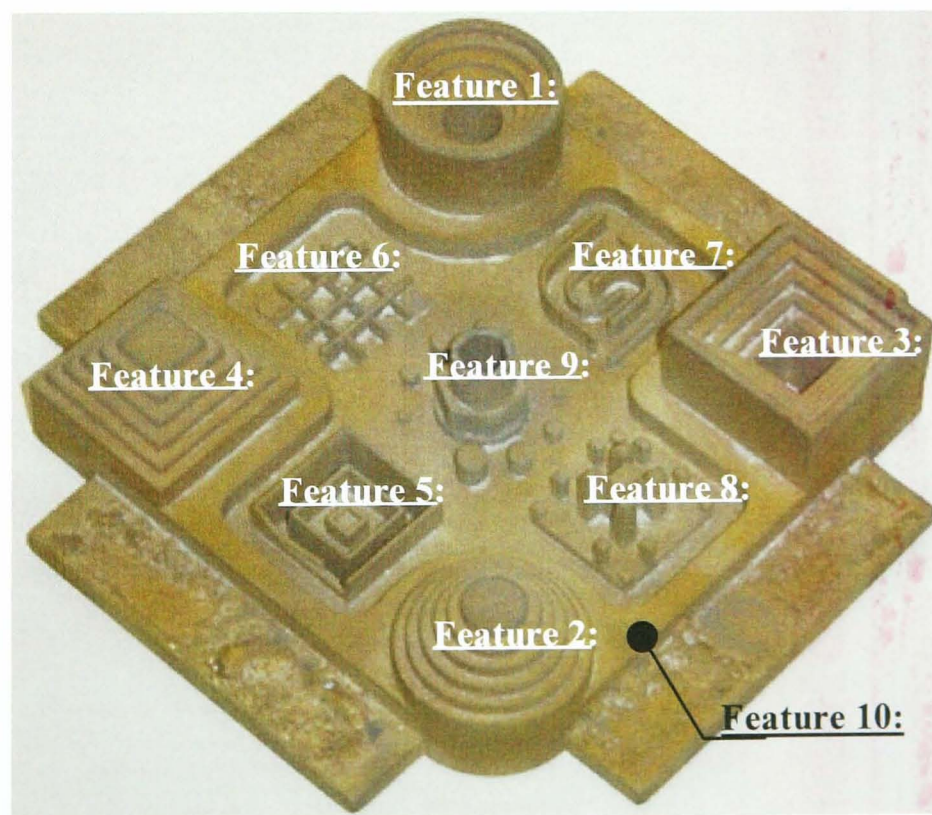


Figure 3-14. Individual Features of the Model

Table 3-3. Identifications of the Model Features

Feat.	Identification	Measurement	Target of Measurements
1	Internal Circle	Radial & Linear	Internal diameter/radius, high (Z)
2	External Circle	Radial & Linear	External diameter/radius, high (Z)
3	Internal Square	Linear	Internal dimensions (X & Y), high (Z)
4	External Square	Linear	External dimensions (X & Y), high (Z)
5	Square 1	Linear	Int./Ext. dimensions (X & Y), thickness, high (Z)
6	Square 2	Linear	Thickness, high (Z)
7	Square 3	Linear & radial	Thickness, radius, high (Z)
8	Square 4	Linear	Thickness, high (Z)
9	Square 5	Radial & linear	External dimensions (X & Y), diameter/radius, cylindrical, high (Z)
10	Square 6	Linear	External dimensions (X & Y), high (Z), flatness

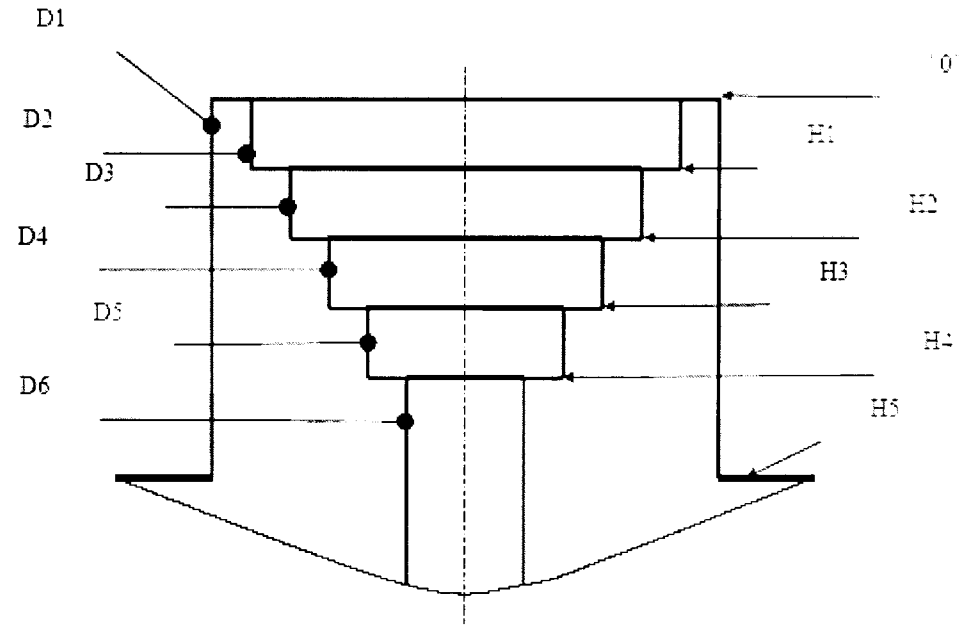
The average measurements of dimensions were recorded from three samples of measurement on each dimension. Thus, an average absolute error ( $\Delta X$  mm) is calculated by determining the difference between the average actual measurements ( $X_0$ ) and the expected/designed dimension ( $X$ ). The relative error ( $\delta X$ ) is then calculated by determining the ratio of the absolute error/deviation ( $\Delta X$ ) with the expected/designed dimension ( $X$ ). Thus, the percentage error ( $\delta X\%$ ) is determined by multiplying the relative error ( $\delta X$ ) with 100% as it is set out in equation (3-1) [Weisstein, 2004]. This percentage value can therefore be utilised to evaluate the scaling factor in building the green part.

$$\delta X(\%) = \frac{\Delta X}{X} \cdot 100\% = \frac{(X_0 - X)}{X} \cdot 100\% \dots (3-1)$$

#### 3.4.1.3. Results

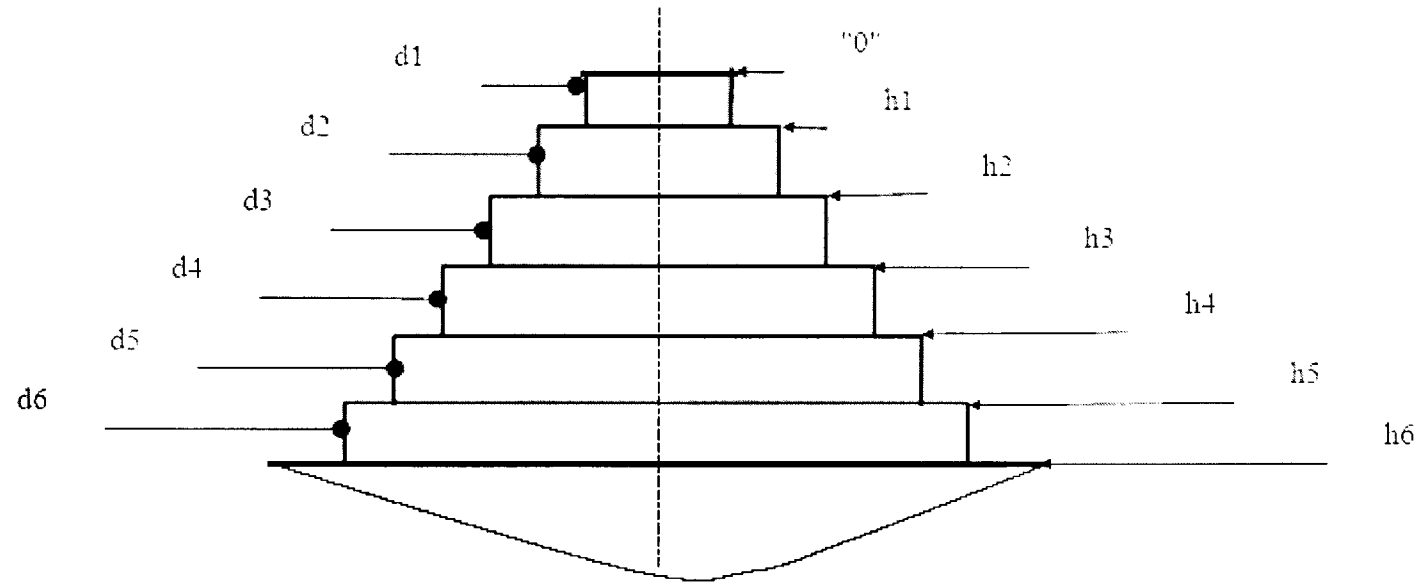
The results of the individual measurements for all indicated features are presented in Table 3-4a to j together with designed geometry and dimensions. To characterize linear errors, the average absolute and relative error against the nominal dimension of all features linear (X, Y, and Z) measurements are then summarised as shown in Figure 3-15 a to f.

Table 3-4a. Feature 1



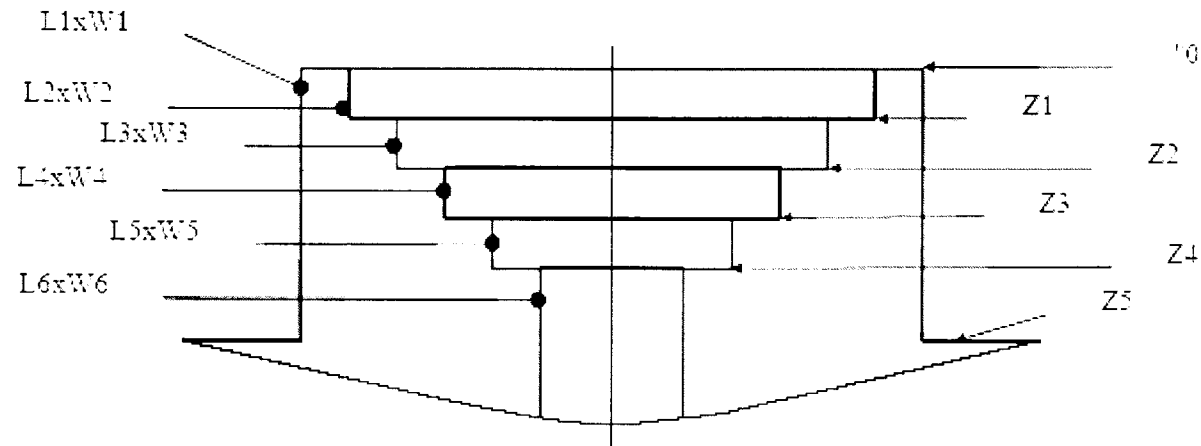
Dim. ID	Measurement	Nominal Dimensions								Ave. Error	
		Expected (mm)				Actual (mm)				Absolute (mm)	Relative (%)
		CAD Model	Scaling Factor	Green Part	After Infiltration	1	2	3	Ave.		
D 1	Radial	30.00	1.01	30.30	30.00	29.877	29.892	29.932	29.900	0.10	0.33
D 2		26.00	1.01	26.26	26.00	25.947	25.913	25.937	25.930	0.07	0.26
D 3		22.00	1.01	22.22	22.00	21.954	21.991	21.974	21.970	0.03	0.12
D 4		18.00	1.01	18.18	18.00	17.935	17.943	17.945	17.940	0.06	0.33
D 5		14.00	1.01	14.14	14.00	13.949	13.956	13.933	13.950	0.05	0.39
D 6		10.00	1.01	10.10	10.00	10.002	10.026	9.984	10.000	0.00	0.04
H 1	Linear (Z)	-2.00	1.00	-2.00	-2.00	-1.957	-1.954	-1.947	-1.950	0.05	2.37
H 2		-4.00	1.00	-4.00	-4.00	-3.924	-3.944	-3.911	-3.930	0.07	1.84
H 3		-6.00	1.00	-6.00	-6.00	-5.970	-5.973	-5.954	-5.970	0.03	0.57
H 4		-8.00	1.00	-8.00	-8.00	-7.932	-7.932	-7.918	-7.930	0.07	0.91
H 5		-15.00	1.00	-15.00	-15.00	-15.070	-14.652	-15.021	-14.910	0.09	0.57

Table 3-4b. Feature 2



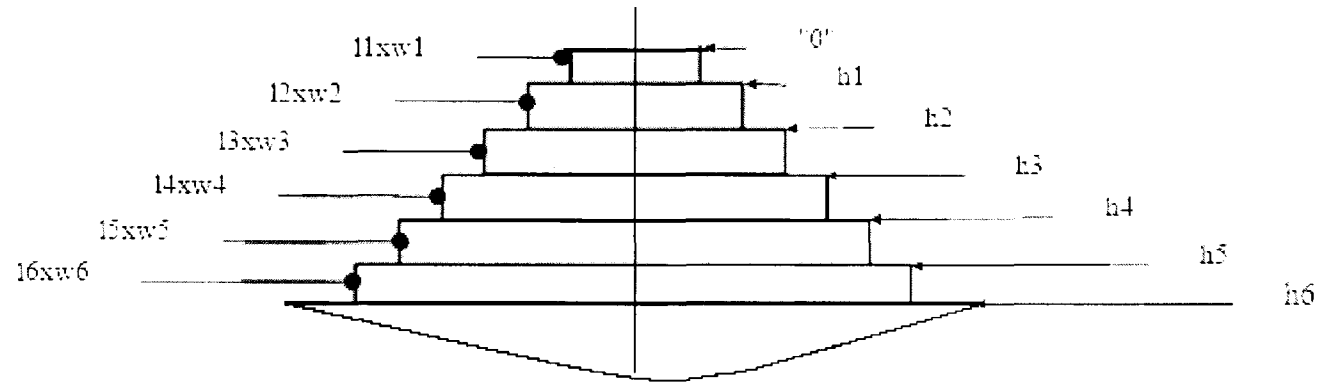
Dim. ID	Measurement	Nominal Dimensions								Ave. Error	
		Expected (mm)				Actual (mm)				Absolute (mm)	Relative (%)
		CAD Model	Scalling Factor	Green Part	After Infiltration	1	2	3	Ave.		
d 1	Radial	30.00	1.01	30.30	30.00	29.909	29.897	29.913	29.91	0.09	0.31
d 2		26.00	1.01	26.26	26.00	25.925	25.946	25.950	25.94	0.06	0.23
d 3		22.00	1.01	22.22	22.00	21.917	21.957	21.928	21.93	0.07	0.30
d 4		18.00	1.01	18.18	18.00	17.928	17.948	17.939	17.94	0.06	0.34
d 5		14.00	1.01	14.14	14.00	13.966	13.960	13.949	13.96	0.04	0.30
d 6		10.00	1.01	10.10	10.00	9.937	9.913	9.923	9.92	0.08	0.76
h 1	Linear (Z)	-2.00	1.00	-2.00	-2.00	-1.962	-1.914	-1.994	-1.96	0.04	2.17
h 2		-4.00	1.00	-4.00	-4.00	-3.962	-3.871	-3.911	-3.91	0.09	2.13
h 3		-6.00	1.00	-6.00	-6.00	-5.955	-6.030	-5.974	-5.99	0.01	0.23
h 4		-8.00	1.00	-8.00	-8.00	-7.909	-7.834	-7.903	-7.88	0.12	1.48
h 5		-10.00	1.00	-10.00	-10.00	-9.865	-9.982	-9.870	-9.91	0.09	0.94
h 6		-15.00	1.00	-15.00	-15.00	-14.931	-14.812	-14.720	-14.82	0.18	1.19

Table 3-4c. Feature 3



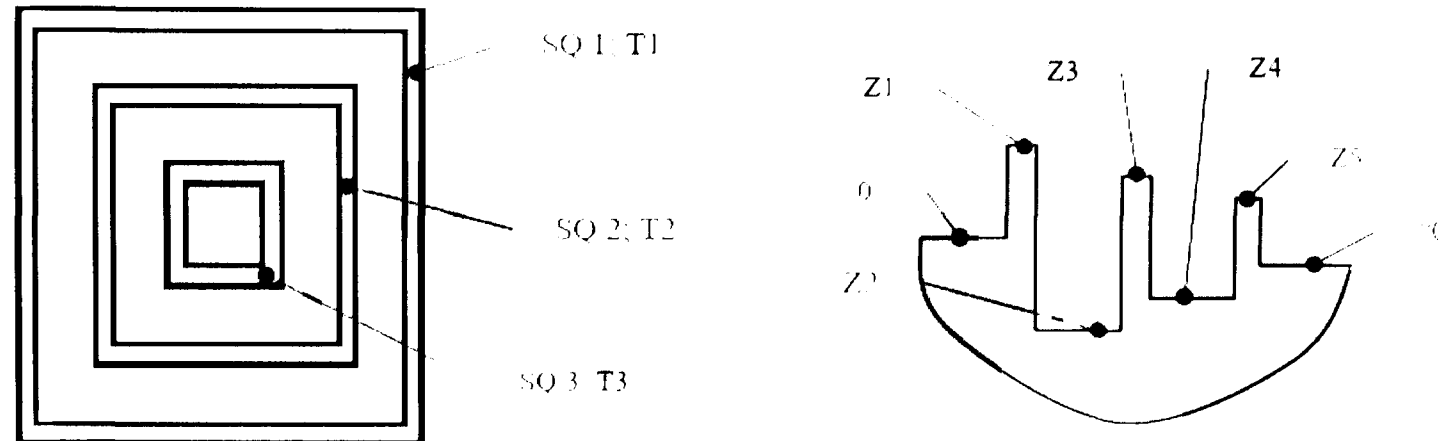
Dim. ID	Measurement	Nominal Dimensions								Ave. Error	
		Expected (mm)				Actual (mm)				Absolute (mm)	Relative (%)
		CAD Model	Scaling Factor	Green Part	After Infiltration	1	2	3	Ave.		
L 1	Linear (X=L; Y=W)	30.00	1.01	30.30	30.00	30.012	30.037	30.008	30.02	0.02	0.06
W 1		30.00	1.01	30.30	30.00	29.938	29.872	29.936	29.92	0.08	0.28
L 2		26.00	1.01	26.26	26.00	26.069	26.077	26.037	26.06	0.06	0.23
W 2		26.00	1.01	26.26	26.00	25.982	26.012	25.997	26.00	0.00	0.01
L 3		22.00	1.01	22.22	22.00	22.063	22.061	21.994	22.04	0.04	0.18
W 3		22.00	1.01	22.22	22.00	21.962	21.996	22.018	21.99	0.01	0.04
L 4		18.00	1.01	18.18	18.00	18.034	18.043	18.005	18.03	0.03	0.15
W 4		18.00	1.01	18.18	18.00	17.988	18.003	18.012	18.00	0.00	0.01
L 5		14.00	1.01	14.14	14.00	13.992	14.025	14.001	14.01	0.01	0.04
W 5		14.00	1.01	14.14	14.00	13.986	14.002	14.002	14.00	0.00	0.02
L 6		10.00	1.01	10.10	10.00	9.966	9.993	9.99	9.98	0.01	0.17
W 6		10.00	1.01	10.10	10.00	9.973	10.005	9.982	9.99	0.01	0.13
Z 1	Linear Z	-2.00	1.00	-2.00	-2.00	-1.977	-1.934	-1.942	-1.95	0.05	2.45
Z 2		-4.00	1.00	-4.00	-4.00	-3.964	-3.883	-3.914	-3.92	0.08	1.99
Z 3		-6.00	1.00	-6.00	-6.00	-5.955	-5.963	-5.909	-5.94	0.06	0.96
Z 4		-8.00	1.00	-8.00	-8.00	-7.877	-7.916	-7.917	-7.90	0.10	1.21
Z 5		-15.00	1.00	-15.00	-15.00	-14.968	-14.779	-14.87	-14.87	0.13	0.85

Table 3-4d. Feature 4



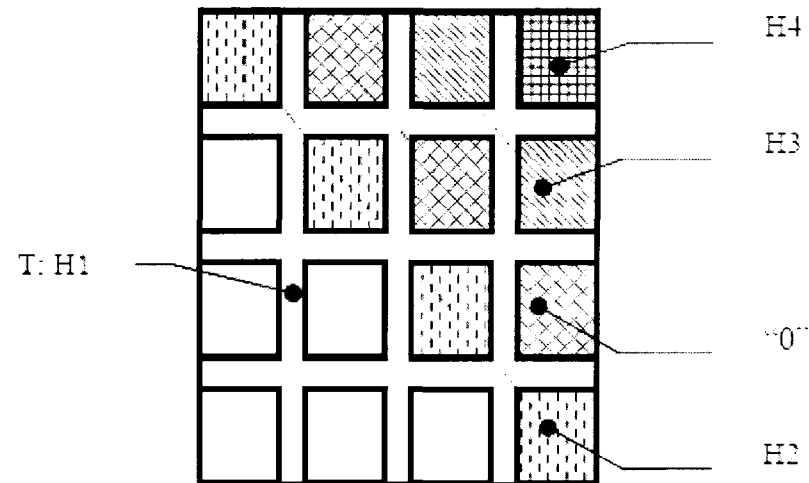
Dim. ID	Measurement	Nominal Dimensions								Ave. Error	
		Expected (mm)				Actual (mm)				Absolute (mm)	Relative (%)
		CAD Model	Scaling Factor	Green Part	After Infiltration	1	2	3	Ave.		
11	Linear (X=l; Y=w)	30.00	1.01	30.30	30.00	29.936	29.854	29.850	29.88	0.12	0.40
w 1		30.00	1.01	30.30	30.00	29.833	29.856	29.898	29.86	0.14	0.46
12		26.00	1.01	26.26	26.00	25.948	25.939	25.917	25.93	0.07	0.25
w 2		26.00	1.01	26.26	26.00	25.922	25.907	25.941	25.92	0.08	0.29
13		22.00	1.01	22.22	22.00	21.968	21.966	21.947	21.96	0.04	0.18
w 3		22.00	1.01	22.22	22.00	21.933	21.950	21.955	21.95	0.05	0.25
14		18.00	1.01	18.18	18.00	17.959	17.969	17.963	17.96	0.04	0.20
w 4		18.00	1.01	18.18	18.00	17.962	17.952	17.964	17.96	0.04	0.23
15		14.00	1.01	14.14	14.00	13.991	13.991	13.967	13.98	0.02	0.12
w 5		14.00	1.01	14.14	14.00	13.954	13.972	13.972	13.97	0.03	0.24
16		10.00	1.01	10.10	10.00	9.991	10.009	9.994	10.00	0.00	0.02
w 6		10.00	1.01	10.10	10.00	9.964	9.990	9.978	9.98	0.02	0.23
h 1	Linear Z	-2.00	1.00	-2.00	-2.00	-1.943	-1.940	-1.966	-1.95	0.05	2.35
h 2		-4.00	1.00	-4.00	-4.00	-3.943	-3.927	-3.916	-3.93	0.07	1.78
h 3		-6.00	1.00	-6.00	-6.00	-5.920	-5.952	-5.978	-5.95	0.05	0.83
h 4		-8.00	1.00	-8.00	-8.00	-7.958	-7.933	-7.907	-7.93	0.07	0.84
h 5		-10.00	1.00	-10.00	-10.00	-9.795	-9.866	-9.872	-9.84	0.16	1.56
h 6		-15.00	1.00	-15.00	-15.00	-14.832	-14.685	-14.892	-14.80	0.20	1.31

Table 3-4e. Feature 5



Dim. ID	Measurement	Nominal Dimensions								Ave. Error		
		Expected (mm)				Actual (mm)				Absolute (mm)	Relative (%)	
		CAD Model	Scaling Factor	Green Part	After Infiltration	1	2	3	Ave.			
SQ1	L 1	Linear (X 1: Y W)	21.00	1.01	21.21	21.00	20.960	20.900	20.964	20.94	0.06	0.3
	W 1		21.00	1.01	21.21	21.00	20.881	20.836	20.930	20.88	0.12	0.6
SQ2	L 2		13.00	1.01	13.13	13.00	13.015	12.985	13.023	13.01	0.01	0.1
	W 2		13.00	1.01	13.13	13.00	12.944	12.909	12.950	12.93	0.07	0.5
SQ3	L 3		5.00	1.01	5.05	5.00	5.008	4.989	4.993	5.00	0.00	0.1
	W 3		5.00	1.01	5.05	5.00	4.966	4.965	4.956	4.96	0.04	0.8
I 1	Linear X	1.00	1.01	1.01	1.00	0.985	0.941	0.948	0.95	0.05	5.2	
I 2		1.00	1.01	1.01	1.00	0.983	0.966	1.001	0.98	0.02	1.7	
I 3		1.00	1.01	1.01	1.00	0.925	0.915	0.928	0.92	0.08	7.7	
Z 1	Linear Z	6.00	1.00	6.00	6.00	5.838	6.040	5.914	5.93	0.07	1.2	
Z 2		4.00	1.00	4.00	4.00	-3.919	-3.715	-4.010	3.89	0.11	2.7	
Z 3		4.00	1.00	4.00	4.00	3.843	4.017	3.904	3.92	0.08	2.0	
Z 4		-2.00	1.00	-2.00	-2.00	-1.999	-1.941	-2.034	-1.99	0.01	0.4	
Z 5		2.00	1.00	2.00	2.00	1.936	2.000	1.992	1.98	0.02	1.2	

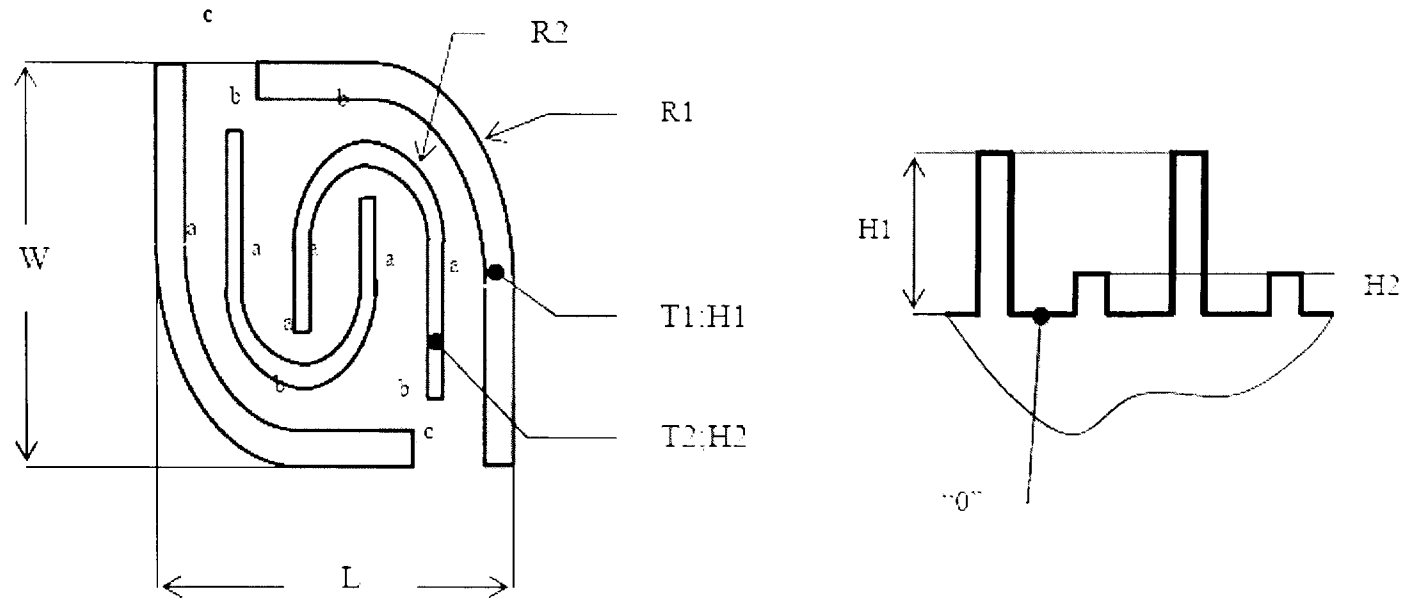
Table 3-4f. Feature 6



Dim. ID	Measurement	Nominal Dimensions								Ave. Error	
		Expected (mm)				Actual (mm)				Absolute (mm)	Relative (%)
		CAD Model	Scaling Factor	Green Part	After Infiltration	1	2	3	Ave.		
T	Linear X	1.00	1.01	1.01	1.00	0.950	1.031	0.958	0.98	0.02	2.03
H1	Linear Z	3.00	1.00	3.00	3.00	2.980	2.915	2.859	2.92	0.08	2.75
H2		-1.00	1.00	-1.00	-1.00	-0.975	-0.999	-0.940	-0.97	0.03	2.87
H3		1.00	1.00	1.00	1.00	1.076	0.810	0.939	0.94	0.06	5.73
H4		2.00	1.00	2.00	2.00	1.936	2.104	2.019	2.02	0.02	0.99

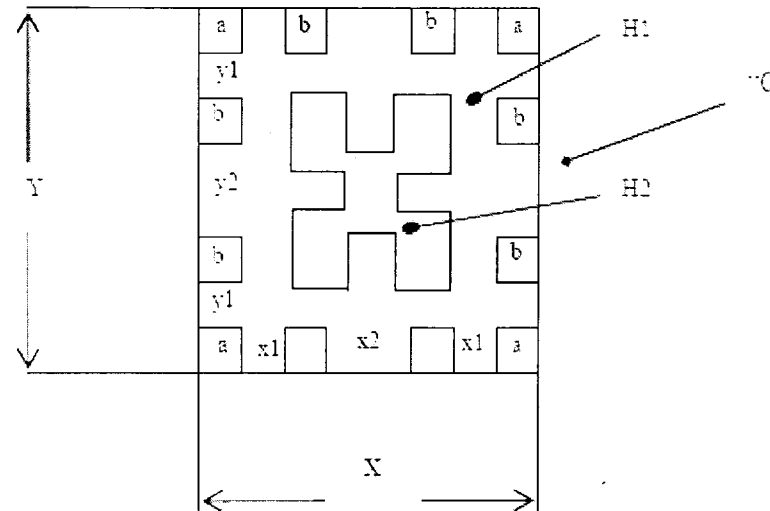


Table 3-4g. Feature 7



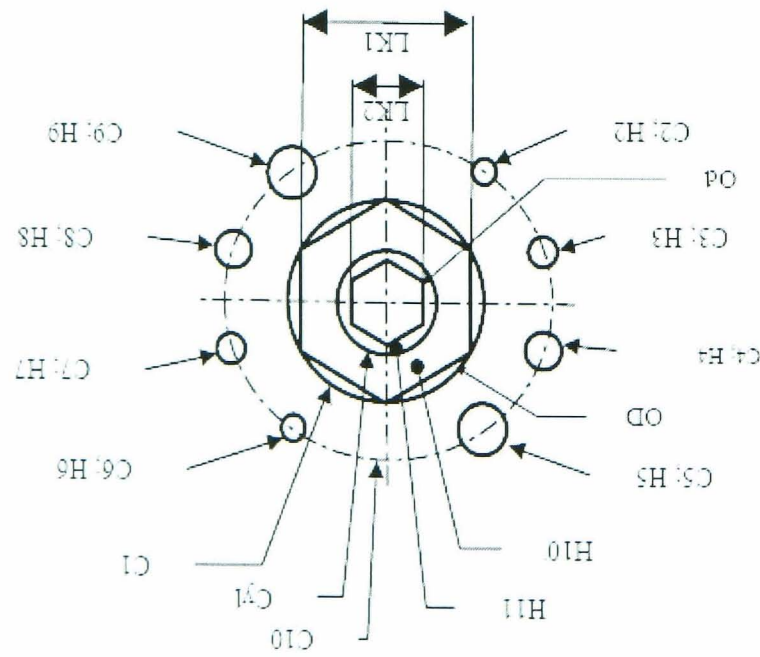
Dim. ID	Measurement	Nominal Dimensions								Ave. Error	
		Expected (mm)				Actual (mm)				Absolute (mm)	Relative (%)
		CAD Model	Scaling Factor	Green Part	After Infiltration	1	2	3	Ave.		
L	Linear	20.50	1.01	20.71	20.50	20.367	20.312	20.232	20.30	0.20	0.96
W	(X=L; Y=W)	20.00	1.01	20.20	20.00	20.078	20.023	19.982	20.03	0.03	0.14
T 1	Linear X	1.00	1.01	1.01	1.00	1.005	1.162	0.994	1.05	0.05	5.37
T 2		1.00	1.01	1.01	1.00	0.995	1.004	0.971	0.99	0.01	1.00
H 1	Linear Z	3.00	1.00	3.00	3.00	3.047	2.858	2.890	2.93	0.07	2.28
H 2		5.00	1.00	5.00	5.00	4.808	4.867	5.095	4.92	0.08	1.53
R 1	Radial	8.25	1.01	8.33	8.25	8.079	8.128	8.101	8.10	0.15	1.78
R 2		4.25	1.01	4.29	4.25	4.178	4.185	4.179	4.18	0.07	1.61
a	Linear (X=a, c; Y= b)	3.00	1.01	3.03	3.00	2.935	2.935	3.015	2.96	0.04	1.28
b		3.00	1.01	3.03	3.00	2.973	3.119	2.964	3.02	0.02	0.62
c		3.00	1.01	3.03	3.00	3.121	3.045	3.078	3.08	0.08	2.77

Table 3-4h. Feature 8



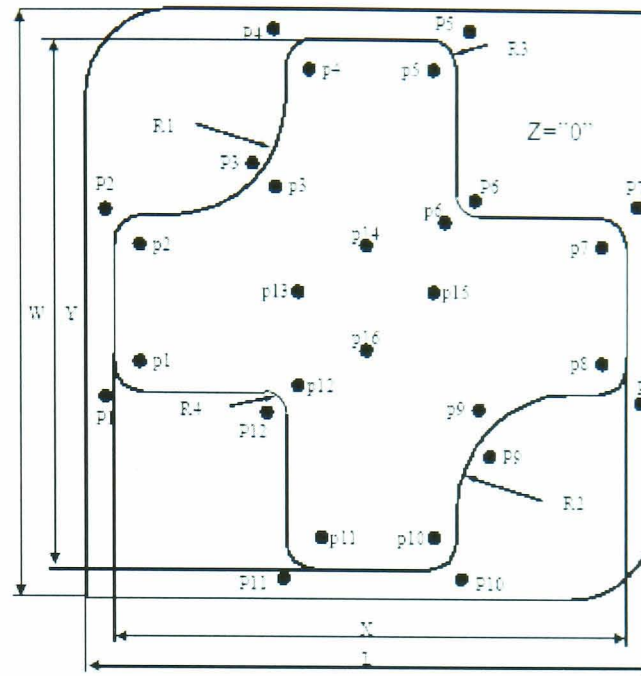
Dim. ID	Measurement	Nominal Dimensions								Ave. Error		
		Expected (mm)				Actual (mm)				Absolute (mm)	Relative (%)	
		CAD Model	Scalling Factor	Green Part	After Infiltration	1	2	3	Ave.			
a	L	Linear (X=L; Y=W)	2.00	1.01	2.02	2.00	1.980	2.016	2.001	2.00	0.00	0.05
	W		2.00	1.01	2.02	2.00	1.950	1.997	1.997	1.98	0.02	0.93
b	L		2.00	1.01	2.02	2.00	1.939	1.988	1.975	1.97	0.03	1.63
	W		2.00	1.01	2.02	2.00	1.988	1.943	2.002	1.98	0.02	1.12
X	Linear X	20.00	1.01	20.20	20.00	19.965	19.956	19.969	19.96	0.04	0.18	
x1		3.00	1.01	3.03	3.00	2.967	3.033	3.057	3.02	0.02	0.63	
x2		6.00	1.01	6.06	6.00	5.982	6.001	6.035	6.01	0.01	0.10	
Y	Linear Y	20.50	1.01	20.71	20.50	20.468	20.450	20.463	20.46	0.04	0.19	
y1		3.00	1.01	3.03	3.00	3.022	3.006	3.004	3.01	0.01	0.36	
y2		6.51	1.01	6.57	6.51	6.495	6.524	6.582	6.53	0.03	0.44	
Ha	Linear Z	4.00	1.00	4.00	4.00	3.866	3.923	3.894	3.89	0.11	2.64	
Hb		7.00	1.00	7.00	7.00	6.894	6.907	6.873	6.89	0.11	1.55	
H1		2.00	1.00	2.00	2.00	1.918	1.937	1.957	1.94	0.06	3.13	
H2		12.00	1.00	12.00	12.00	11.799	11.795	11.795	11.80	0.20	1.70	

Table 3-41. Feature 9



Dim. ID	Measurement	Expected (mm)			Actual (mm)			Ave. Error	Absolute (mm)	Relative (%)
		CAD Model	Scaling Factor	Green Part Infiltration	1	2	3			
C1	Radial	15.00	1.01	15.15	14.953	14.987	14.995	14.98	0.02	0.14
C2		2.00	1.01	2.02	1.861	1.895	1.887	1.88	0.12	5.95
C3		3.00	1.01	3.03	2.896	2.941	2.909	2.92	0.08	2.82
C4		4.00	1.01	4.04	3.928	3.945	3.941	3.94	0.06	1.55
C5		5.00	1.01	5.05	4.916	4.956	4.940	4.94	0.06	1.25
C6		2.00	1.01	2.02	1.861	1.896	1.908	1.88	0.11	5.58
C7		3.00	1.01	3.03	2.906	2.839	2.909	2.92	0.12	3.84
C8		4.00	1.01	4.04	3.930	3.946	3.938	3.94	0.06	1.55
C9		5.00	1.01	5.05	4.920	4.955	4.942	4.94	0.06	1.22
DP		25.00	1.01	25.25	24.987	24.989	24.997	24.96	0.04	0.17
OD		15.00	1.01	15.15	14.918	14.995	14.960	14.96	0.04	0.28
O4	8.00	1.01	8.08	8.038	8.053	8.039	8.04	0.04	0.54	
C10	10.10	1.01	10.10	9.937	9.913	9.923	9.92	0.08	0.76	
H2	Linear Z	2.00	1.00	2.00	2.058	2.045	2.051	2.05	0.05	2.57
H3		3.00	1.00	3.00	2.882	2.962	2.922	2.92	0.08	2.60
H4		4.00	1.00	4.00	3.870	3.913	3.889	3.89	0.11	2.73
H5		5.00	1.00	5.00	4.930	4.896	4.907	4.91	0.09	1.78
H6		2.00	1.00	2.00	2.056	2.050	2.048	2.05	0.05	2.57
H7		3.00	1.00	3.00	2.902	2.959	2.924	2.92	0.07	2.39
H8		4.00	1.00	4.00	3.866	3.908	3.901	3.89	0.11	2.71
H9		5.00	1.00	5.00	4.897	4.905	4.965	4.91	0.08	1.55
H10		7.00	1.00	7.00	7.007	7.161	7.085	7.08	0.08	1.20
H11		15.00	1.00	15.00	14.990	14.960	14.933	14.96	0.04	0.26
LK1		Linear X	12.99	1.01	13.12	12.989	12.955	12.959	12.97	0.02
LK2	6.93		1.01	7.00	6.963	6.959	6.961	6.96	0.03	0.45

Table 3-4j. Feature 10



Dim. ID	Measurement	Nominal Dimensions								Ave. Error	
		Expected (mm)				Actual (mm)				Absolute (mm)	Relative (%)
		CAD Model	Scaling Factor	Green Part	After Infiltration	1	2	3	Ave.		
R1	Radial	20.00	1.01	20.20	20.00	20.085	20.013	20.008	20.04	0.04	0.2
R2		20.00	1.01	20.20	20.00	20.145	19.988	20.110	20.08	0.08	0.4
R3		5.00	1.01	5.05	5.00	4.988	4.885	5.010	4.96	0.04	0.8
R4		5.00	1.01	5.05	5.00	4.915	4.991	4.988	4.96	0.04	0.7
X	Linear (X=L; Y=W)	90.00	1.01	90.90	90.00	89.767	89.774	89.792	89.78	0.22	0.2
Y		90.00	1.01	90.90	90.00	89.754	89.745	89.746	89.75	0.25	0.3
L		100.00	1.01	101.00	100.00	99.749	99.677	99.726	99.72	0.28	0.3
W		100.00	1.01	101.00	100.00	99.593	99.633	99.585	99.60	0.40	0.4
p1	Linear Z	-5.00	1.00	-5.00	-5.00	-4.994	-4.989	-4.990	-4.99	0.01	0.2
p2		-5.00	1.00	-5.00	-5.00	-4.752	-4.748	-4.750	-4.75	0.25	5.0
p3		-5.00	1.00	-5.00	-5.00	-4.425	-4.420	-4.419	-4.42	0.58	11.6
p4		-5.00	1.00	-5.00	-5.00	-4.512	-4.498	-4.508	-4.51	0.49	9.9
p5		-5.00	1.00	-5.00	-5.00	-4.875	-4.873	-4.885	-4.88	0.12	2.4
p6		-5.00	1.00	-5.00	-5.00	-4.932	-4.929	-4.930	-4.93	0.07	1.4
p7		-5.00	1.00	-5.00	-5.00	-4.984	-4.979	-4.985	-4.98	0.02	0.3
p8		-5.00	1.00	-5.00	-5.00	-4.873	-4.869	-4.870	-4.87	0.13	2.6
p9		-5.00	1.00	-5.00	-5.00	-4.885	-4.905	-4.879	-4.89	0.11	2.2
p10		-5.00	1.00	-5.00	-5.00	-4.818	-4.798	-4.790	-4.80	0.20	4.0
p11		-5.00	1.00	-5.00	-5.00	-4.887	-4.902	-4.891	-4.89	0.11	2.1
p12		-5.00	1.00	-5.00	-5.00	-4.827	-4.796	-4.831	-4.82	0.18	3.6
p13		-5.00	1.00	-5.00	-5.00	-4.811	-4.779	-4.809	-4.80	0.20	4.0
p14		-5.00	1.00	-5.00	-5.00	-4.674	-4.668	-4.669	-4.67	0.33	6.6
p15		-5.00	1.00	-5.00	-5.00	-4.837	-4.840	-4.836	-4.84	0.16	3.2
p16		-5.00	1.00	-5.00	-5.00	-4.655	-4.660	-4.649	-4.65	0.35	6.9

For the average absolute error ( $\Delta X$ ), Figure 3-15. a, c and e show that the error in all building directions tends to increase as the nominal dimensions of the features increase. Furthermore, it is noted that the ranges of the error within nominal dimension range of 0 mm and 30 mm for X, Y, and Z building direction are: 0.1 mm to -0.2 mm, 0.05 mm to -0.15 mm, and 0.25 mm to -0.25 mm respectively.

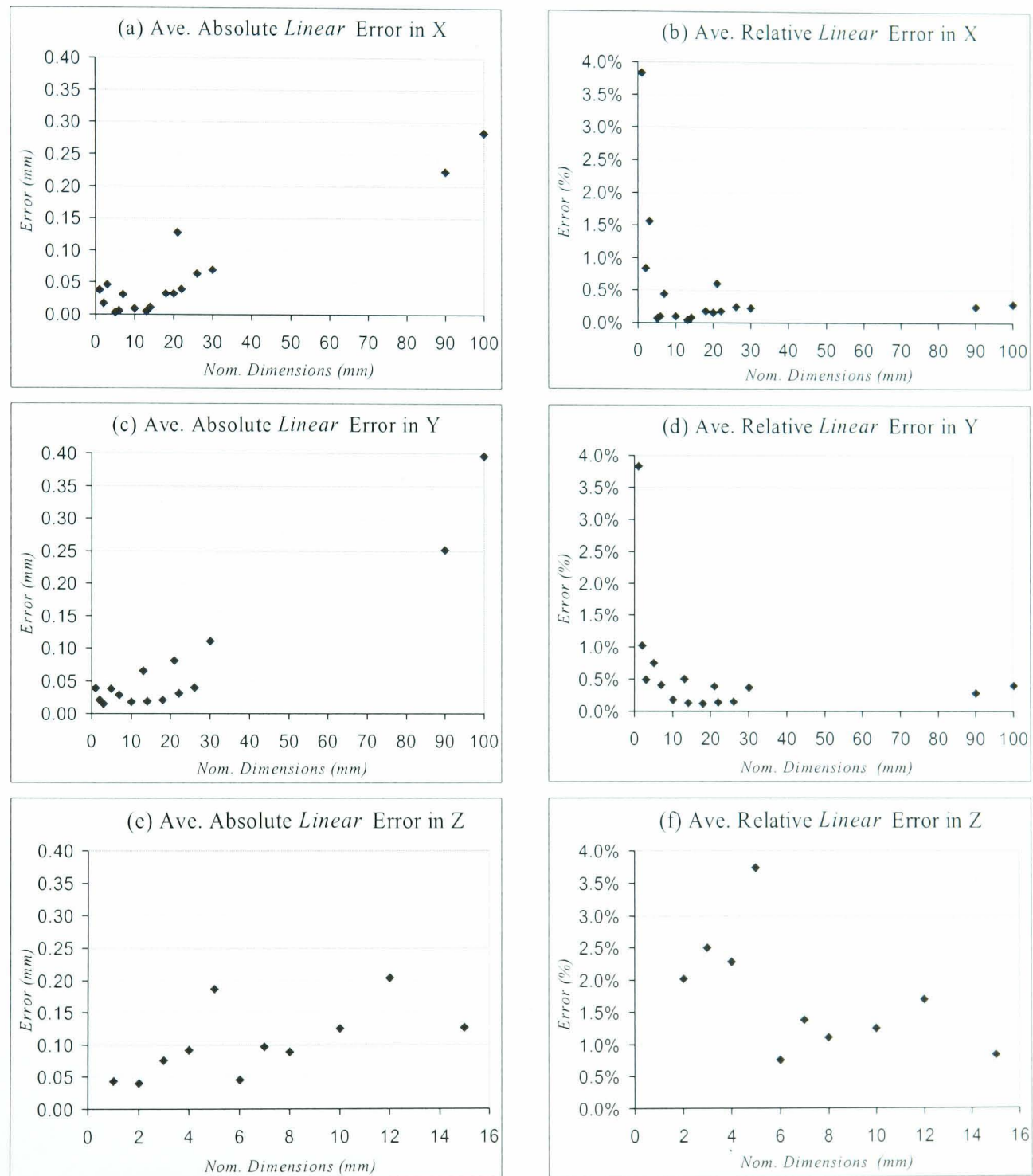


Figure 3-15. Average Linear Errors

In the case of the average relative errors, Figure 3-15. b, d and f show that the average relative error ( $\delta X\%$ ) tend to be highest (up to 3.0%) at the small nominal dimension ( $< 5$  mm) and predominantly in the range 0.0% to 0.5% as the nominal dimensions increase to between 5 mm to 25 mm in all direction.

From both average absolute and relative errors, it is furthermore interesting to find out that the scale factor of 1.00% for both the X and Y building directions, which is set up in developing the green part of the benchmark model, seems to be an appropriate value because the dimensions in these building directions are achieved as expected. However, this is not the case in the Z building direction. The results show that the scale factor of 0.0% set up for the Z building direction needs to be reconsidered due to the significant percentage errors (0.5% to 2.0%) which occur in this direction at nominal dimensions between 5 mm to 15 mm (Figure 3-15.f). Since the Z relative errors range closely similar to X and Y, the same scaling factor might also be applied to compensate for dimensional changes in the Z direction.

Figure 3-16 summarises the average absolute and relative errors for all radial measurements from the circular-based shapes on features 1, 2, 7, 9 and 10 (see Table 3-4. a, b, g, I and j). The results show that the absolute radial error (Figure 3-16.a) is fairly constant as the nominal diameter increases. However, the tendency of the relative radial error (Figure 3-16.b) is similar to the tendency shown in the linear relative error. The average percentage of the relative radial errors tends to be highest up to 3.3% at the diameter less than 5 mm and fairly constant between 0.0% to 0.5% at feature diameter between 5 mm to 40 mm.

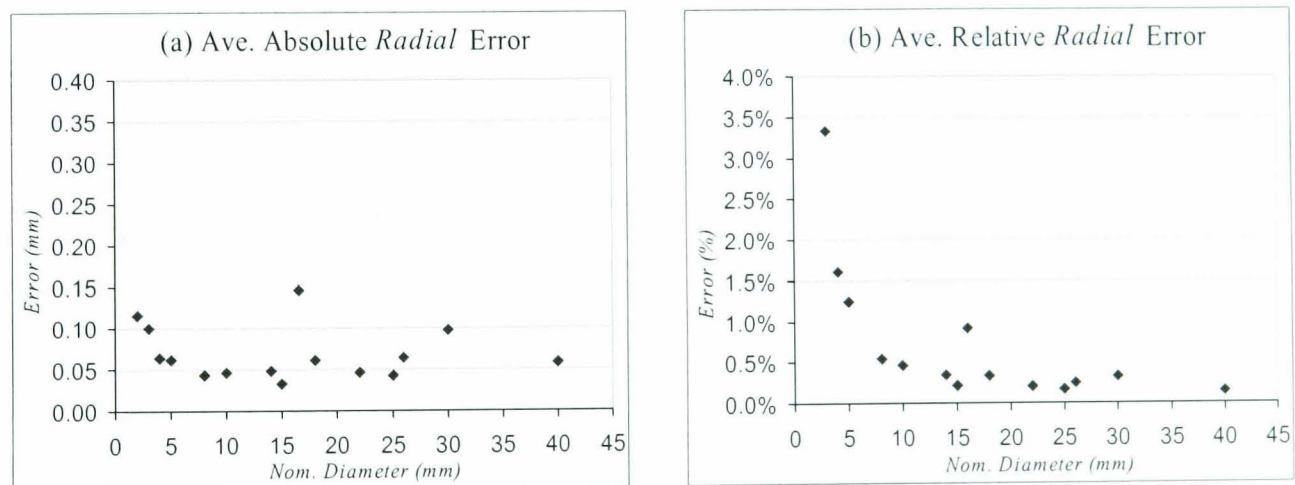


Figure 3-16. Average Radial Error

Concerning paired features indicated in Figure 3-14, the following Figure 3-17 presents the average absolute errors in the X and Y building directions for both features 3 (internal dimensions) and 4 (external dimensions). The average errors indicate that the absolute errors for internal and external dimensions in both X and Y direction are fairly constant at 0.0mm to 0.1mm between the nominal dimension 10mm to 30mm.

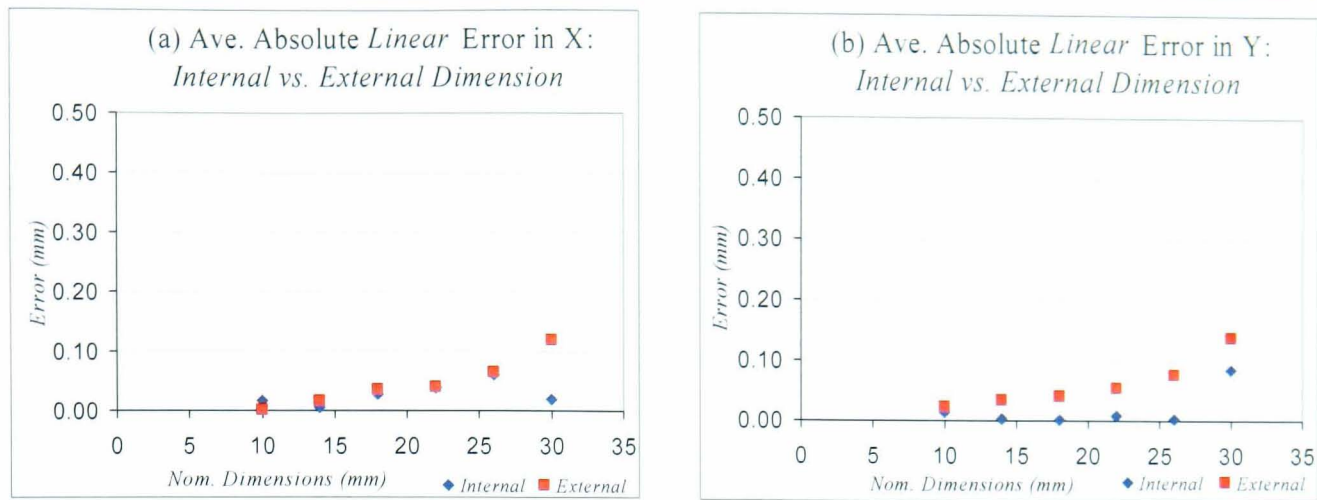


Figure 3-17. Average Absolute Linear Error: Internal vs. External Dimension

Figure 3-18 shows the range of the average relative linear errors for both internal and external dimensions in X and Y building direction. It is indicated that the average errors for both internal and external dimensions in these building direction are also considered constant at 0.0% to 0.3% between 10mm to 30mm.

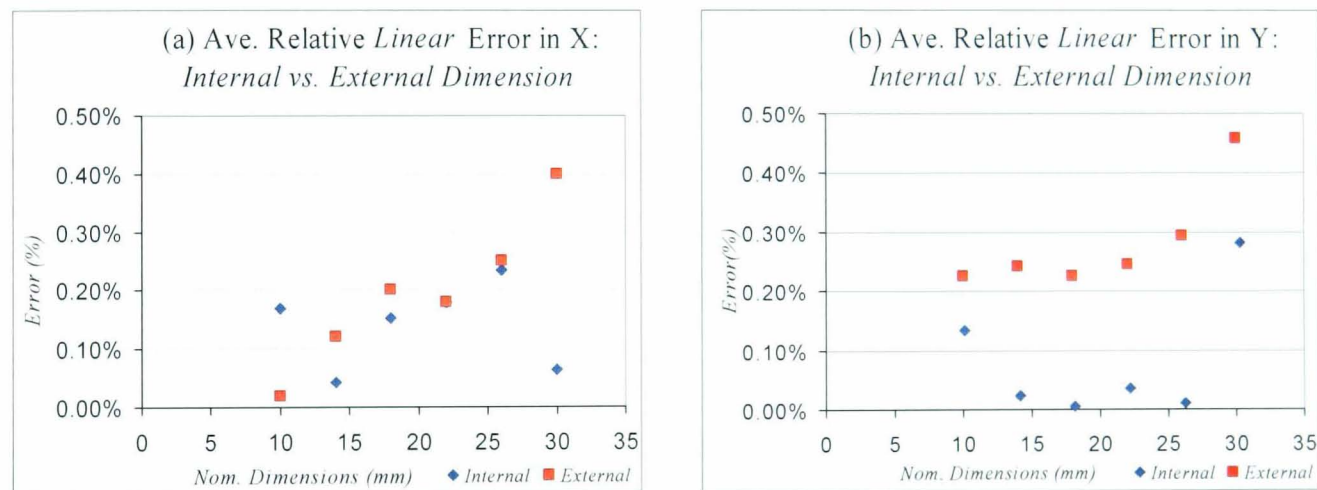


Figure 3-18. Average Relative Linear Error: Internal vs. External Dimension

Furthermore, Figure 3-19 summarizes the average radial errors for paired internal and external diameter for features 1 and 2. The average absolute errors (Figure 3-19.a) for both feature dimensions tend to be constant between 0.0mm to 0.1mm at the diameter of 10mm to 30mm. This result provides a predominantly constant range of an average relative error between 0.2% to 0.4% at the same diameter range.

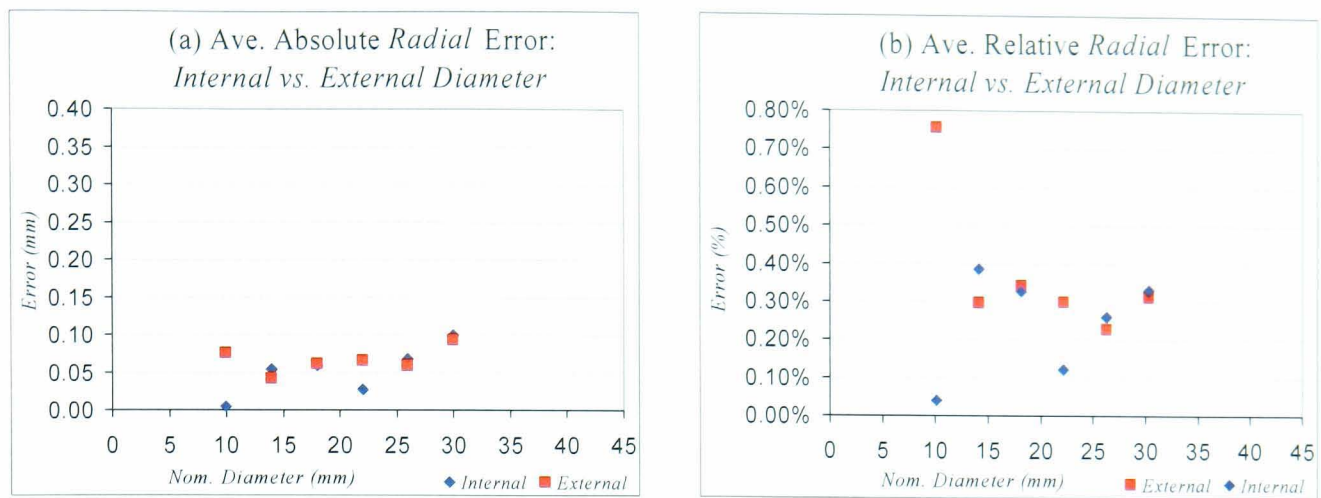


Figure 3-19. Average Absolute and Relative Error: Internal vs. External Diameter

#### 3.4.1.4. Building Limitations

The main purpose of this study was to investigate the capability of the SLS system to create small features. Therefore, the benchmark model of the previous dimensional accuracy study was used because the various features geometrical shape and dimensions can be utilised for representing the result of the study. In the green part stage, two observations concerning the limitations of the SLS system have been made: the green part is very fragile, and some small parts of the features, with a wall thickness of 0.5 mm, are not built on the model. Figure 3-20 shows all the incomplete features.

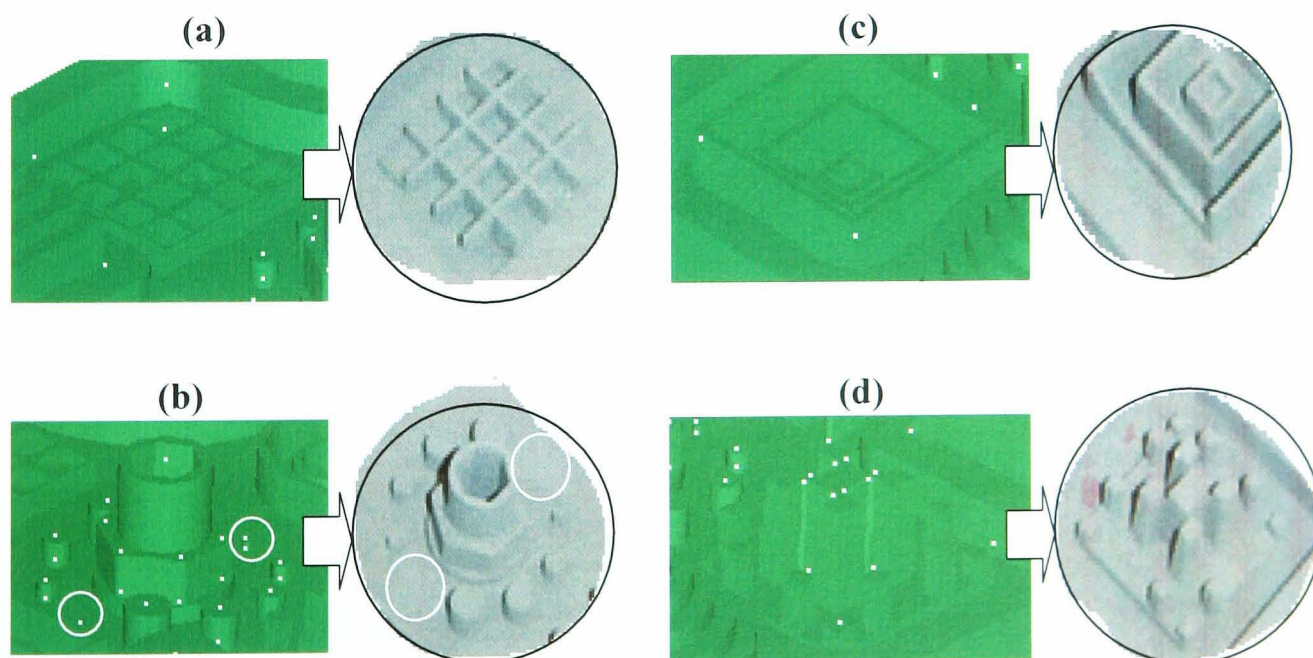


Figure 3-20. Incomplete Features

The fragile green part can cause the smallest geometrical features to be easily broken and brushed away during the cleaning process as is shown in Figure 3-20c and d. Moreover, features not being built at all, however, is attributed to the laser



beam diameter and compensation (offset). In Figure 3-20a, the smallest geometry is the outside wall with the thickness of 0.5 mm. Whilst, the 3D CAD solid model in Figure 3-20b shows two smallest cylinders that have a diameter of 0.5 mm. The intended size of those feature is smaller than the laser beam diameter (~0.6 mm) so it is not possible for them to be created using the SLS machine.

Once the metal part is developed, there are three other important observations. Firstly, there are “sinking marks” on the benchmark model (Figure 3-21). It was visually observed that the relatively thin plate thickness at A (3 mm) and C (1 mm) was the cause of the sinking. Due to the cooling time and material shrinkage, thicker walls cool slower and shrink greater than thinner walls.

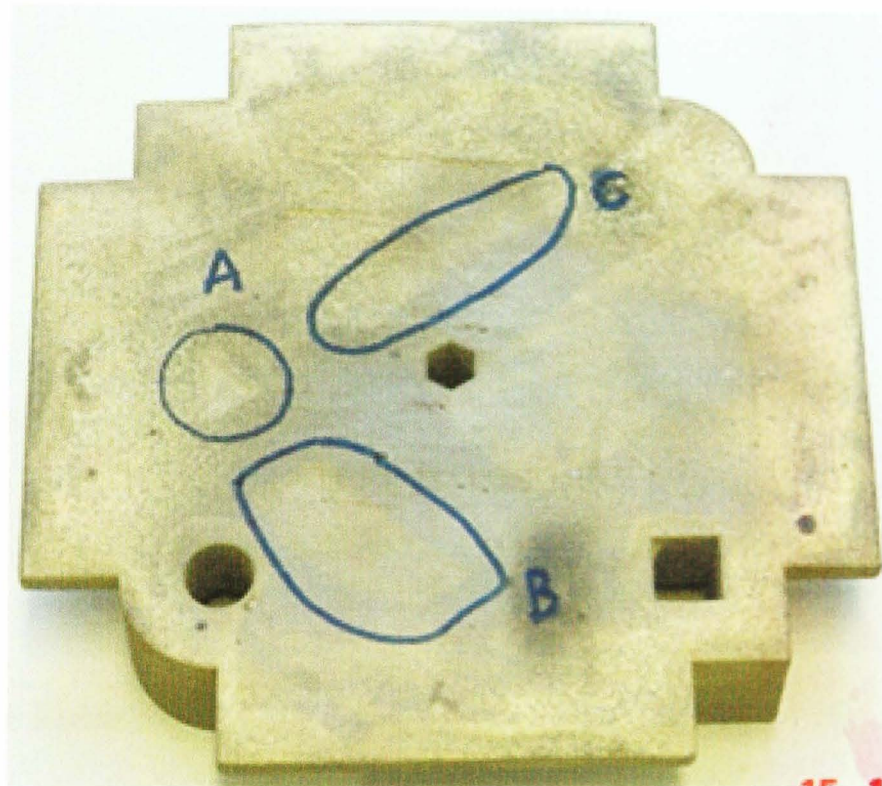


Figure 3-21. Sinking Marks on the Model

The second important observation that the warping causes difficulty in determining a common reference/datum plane for all features. From the measurements, Figure 3-22 illustrates two extreme surface levels between A and B that have a significant difference in average absolute error. This warping is likely to be caused by internal stress due to geometry of the part causing differential cooling when the temperature of the model is lowered.

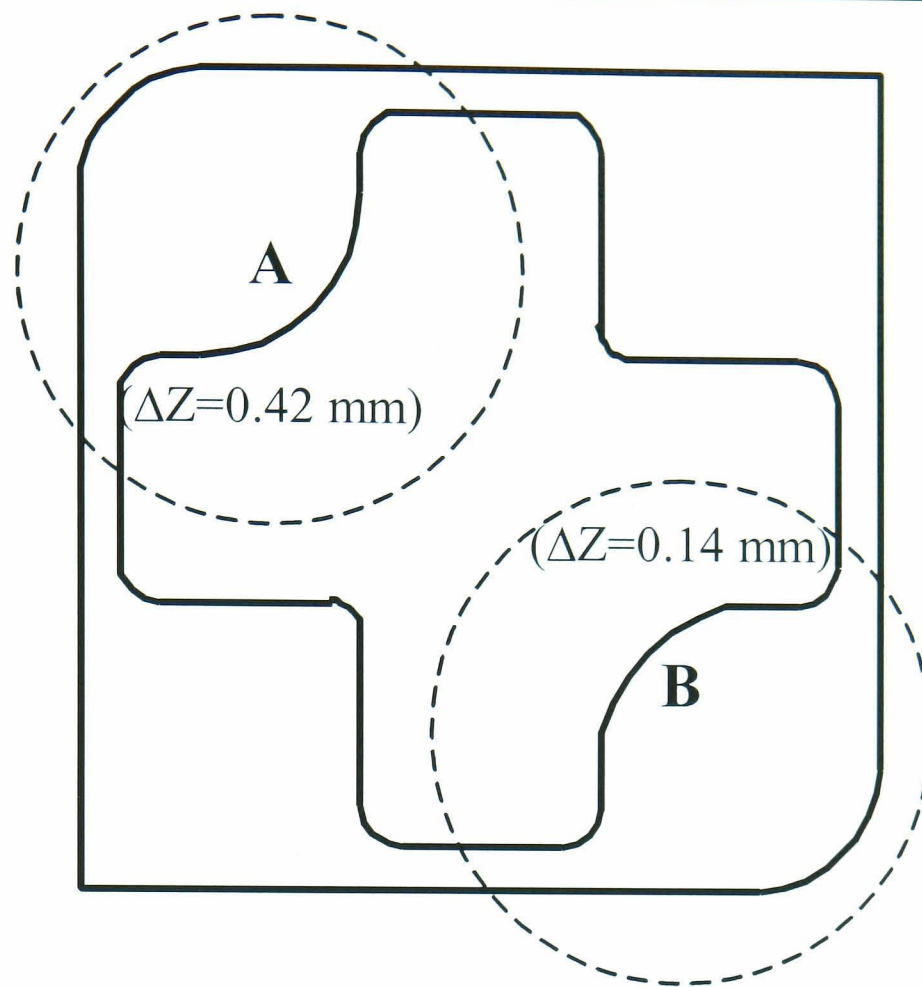


Figure 3-22. Different Absolute Error in Z Direction

The third finding is much more related to the surface finish of the metal part as infiltrated. It is observed that the surface quality of the indirect SLS metal part is relatively rough. A detail study about this surface finish will be explained in section 3.4.3.

### 3.4.2. Surface Flatness

A study on surface flatness was carried out to examine larger scale distortion which could be carried at by looking at the features. In order to characterise surface flatness, a series of measurements in thickness and dimensional changes in Z direction were performed on simple benchmark models (Figure 3-23) which were specifically designed for this study. The models were five 100 x 100 mm plates which had different thicknesses: 5, 10, 15, 20, and 25 mm.

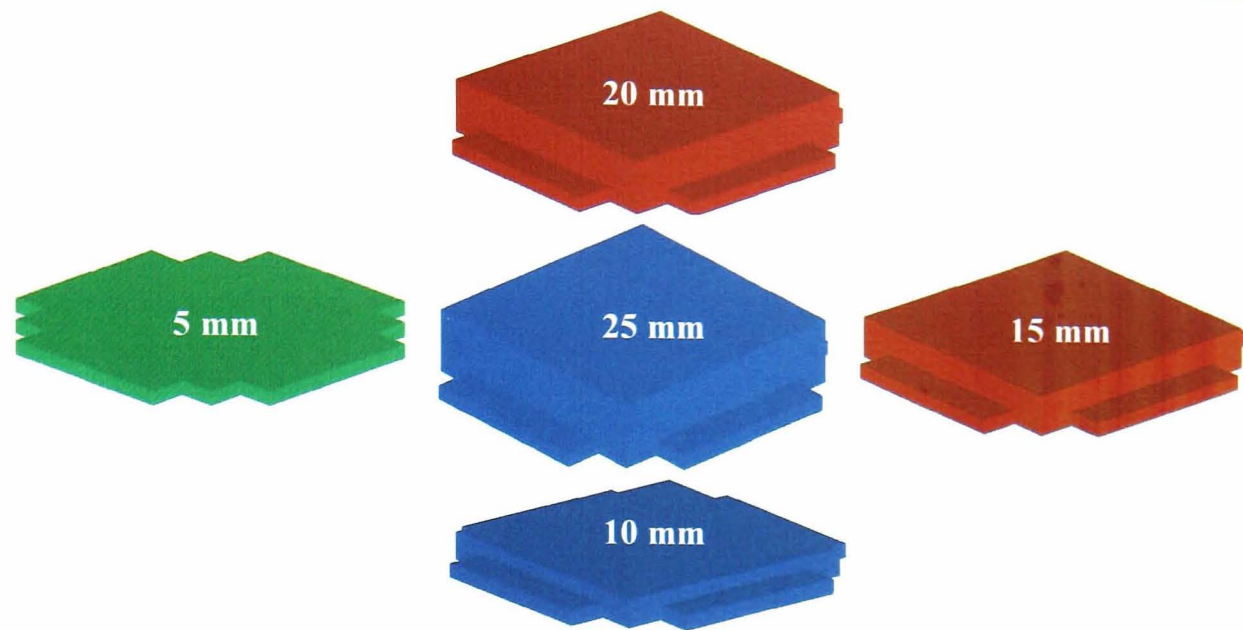


Figure 3-23. 3D CAD Solid Models

The development of the green part (Figure 3-24) and metal part (Figure 3-25) for the benchmark models followed the same procedures as applied previously. In the preparation for bronze infiltration, Table 3-5 shows the total weight of the bronze ingots required proportion to the total weight of each respective green part model.

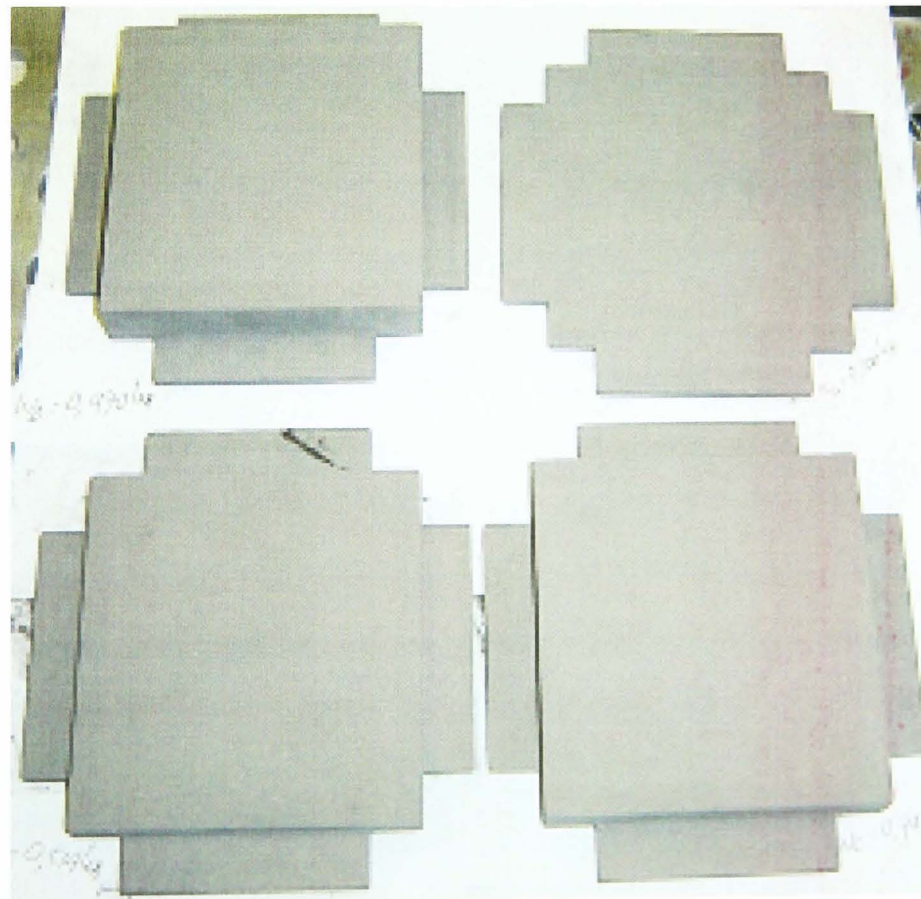


Figure 3-24. Green Part Models

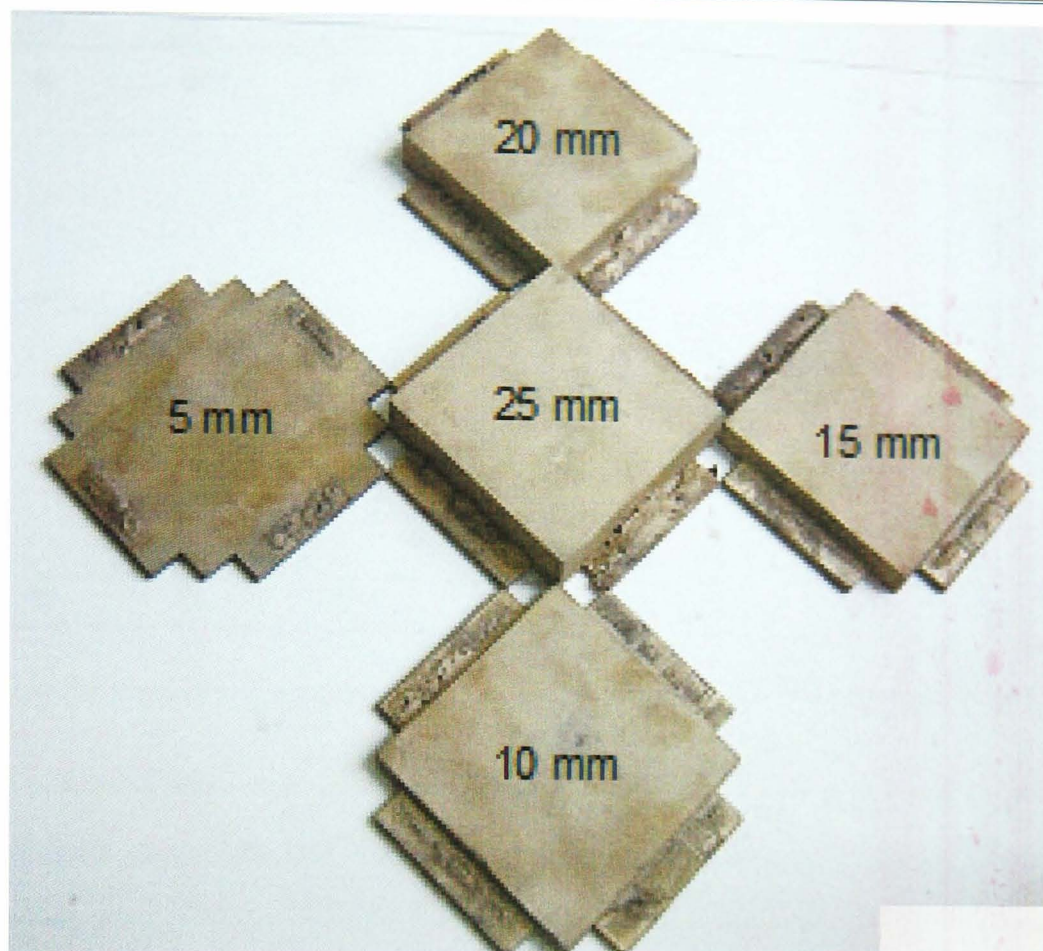


Figure 3-25. Metal Part Models

Table 3-5. Proportion Weight of Bronze Ingots

Plate Thickness (mm)	Tot. Vol (cm <sup>3</sup> )	Weight GP (gr)	Weight Bronze (gr)
5	71	306	220
10	121	514	370
15	171	742	534
20	221	970	698
25	271	1,198	862

To assess the thickness and surface flatness, each model was then measured using a Mitutoyo digital micrometer and the Kemco 400 3D CMM. Figure 3-26 shows the set of the measuring points that is used to determine thickness. Figure 3-27 shows a second set of the measuring points that was used to investigate surface flatness. Equation (3-1) was again used to calculate the average of absolute and relative errors.

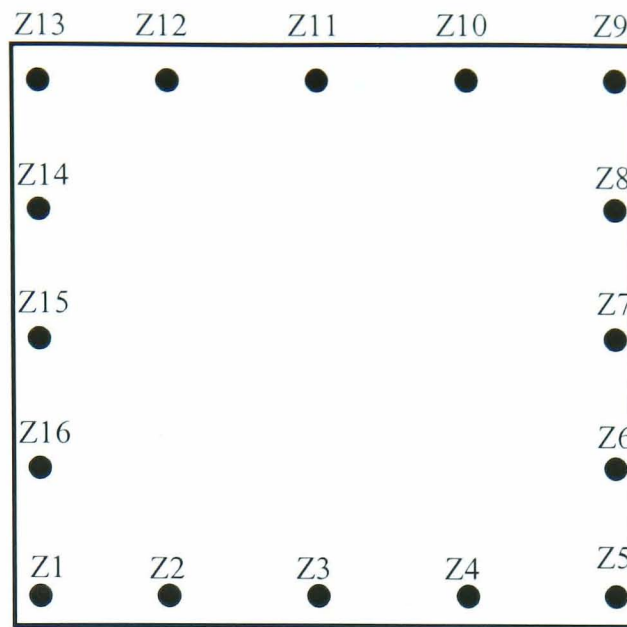


Figure 3-26. Thickness Measuring Points

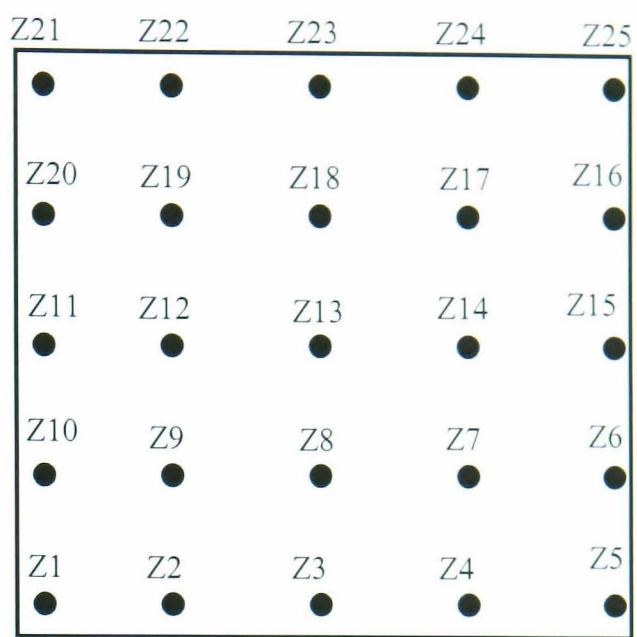


Figure 3-27. Flatness Measuring Points

To investigate the surface flatness of each metal part, the gap between defined datum plane and the Z co-ordinate of the measuring points in Figure 3-27 must be assessed. Figure 3-28 illustrates a schematic diagram of the measurements. The top surfaces of the 3 jaw chuck are defined to be a common datum plane ( $Z = 0$  mm) for the measurements. To analyse and visualise the gap profile and the surface flatness of each benchmark model, the measured Z co-ordinates are then grouped (Figure 3-29) so that they can be plotted relative to the datum plane.

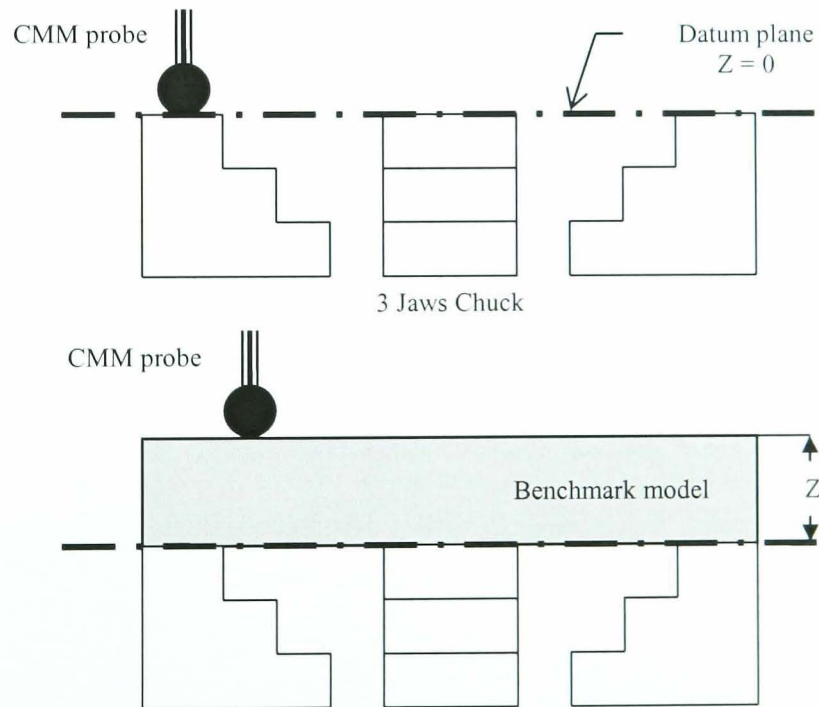
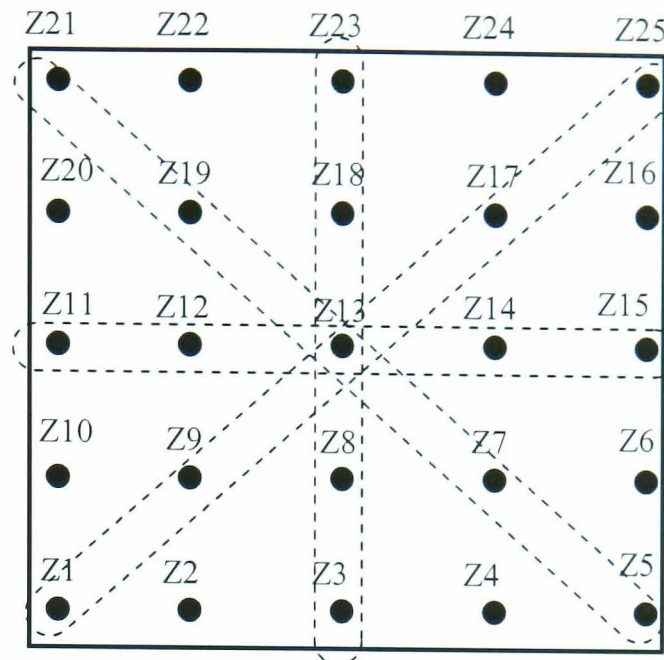


Figure 3-28. Schematic of the Measurements



Points 1	Z1; Z9; Z13; Z17; Z25
Points 2	Z5; Z7; Z13; Z19; Z21
Points 3	Z11; Z12; Z13; Z14; Z15
Points 4	Z3; Z8; Z13; Z18; Z23

Figure 3-29. Groups of Measuring Points

Referring to the defined set points in Figure 3-26, Table 3-6 shows the thickness of each plate as a result of a single measurement at every point, which are then plotted in Figure 3-30. The results show that the absolute error increases with thickness and leaves the plate undersized. The relative error is fairly constant at around 3.0%.

Table 3-6. Thickness Measurements

Thick. Point	5 mm		Ave. Error		10 mm	Ave. Error		15 mm	Ave. Error		20 mm	Ave. Error		25 mm	Ave. Error	
	Abs. (mm)	Rel. (%)	Abs. (mm)	Rel. (%)		Abs. (mm)	Rel. (%)		Abs. (mm)	Rel. (%)		Abs. (mm)	Rel. (%)		Abs. (mm)	Rel. (%)
Z1	4.785	0.215	4.30%	9.690	0.310	3.10%	14.510	0.490	3.27%	19.525	0.475	2.38%	24.935	0.065	0.26%	
Z2	4.825	0.175	3.50%	9.715	0.285	2.85%	14.575	0.425	2.83%	19.465	0.535	2.68%	24.935	0.065	0.26%	
Z3	4.825	0.175	3.50%	9.690	0.310	3.10%	14.545	0.455	3.03%	19.480	0.520	2.60%	24.450	0.550	2.20%	
Z4	4.960	0.040	0.80%	9.640	0.360	3.60%	14.540	0.460	3.07%	19.490	0.510	2.55%	24.360	0.640	2.56%	
Z5	4.750	0.250	5.00%	9.715	0.285	2.85%	14.515	0.485	3.23%	19.550	0.450	2.25%	24.280	0.720	2.88%	
Z6	4.820	0.180	3.60%	9.710	0.290	2.90%	14.580	0.420	2.80%	19.505	0.495	2.48%	24.270	0.730	2.92%	
Z7	4.870	0.130	2.60%	9.650	0.350	3.50%	14.585	0.415	2.77%	19.480	0.520	2.60%	24.275	0.725	2.90%	
Z8	4.875	0.125	2.50%	9.540	0.460	4.60%	14.580	0.420	2.80%	19.520	0.480	2.40%	24.280	0.720	2.88%	
Z9	4.820	0.180	3.60%	9.565	0.435	4.35%	14.550	0.450	3.00%	19.515	0.485	2.43%	24.270	0.730	2.92%	
Z10	4.820	0.180	3.60%	9.560	0.440	4.40%	14.540	0.460	3.07%	19.520	0.490	2.40%	24.295	0.705	2.82%	
Z11	4.875	0.125	2.50%	9.540	0.460	4.60%	14.575	0.425	2.83%	19.510	0.490	2.45%	24.315	0.685	2.74%	
Z12	4.835	0.165	3.30%	9.545	0.455	4.55%	14.610	0.390	2.60%	19.515	0.485	2.43%	24.360	0.640	2.56%	
Z13	4.865	0.135	2.70%	9.520	0.480	4.80%	14.590	0.410	2.73%	19.505	0.495	2.48%	24.345	0.655	2.62%	
Z14	4.850	0.150	3.00%	9.550	0.450	4.50%	14.570	0.430	2.87%	19.510	0.490	2.45%	24.345	0.655	2.62%	
Z15	4.875	0.125	2.50%	9.540	0.460	4.60%	14.530	0.470	3.13%	19.490	0.510	2.55%	24.340	0.660	2.64%	
Z16	4.870	0.130	2.60%	9.665	0.335	3.35%	14.520	0.480	3.20%	19.580	0.420	2.10%	24.360	0.640	2.56%	

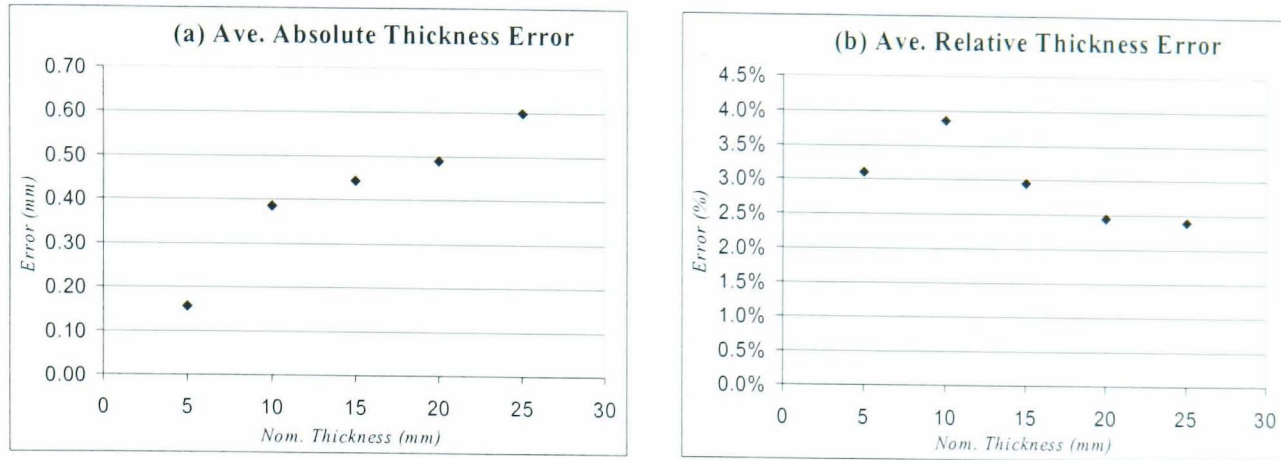


Figure 3-30. Average Absolute and Relative Error of Thickness

Table 3-7 shows the results of measurements of surface flatness. The surface flatness analysis of each metal model is based on the plotted profile gap between the actual Z co-ordinate of the measuring points in Figure 3-29 and the intended thickness of its respective plate. Figure 3-31 illustrates the surface profiles of all benchmark models accordingly.

Table 3-7. Flatness Measurements

Thick.	5 mm		10 mm		15 mm		20 mm		25 mm	
	Z coord. (mm)	Gap (mm)	Z coord. (mm)	Gap (mm)	Z coord. (mm)	Gap (mm)	Z coord. (mm)	Gap (mm)	Z coord. (mm)	Gap (mm)
Z1	4.864	-0.136	9.700	-0.300	14.567	-0.433	19.559	-0.441	24.243	-0.757
Z2	4.912	-0.088	9.701	-0.299	14.555	-0.445	19.526	-0.474	24.274	-0.726
Z3	4.898	-0.102	9.715	-0.285	14.560	-0.440	19.494	-0.506	24.317	-0.683
Z4	4.906	-0.094	9.727	-0.273	14.564	-0.436	19.523	-0.477	24.357	-0.643
Z5	5.027	0.027	9.798	-0.202	14.592	-0.408	19.531	-0.469	24.376	-0.624
Z6	4.760	-0.240	9.751	-0.249	14.587	-0.413	19.534	-0.466	24.345	-0.655
Z7	4.806	-0.194	9.656	-0.344	14.540	-0.460	19.479	-0.521	24.344	-0.656
Z8	4.825	-0.175	9.637	-0.363	14.509	-0.491	19.467	-0.533	24.331	-0.669
Z9	4.864	-0.136	9.671	-0.329	14.533	-0.467	19.507	-0.493	24.281	-0.719
Z10	4.924	-0.076	9.669	-0.331	14.510	-0.490	19.551	-0.449	24.246	-0.754
Z11	4.912	-0.088	9.620	-0.380	14.541	-0.459	19.551	-0.449	24.250	-0.750
Z12	4.924	-0.076	9.610	-0.390	14.500	-0.500	19.512	-0.488	24.300	-0.700
Z13	4.867	-0.133	9.588	-0.412	14.506	-0.494	19.470	-0.530	24.360	-0.640
Z14	4.843	-0.157	9.658	-0.342	14.507	-0.493	19.491	-0.509	24.352	-0.648
Z15	4.845	-0.155	9.664	-0.336	14.574	-0.426	19.554	-0.446	24.362	-0.638
Z16	4.947	-0.053	9.537	-0.463	14.634	-0.366	19.600	-0.400	24.376	-0.624
Z17	4.889	-0.111	9.510	-0.490	14.561	-0.439	19.519	-0.481	24.374	-0.626
Z18	4.888	-0.112	9.505	-0.495	14.534	-0.466	19.497	-0.503	24.362	-0.638
Z19	4.903	-0.097	9.601	-0.399	14.550	-0.450	19.530	-0.470	24.316	-0.684
Z20	4.930	-0.070	9.604	-0.396	14.590	-0.410	19.581	-0.419	24.279	-0.721
Z21	4.936	-0.064	9.607	-0.393	14.668	-0.332	19.613	-0.387	24.305	-0.695
Z22	4.893	-0.107	9.543	-0.457	14.633	-0.367	19.577	-0.423	24.323	-0.677
Z23	4.810	-0.190	9.493	-0.507	14.600	-0.400	19.532	-0.468	24.350	-0.650
Z24	4.797	-0.203	9.519	-0.481	14.616	-0.384	19.556	-0.444	24.374	-0.626
Z25	5.097	0.097	9.502	-0.498	14.677	-0.323	19.569	-0.431	24.402	-0.598

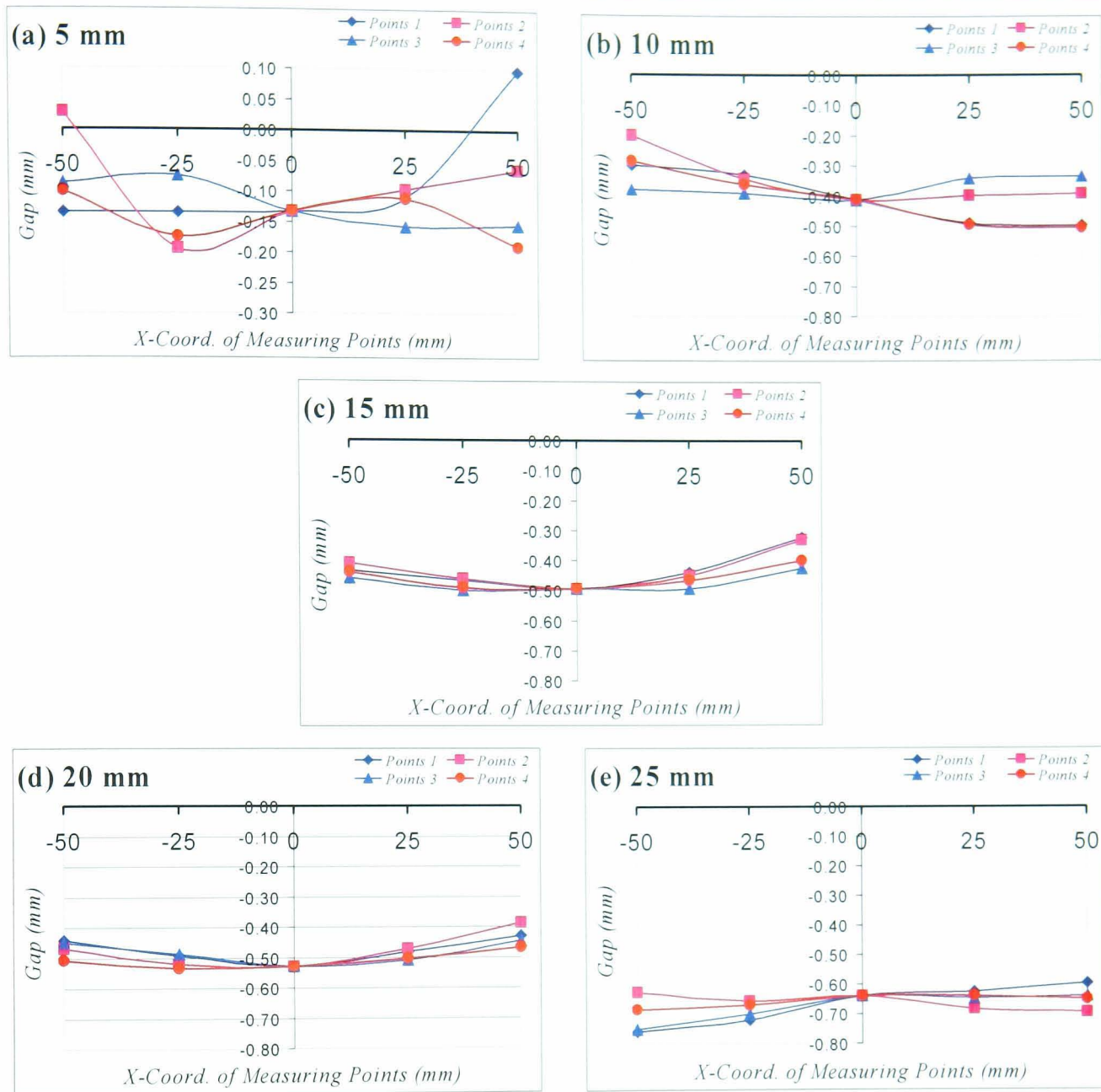


Figure 3-31. Surface Gap Profiles of the Benchmark Models

### 3.4.3. Surface Finish

The main objective of the surface finish study is to assess and investigate the surface roughness of a metal part as a result of the indirect SLS process, as well as a result of the part after post-processing (machining and polishing).

#### 3.4.3.1. Model Development

For the purpose of the study, a simple ST-100 metal plate is designed and manufactured using the same route and operating set up as the previous studies. The metal plate was then machined on a Bridgeport Portal machining centre (high speed milling machine) using a 2 mm diameter ball nose solid carbide cutter, with set-up operating parameters: 15,000 rpm spindle speed, 1200 mm/min federate, 0.2 mm



depth of cut, 0.04 mm feed/tooth, 0.1 mm step over, and 94m/min. This trial was carried out by Delcam (UK) Ltd, an industrial collaborator with the Manufacturing Research Group at the University of Leeds. Following this, the metal plate is then polished to produce six different surface qualities. Figure 3-32 shows the final result of the metal plate after machining and polishing. The figure also indicates measured locations, including the six different polished areas. The differences among those six polished areas were as follows:

- Area 1: prepared with 400 grit paper and then finished with 600 grit paper
- Area 2: polished only with 600 grit paper
- Area 3: prepared with 400 grit paper and then finished with dry 1200 grit paper
- Area 4: prepared with 400 grit paper and then finished with wet 1200 grit paper
- Area 5: prepared with 400 grit paper and then finished with wet 1200 grit paper and 6 $\mu$ m diamond polishing.
- Area 6: prepared with 400 grit paper and wet 1200 grit paper, and then finished with 6 $\mu$ m and 1 $\mu$ m diamond polishing

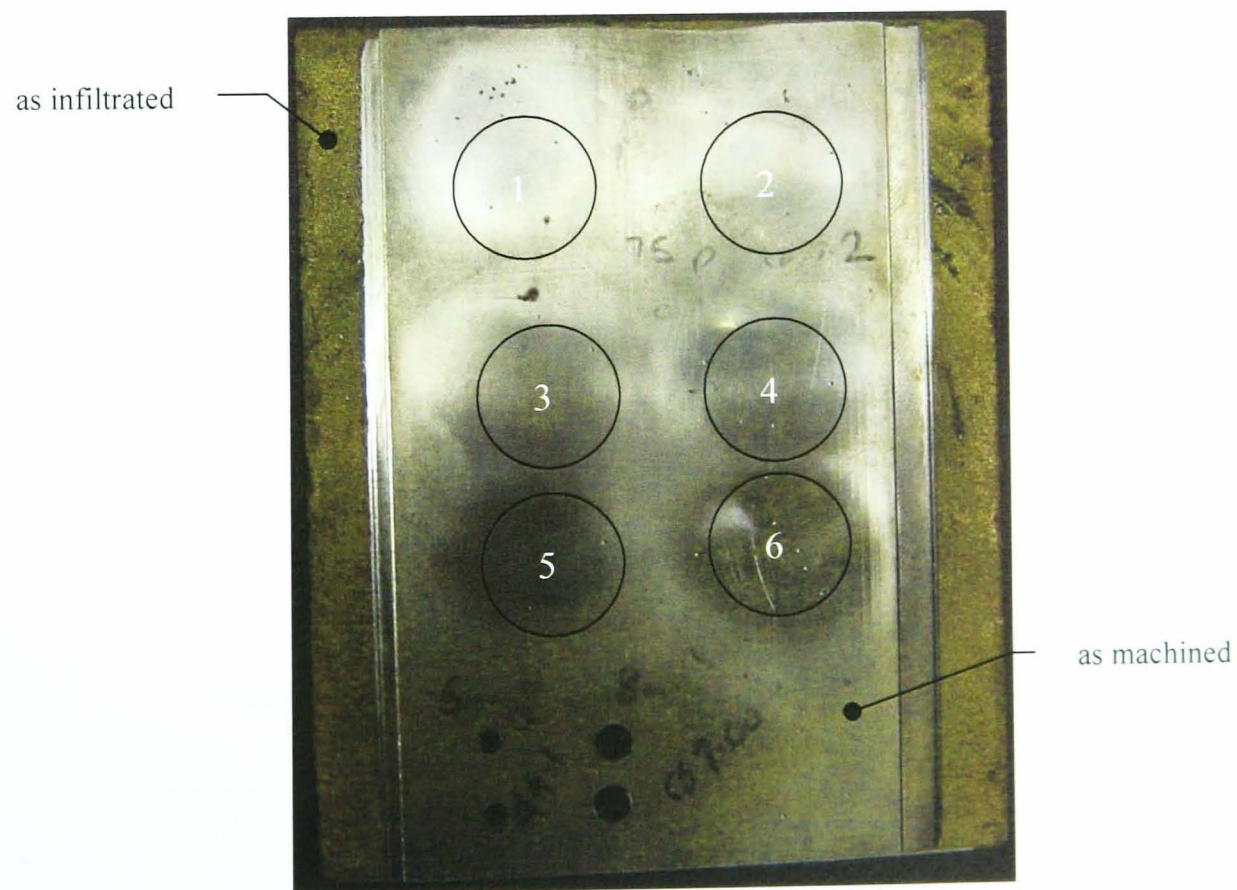


Figure 3-32. SLS Metal Plate for Surface Roughness and Hardness

During polishing process, there are two observations need to be considered when achieving required quality. Firstly, it is observed that a series of grit sizes is required to smooth the surface as a result of the previous grit size. Secondly, cleanliness before diamond polishing, is crucial due to lots of material dirt between grade.

### 3.4.3.2. Model Measurements

A WYKO<sup>®</sup> NT3300S surface profiler was employed to measure the surface roughness and to characterise the surface profile of the metal plate. The schematic diagram in Figure 3-33 shows that this typical machine is a non-contact optical profiler that uses two techniques to measure a wide range of surface heights. Phase-shifting interferometry (PSI) mode is usually used to measure smooth surfaces and small steps, while the vertical scanning interferometry (VSI) mode is to measure rough surfaces and steps up to several millimetre high. The basic interferometric principles are similar in both techniques: light reflected from a reference mirror combines with light reflected from a measured sample to produce interference fringes, where the best-contrast fringe occurs at best focus [Lamb, 1999].

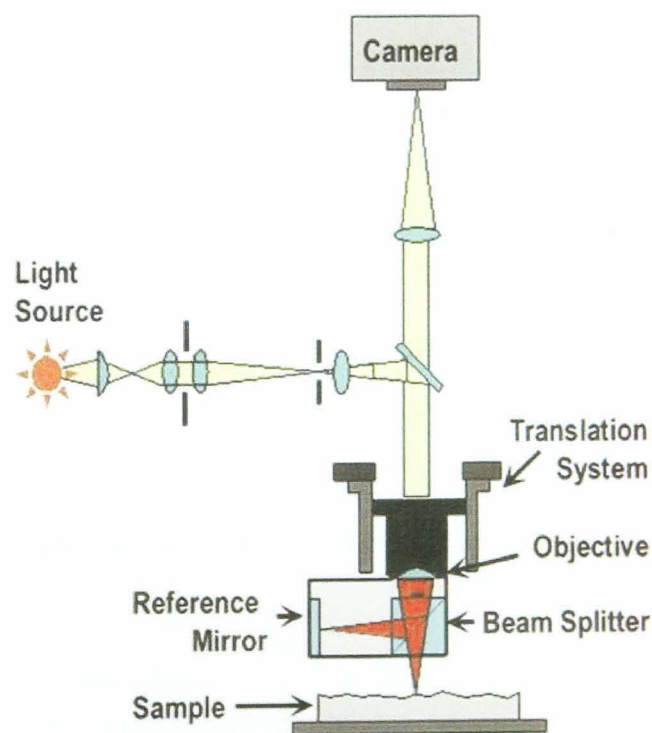


Figure 3-33. Schematic Diagram of an Optical Profiler [Lamb, 1999]

The main measurement made was a surface roughness average ( $R_a$ ). The  $R_a$  is an arithmetical mean of the deviations of the roughness profile from the mean line along the measurement. This  $R_a$  definition is set out in equation (3-2), where  $y(x)$  is the profile values of the roughness profile and  $L$  is the evaluation length.

Graphically,  $R_a$  is the area between the roughness profile and its mean line divided by the evaluation length, which normally equal to five lengths of cut-off filter (Figure 3-34). In practice,  $R_a$  is generally used to describe the roughness of surfaces. It is useful for detecting general variations in overall surface height characteristics and for monitoring an establishing process [Lamb, 1999].

$$R_a = \frac{1}{L} \int_0^L |y(x)| \cdot dx \dots (3-2)$$

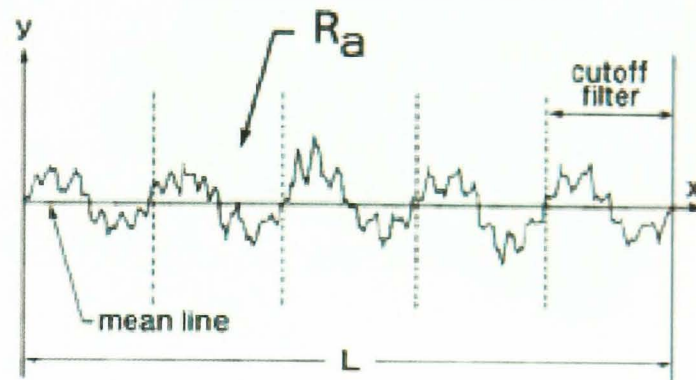


Figure 3-34. Average Surface Roughness  $R_a$  [Lamb, 1999]

### 3.4.3.3. Results

The machine operators at Delcam reported that the ST-100 material was qualitatively similar to nickel aluminium bronze. Tool wear occurred after 90 m or 75 minutes of cutting using the operating parameters mentioned previously. The

Figure 3-35 to 3-42 show the surface profiles and roughness measurement results, whilst, Figure 3-43 summarizes the average surface measurements ( $R_a$  value) on each selected location. These results show that the material could be polished to the quality of surface roughness ( $R_a$ ) of  $0.08 \mu\text{m}$ . However, the surface pores of the material or deep scratches from the machining cannot be completely removed by polishing as they are clearly exposed in the following 3D images of the measurements.

**Surface Stats:**

Ra: 1.92  $\mu\text{m}$   
Rq: 2.43  $\mu\text{m}$   
Rp: 9.99  $\mu\text{m}$   
Rv: -5.22  $\mu\text{m}$   
Rt: 15.21  $\mu\text{m}$   
Rpm: 9.42  $\mu\text{m}$   
Rvm: -4.57  $\mu\text{m}$   
Rsk: 0.92

**Measurement Info:**

Magnification: 10.37  
Measurement Mode: VSI  
Sampling: 809.93 nm  
Array Size: 736 X 480  
Filtering: None

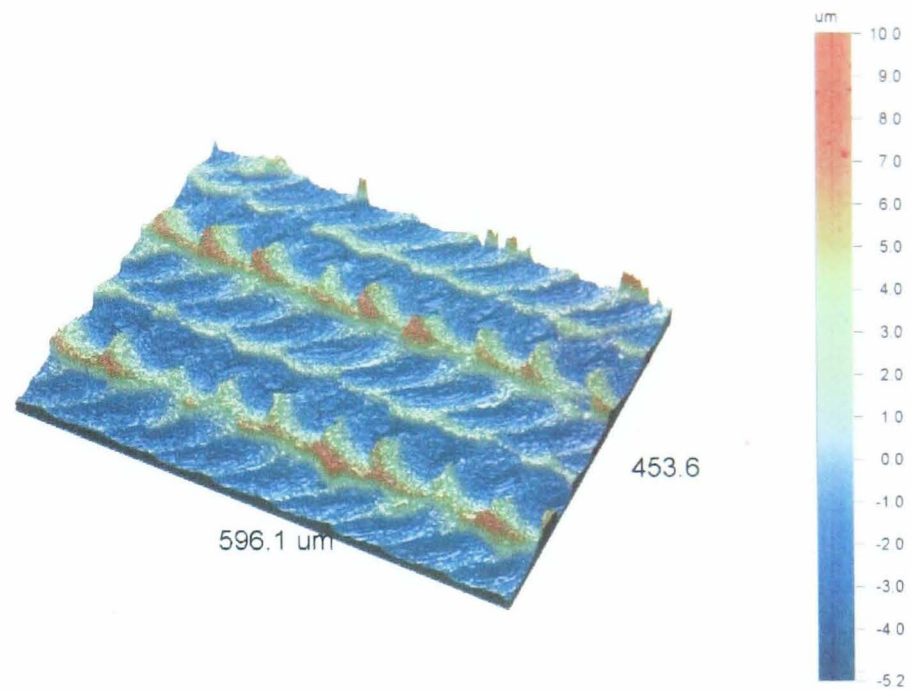


Figure 3-35. As Infiltrated

**Surface Stats:**

Ra: 1.25  $\mu\text{m}$   
Rq: 1.52  $\mu\text{m}$   
Rp: 5.57  $\mu\text{m}$   
Rv: -3.99  $\mu\text{m}$   
Rz: 8.70  $\mu\text{m}$   
Rpm: 5.01  $\mu\text{m}$   
Rvm: -3.69  $\mu\text{m}$   
Rsk: 0.33  
**Rt: 9.56  $\mu\text{m}$**

**Measurement Info:**

Magnification: 10.37  
Measurement Mode: VSI  
Sampling: 809.93 nm  
Array Size: 736 X 480  
Filtering: Median

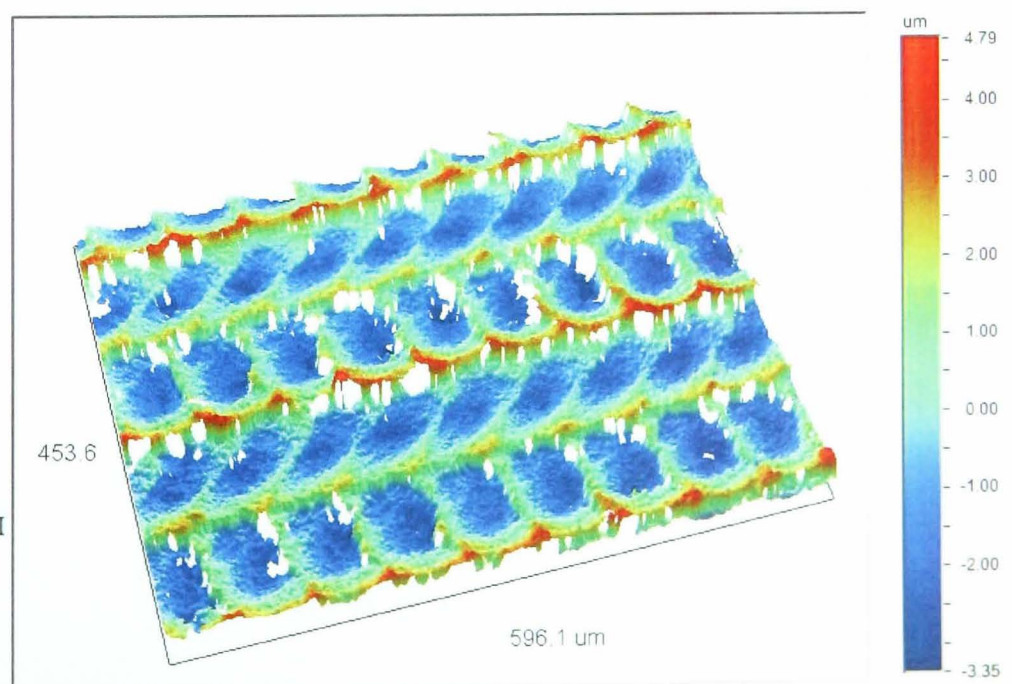


Figure 3-36. As Machined

**Surface Stats:**

Ra: 141.93 nm  
 Rq: 180.88 nm  
 Rp: 805.92 nm  
 Rv: -1.03 um  
 Rz: 1.58 um  
 Rpm: 722.06 nm  
 Rvm: -853.58 nm  
 Rsk: -0.30

**Rt: 1.84 um**

**Measurement Info:**

Magnification: 10.37  
 Measurement Mode: VSI  
 Sampling: 809.93 nm  
 Array Size: 736 X 480  
 Filtering: Median

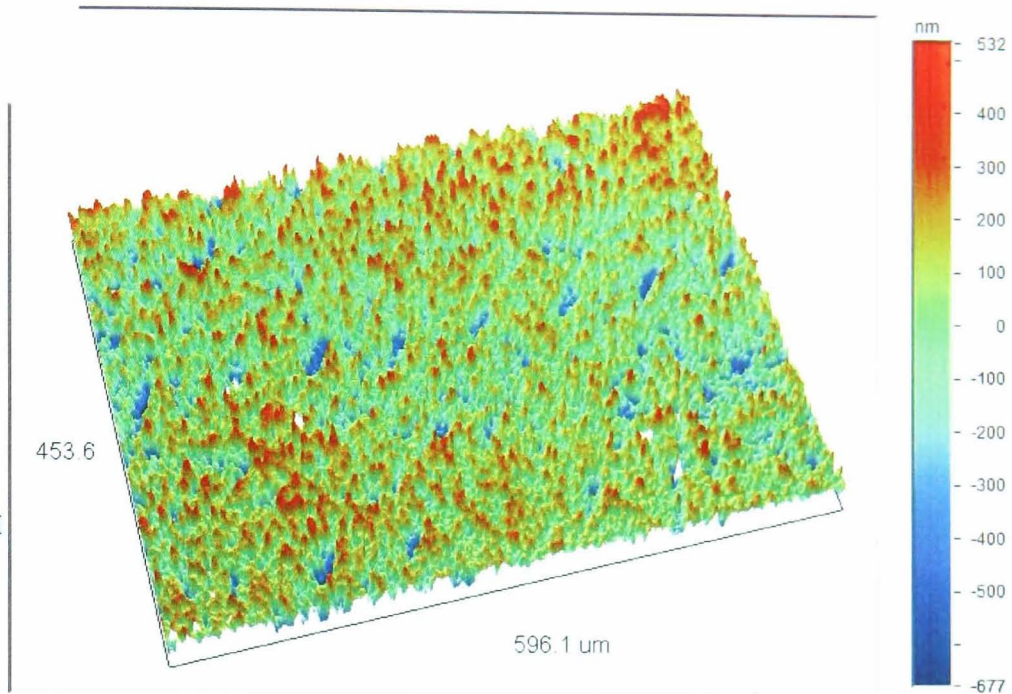


Figure 3-37. As Polished (area 1)

**Surface Stats:**

Ra: 176.89 nm  
 Rq: 231.94 nm  
 Rp: 899.64 nm  
 Rv: -1.16 um  
 Rz: 1.91 um  
 Rpm: 829.71 nm  
 Rvm: -1.08 um  
 Rsk: -0.71

**Rt: 2.06 um**

**Measurement Info:**

Magnification: 10.37  
 Measurement Mode: VSI  
 Sampling: 809.93 nm  
 Array Size: 736 X 480  
 Filtering: Median

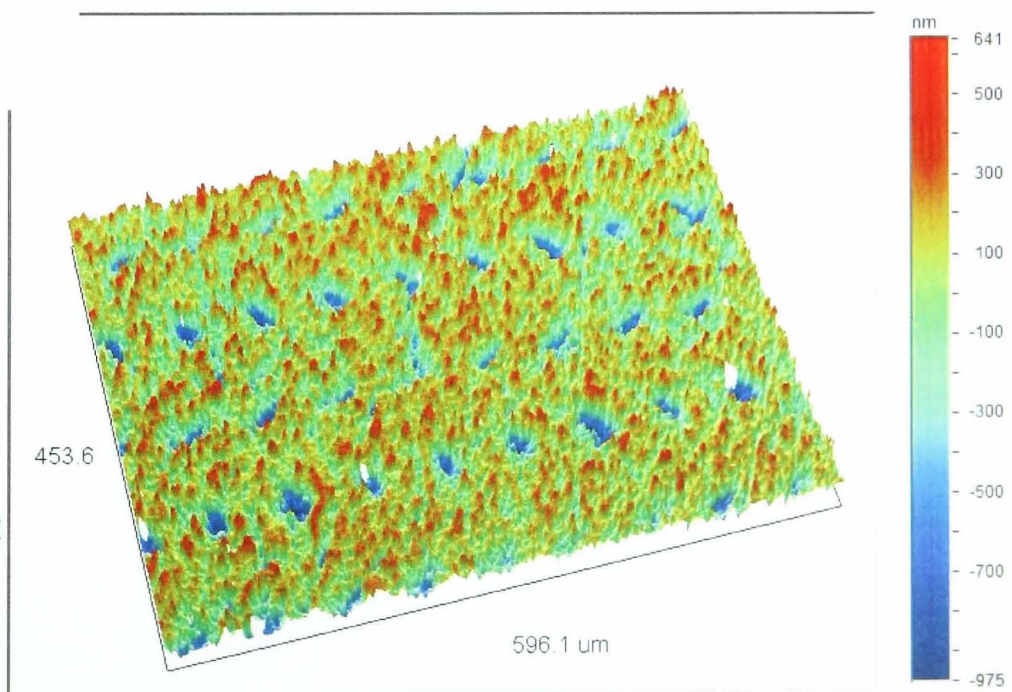


Figure 3-38. As Polished (area 2)

**Surface Stats:**  
Ra: 164.01 nm  
Rq: 215.23 nm  
Rp: 816.09 nm  
Rv: -1.43 um  
Rz: 1.92 um  
Rpm: 682.96 nm  
Rvm: -1.24 um  
Rsk: -0.99  
**Rt: 2.24 um**  
**Measurement Info:**  
Magnification: 10.37  
Measurement Mode: VSI  
Sampling: 809.93 nm  
Array Size: 736 X 480  
Filtering: Median

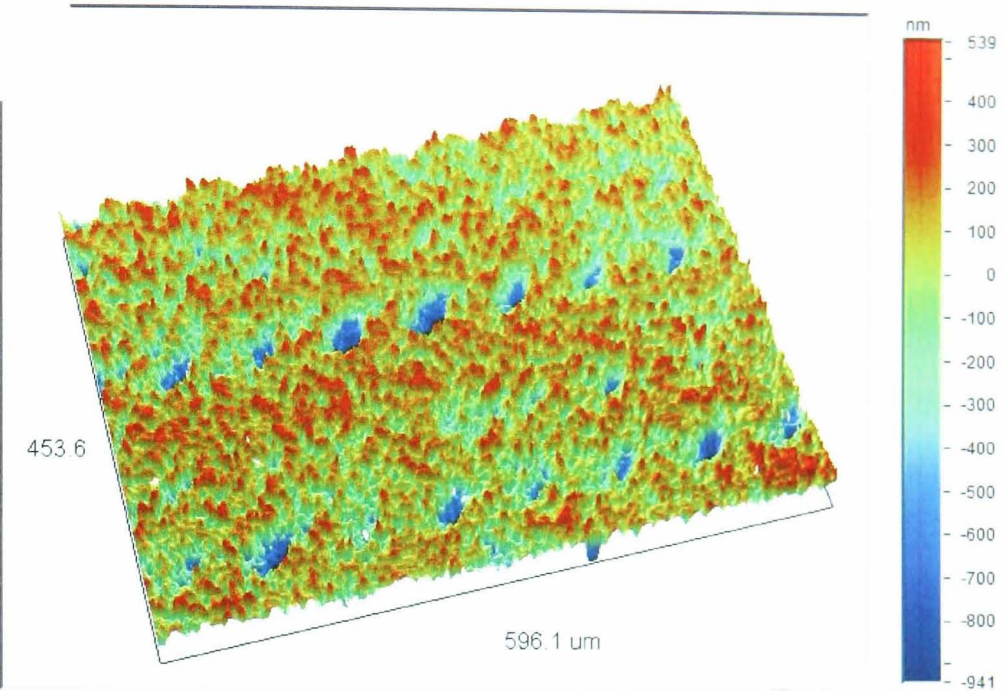


Figure 3-39. As Polished (area 3)

**Surface Stats:**  
Ra: 120.61 nm  
Rq: 153.26 nm  
Rp: 905.12 nm  
Rv: -1.15 um  
Rz: 1.63 um  
Rpm: 710.40 nm  
Rvm: -918.16 nm  
Rsk: -0.42  
**Rt: 2.06 um**  
**Measurement Info:**  
Magnification: 10.37  
Measurement Mode: VSI  
Sampling: 809.93 nm  
Array Size: 736 X 480  
Filtering: Median

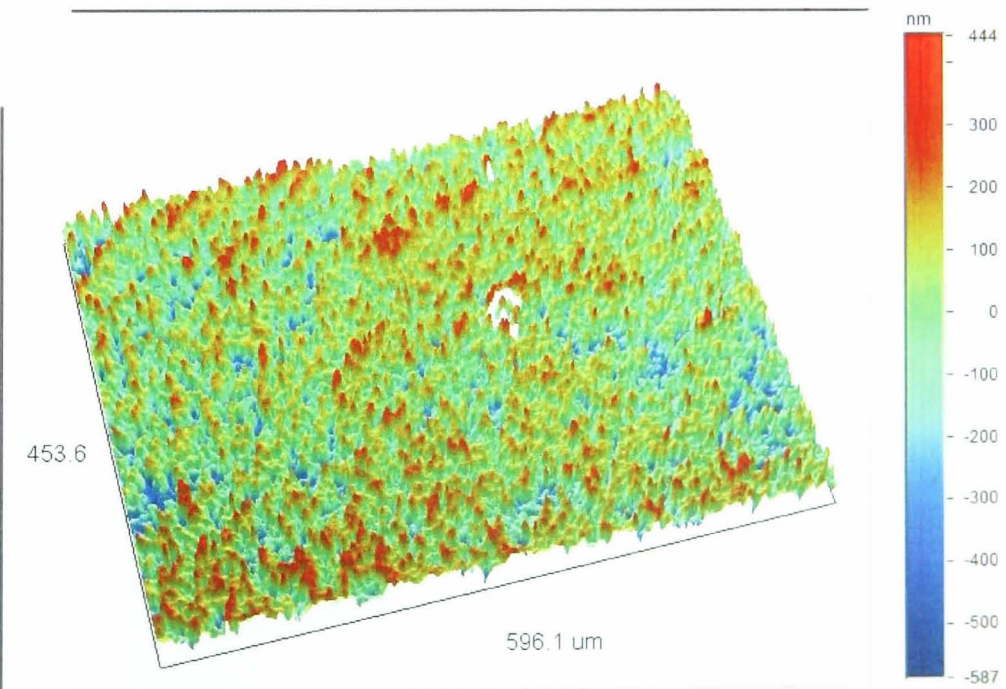


Figure 3-40. As Polished (area 4)

**Surface Stats:**

Ra: 166.06 nm  
Rq: 222.97 nm  
Rp: 736.26 nm  
Rv: -1.40 um  
Rz: 1.90 um  
Rpm: 654.25 nm  
Rvm: -1.24 um  
Rsk: -1.30  
**Rt: 2.14 um**  
**Measurement Info:**  
Magnification: 10.37  
Measurement Mode: VSI  
Sampling: 809.93 nm  
Array Size: 736 X 480  
Filtering: Median

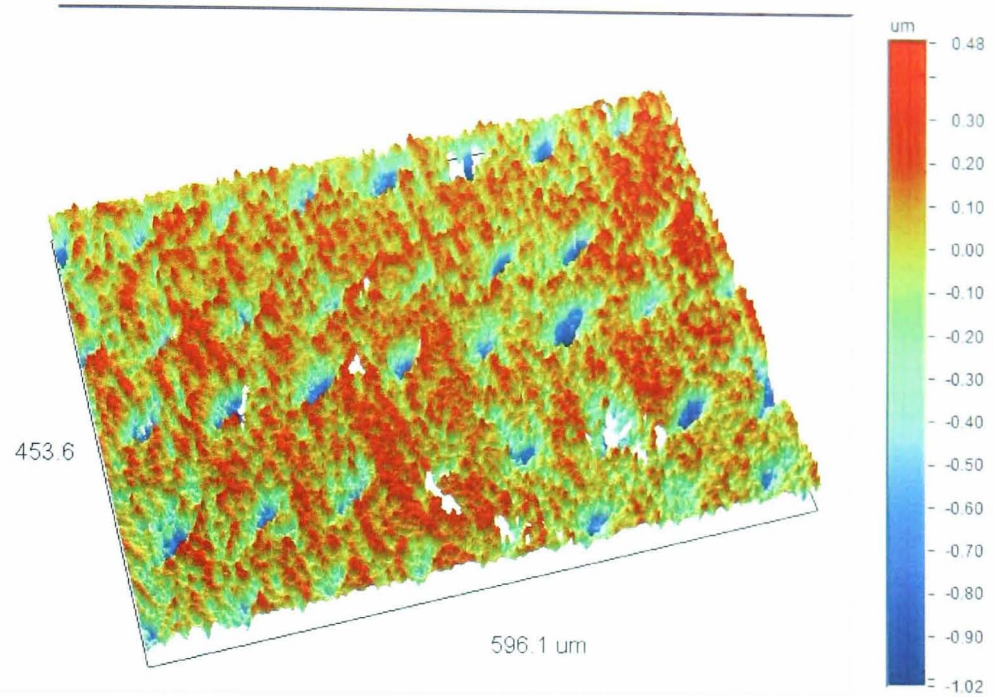


Figure 3-41. As Polished (area 5)

**Surface Stats:**

Ra: 83.81 nm  
Rq: 116.06 nm  
Rp: 648.70 nm  
Rv: -780.08 nm  
Rz: 1.18 um  
Rpm: 527.59 nm  
Rvm: -657.12 nm  
Rsk: -1.17  
**Rt: 1.43 um**  
**Measurement Info:**  
Magnification: 10.37  
Measurement Mode: VSI  
Sampling: 809.93 nm  
Array Size: 736 X 480  
Filtering: Median

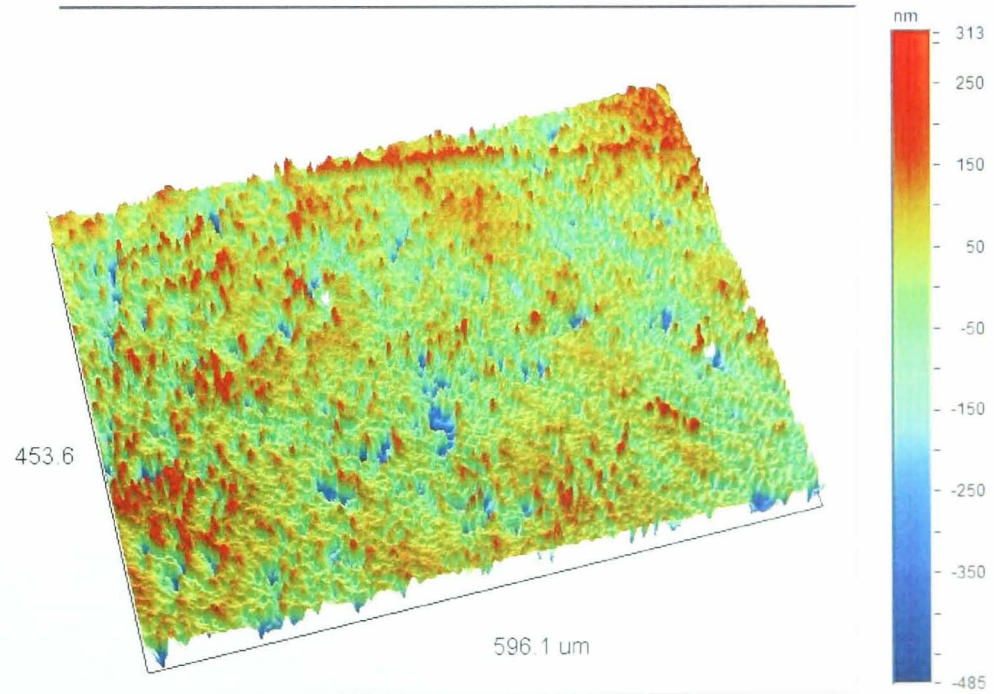


Figure 3-42. As Polished (area 6)

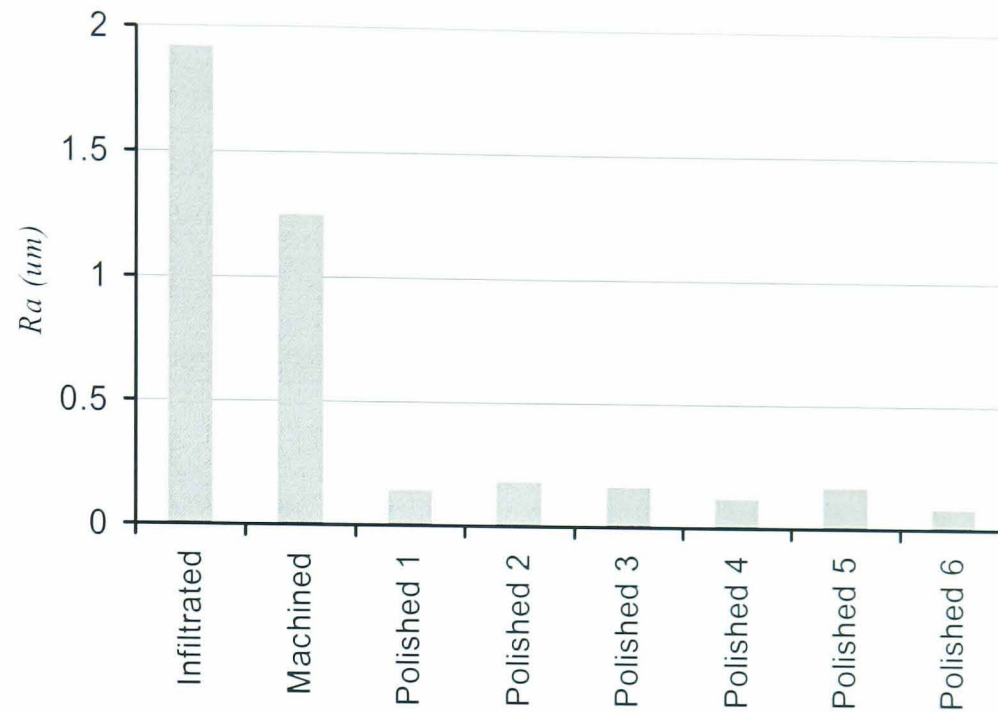


Figure 3-43. Average Surface Roughness Summary

#### 3.4.4. Surface Hardness

In measuring surface hardness, the same SLS metal plate used in the previous surface finish study was used, with the material hardness also measured at the eight locations indicated on Figure 3-32. The measurements were carried out using an INDENTEC 6187.5LK hardness testing machine (Figure 3-9) using standard measuring procedure of the Rockwell scale B test. The machine are equipped with 1/16" steel-ball indenter and  $\varnothing$  70 mm flat anvil. Three samples of the measurements are taken at each selected location as shown in Table 3-8.

Table 3-8. The Hardness Measurement Results

Measurements Location		Hardness (HR <sub>B</sub> )			
		1	2	3	Average
As Infiltrated		84.6	81.3	81.2	<b>82.4</b>
As Machined		82.8	79.1	83.2	<b>81.7</b>
As Polished	Area 1	83.9	83.6	84.2	<b>83.9</b>
	Area 2	86.1	83.6	85.0	<b>84.9</b>
	Area 3	82.8	83.8	84.0	<b>83.5</b>
	Area 4	83.9	84.0	84.8	<b>84.2</b>
	Area 5	84.8	84.9	85.3	<b>85.0</b>
	Area 6	86.1	85.1	84.4	<b>85.2</b>



### 3.4.5. Material Porosity

The primary objective of the material porosity study is to investigate whether the SLS metal part would leak as a result of porosity. Figure 3-44 shows the 3D CAD solid model of a test piece, which was designed to have an 8 mm diameter cooling line to represent cooling channel inside the mould inserts. The metal test piece (Figure 3-45) is developed under the same route and operating parameters.

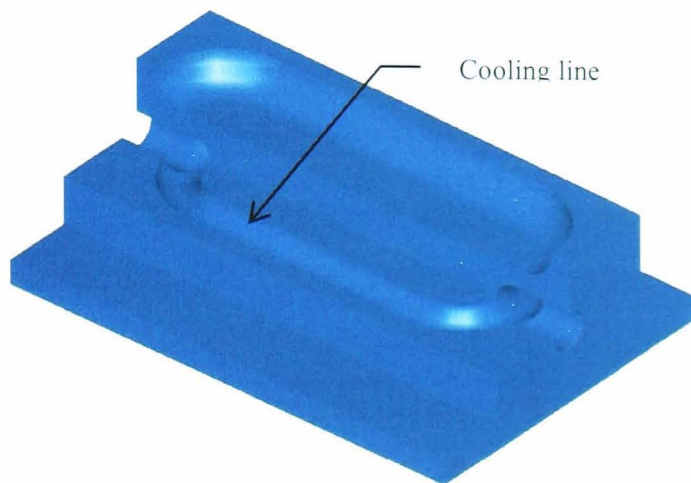


Figure 3-44. 3D CAD Solid Model

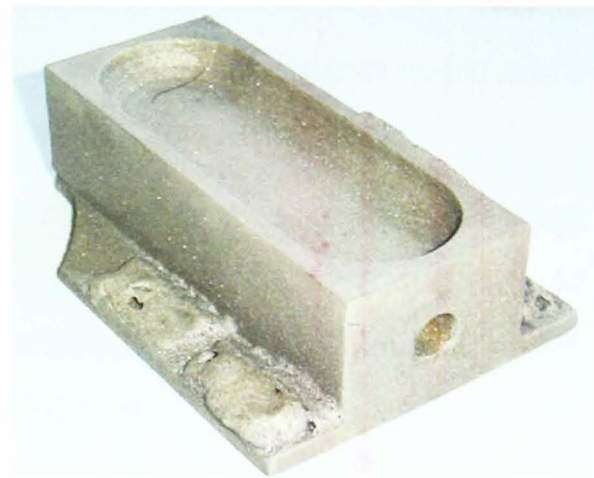


Figure 3-45. 3D Metal Model

A simple leak test was performed. With one end blocked, the cooling line was then filled with water and left for five days. During this period of time, the level of water at the open end observed in order to indicate whether there leaking due to material porosity. The level of the water surface at the open end of the cooling line was found not to change.

### 3.5. Discussion and Summary

This chapter has examined benchmark studies associated with the technological capability of indirect SLS process in developing metal parts using LaserForm ST-100. Given the information gathered from this study, the results have demonstrated that the indirect SLS process has limitations which need to be considered before using current indirect SLS metal part for tooling solution. Comparing with conventional tooling, the followings highlight a number of issues regarding the limitations of indirect SLS.

The dimensional accuracy study have indicated that the maximum average relative errors are approximately between 1.00% to 1.20% in X, Y, and Z directions for feature dimension of between 5 mm and 25 mm. However, this is more pronounced in Z than in X and Y, where, above 25 mm, the relative error in X and Y

is within 0.0% to 0.4%. For dimensions of less than 5 mm, larger errors are observed. In the surface flatness study, the results have shown that the average absolute error increases with nominal thickness, providing average relative error which is fairly consistent at around 3.0% undersize. Moreover, the results on surface profiles have shown that the flatness of parts which are 10 mm thick and over is  $\pm 0.1$  mm. However, it is considered that thicknesses less than 10 mm are not be able to withstand warping in the furnace process where complex geometries are involved. In the observation of building limitations, a number of small features at the green part stage were missing, either damaged or not built at all in the process.

Concerning these constraints, it is recommended to consider appropriate machining allowances that should be provided in designing near-net shape mould inserts. Based on the results, a machining allowance of at least 0.5 mm in X and Y building direction is recommended to be provided to ensure sufficient stock material for finishing items of up to 100 mm in size. Above this, an oversize of 0.4% is an appropriate allowance. To anticipate 3.0% undersize in Z, an additional 0.5 mm of machining allowance to ensure sufficient stock to work with is also considered necessary. Concerning the limitations in building process and a fragile green part, small features that have dimensions of less 2 mm are best produced by machining.

From the surface finish study, it is indicated that the average surface roughness  $R_a$  of the indirect SLS metal part can be polished up to  $0.08 \mu\text{m}$ , which provides ‘glossy’ surface quality with very small or acceptable visible scratches. This surface quality is better than N3 ( $R_a \sim 0.1 \mu\text{m}$ ) surface finish class according to ISO 1302.

The results of the surface hardness study furthermore indicate that the average hardness of the ST-100 metal part as polished is between 84 to 85  $\text{HR}_B$  which is approximately equal to 2 to 3  $\text{HR}_C$ . This typical hardness is considerably very low for the mould inserts compared to the average hardness of pre-hardened P-20 steel and 420 stainless steel which is between 30 to 36  $\text{HR}_C$ . However, the average hardness of the ST-100 metal part is slightly higher than the average hardness of the Aluminium alloy ( $\sim 60 \text{HR}_B$ ). Finally, Leak testing has shown the ST-100 metal part did not leak due to the material porosity.

However, the indirect SLS process offer advantages. The indirect SLS process works well in developing rapidly complex geometries that would take a

considerable amount of time and difficult to achieve using a conventional method, especially in constructing a free-form internal feature (i.e. conformal cooling channel) inside the parts. If the metal part for mould inserts require a great deal of machining detail and tight tolerance features, the time and cost savings over conventional tooling method would be reduced. For a better results, the design of the metal part using indirect SLS should be suitable for the process.

## Chapter 4

# **Case Studies**

## **Chapter 4. Case Studies**

This chapter describes three major case studies which were carried out to support the research work. The three major case studies were from Seaquist Closures Ltd. (Case Study 1), Trisport Ltd. (Case Study 2), and Unilever Ltd. (Case Study 3). The case studies were carried out as part of a larger research project which was carried at the University of Leeds. The studies aimed to assess the input of conformal cooling on cycle time, and worked through the redesign of the existing core and cavity inserts. This meant that the case studies were constrained to use the existing ejection systems, that the entry/exit points for coolant were fixed, and that the position of the gate was also fixed. The work reported in this chapter was carried out in collaboration with Dr. C.M. Taylor, who worked on the research project which the case studies supported.

### **4.1. Introduction**

The following Figure 4-1 outlines the procedure which was employed in the development of the case studies. There are four important process areas which are focused on in the development of new inserts: the design process, the manufacture process, moulding and production trials, and performance evaluation. In the design process, reviewing the design of both selected product and mould inserts (core and cavity) of each case study was crucial in generating an optimum design of the new mould inserts. In product design, geometry, tolerance, surface finish, volume, material, gate point and parting-line were crucial information which had to be reviewed and evaluated. In insert design, information on surface finish, runner and gate system, cooling system, and ejector system were the main concern.

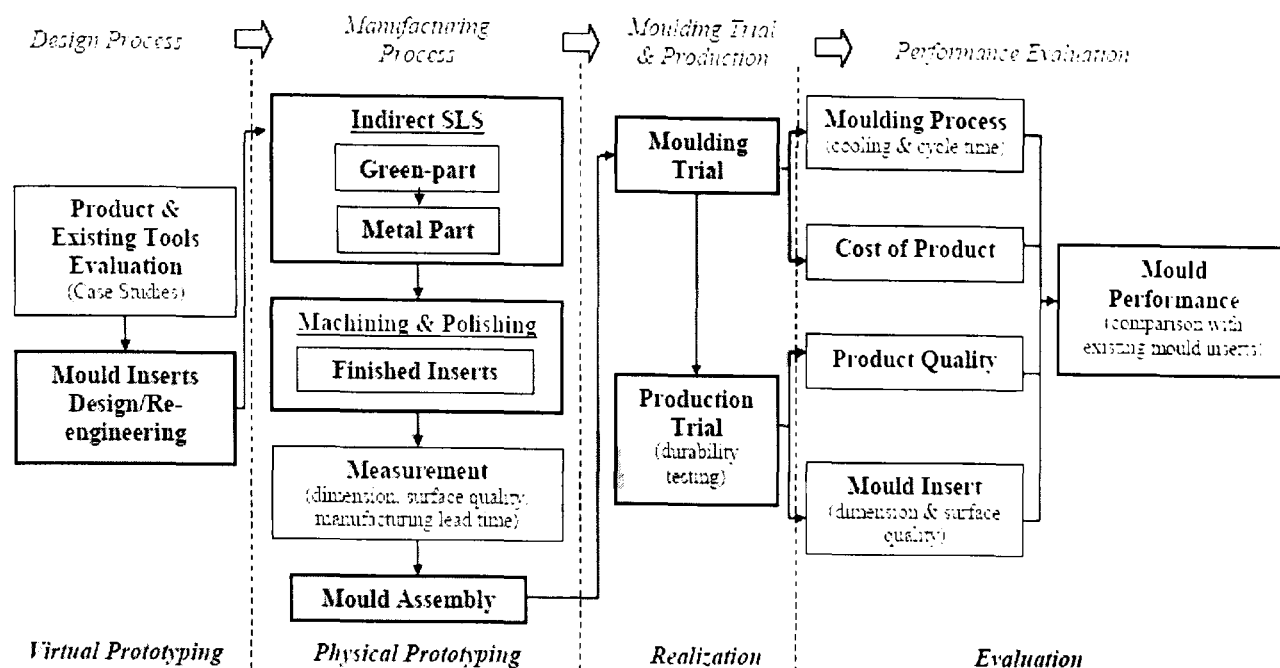


Figure 4-1. Development Procedures

As the design of the new inserts proceeded, an important consideration was to generate a near-net shape model of the inserts. At this stage, the main consideration was on the general limitations of the indirect SLS process in producing a metal part which were discussed previously in Chapter 3. Once the near-net shape models had been defined, the indirect SLS process was used to produce the green-parts. The green parts were then sent to the furnace for bronze infiltration. In this process, the orientation and location of the inserts in the furnace was considered to provide good infiltrant flow into the green part and surface flatness after infiltration. After infiltration, a high-temperature resin infiltration process on the metal insert was used to guarantee sealed surfaces. To achieve the required production specifications, the inserts were then sent out for finishing.

To evaluate the overall performance of the new developed inserts, moulding trials were carried out. Basically, the focus in these trials was assessment of using the new inserts, an analysis of moulding cost, and an evaluation of the inserts durability. The assessment and performance evaluation results of the new inserts were benchmarked against the original inserts. Table 4-1 lists and summarises the required data and information from the tool owner that was used for performance evaluation.

Table 4-1. Performance Parameter and Data/Information Required

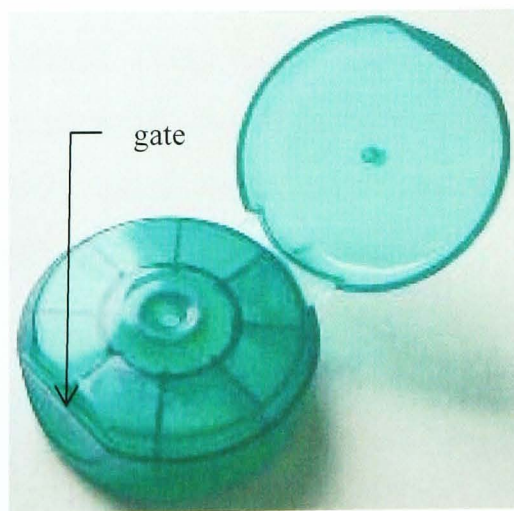
Parameters	Data & Information
Productivity	<ul style="list-style-type: none"> <li>• Projected volume of production</li> <li>• Expected tool (mould inserts) life</li> <li>• Total moulding cycle time</li> <li>• Cooling time</li> </ul>
Manufacturing Lead-Time	<ul style="list-style-type: none"> <li>• A total manufacturing lead-time for a set of inserts (core and cavity)</li> <li>• A total manufacturing lead-time for a complete mould</li> </ul>
Cost	<ul style="list-style-type: none"> <li>• A total cost required for manufacturing a set of inserts (core and cavity)</li> <li>• A total cost required for manufacturing a complete mould</li> <li>• Time required for replacing the mould from/to the moulding machine</li> <li>• Moulding operational hourly rate (incl. machine, operator and utilities)</li> <li>• Moulding machine utilization per year</li> </ul>

In the moulding trial, the manufacturing time and costs collected, and then fed into a cost model. The cost model in section 2.1.3.1.4 which was developed in previous research by Dalgarno et. al. [Dalgarno, 2001] was employed.

## 4.2. Case Study 1: 50 mm Snap-On Tube Top

### 4.2.1. Product Evaluation

For the first case study (CS1), a Snap-On Tube Top (Figure 4-2), a closure product from Seaquist Closures Ltd was selected. According to the information provided, the average production volume for this product is approximately 100,000 to 200,000 products per year. With an average product life of 5 years, the existing mould inserts are therefore designed to be able to stand 500,000 to 1,000,000 shots. The total cycle and cooling time to mould this typical product using the existing mould insert are 14.1 s and 7.0 s respectively.



<b>Dimension:</b>	Ø 48 x 24.5 mm
<b>Orifice Size:</b>	3.2 mm
<b>Sealing System:</b>	Plug Seal
<b>Hinge Style:</b>	Protrusionless
<b>Lid:</b>	Flat Lid
<b>Surface Finish:</b>	Glossy all over
<b>Material:</b>	Polypropylene (PP)
<b>Shrinkage</b>	1.6%
<b>Weight:</b>	~ 7.0 g

Figure 4-2. 50 mm Snap-On Tube Top [Seaquist Closure Ltd.]

For the insert, the following product information were counted to be important design considerations

- *Wall thickness*: varies from 0.1 to 2.7 mm
- *Small features*: (i) a 'number mark' on the hinge, (ii) retention bead on the collar, and (iii) lid locks. (Figure 4-3)
- *Draft angle*:  $0.5^{\circ}$  to  $1.0^{\circ}$
- *Surface finish*: glossy finish of external and major internal surfaces ( $R_a \approx 0.02\mu\text{m}$ )



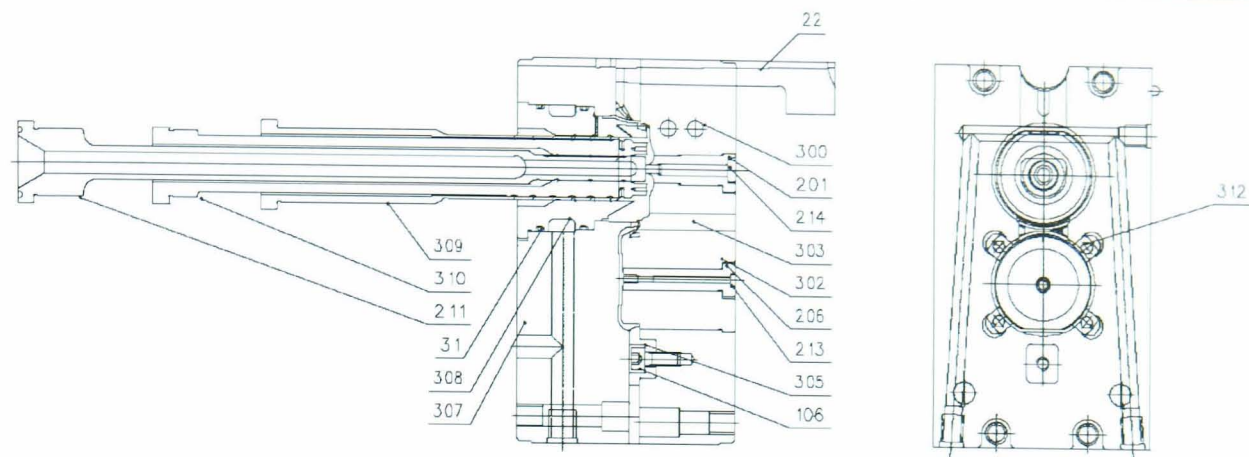
Figure 4-3. Small Features

Furthermore, the gate location where the melted plastic was injected into the mould cavity is also considered and indicated on Figure 4-2.

#### 4.2.2. Insert Design

The design of the new CS1 inserts was focused on the key advantages of indirect SLS. Indirect SLS can provide more design freedom in developing a 3D solid object [Hague, 2003] which has been utilised to simplify the complexity of the existing CS1 inserts (Figure 4-4). An assembly drawing of the original CS1 inserts (a) shows that the existing top insert (b) and bottom insert (c) contains a number of inserted components (201, 300, 302, 303, 305, 307 and 308). From these components, the main body of both top (300) and bottom (307) insert, cap insert (302), hinge insert (303) and rib insert (308) are potential candidates that were selected to be manufactured by SLS.

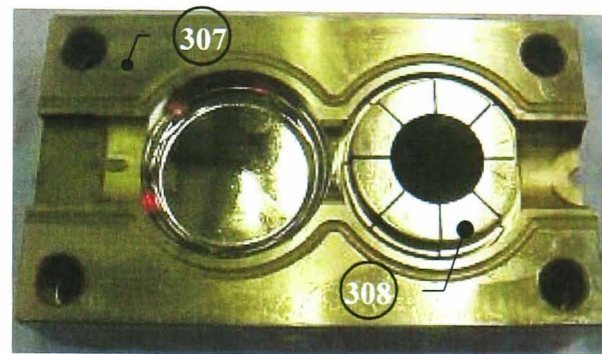




(a) Assembly of the Inserts



(b) Top CS1 insert



(c) Bottom Insert

Figure 4-4. Existing CS1 Inserts

Considering for a better cooling system inside the inserts, both top and bottom inserts were redesigned by merging as many as possible of the inserted components into one solid component. However, machining and finishing as well as a process accessibility were becoming major design constraints that need to be considered. From the original inserts, it was identified that there are deep slots on the rib inserts, surface textures on the hinge, and undercuts for lid lock which require EDM finishing. Since a glossy finish of the product external and major internal surfaces is required, it was also indicated that most surfaces on the features that form mould cavity require a polished quality surface finish. The followings explain the redesign process of the new CS1 inserts

For a new top insert (a), cap (302) and hinge (303) components were selected to be merged to the main body in order to provide a better penetration in constructing conformal cooling channel, and to improve cooling process. For manufacturing concerns, merging both 302 and 303 allows tightest tolerances for fitting to be removed, and reduces significant numbers of surfaces to be machined, which can save lead-time significantly. For component 201, 305, and 312, the existing component were used. A decision taken of using these existing components

was mainly based on manufacturing constraints, interchangeable components, moving components, and replacement of worn components.

Component 201 is a module of an interchangeable insert for different nozzle and orifice diameters. Component 305 was unmerged basically due to ease EDM operation in developing undercuts that will be used to mould the lid lock. Thus, component 312 is spring ejectors which will be functioned to eject and force out the cap from the lid lock undercuts on the component 305 when the mould is opened. For the new bottom insert (b), the idea of the original CS1 insert not to merge component 308 into the main body was adopted due to the requirement of a polished quality surface finish on both external and internal surfaces that form a rib insert. Therefore, a two separate plates design of the new bottom insert was generated in order to provide polishing accessibilities. To fit both plates together, a locating pin had been considered.

In reference to the above design considerations and manufacturing constraints, Figure 4-5 show the final CAD design model of the new CS1 inserts.

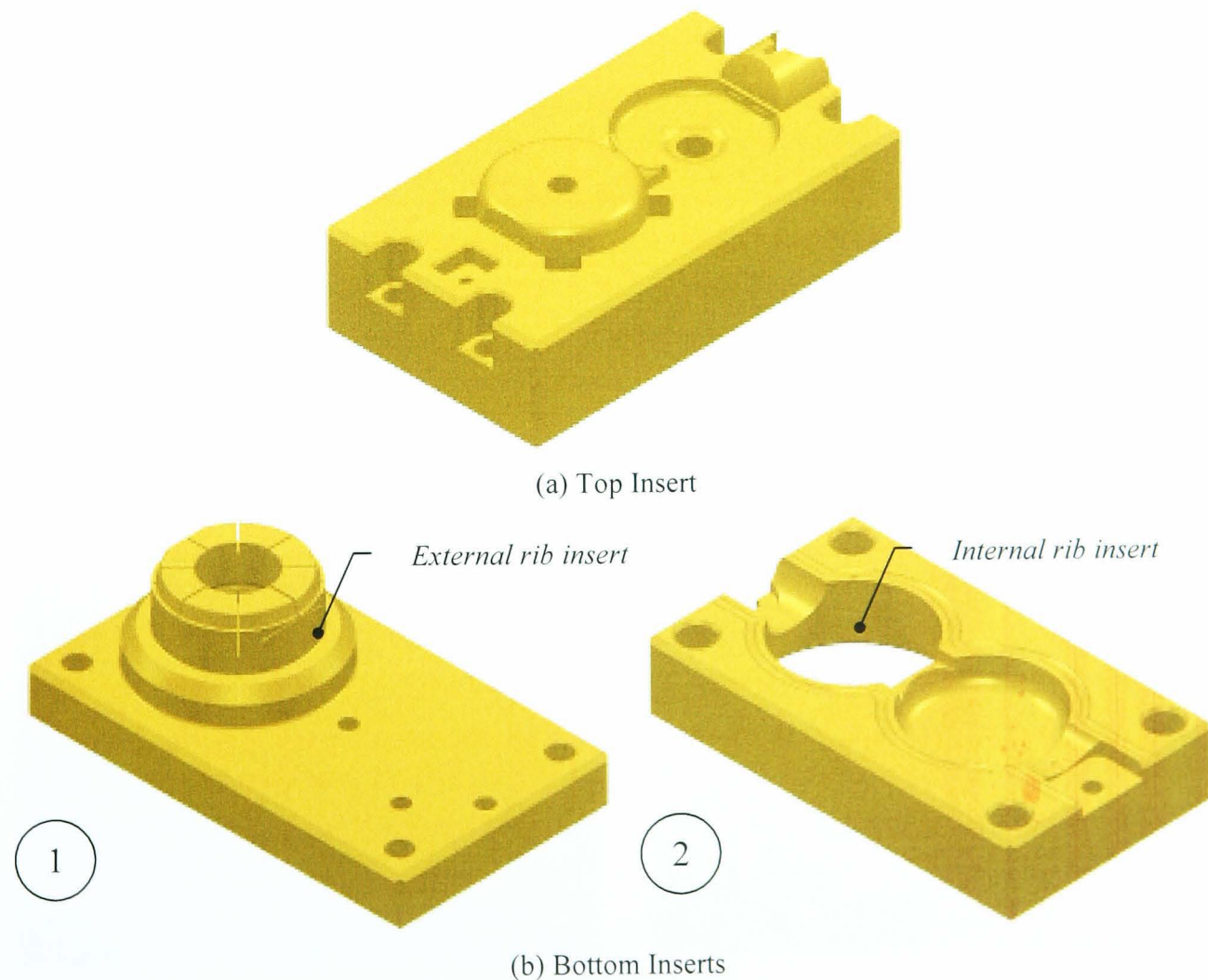


Figure 4-5. The Design of the New CS1 Inserts

Indirect SLS also allows a conventional straight-drilled cooling channels to be replaced by complex conformal cooling channels. Merging components in redesigning the new insert, also allow better penetration and freeform construction of conformal cooling channels into the inserts. As a final design of the channels, Figure 4-6 shows a comparison between the original and new cooling channel designs, and Figure 4-7 shows the new cooling channel designs implemented into the inserts.

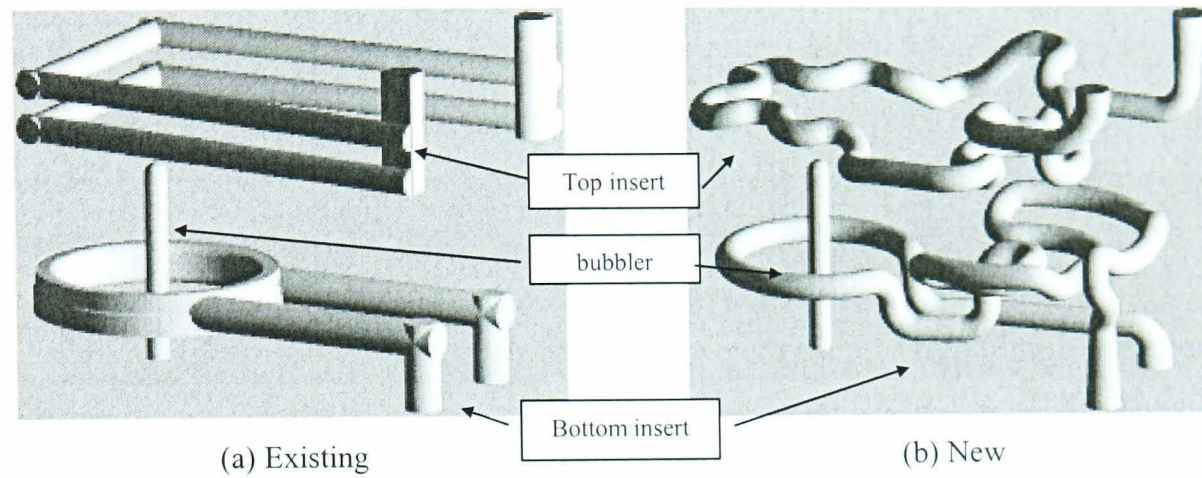


Figure 4-6. Cooling Channels: Existing vs. New Mould Inserts

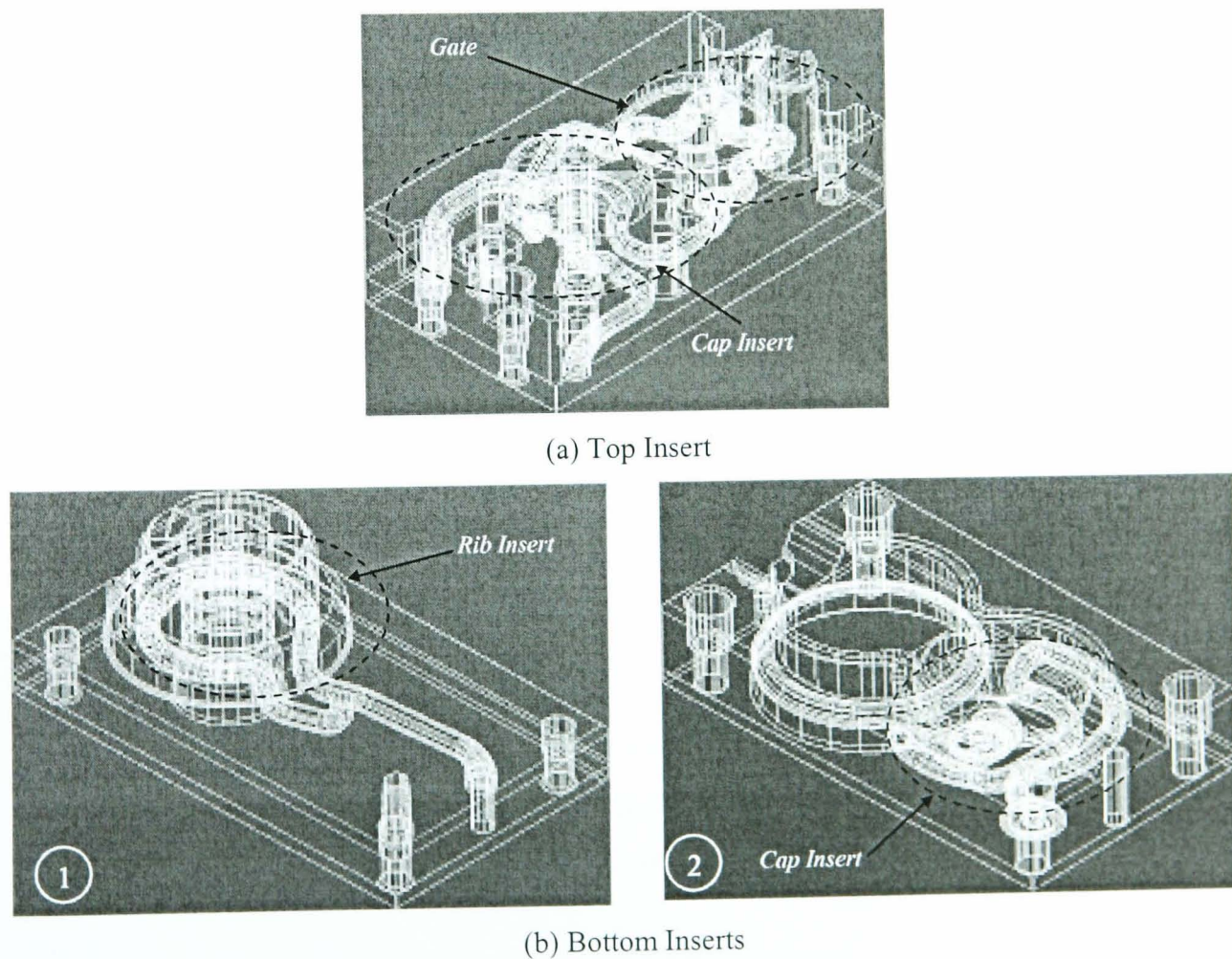


Figure 4-7. Conformal Cooling Channels

For the new CS1 inserts, the parameters (diameter, length, geometrical complexity and location) employed in designing the new cooling channels are mostly based on the rules developed previously by Dalgarno et al. [Dalgarno, 2001] as described in section 2.1.3.1.2.2. Both channels diameter and a distance between the cavity surfaces and cooling channel centre line and between adjacent channels were designed with 8 mm. Since the new CS1 inserts are contained into the existing mould base, the inlet and outlet position of the new cooling channel in both inserts are constrained and fixed to the existing channel positions in the mould base. Following the previous rules, an 8 mm diameter cooling channel is employed, and an average shortest distance of the channels from the cavity surfaces is kept roughly constant at that value. To increase contact cooling area, the channel path in the top insert is wound around the gate and cap insert area (see Figure 4-7a). In both areas, the winding path of the channels is outlined according to the availability of the material. For bottom inserts, a ring cooling channel is constructed inside the rib insert area, while several winding channels are outlined conformal to the cap insert (see Figure 4-7b). To ensure no leakage, the channels which run vertically through inter-plate surfaces between the bottom insert 1 and 2 are sealed with o-rings as it is shown in Figure 4-8.

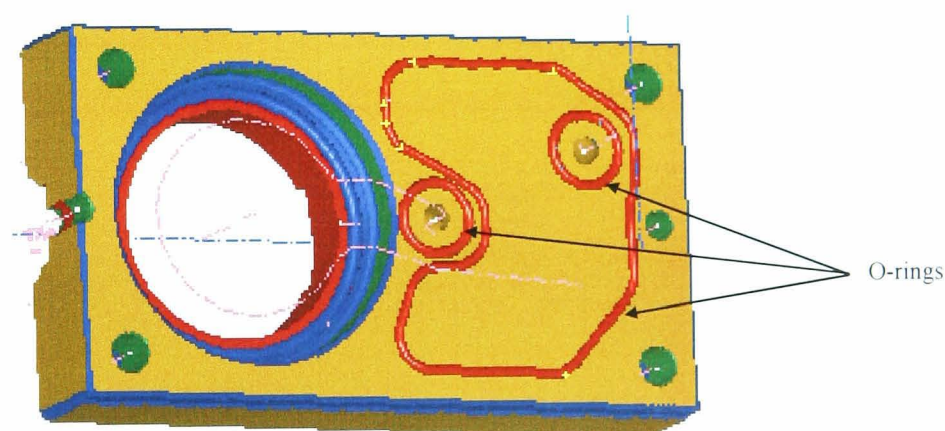
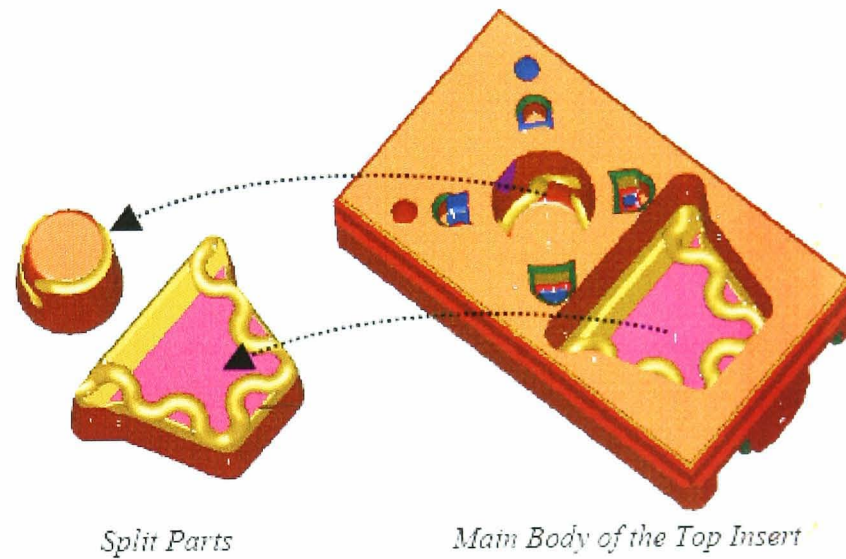


Figure 4-8. O-Ring Seals

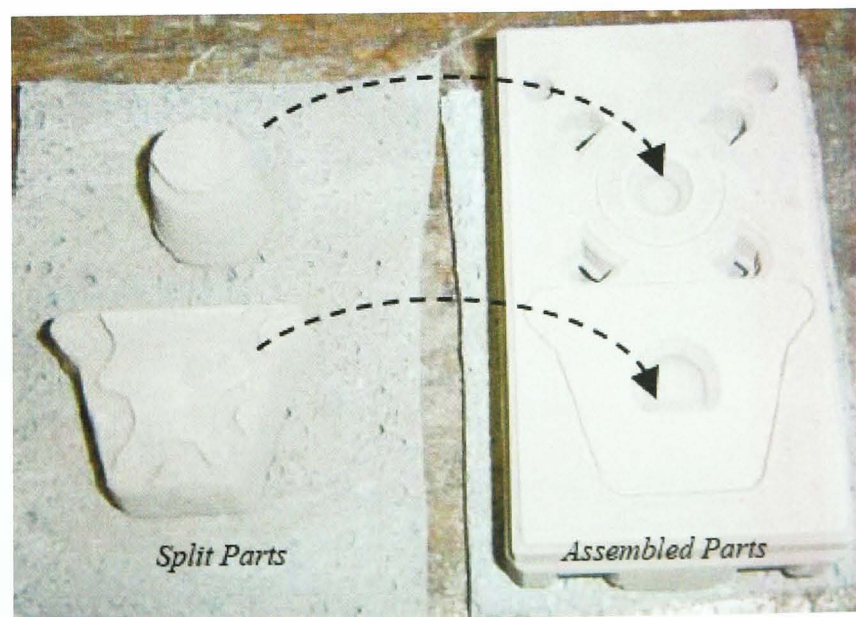
Considering the general limitations of the indirect SLS, all small/delicate features, deep narrow slots, and drilled holes on the new CS1 inserts were considered to be added and finished later by the required post-processing. To anticipate oversize during the process and to ensure sufficient material for finishing, additional 0.5 mm machining allowance was then added to all surfaces of the CS1 inserts.

Moreover, a 'split' design models of the near-net shape inserts were decided

in green part stage. A main idea was to provide an effective and efficient approach in clearing the loose powder inside the new conformal cooling channels constructed inside the inserts. Figure 4-9 illustrates the split approach implemented on the new CS1 top insert. In a 3D CAD model (a), it shows that two split parts were cut-off from the main body of the inserts and bisected the cooling channels. In the green part stage (b), it then shows these split parts were assembled back to the main body of the inserts. Concerning this idea, the main issues were related on decision on determining split lines, aligning features for assembly, geometry and tolerances. For matching them, building orientation and location of the split pairs were further taken into account. A clean pair was required in aligning and fitting them to avoid any destruction. To assure a firm alignment, resin and glue were then put on their matched surface.



(a) 3D CAD of Split Model

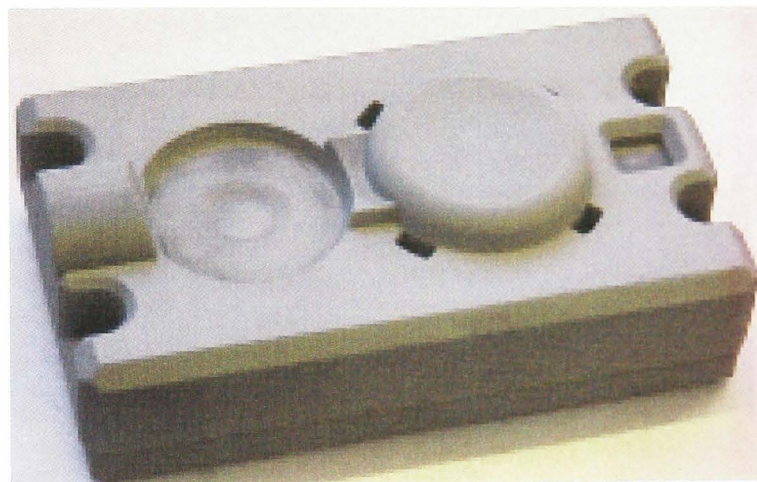


(a) Split and Assembled Green-Part

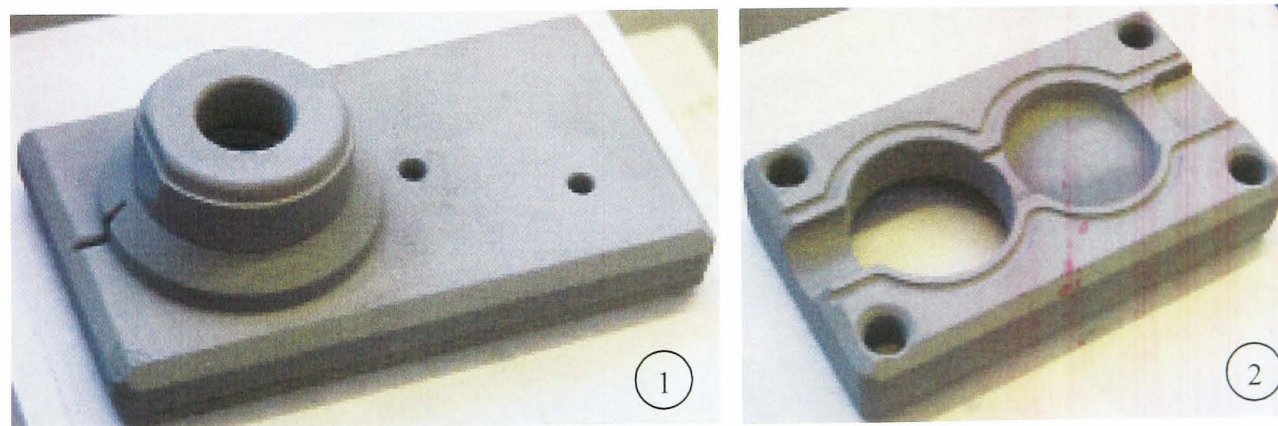
Figure 4-9. Split Approach of the new CS1 Top Insert

### 4.2.3. Inserts Manufacture

Figure 4-10 shows the green part of the new CS1 top (a) and bottom (b) inserts after SLS process. After cleaning and clearing all the loose powder, these green parts were then sent to an oven for bronze infiltration to produce metal inserts. Figure 4-11 shows the metal part of the top (a) and component 2 of the bottom (b) inserts. Before sending out all of the inserts to Delcam for finishing, the inserts were first sealed with a high-temperature resin (ultraseal PC504/66 methacrylate) using vacuum impregnation process. The process basically infiltrates the resin in order to fill any porosity inside the inserts which may cause water leaking from the cooling channels. After the process, the inserts were washed and then heated to cure. From technical information provided, this PC504/66 sealant can be operated at the temperature between -50 to 200°C [Ultraseal International, 2004].



(a) Top CS1 Insert



(b) Bottom CS1 Inserts

Figure 4-10. The Green Part of the New Inserts

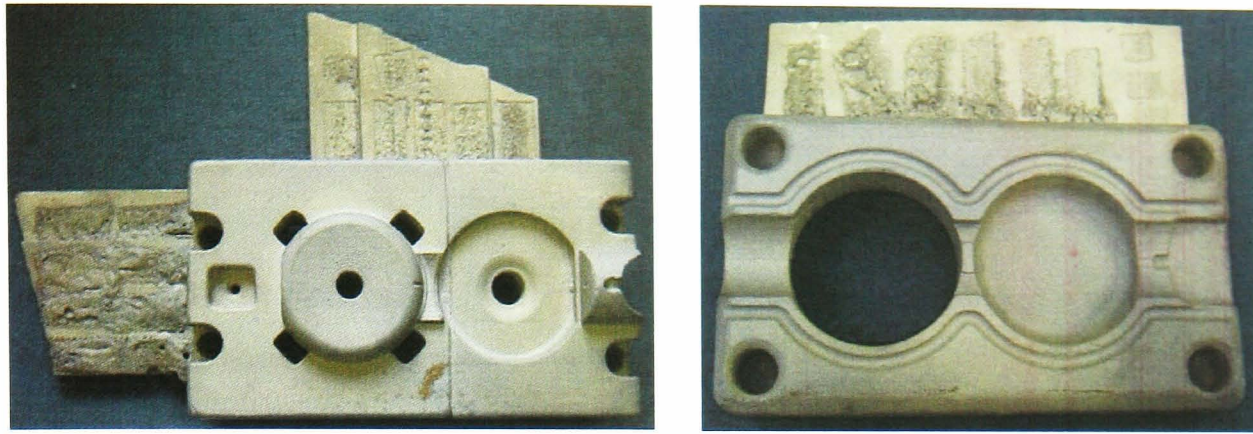


Figure 4-11. SLS Metal Part of the New CS1 Inserts

In machining and finishing the inserts, it was reported that a high-speed milling machine (HSM), electro-discharge machines (electrode and wire EDM) and polishing are the main processes required to produce final new CS1 insert with required production specifications. For manufacturing operations, the following Figure 4-12 and Figure 4-13 illustrates colour codes (brown, red, green, pink, blue and yellow) which were used to explain machining and finishing processes that form the features on both top and bottom inserts respectively.

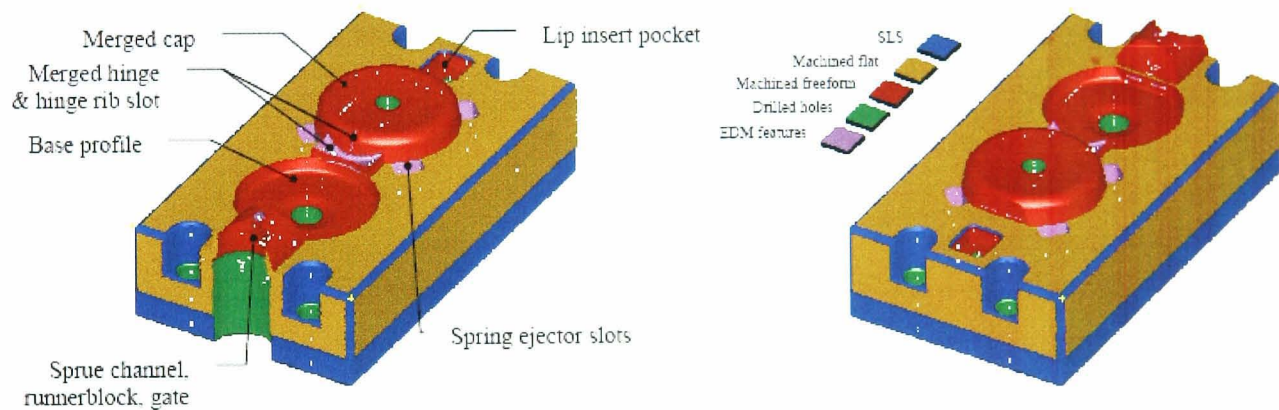


Figure 4-12. Manufacturing Operations of the Top Insert

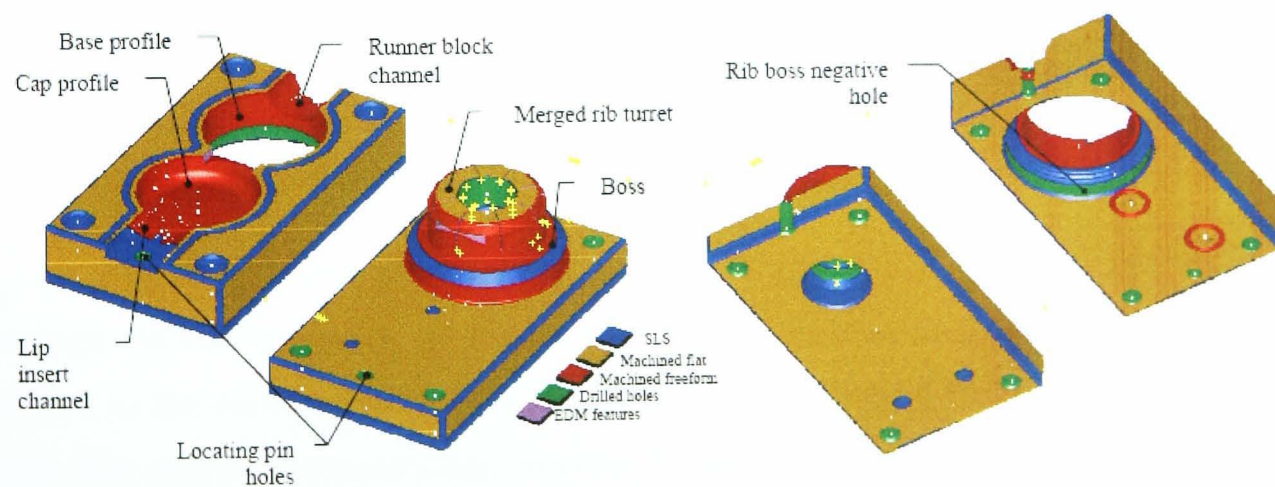


Figure 4-13. Manufacturing Operation of the Bottom Inserts

A brown colour represents the flat features that had been machined using HSM for blocking out all components of both inserts. These operations include

machining all six faces of each component and the flat top face of the rib turret on the bottom insert 1. A red colour code represents the HSM operations that had been used to machine freeform surface of all the features (merged cap, hinge and rib turret; base and cap profile; sprue and runner block channel; and lip insert pocket) that mostly form the mould cavity, including the grooves prepared for the o-rings on the bottom insert 1. A green code represents drilling and boring operations that had been used to add mostly holes for bolts, holes for nozzle and orifice, rib boss and turret, located pins, and sprue puller channel.

Thus, a pink colour represents the features that require EDM operation. In this operation, spring ejector, ribs and hinge rib slots, gate, and hinge freeform surfaces were included. For a blue colour code, it represents the features that did not require further machining or finishing. They were formed as is of the indirect SLS process. The features which were included in this code are vents, chamfers, and clearance holes. For enhancing the insert final quality, Figure 4-14 furthermore shows a yellow colour code used to indicate the surfaces of the main cavity features (merged cap, hinge, rib turret, gate, base and cap profile) that require polished finishing

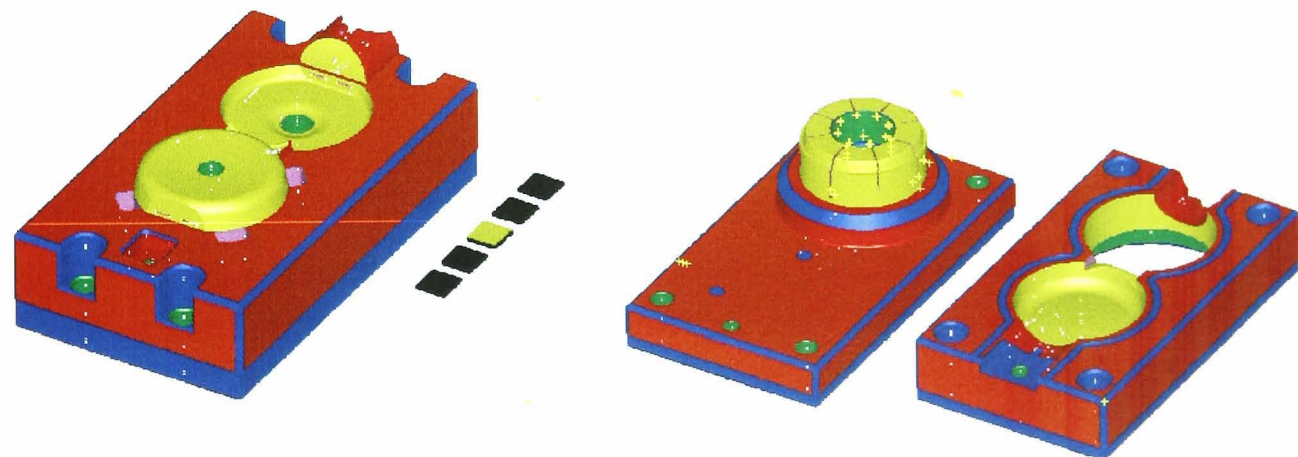


Figure 4-14. Polishing Colour Code of the Inserts

Figure 4-15 show finished CS 1 inserts. As required, it was measured that an average surface roughness of the polished cavity surfaces area was achieved and similar to the surface finish at the same area of the original tool cavity ( $R_a = 0.02 \mu\text{m}$ ). For overall manufacturing process, it was calculated that a total amount of lead-time and cost required to manufacture both new CS1 top and bottom inserts from 3D CAD model were about 301 hours and £ 11,000 respectively.



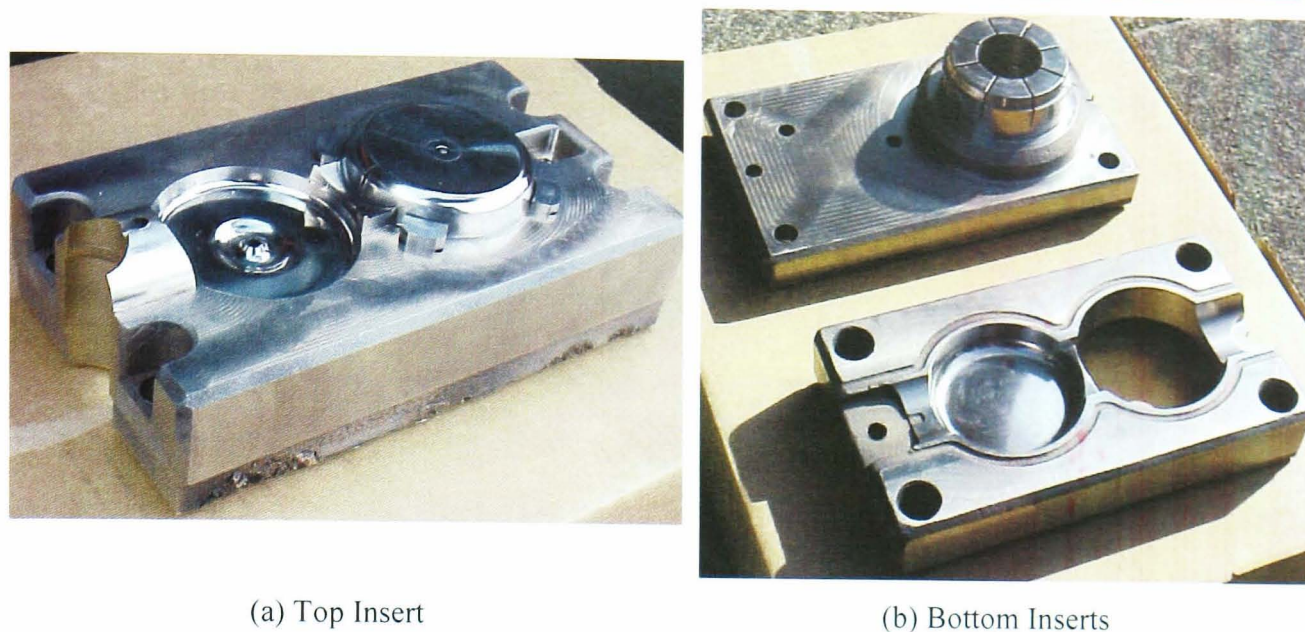


Figure 4-15. Finished Mould Inserts

#### 4.2.4. Moulding Trial

A moulding trial with the new CS1 inserts was run in the production workshop of the Seaquist Closures Ltd. using a Kloeckner Ferromatik FM-85 injection machine. The parameters for running the new CS1 inserts were set up similar to the operating parameters of running the existing insert in the production. Table 4-2 lists the specification of the material used and summarizes the main process parameters.

Table 4-2. CS1 Material and Process Parameters

<b>A</b>	<b>Material Specifications</b>	
1.	Material:	RE420MO - Polypropylene (PP) - Copolymer
2.	Density:	0.9 g/cm <sup>3</sup>
3.	Sp. Heat	2.1 J/g °C
<b>B</b>	<b>Process Parameters</b>	
1.	Injection Temp.:	ave. 230 °C
2.	Ejection Temp.:	ave. 65 °C
3.	Mould Temp.:	ave. 40 °C
<b>C</b>	<b>Coolant</b>	
1.	Coolant:	water
2.	Temp Different:	ave. 8 °C
3.	Flow Rate	ave. 7.5 l/min

##### 4.2.4.1. Procedure and Measurements

In carrying out the trial and assessing productivity, the moulding cycle time was reduced incrementally. For warming up and reaching a process steady state, the

production cycle time of the existing inserts (14.1s) was used for the first 2 hours. The cycle time is then reduced every 2 hours of running in the following order: 5% (13.4s), 15% (12s) and 20% (11.3s). The cycle time reduction could not be continued because the machine mechanism would not be able to keep up with the cooling cycle.

Simultaneously, machine energy consumptions for each set up cycle time were monitored and measured. Both apparent (actual) and effective (desired) power consumptions were calculated. Two sets of readings from injection machine were therefore taken for calculating both power consumptions: instantaneous measurements of power/current/voltage, and integrated measurement of energy. The following Figure 4-16 is an example graph was used in measuring both energy consumptions using both instantaneous and integrated methods.

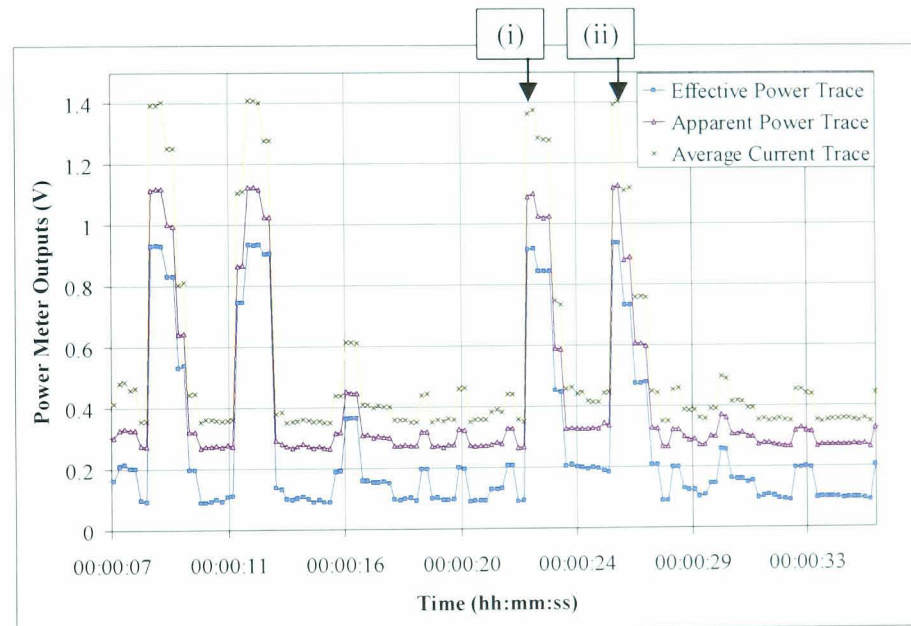
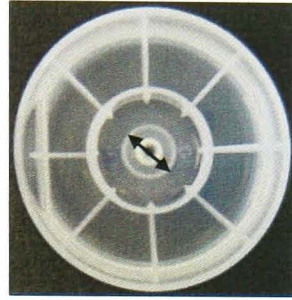


Figure 4-16. Example of Readings

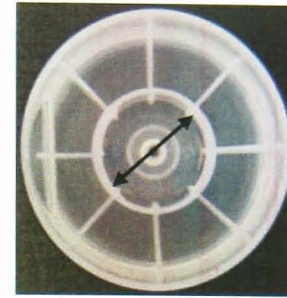
The graph shows that a y-axis represents output voltage (0 to 5 Volt) from power meter, and an x-axis is the elapsed time. To provide power or current values, a scaling factor which is similar for both readings was required. Furthermore, the graph also illustrates two important injection moulding cycles, which each of them was represented by two major spikes in power consumptions: (i) ejection and (ii) clamping/injection cycle. Based on this graph, energy consumed can be estimated by calculating the area under each power curve.

Samples for each cycle time were collected for a quality inspection. Seaquist's standard procedures for quality inspection were used. Figure 4-17

indicates dimensions of two important features (plug outside diameter and snap inside diameter) that have to be measured and which have been used to represent the product quality. The expected dimensions of the plug O/D and snap I/D are  $10.00 \begin{pmatrix} +0.40 \\ 0.00 \end{pmatrix}$  mm and  $19.80 (\pm 0.20)$  mm respectively.



(a) Plug Outside Diameter (O/D)

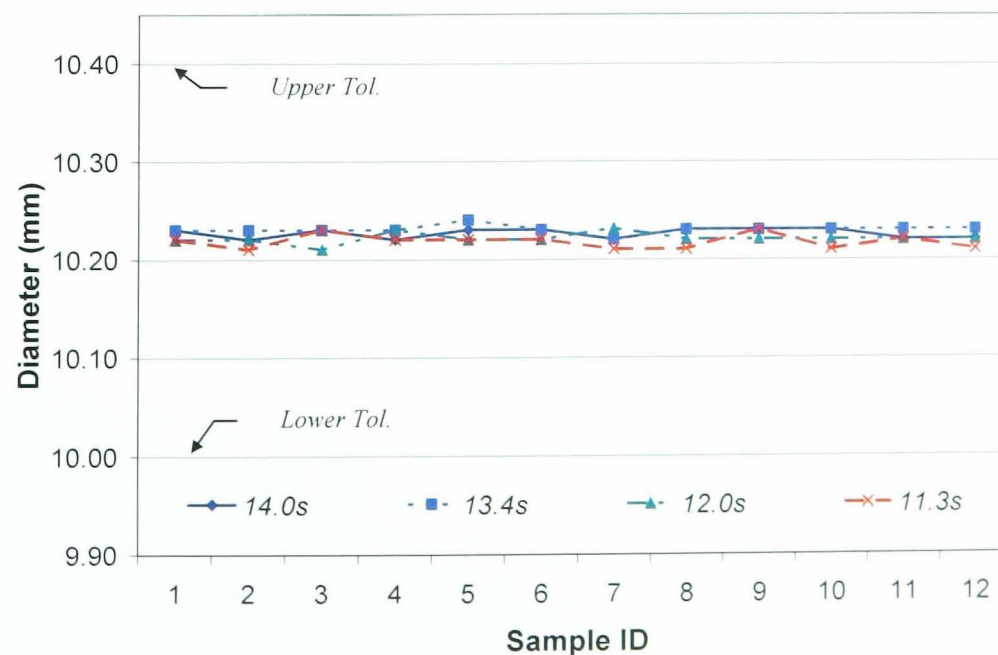


(b) Snap Inside Diameter (I/D)

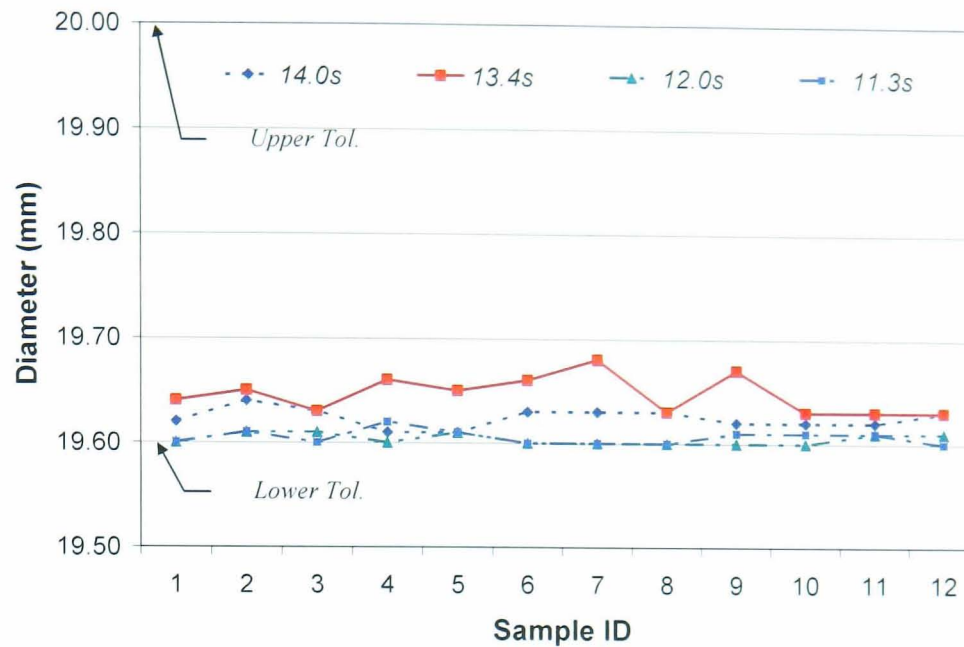
Figure 4-17. CS1 Product Quality

#### 4.2.4.2. Results

From the product quality inspection (Figure 4-18), the measurements have shown that the designated dimensions on all samples lie within the tolerance band. For the plug O/D (Figure 4-18a), average measured dimensions for every cycle time are consistent within the designated tolerance band. In the case of snap I/D (Figure 4-18b), the average dimensions at every cycle time are also within the expected tolerance even though most of them are distributed close to a lower tolerance limit. These results indicates that the new CS1 inserts were able to performed its function under every set up cycle time, as expected.



(a) Plug O/D



(b) Snap I/D

Figure 4-18. Feature Measurements

Moreover, the energy measurement indicated that the machine energy consumption has improved using the new CS1 inserts compared to the energy required (124 kJ/part) by the existing inserts. At 5%, 15% and 20% cycle time reduction, the new CS1 inserts is able to reduce the machine energy consumption by approximately 4% (119 kJ/part), 10% (112 kJ/part) and 13% (108 kJ/part) respectively. Figure 4-19 shows an effective and apparent power consumption measurement at 20% (11.3s) cycle time reduction [Taylor, 2004b]. Two typical cycle in the process are shown with injection and ejection points are indicated.

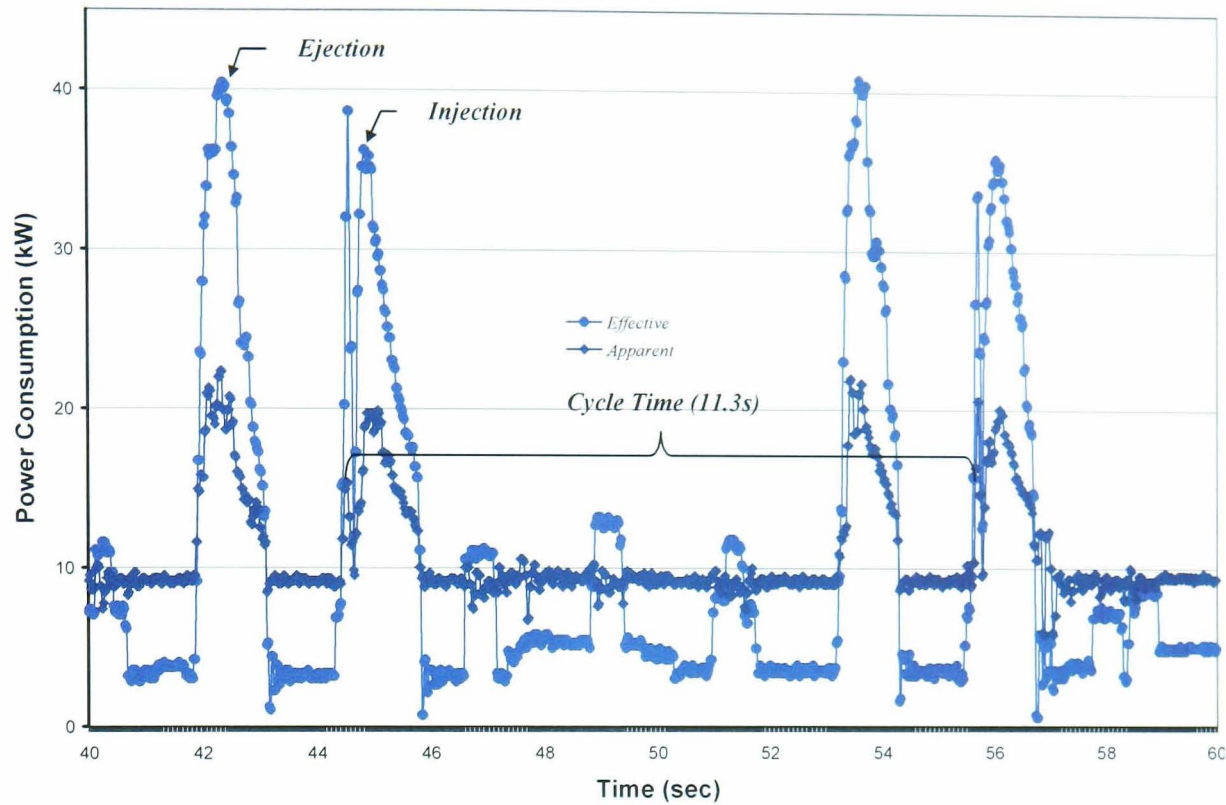
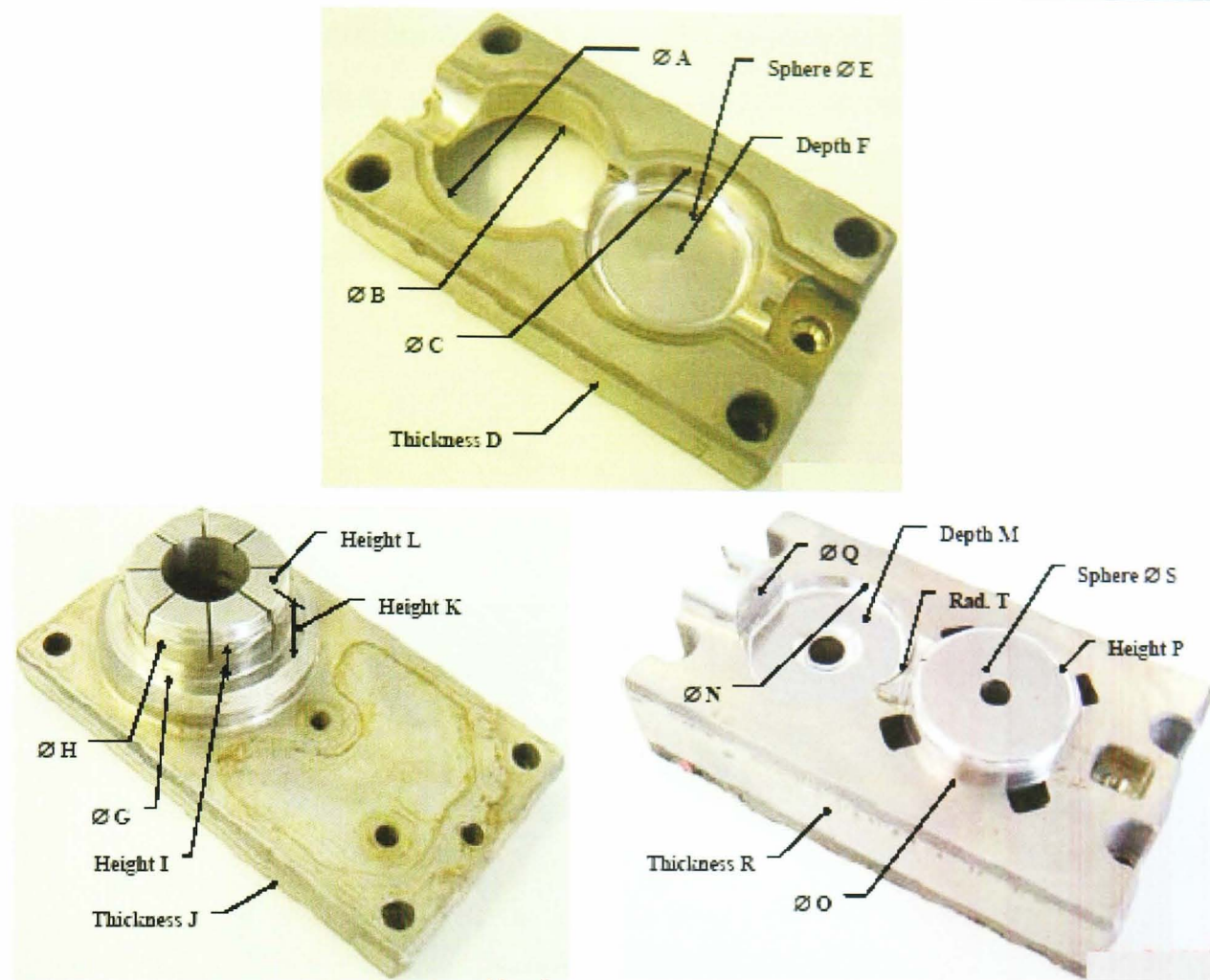


Figure 4-19. Power Consumption at 20% Cycle Time Reduction [Taylor, 2004b]

#### 4.2.5. Production/Durability Trial

A durability trial was carried out using a Kloeckner Ferromatik FM-85 injection machine at Seaquist Closures production workshop. The same set-up parameters as for the moulding trial at 12s cycle time and 6s cooling time. To evaluate the process, a quality inspection on the mouldings was carried out. Twenty samples were taken just after the moulding process reached its steady state. Then, consecutive batches of twenty moulding were taken every 1000 mouldings. The trial continued for 86 hours and 48 minutes and produced about 25,000 mouldings.

To evaluate the insert performance, Figure 4-20 shows the comparison of dimensional measurements on the inserts before and after producing 25,000 mouldings. From the table in the figure, it was observed that there was no significant changes on the most dimension measured except for the diameter 'O'. After producing 25,000 mouldings, it was measured that a change on diameter 'O' from 46.22mm to 45.79mm (reduced by 0.43mm or 0.94%) were considerably high because it was outside of the expected tolerance ( $\pm 0.2\text{mm}$ ).



Dim. ID	Values (mm)		$\Delta\%$	Dim. ID	Values (mm)		$\Delta\%$	Dim. ID	Values (mm)		$\Delta\%$
	Before	After			Before	After			Before	After	
A	48.71	48.72	0.04%	H	45.76	45.65	-0.25%	O	46.22	45.79	-0.94%
B	48.20	48.18	-0.04%	I	15.54	15.59	0.35%	P	8.64	8.73	0.96%
C	48.57	48.66	0.18%	J	18.04	18.06	0.11%	Q	0.83	0.84	0.60%
D	27.05	27.04	-0.04%	K	18.70	18.75	0.24%	R	35.02	35.02	0.00%
E	121.96	121.93	-0.02%	L	48.50	48.35	-0.31%	S	115.38	115.57	0.17%
F	8.16	8.19	0.37%	M	4.53	4.56	0.58%	T	4.00	3.97	-0.96%
G	45.90	45.84	-0.13%	N	45.63	45.87	0.52%				

Figure 4-20. Dimensions of the Inserts

To investigate the above significant deficiency, further assessment on a product diameter as a results of ‘O’ was carried out. Based on the expected dimension of  $\text{Ø}45.3$  mm (expected tolerance:  $\pm 0.2\text{mm}$ ), Figure 4-21 shows the actual diameters of the selected feature were within the expected tolerances during the trial of producing 25,000 mouldings. From a trend line, its equation indicates a negative linear slope which represents a rate of 0.0013mm diameter reduction on the mouldings produced every 1000 shots. Assuming that this value reflects a wear rate of the insert material, the reduction of 0.0013mm/1000 shots on the product can therefore be utilised to predict a maximum durability (life time) of the insert in producing a part which dimensionally accurate within expected tolerances. Utilising the trend line equation and the acceptable minimum diameter (45.1mm), it was then

calculated that this minimum diameter would be reached at 195,000 shots. As this is the case, it was therefore predicted that this will be an experimental value of a maximum durability of the insert material (LaserForm ST-100).

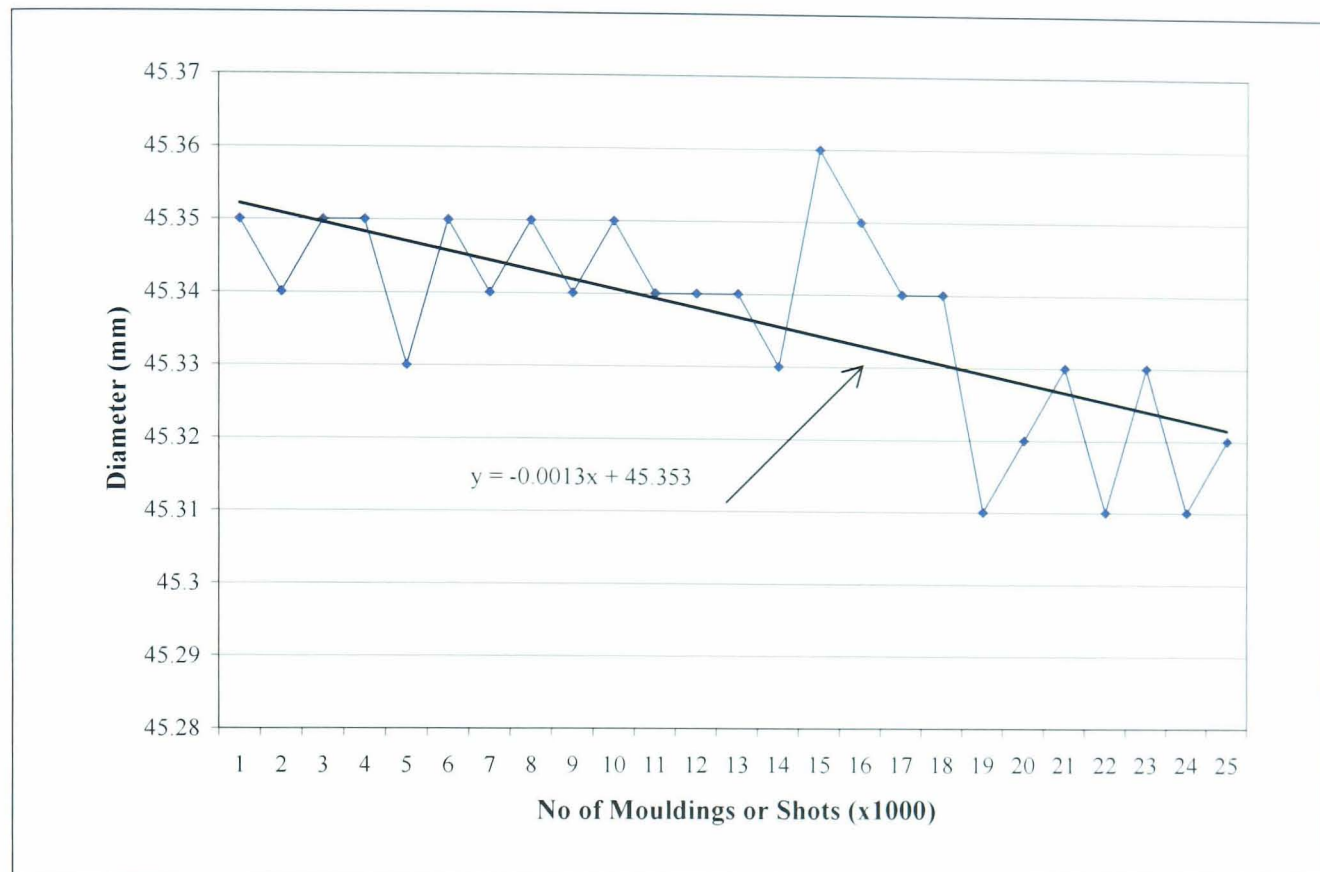


Figure 4-21. Wear Rate

Whilst, Figure 4-22 indicates the areas on the inserts where the surface finish was assessed. Comparing to the average surface roughness ( $R_a = 0.02\mu\text{m}$ ) measured before the trial, the surface roughness after trial are smoother by: 10.0% ( $0.018\mu\text{m}$ ) at the indicated surface area A.

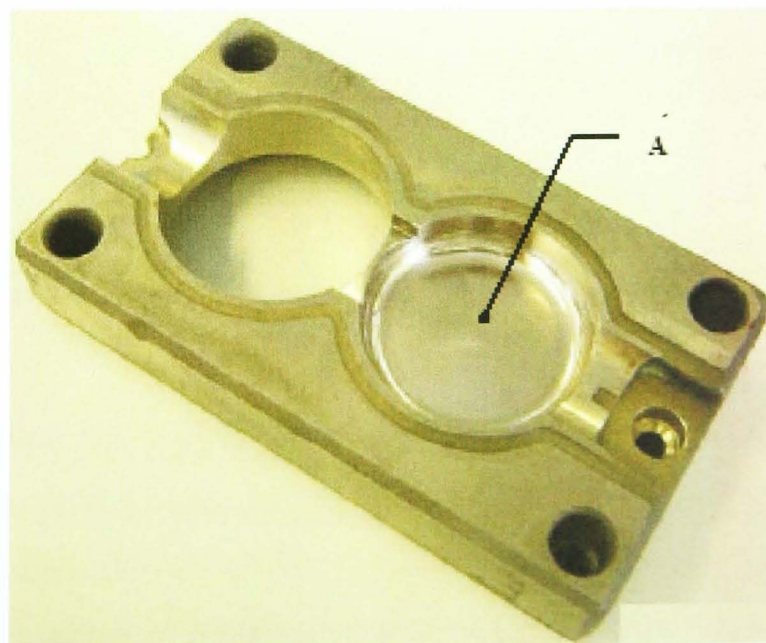


Figure 4-22. Surface Finish Area

#### 4.2.6. Cost Analysis

With a new conformal cooling channels constructed inside the new CS1 inserts, the moulding trial has indicated a significant improvement in moulding productivity. Thus, the development of the new CS1 inserts has also indicated that combining indirect SLS with the HSM process has able to reduce the manufacturing time and cost required. Table 4-3 summarises the time advantages of using the new CS1 inserts compared to its existing inserts. To evaluate an economic impact, these advantages were then fed into the cost model for a product cost analysis. For this purpose, a condition at 12s moulding cycle time (15% reduction) was decided to use because products at 11.3s moulding cycle time (20% reduction) was failed (Figure 4-23).

Table 4-3. CS1 Manufacturing and Moulding Comparison

No	Data/Parameters	Unit	Existing	New CS1	Diff. (%)
1	Manufacturing lead-time	Hours	486	270	(44.3)
2	Moulding cycle time	sec	14.1	12.0	(15.0)
3	Production rate	Part/hour	255	300	17.6
4	Total moulding time required**	hour	3,922	3,333	15.0

\*\* Total time required to mould 1,000,000 products



Figure 4-23. Failed Products at 11.3s Cycle Time

To overview the impact on the product cost, Table 4-4 lists the percentage differences of the product cost using the new CS1 inserts, analysed on the basis of: (a) the expected durability for moulding projected number of products required, and (b) the projected number of products relative to the assumed/predicted durability. To protect commercial confidentiality, the results are presented as a ratio rather than as



absolute. Both tables also indicate the replacements required of the new CS1 insert to produce the projected number of the products at expected durability.

Table 4-4. CS1 Product Cost Analysis

*Expected Durability	No. of Replacement		Prod. Cost Diff. (%)
	Exist.	New	
100,000	1	10	82.4
200,000		5	11.7
300,000		4	(2.4)
400,000		3	(16.5)
500,000		2	(30.6)
600,000		2	(30.6)
700,000		2	(30.6)
800,000		2	(30.6)
900,000		2	(30.6)
1,000,000		1	(44.8)

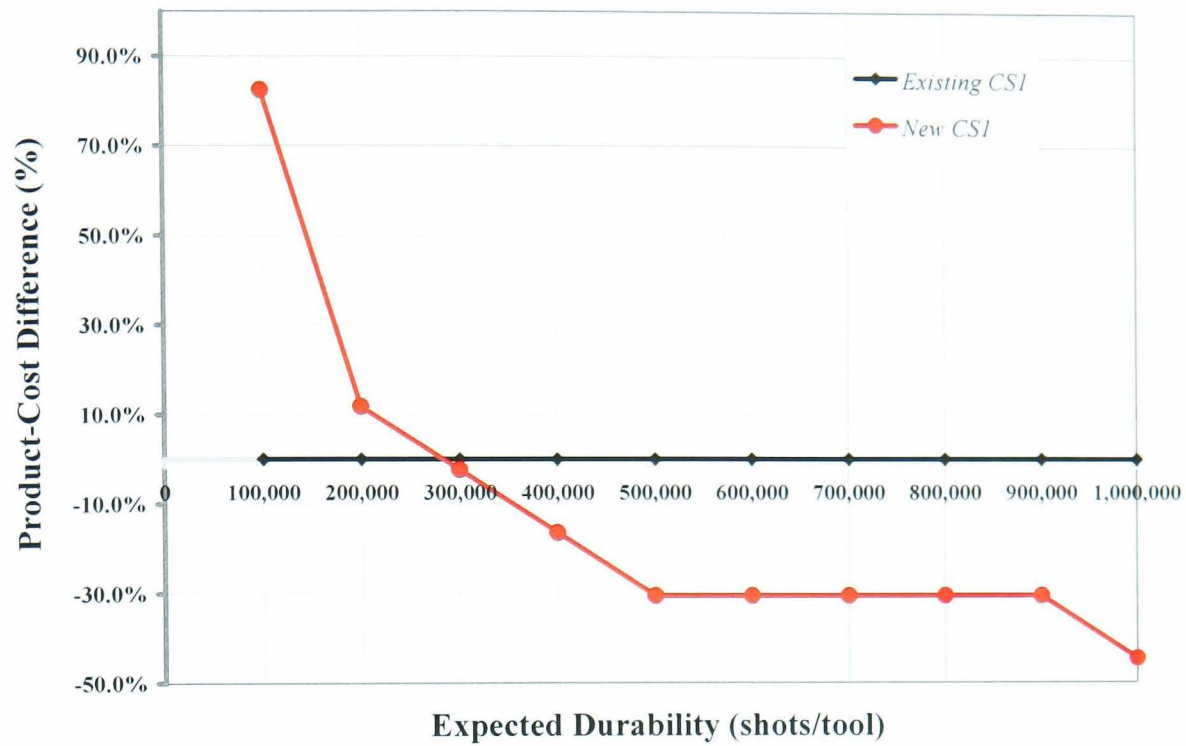
\* Expected durability of LaserForm material

(a) Product Cost vs. Expected Durability

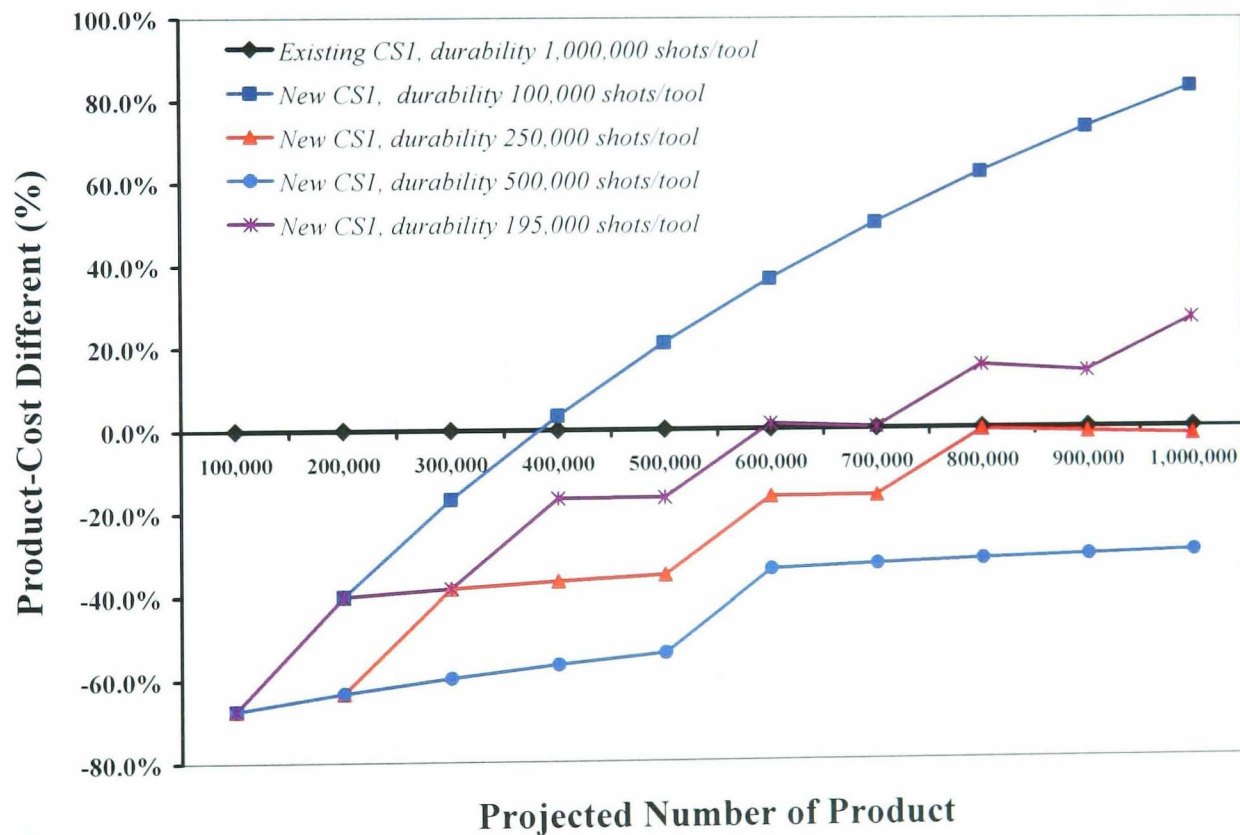
Projected Products	No. of Replacements					Product Cost Different (%)			
	Exist.	New							
		100k	195k	250k	500k	100k	195k	250k	500k
100,000	1	1	1	1	1	(67.5)	(67.5)	(67.5)	(67.5)
200,000		2	2	1	1	(40.1)	(40.1)	(63.4)	(63.4)
300,000		3	2	2	1	(16.8)	(38.3)	(38.3)	(59.8)
400,000		4	3	2	1	3.3	(16.7)	(36.7)	(56.7)
500,000		5	3	2	1	20.9	(16.6)	(35.3)	(54.0)
600,000		6	4	3	2	36.3	1.1	(16.5)	(34.1)
700,000		7	4	3	2	50.0	0.2	(16.4)	(33.0)
800,000		8	5	4	2	62.2	15.1	(0.6)	(32.0)
900,000		9	5	4	2	73.2	13.6	(1.3)	(31.2)
1,000,000		10	6	4	2	83.1	26.4	(2.0)	(30.4)

(b) Product Cost vs. Projected Number of Products

To analyse whether the new CS1 inserts is economically viable as production tool, Figure 4-24 shows a percentage difference of the product cost between the new and existing CS1 insert. From the percentage difference, the graphs in both Figure 4-24a and b have generally indicated that the usage of the new CS1 inserts can be competitive (lower product cost) against its existing inserts as long as the durability of the new CS1 inserts is able to stand at least 250,000 shots. Moreover, Figure 4-24b indicates that the new CS1 inserts - regardless its durability - always more economic compared to the existing for small volume production (less than 350,000 shots). However, a production/durability trial for CS1 has predicted (with a maximum durability of 195,000 shots) that a product cost benefit will be achieved if this new CS1 insert is run to produce up to 550,000 – 600,000 products.



(a) Product Costs at Expected Insert Durability to Produce 1,000,000 Products



(b) Product Costs at Assumed Inserts Durability to Produce Projected Products

Figure 4-24. CS1 Product Costs Analysis

### 4.3. Case Study 2: Receptacle Spoke

#### 4.3.1. Product Evaluation

The second case study (CS2) considered a receptacle spoke (Figure 4-25) from Trisport Ltd. According to the information provided by Trisport [Clark, 2006],

typical production volume for this product is 40,000,000 per year using a 16 cavity mould. With an average product life of 2 to 5 years, the existing mould inserts are designed to be able to stand up to 5,000,000 to 12,500,000 shots. The required cycle and cooling time to mould this product using the existing mould insert were 8.0 s and 2.5 s respectively. As evaluated from its detail drawing, the following important information and specifications are considered.

- *Wall thickness*: various from 1.2 to 3.3 mm
- *Special features*: internal thread
- *Draft angle*: 5° is provided to the product
- *Surface finish*: fine spark eroded finish all over the surfaces, except internal thread (polished all over)



Figure 4-25. Receptacle Spoke [Trisport Ltd.]

#### 4.3.2. Insert Design

For this case study, the redesign of the CS2 inserts was focused on modification of the cooling channel on the existing inserts. Figure 4-26 shows an assembly drawing of both (a) existing and (b) new CS2 inserts as well as a 3D CAD model of the new moving (c) and fixed (d) inserts. Figure 4-26a clearly shows that the design of the existing inserts has the cooling channels for both moving and fixed inserts externally constructed as turned grooves which are located approximately 9 mm from the cavity. With a new modification, the new CS2 cooling channel was constructed inside the inserts and laid out conformal to the cavity. In designing the channel, a limited working area for locating the channel in the fixed insert was a major constraint because at this insert the off-centre hole for hot runner nozzle was constructed. As a result, the new cooling channel was then progressed and located approximately 4 mm from the cavity (Figure 4-26b). To view the cooling channels geometry, Figure 4-27 furthermore illustrates the 3D CAD channel models designed for both moving (a) and fixed (b) inserts.

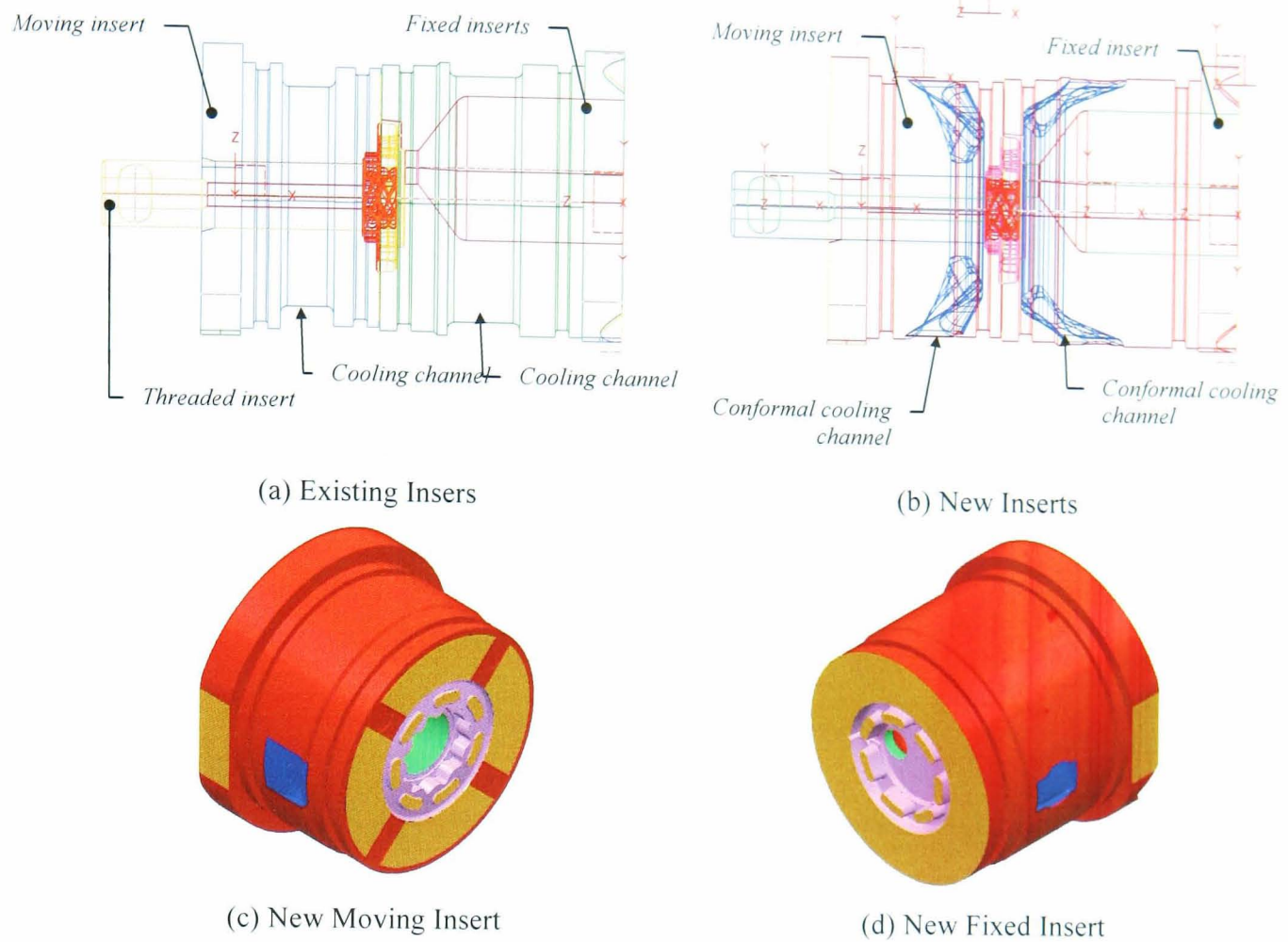


Figure 4-26. CS2 Inserts

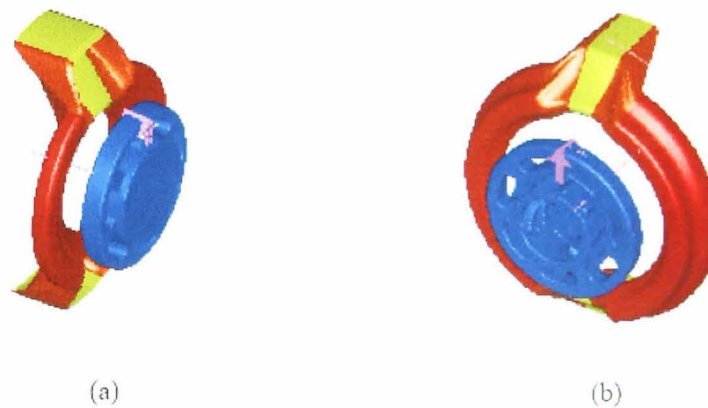
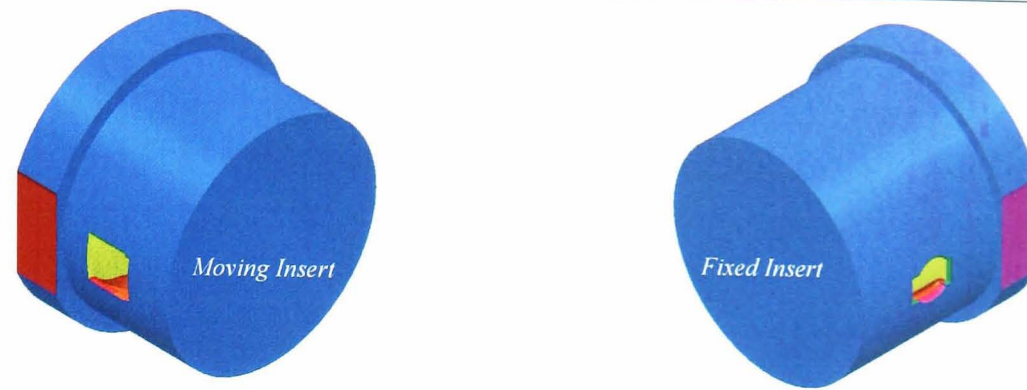


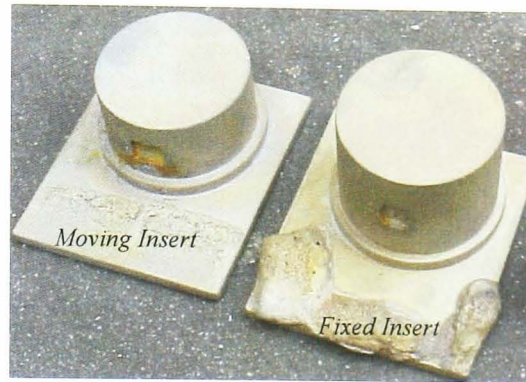
Figure 4-27. The New CS2 Cooling Channels Geometry

### 4.3.3. Insert Manufacture

As the inserts contained a large number of small features, both the new CS2 moving and fixed inserts were designed as simple cylinders with conformal cooling channels constructed inside them. Referring to CS1, a larger 1mm machining allowance was added to all external dimensions to provide more stock for machining/finishing. Figure 4-28 shows (a) 3D CAD and (b) the SLS metal models after infiltration.



(a) 3D CAD Models



(b) SLS Metal Models

Figure 4-28. Near-Net Shape Design of the New CS2 Inserts

Sixteen sets of moving and fixed inserts were developed. No special treatment was taken for powder clearing as it was believed that the powder could be cleared easily. Also, additional high temperature resin infiltration for sealing was not necessary. For finishing to final production specification, the inserts were manufactured at Leeds University (lathe work and surface grinding), Craftsman Tools (cylindrical grinding), and Delcam (HSM and EDM).

As in CS1, Figure 4-29 shows the colour codes used to explain turning and grinding operations in producing the features on the inserts. A blue colour represents the features that require only SLS process, no further machining and finishing required. A green colour shows the features that require only surface turning operation, while a red colour show the features that require both turning and grinding operation. A yellow colour indicate turned grooves which are required for o-ring. Thus, a pink colour represents drilled and bored features.

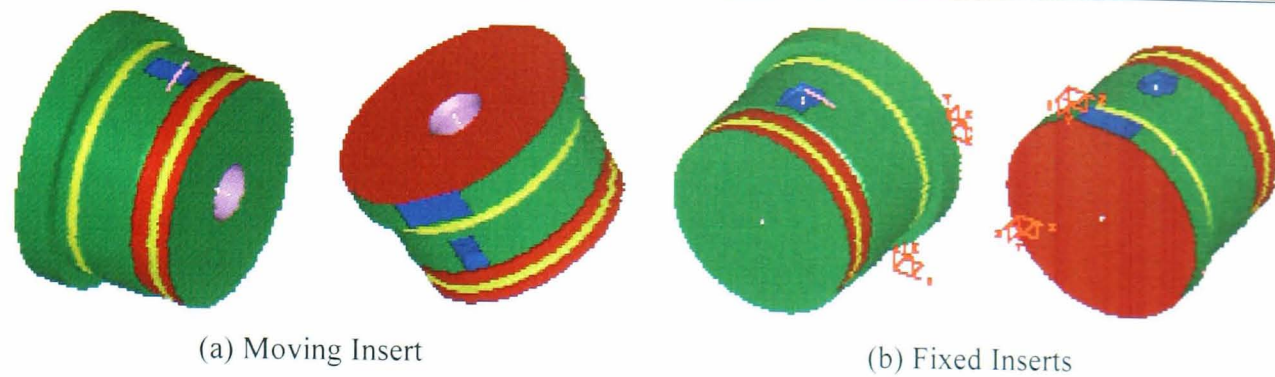


Figure 4-29. Colour Code of Turning and Grinding Operation

Furthermore, Figure 4-30 show the colour codes that explain machining and finishing operations required following the above operations. In this case, a blue represents the surfaces of the completed features from the previous operations. An orange show HSM operation for facing flat surfaces, while a red colour for forming freeform surfaces. A green colour represents drilled or bored holes. For a pink colour, it represents the features that require an EDM operations

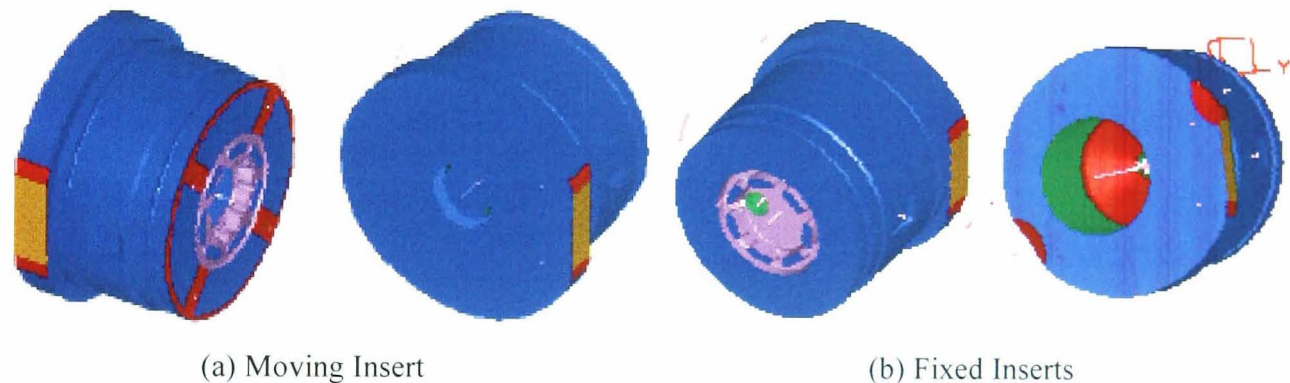


Figure 4-30. Colour Code of HSM and EDM Operations

During turning operation at Leeds University, the operator indicated that back face of every insert was found curl on one edge, due to SLS process. For programming purposes, the operator therefore decided to attempt full surface clean-up at this back face. Consequently, a length of 2 moving and 8 fixed inserts before grinding was undersized as illustrated in Figure 4-31. To solve the problem, two approaches was performed. The back face of the undersized inserts was: (i) used as a datum when programming HSM and EDM operations to develop core and cavity, and (ii) chrome plated and reground back to standard length. Overall, it was evaluated that the manufacturing of the new CS2 inserts reduced the lead time by 13.6% and increased the cost by 24%.

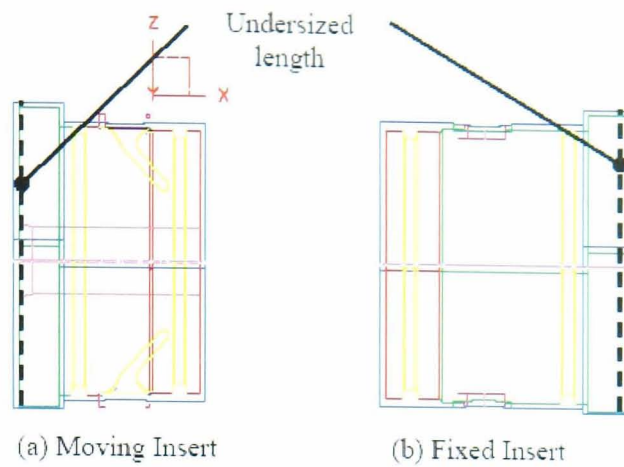


Figure 4-31. Underized Inserts

#### 4.3.4. Moulding Trial

The moulding trial was run in the Trisport production workshop. Before trial, it was found that 3 sets out of the 16 sets inserts could not be used for trials due to blocked cooling channels. Therefore, 13 sets of the new and 3 sets of existing inserts were then combined and contained in the exiting mould base. Figure 4-32 shows both moving (a) and fixed (b) halves was mounted on the injection machine, and illustrates an arrangement of the inserts (c) located in mould halves. From this arrangement, it is indicated (see Figure 4-32c) that the sets of the inserts (impressions) number 3, 7 and 16 were allocated for the 3 existing inserts. For the trial, the moulding parameters were set up using the operating parameters as run in production. Table 4-5 lists the specification of the material used and summarizes the main process parameters.

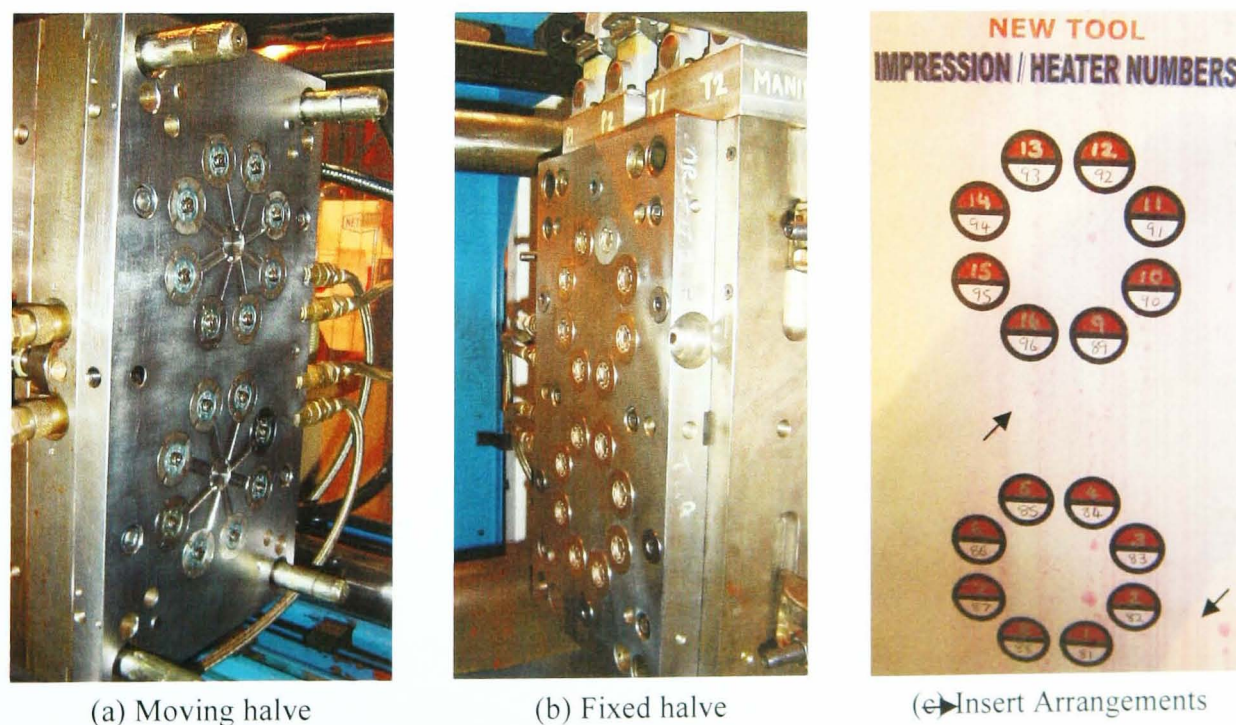


Figure 4-32. Mould halves and Inserts Arrangement

Table 4-5. CS2 Material and Process Parameters

<b>A</b>	<b>Material Specificatios</b>	
1.	Material:	Stanyl TW341 Natural
2.	Density:	1.18 g/cm <sup>3</sup>
3.	Sp. Heat	2.1 J/g °C
<b>B</b>	<b>Process Parameters</b>	
1.	Injection Temp.:	ave. 310 °C
2.	Ejection Temp.:	ave. 120 °C
3.	Mould Temp.:	ave. 80 °C
<b>C</b>	<b>Coolant</b>	
1.	Coolant:	water
2.	Temp. Diff:	ave. 10 °C
3.	Flow Rate	ave. 15 l/min

#### 4.3.4.1. Procedure and Measurements

As in CS1, the moulding trial progressed by reducing the cycle time gradually. During the cycle time reduction, a machine energy consumption was also measured. At the beginning of the trial, the moulding process was warmed up for about an hour at the optimum production cycle time of the existing inserts (7.7s) until process steady state was reached. Cycle time reduction was then carried out in the following reduction order every 1 hour of running: 4% (7.4s), 8% (7.1s), 12% (6.8s) until reaching the machine limits of 16% (6.5s).

Sample mouldings for each cycle time were then collected for quality inspection. Figure 4-33 indicates four targeted dimensions on the mouldings that have to be measured in order to represent the product quality. These four targeted dimensions are: Main (M) diameter = 22.00 ( $\pm 0.20$ ) mm; Ratchet (R) diameter = 13.70 ( $\pm 0.04$ ) mm; Bore (B) diameter = 6.54 ( $\pm 0.02$ ) mm; Height (H) = 6.2 ( $\begin{smallmatrix} +0.20 \\ 0.00 \end{smallmatrix}$ ) mm.



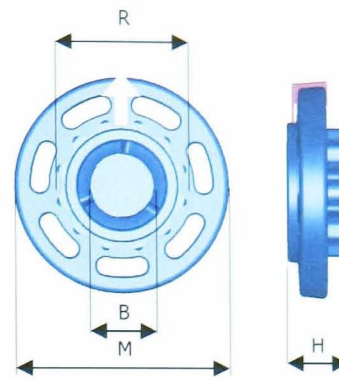


Figure 4-33. CS2 Product Quality

#### 4.3.4.2. Results

The trial had showed that the new CS2 inserts were able to be operated at a 6.5s cycle time. At this condition, visually there was no evidence that indicate product failure on the mouldings at every cycle time reduction, including the mouldings which were produced by the 3 sets of the existing inserts. From given information, the original cycle time of 7.7s is chosen in running the existing inserts is actually to minimise scrap due to un-acceptable product quality such as out of tolerance, burning, and voids [Clark, 2006].

The trial was also indicated that the machine energy consumption improved as the cycle time reduced. The machine energy consumed to moulding 16 products per shot was reduced from 163 kJ at 7.7s down to 140 kJ (14%) at 6.5s cycle time. Figure 4-34 show the profiles of the effective power consumed against the elapsed time for both cycle time 7.7s and 6.5s.

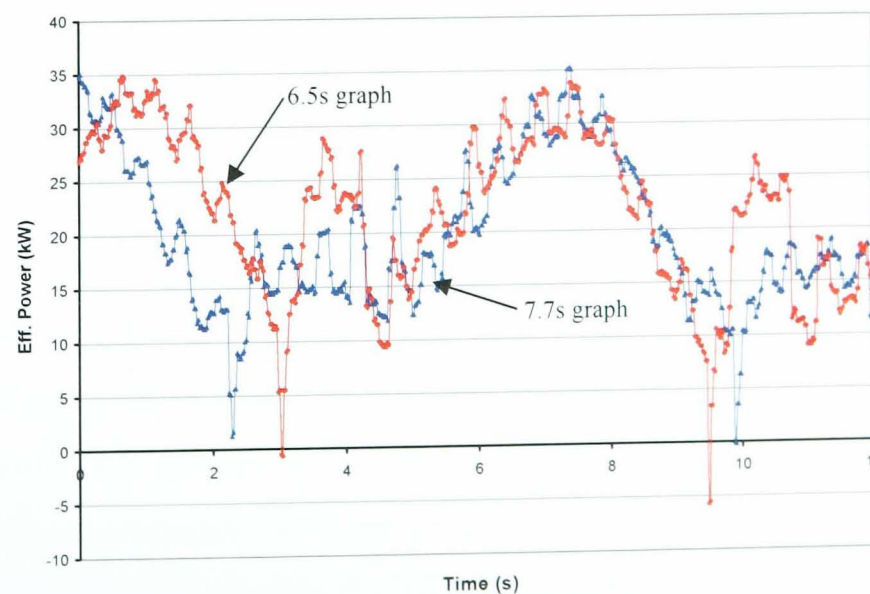


Figure 4-34. Energy Measurement.

Furthermore, the trial also showed that the new CS2 inserts performed as expected. The average measurements of each targeted dimension are shown in Figure 4-35.

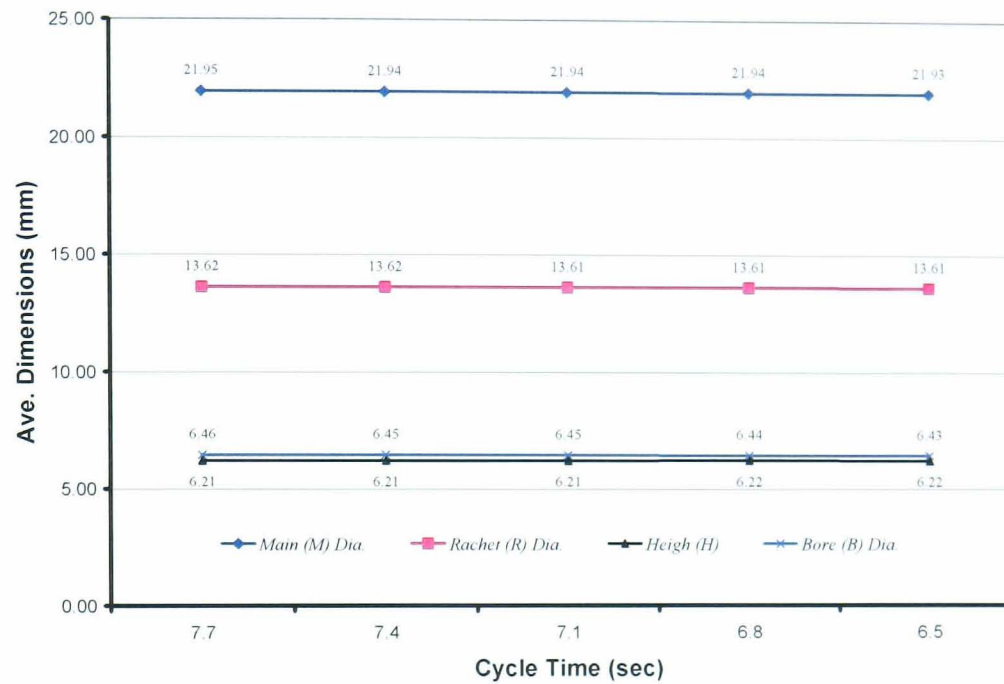


Figure 4-35. CS2 Product Measurements

In general, the graph has shown that the average of four targeted feature dimensions was consistent even though two of them - ratchet (R) and bore (B) diameter- are out of tolerance band (smaller) as mentioned in section 4.3.4.1. From the results of both quality inspection and energy measurement, it is indicated that the inserts are capable to produce quality moulding consistently and offer a robust operation. To evaluate its economic impact, these results together with the outputs from the manufacturing processes were then included for analysing the product cost, which will be discussed in the next following section.

#### 4.3.5. Cost Analysis

In CS2, combining indirect SLS with HSM in developing the inserts has been unable to offer overall cost benefits even though the overall manufacturing processes and moulding productivity improved. To analyse the overall impact, the cost analysis using these new CS2 was then carried out, and a cycle time at 6.8s (12% reduction) was chosen to be employed in calculation. This cycle time was chosen only for concerning the limit of the machine and avoiding too optimistic analysis results when employing the minimum cycle time of 6.5s. To review the results, Table 4-6 summarises four important key advantages and improvements in developing the new CS2 insert comparing to its existing inserts.

Table 4-6. CS2 Manufacturing and Moulding Comparison

No	Data/Parameters	Unit	Existing	New CS2	Diff. (%)
1	Manufacturing lead-time	hour	640	553	(13.6)
2	Moulding cycle time	sec	7.7	6.8	(12.0)
3	Production rate	Product/hour	7,481	8,471	13.2
4	Total moulding time required**	hour	2,139	1,889	(12.0)

\*\* Total time required to mould 16,000,000 products

The product costs as a result of using the new CS2 is analysed against the product cost using the existing insert (Table 4-7). As in CS1, the table shows the product cost percentage differences based on (a) an expected durability of one set of the new CS2 inserts in moulding the projected number (16,000,000) of the products, and (b) projected numbers of the products at assumed durability. Figure 4-36 plots these product costs differences, and both figures indicate that the product costs using the new CS2 inserts are higher than in using the existing insert at every assumed/predicted durability. The main reason of the results is due to the significant impact of 73% cost increase inquired during manufacturing the 16 sets of the CS2 inserts.

Table 4-7. CS2 Product Cost Analysis

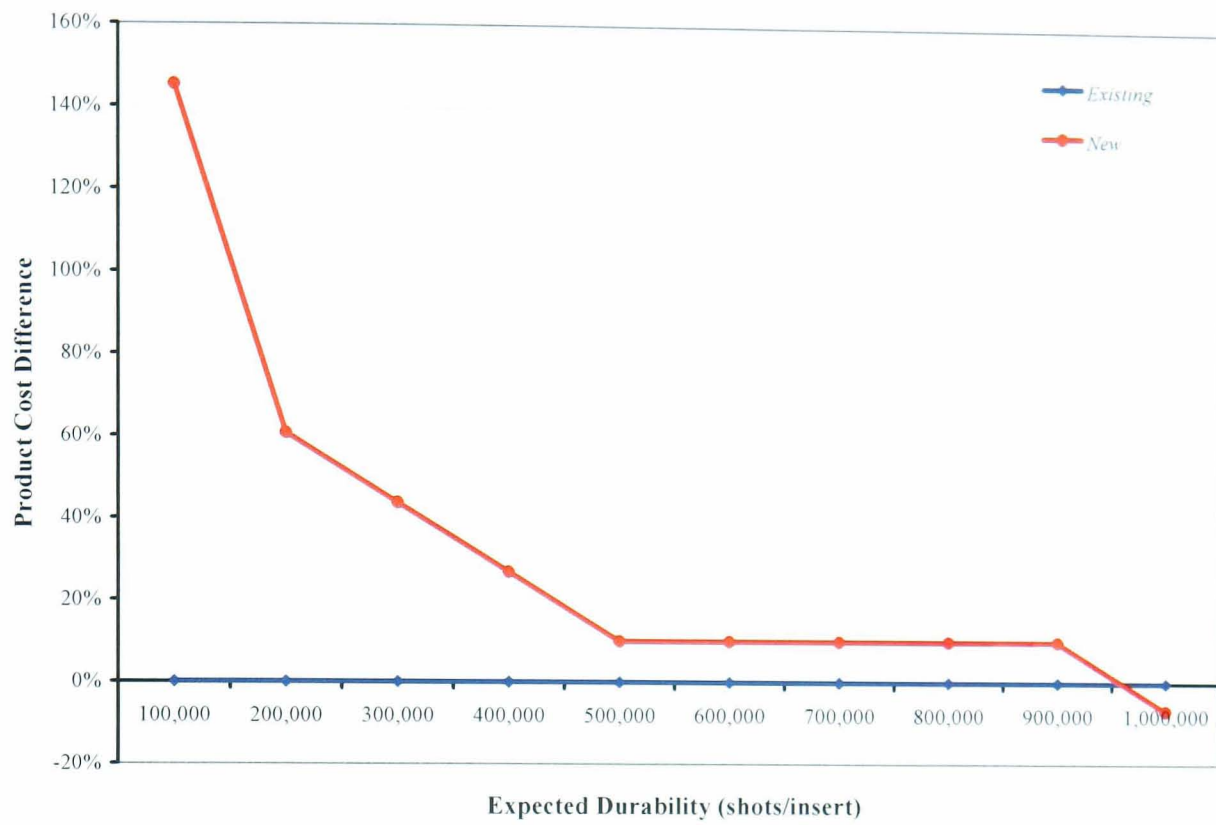
*Expected Durability	No. of Replacements		Product Cost Diff. (%)
	Exist.	New	
100,000	1	10	303.9%
200,000		5	107.4%
300,000		4	68.1%
400,000		3	28.8%
500,000		2	(10.5)
600,000		2	(10.5)
700,000		2	(10.5)
800,000		2	(10.5)
900,000		2	(10.5)
1,000,000		1	(49.8)

(\*) Expected durability of LaserFom material

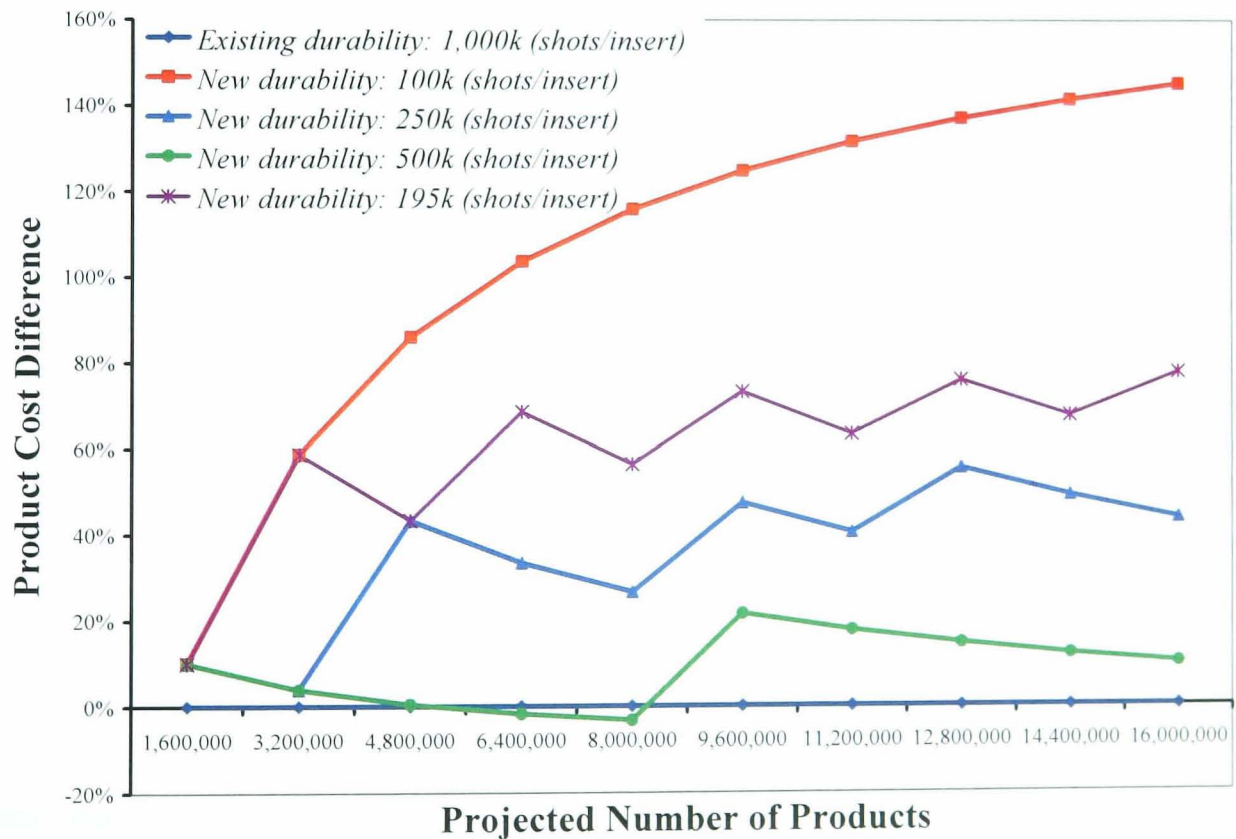
(a) Product Cost vs. Expected Durability

Projected Products	No. of Replacements				Product Cost Different (%)				
	Exist.	New							
		100k	195k	250k	500k	100k	195k	250k	500k
1,600,000	1	1	1	1	1	9.9	9.9	9.9	9.9
3,200,000		2	2	1	1	58.6	58.6	3.9	3.9
4,800,000		3	2	2	1	86.0	43.2	43.2	0.5
6,400,000		4	3	2	1	103.5	68.5	33.4	-1.7
8,000,000		5	3	2	1	115.8	56.3	26.5	-3.2
9,600,000		6	4	3	2	124.8	73.1	47.3	21.5
11,200,000		7	4	3	2	131.6	63.2	40.4	17.6
12,800,000		8	5	4	2	137.1	75.8	55.4	14.5
14,400,000		9	5	4	2	141.5	67.5	49.1	12.1
16,000,000		10	6	4	2	145.2	77.6	43.8	10.0

(b) Product Cost vs. Projected Number of Products



(a) Product Costs at Expected Durability of One Set Insert to Produce 1,000,000 product



(b) Product Costs at Assumed Inserts Durability to Produce Projected Number of Product

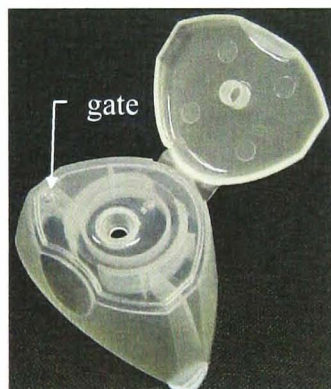
Figure 4-36. CS2 Product Cost Analysis

#### 4.4. Case Study 3: Cassio 200 ml Bottle Top

##### 4.4.1. Product Evaluation

In a case study three (CS3), a Cassio 200ml tube top from Unilever Ltd. was selected (Figure 4-37). According to the information provided [Leech, 2006], the existing mould runs non stop with a cycle time of 15 seconds using 24 cavities. An average production volume per year from this mould is within the range 24,000,000 to 48,000,000. For this product, the average expected life is 3 years. Other information regarding the product design are:

- *Wall thickness*: various from 0.1 to 2.3 mm
- *Special features*: internal thread
- *Draft angle*: 5° is provided to the product
- *Surface finish*: fine spark eroded finish all over the surfaces, except internal thread (polished all over)

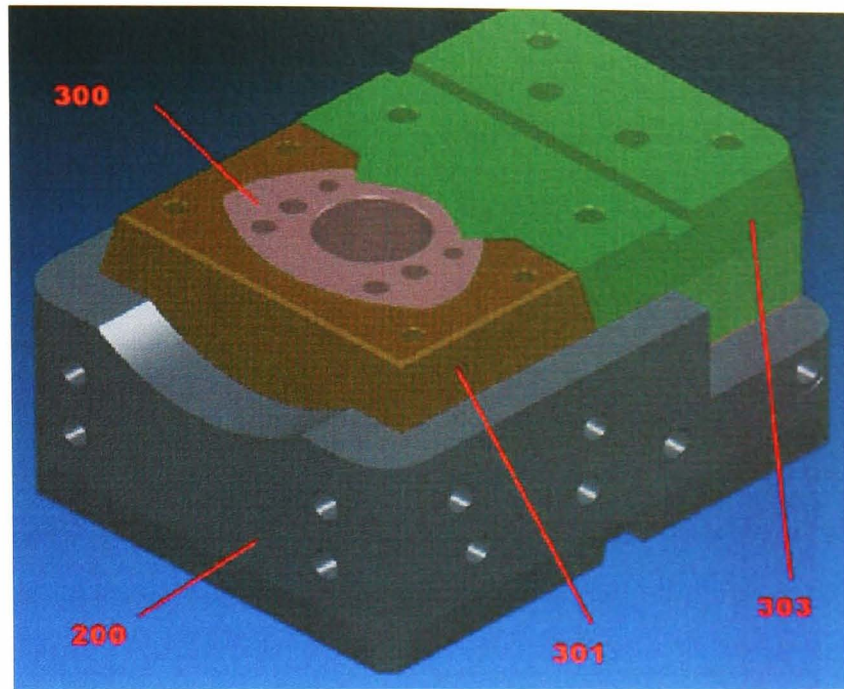


<b>Dimension:</b>	41 x 61 x 29.6 mm
<b>Orifice Size:</b>	6.0 mm
<b>Hinge Style:</b>	Protrusionless
<b>Lid:</b>	Flat Lid
<b>Surface Finish:</b>	Glossy, Fine machine finishing
<b>Material:</b>	Polypropylene (PP)
<b>Shrinkage</b>	1.6%
<b>Weight:</b>	6.6g

Figure 4-37. A Cassio 200ml Tube Top [Uniliver Ltd.]

##### 4.4.2. Insert Design

In this case study, the major concern in redesign was focused on modification of the cooling channels design inside two components (200 and 300) out of the total of six components that form the existing CS3 insert (Figure 4-38). The original external geometry of the modified components was kept the same components 200 and 300 as a main cavity and core respectively. In support of this case study, an initial analysis of moulding performance of the existing cooling channels was carried out by running a filling/packing and cooling simulation by John Gosden using a Moldex3D analysis software from FlowHow®.



(a) Assembly of Inserts



(b) Cavity (200)



(c) Core (300)

Figure 4-38. Existing CS3 Inserts (Unilever)

The filling/packing simulation analyses the moulding from when melting plastic enters into the moulding cavity, through to ejection. The cooling simulation analyses the performance of the cooling system by assessing the cooling efficiency of every channel in removing heat from the moulding cavity. In running these simulations, the moulding parameters are set up the same as the conditions when running the insert for production. Table 4-8 shows basic moulding conditions used for the analysis.

Table 4-8. Moulding Parameters (Gosden, 2005)

Filling/Packing		Cooling	
Filling time (sec)	0.6	Cooling time (sec)	5
Pack time (sec)	5	Open time (sec)	1
Melt temperature (°C)	230	Air temperature (°C)	25
Mould temperature (°C)	40	Eject temperature (°C)	120
Max. injection pressure (MPa)	150	Inlet coolant temperature (°C)	12
Max. pack pressure (MPa)	50	Re Number	16,278

As a result of filling/packing simulation, Figure 4-39 presents surface temperature scales at ejection on both (a) inside and (b) outside of the product. The results have indicated that there are several critical areas on the product that need to be carefully considered in designing the cooling system. The most critical is on the inside area where the product has a direct contact with the core (300). The highest range of the surface temperature of 84°C is spotted in this area. Other considered critical areas are spotted on the surface of hinge and inside the product lid. The average surface temperature at these areas was projected as 63°C. Using the existing cooling system, the model also indicated that the lowest surface temperature of the product at ejection is 20°C.

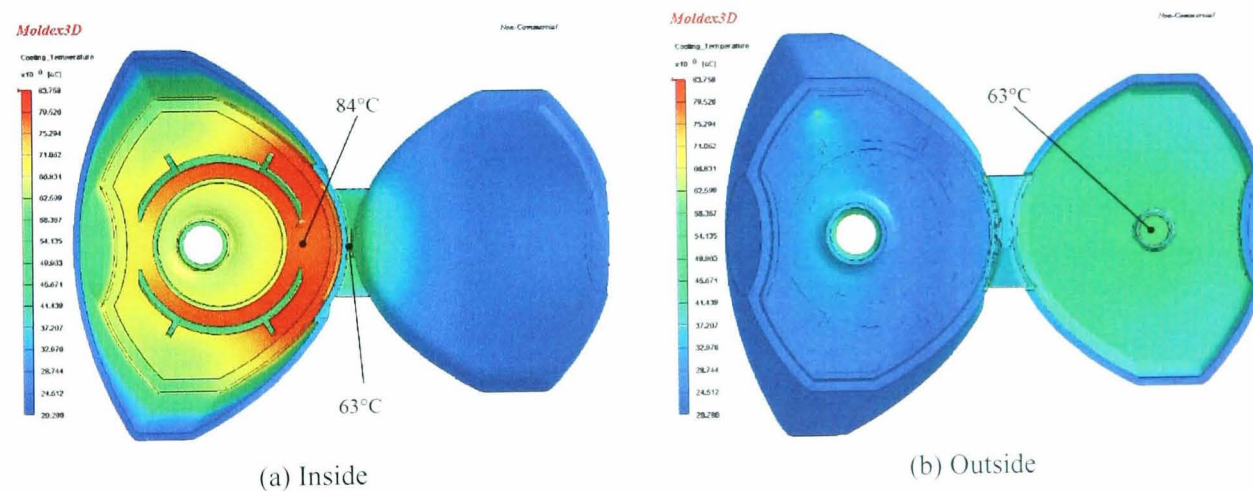


Figure 4-39. Surface Temperature Scales (Gosden, 2006)

In the case of the cooling simulation, Figure 4-40 shows the performance results of the cooling systems inside the existing inserts by indicating the cooling efficiency scales of every cooling channels. The simulation has indicated that the most efficient channels (34%) is at S-shaped channel constructed inside the cavity. The cooling efficiency at the C-shaped channels is only about 15%. The second highest cooling efficiency of 23% is indicated at the two-side bubblers constructed inside the core, with the lowest efficiency channel (10%) the central bubbler in the core.

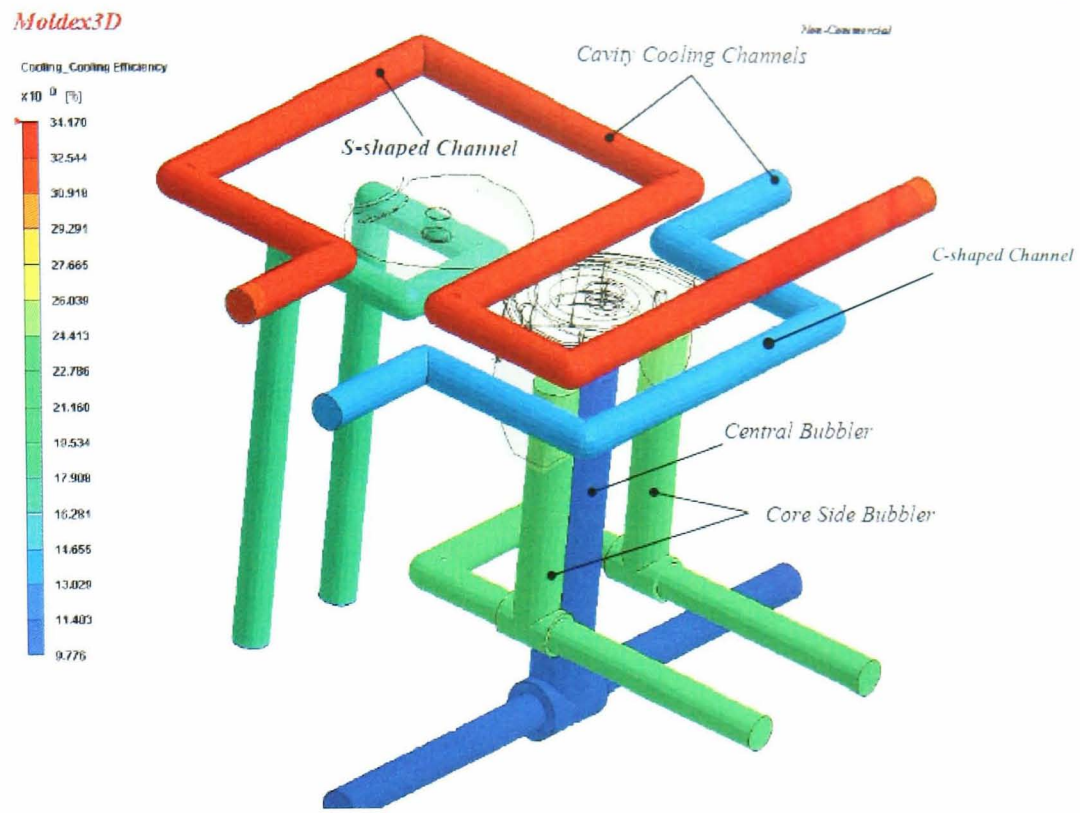
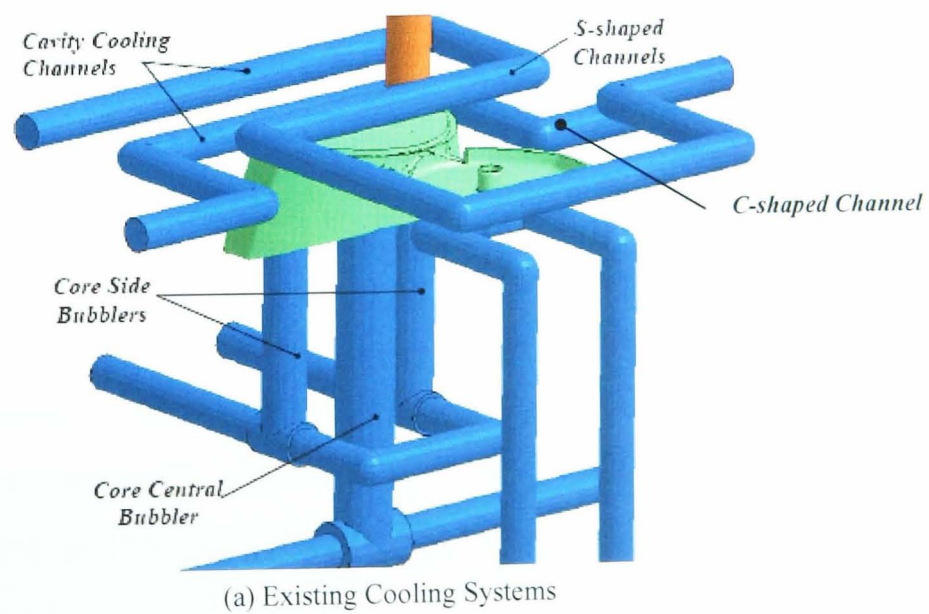


Figure 4-40. Cooling Efficiency [Gosden, 2005]

The proposed new design of the CS3 conformal cooling channels for cavity and core were also simulated. The main objective of the design is to reduce the surface temperature in the critical area of the product by improving cooling. Figure 4-41 shows the design transformation from (a) the existing cooling system to (b) the new CS3 conformal cooling system. Thus, the figure also details the design of the new modified conformal cooling channel constructed inside both cavity (c) and core (d) insert.





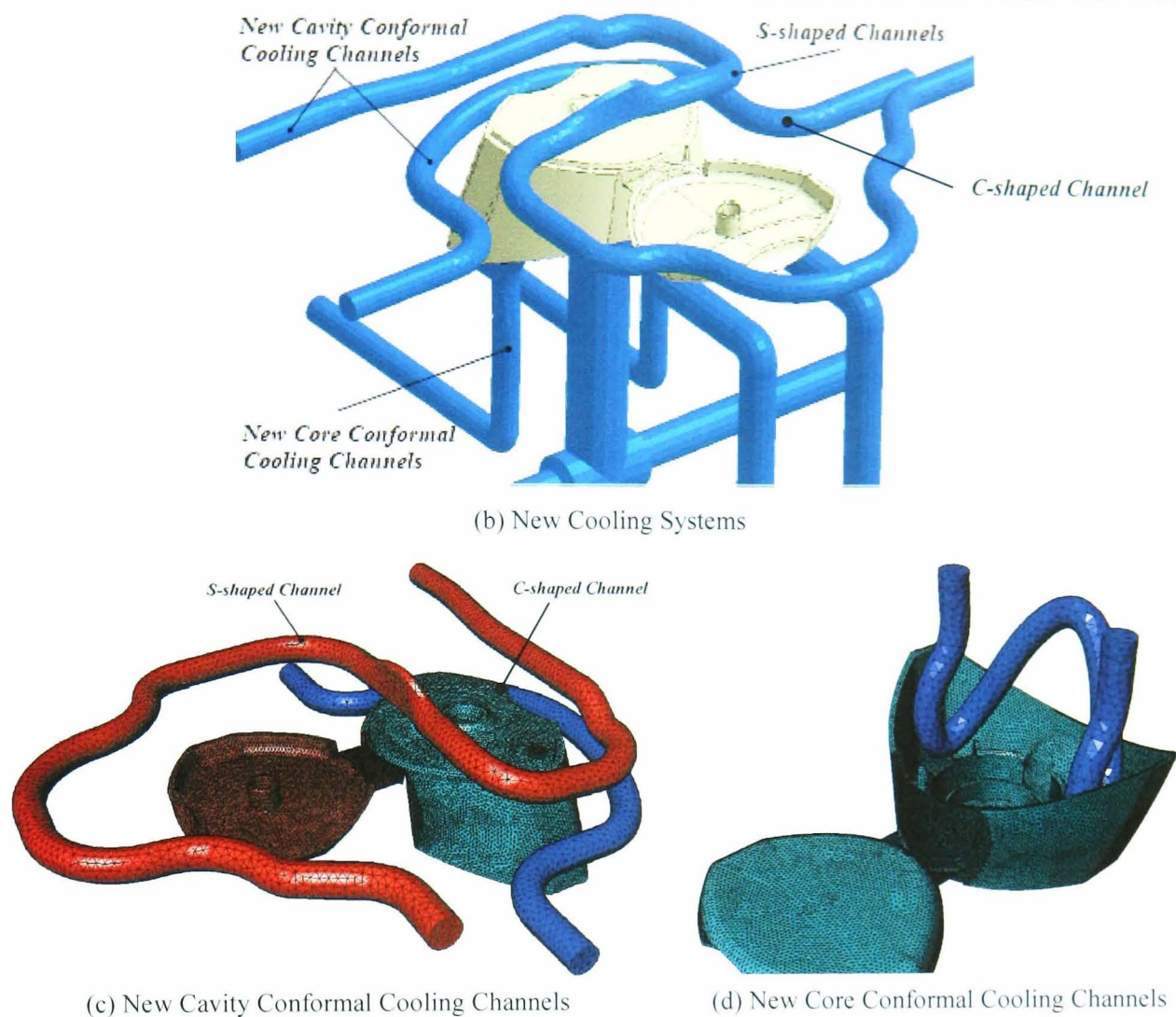


Figure 4-41. Existing vs. New CS3 Cooling Systems [Gosden, 2005]

Restricted by the original geometry, the space available, and the cooling channel inlet and outlet positions, the basic design of the new conformal cooling channels inside the cavity inserts (Figure 4-41c) are mostly similar to the existing cooling channels. The main modification is only to take the channels closer to the mould cavity. In the case of the new conformal cooling channels inside the core (Figure 4-41d), a major modification is the replacement of the existing two-sided bubblers.

The filling/packing result with the new insert designs (Figure 4-42) indicates that the new conformal channels have able to reduce the surface temperature at the critical areas mentioned previously (see Figure 4-39): 23% ( $84^{\circ}\text{C}$  to  $65^{\circ}\text{C}$ ) inside the product, 25% ( $63^{\circ}\text{C}$  to  $47^{\circ}\text{C}$ ) at the hinge, and 36.5% ( $63^{\circ}\text{C}$  to  $40^{\circ}\text{C}$ ) inside the lid.

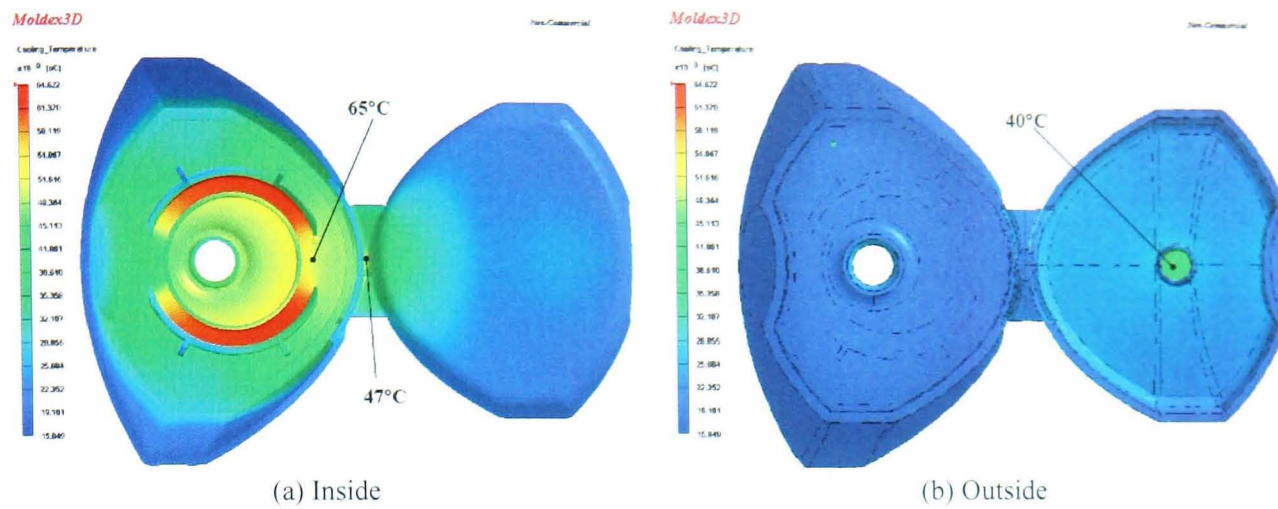


Figure 4-42. New Surface Temperatures [Gosden, 2005]

In the case of the cooling simulation, the results have furthermore indicated that the new design of the CS3 conformal cooling channels are also able to improve the cooling efficiency of the channels (Figure 4-43). For the conformal cooling channels inside the cavity, the average cooling efficiency of both channels is improved by 1%. The new core conformal cooling channel has able to increase its performance significantly by increasing the cooling efficiency from 23% using two-side bubblers to 32%. To evaluate further performance between existing and new cooling system, a simulation on cooling time reductions was also run. The results (Table 4-9) have shown the impact on product surface temperature as cooling time reduced to 1s, which also indicated a potential of the new CS3 to improve the moulding performance [Gosden, 2005].

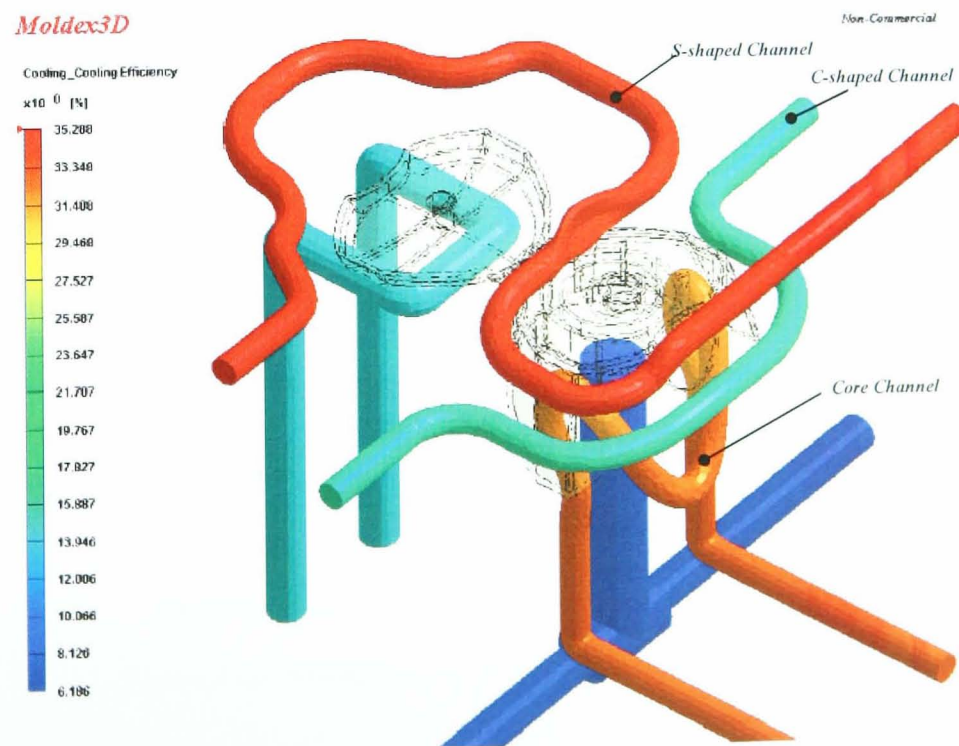


Figure 4-43. New Cooling Efficiency [Gosden, 2005]

Table 4-9. Comparison Effects on Surface Temperature [Gosden, 2005]

Design	Cooling Time (s)	Min Surface Temp. (°C)	Max Surface Temp. (°C)
Existing Insert	5	20.2	83.8
New Insert	5	15.9	64.6
	4	16.4	70.7
	3	17.1	77.6
	2	17.9	84.0
	1	18.1	85.8

#### 4.4.3. Insert Manufacture

A near-net shape design of the new CS3 cavity and core inserts for indirect SLS process was first generated (Figure 4-44). A general machining allowance of 1mm was applied to most surfaces. A larger 2mm allowance was applied to the horizontal surfaces of the cavity inserts to anticipate larger furnace deformation due to the large part volume (green part weight is 5kg). For clearing powder inside the channels, access holes at several selected locations were prepared on both inserts at green-part stage, as indicated in Figure 4-45. Simultaneously, the plugs (bungs) required for closing the holes were also developed at this stage. Because of the large part volume, a special design of plates for bronze ingots to stand was added only on the cavity insert (Figure 4-45a) in order to provide sufficient spaces for the ingots, and to allow uniformly flow distribution of the bronze during infiltration process.

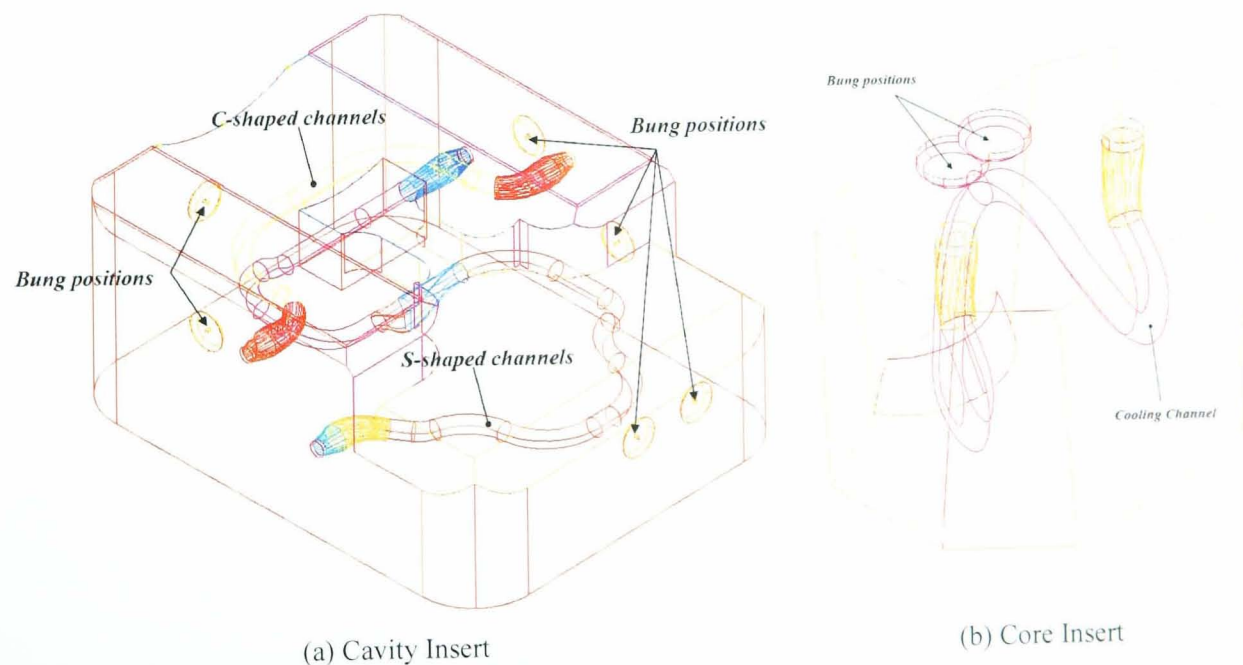
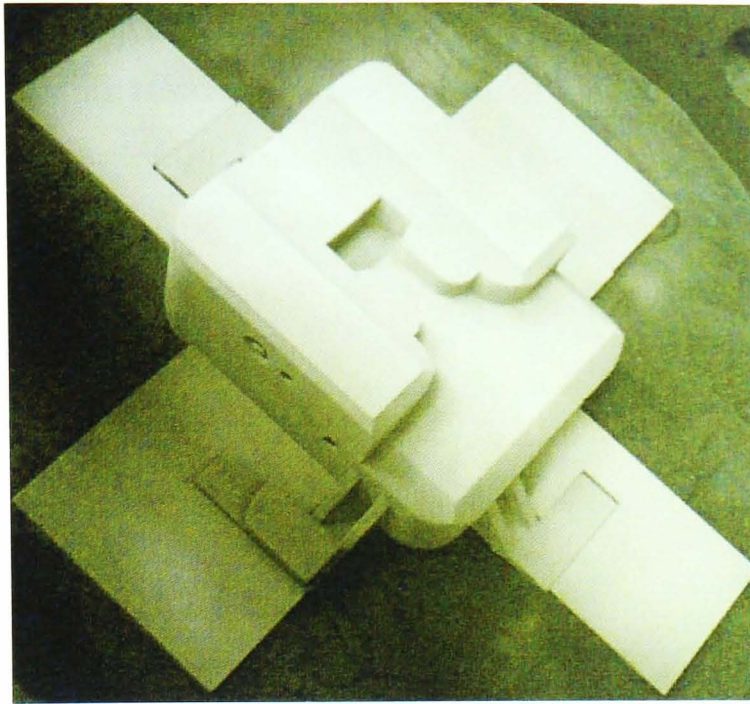


Figure 4-44. Wireframe of the CS3 Near-Net Shape Inserts



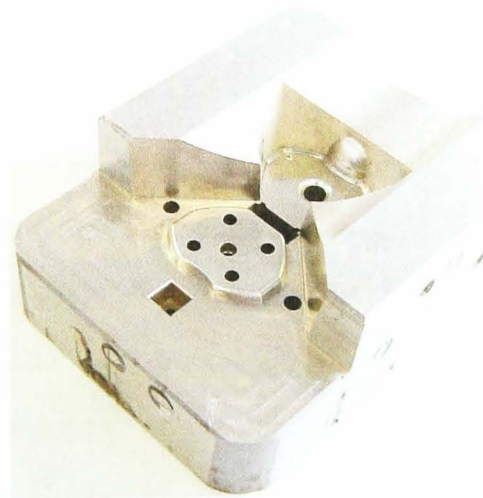
(a) Cavity Insert



(b) Core Insert

Figure 4-45. Green Parts of the New CS3 Inserts

To achieve final production specifications, the metal models of the new CS3 inserts were sent to and machined at Delcam. Figure 4-46 shows the finished inserts of both new core and cavity inserts. A  $0.1\mu\text{m}$  surface roughness (Ra) on the moulding cavity was achieved. As two previous case studies, colour codes were applied in order to explain machining and finishing operations required in developing the features on both inserts.



(a) Cavity Insert



(b) Core Insert

Figure 4-46. Finished CS3 Inserts

Figure 4-47 shows the colour codes for machining operations both cavity (a) and core (b) inserts. A blue colour represents the features that only require SLS process, which mostly the cooling channels and four fillet corners on cavity inserts. A golden-orange represents an operation of HSM to blocking out and machining the

all flat surfaces on the inserts, while a red colour represents the HSM operation in forming freeform surfaces. A green colour represent drilling or boring operation of most holes. Pink shows the EDM features, which are base impression and hot sprue hole on the cavity, and rib slots on the core, as indicated on the figure.

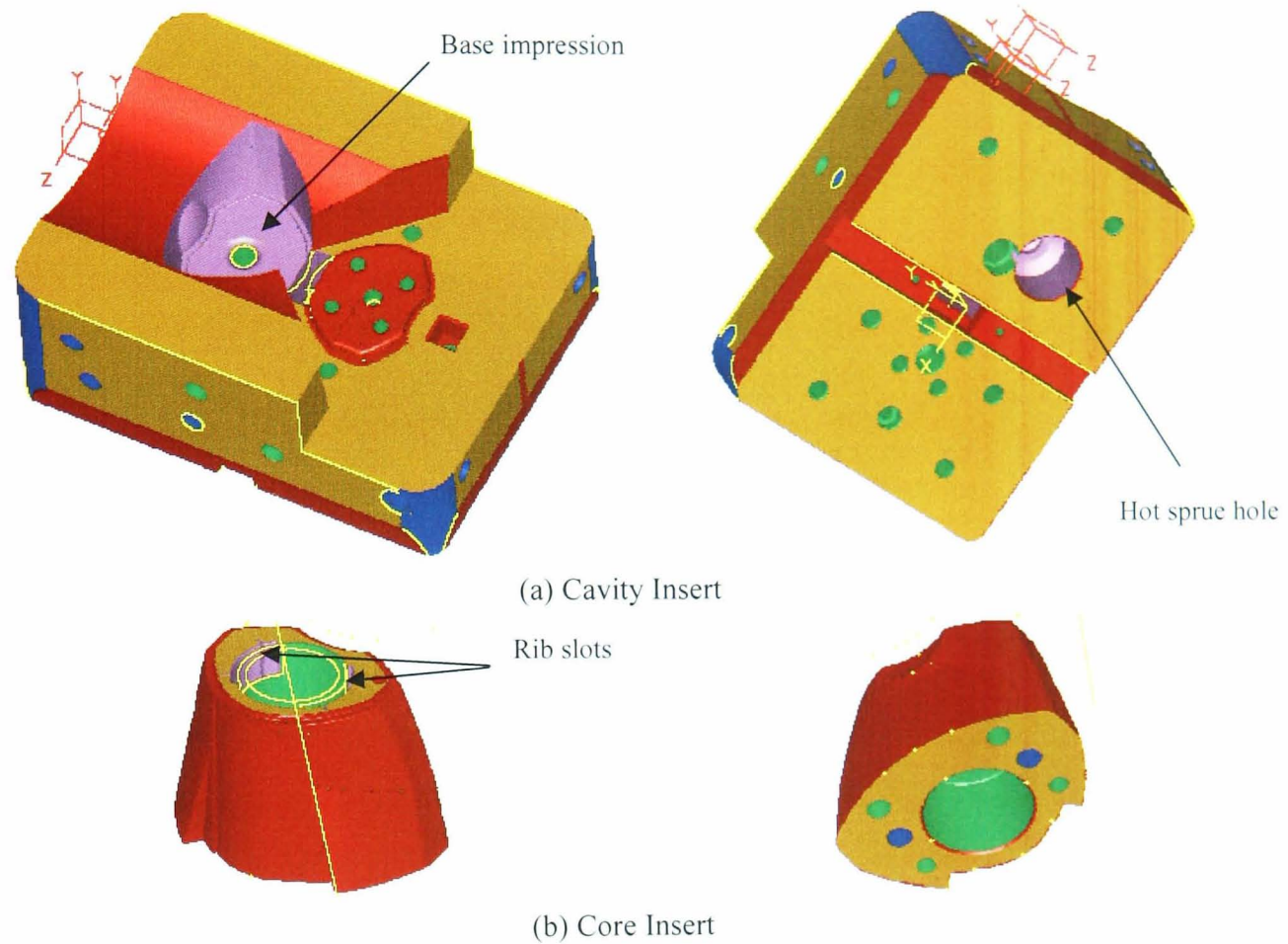


Figure 4-47. Machining Operation of the New CS3 Inserts

Figure 4-48 furthermore shows the colour code employed for polish finishing the features that form the mould cavity (impression). A yellow colour on the cavity insert represents the operation employed for finishing both base and cap impressions using a diamond compound, while a light blue represents a draw polished on the core outer profile using 600 grid stone paper. As an overall evaluation, the total costs required in manufacturing were reduced by 61.5% compared to the existing inserts. However, it was found that the amount of time required was 51% higher than was required for manufacturing the existing inserts.

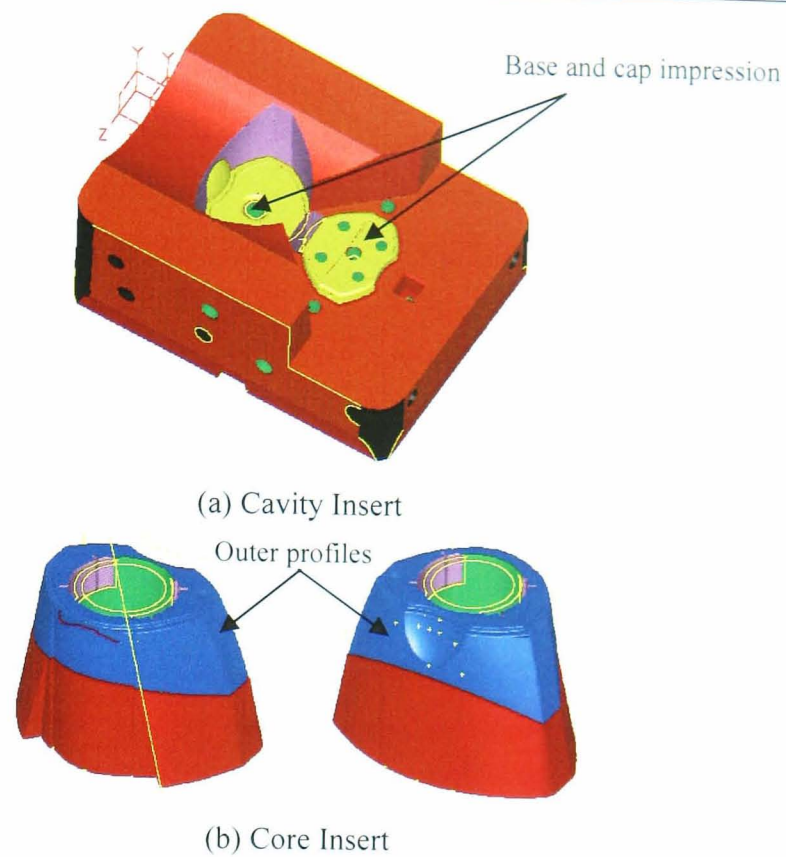


Figure 4-48. Polishi Finishing of the New CS3 Inserts

#### 4.4.4. Moulding Trial

A moulding trial for the new CS3 inserts was run using a Kloeckner Ferromatik FM-160 injection machine at the Seaquist Closures production workshop. As for the two previous case studies, the trial was run at the same operating parameters as used for running the existing insert for production. Table 4-10 lists the specification of the material used and summarizes the main process parameters.

Table 4-10. Material and Process Parameters

<b>A</b>	<b>Material Specificatios</b>	
1.	Material:	RE420MO - Polypropylene (PP) - Copolymer
2.	Density:	0.9 g/cm <sup>3</sup>
3.	Sp. Heat	2.1 J/g °C
<b>B</b>	<b>Process Parameters</b>	
1.	Injection Temp.:	ave. 230 °C
2.	Ejection Temp.:	ave. 65 °C
3.	Mould Temp.:	ave. 40 °C
<b>C</b>	<b>Coolant</b>	
1.	Coolant:	water
2.	Temp Diff:	ave. 5 °C
3.	Flow Rate	ave. 7.5 l/min

4.4.4.1. Procedure and Measurements

Similar to other two earlier case studies, the productivity of the new CS3 inserts were investigated by reducing the cooling and cycle time gradually. To reach process steady state, the mould was first run for about an hour at the conventional production cooling (4.7s) and cycle (9.9s) times. Table 4-11 lists the results of the cycle times reductions with corresponding cooling time reductions.

Table 4-11. Cooling and Cycle Time Reductions

Cooling Time (s)	Cycle Time (s)
4.7	9.9
4	9.2
3	8.2
2	7.2
1	6.2

To investigate the impact, product samples were taken at the adjusted cycle time for inspection. Figure 4-49 indicates two critical dimensions (Plug O/D and Snap I/D) that have to be measured to represent the product quality. The expected nominal and tolerance values of these dimensions are: plug outside diameter (O/D) = 20.50 ( $\pm 0.20$ ) mm, and snap inside diameter (I/D) = 24.30 ( $\pm 0.20$ ) mm.

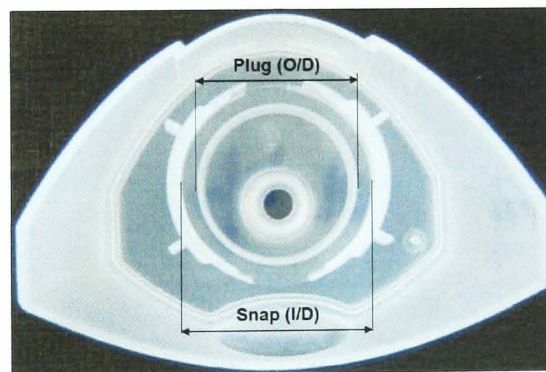
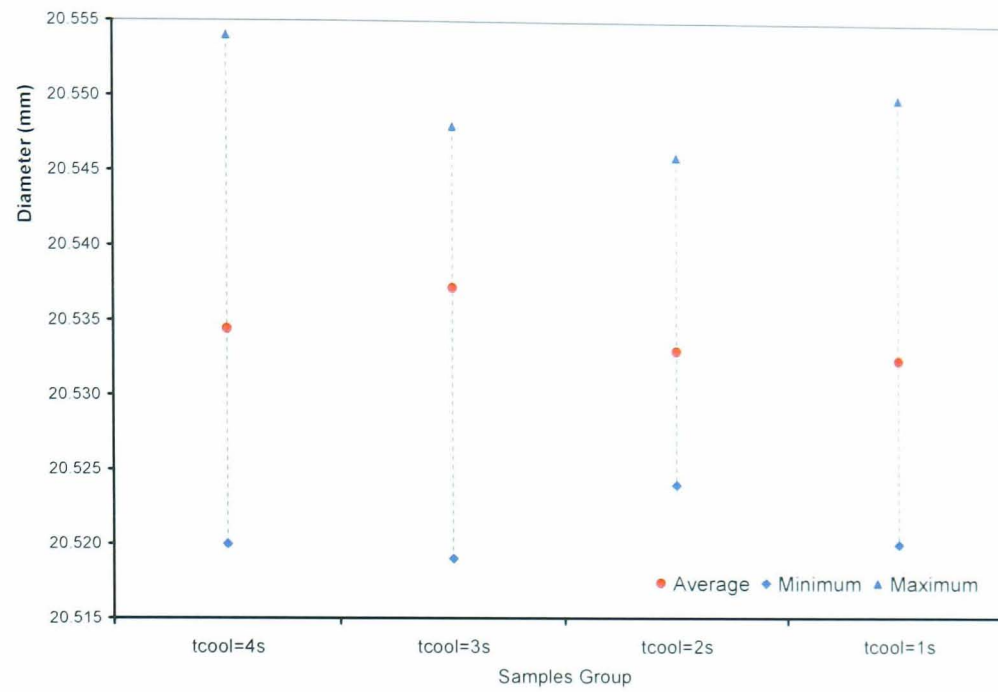


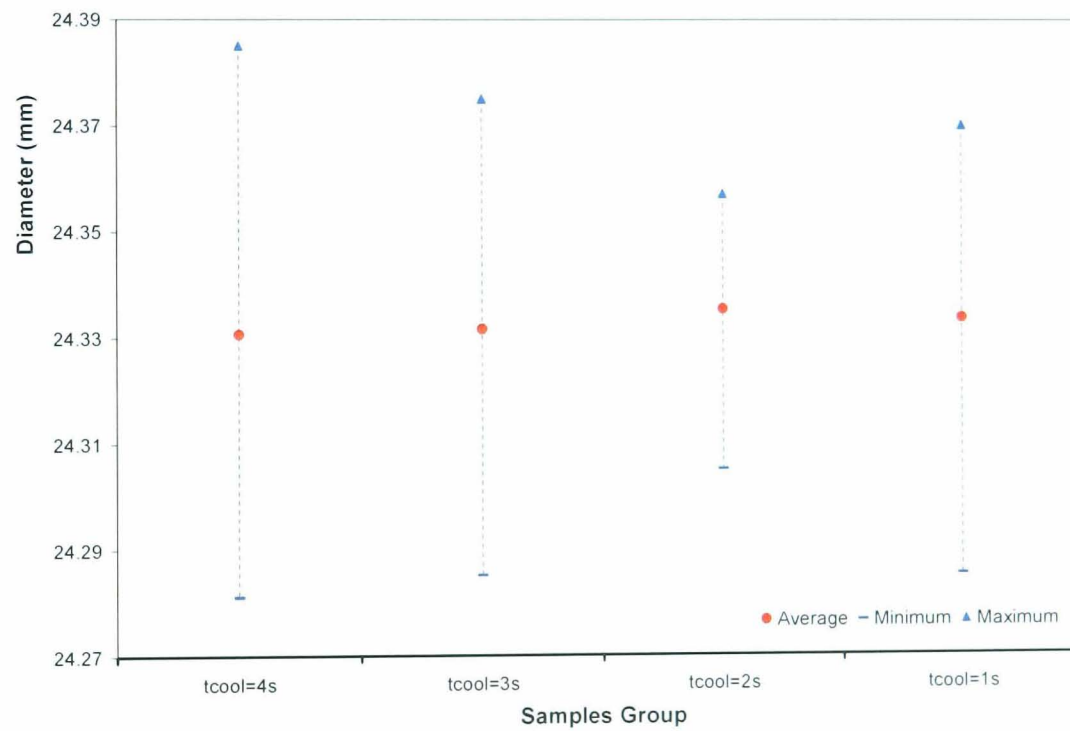
Figure 4-49. CS3 Product Quality

4.4.4.2. Results

Moulding trial showed that the new CS3 insert functioned at all the cycle times. From the results of the quality inspections (Figure 4-50), the average measurement of the both plug O/D and snap I/D have shown the consistency of the new inserts in moulding quality products. Energy measurements indicated that the machine energy consumption in moulding per shot was reduced by 20% from 130 kJ/part at 9.9s cycle time down to 104 kJ at 6.2s cycle time.



(a) Plug O/D



(b) Snap I/D

Figure 4-50. CS3 Product Measurements

### Cost Analysis

Table 4-12 summarises the important results and compares them against the existing inserts. In the relation to moulding productivity, the results have shown that the new CS3 insert is able to improve significantly the production rate by 59.6% from 364 to 581 products per hour at moulding cycle time of 6.2s.



Table 4-12. CS3 Manufacturing and Moulding Comparison

No	Data/Parameters	Unit	Existing	New CS3	Diff. (%)
1	Manufacturing Lead-Time	hours	232	350	51.0
2	Moulding cycle time	sec	9.9	6.2	(37.0)
3	Production rate	Product/hour	364	581	59.6
4	Total moulding time required**	hour	2,750	1,772	(37.4)

\*\* Total time required to mould 1,000,000 products

Using a similar approach to both previous case studies, Table 4-13 shows the percentage differences of the product cost of using the new CS3 inserts related to (a) the expected durability of the LaserForm ST-100 material in moulding 1,000,000 products, and (b) the projected number of products relative to the assumed durability. Based on the product cost percentage differences present on the graphs plotted in Figure 4-51, it is identified that the new CS3 inserts is competitive if the inserts can survive between 300,000 and 400,000 shots. With predicted durability of 195,000 shots, the graph however indicates that the product cost benefit will be achieved if the insert (single cavity) is run to produce up to 350,000 quality parts.

Table 4-13. CS3 Product Cost vs. Expected Insert Durability

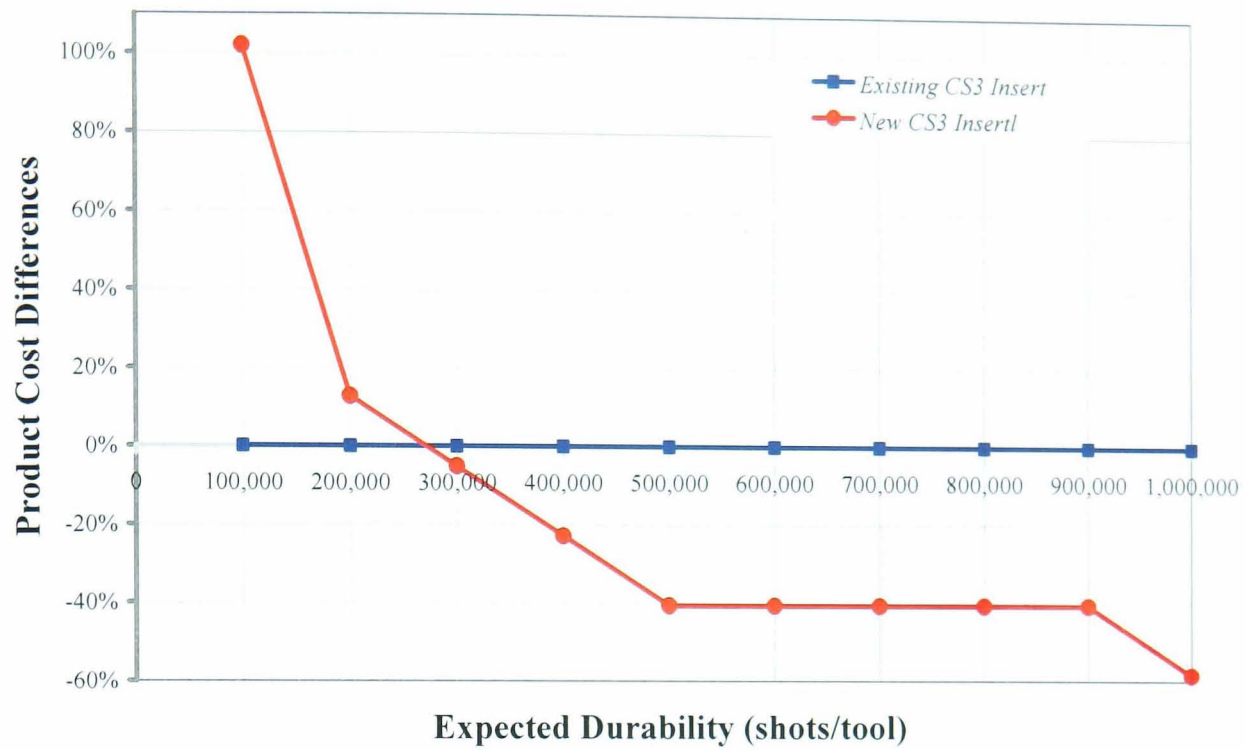
Expected Durability*	No. of Replacements		Prod. Cost Diff. (%)
	Exist.	New	
100,000	1	10	101.8
200,000		5	12.7
300,000		4	(5.1)
400,000		3	(23.0)
500,000		2	(40.8)
600,000		2	(40.8)
700,000		2	(40.8)
800,000		2	(40.8)
900,000		2	(40.8)
1,000,000		1	(58.6)

(a) Product Cost vs. Expected Durability

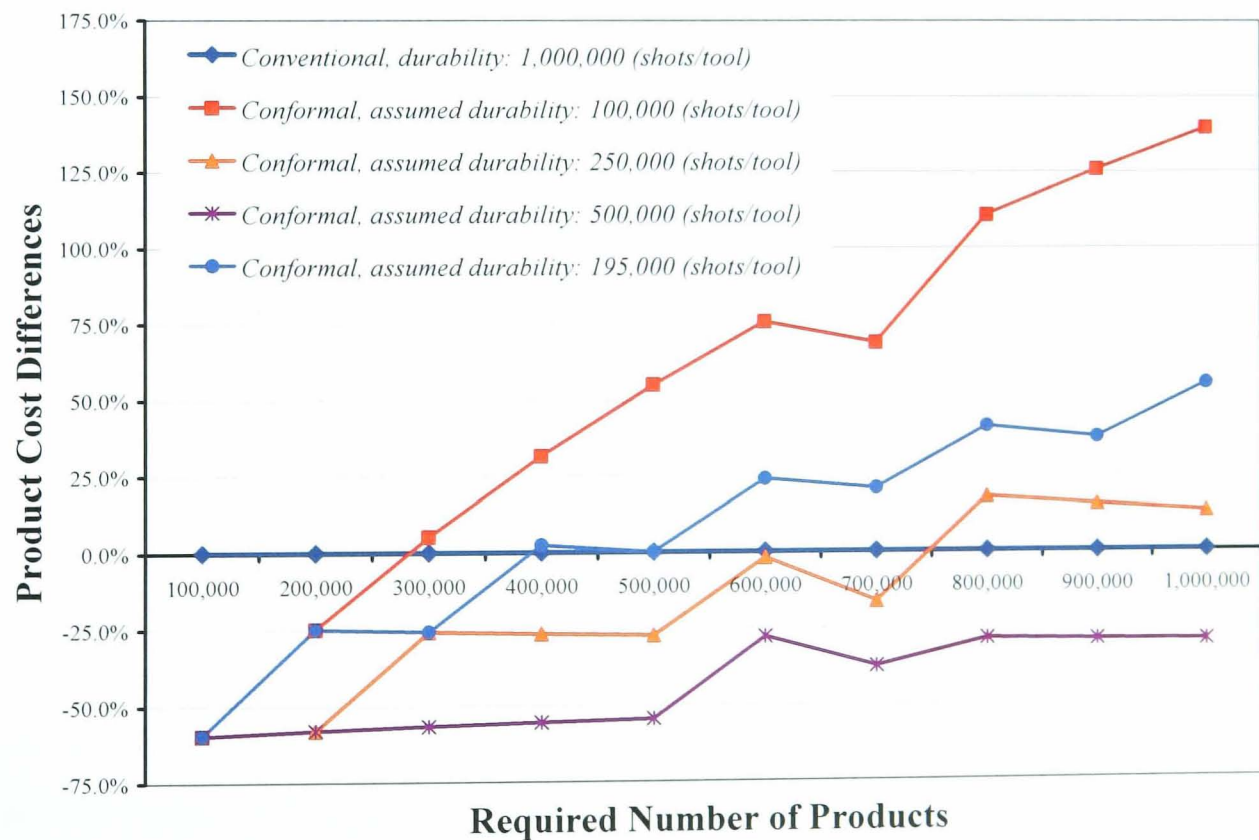
Projected Products	No. of Replacements			Prod. Cost Diff. (%)			
	Exist.	New			100k	250k	500k
		100k	250k	500k			
100,000	1	1	1	1	(59.7)	(59.7)	(59.7)
200,000		2	1	1	(25.0)	(58.1)	(58.1)
300,000		3	2	1	5.2	(25.8)	(56.8)
400,000		4	2	1	31.7	(26.5)	(55.6)
500,000		5	2	1	55.0	(27.1)	(54.5)
600,000		6	3	2	75.9	(1.8)	(27.7)
700,000		7	3	2	68.4	(16.6)	(37.8)
800,000		8	4	2	111.4	18.0	(28.7)
900,000		9	4	2	126.6	15.4	(29.1)
1,000,000		10	4	2	140.5	13.0	(29.4)

(b) Product Cost vs. Projected Number of Products

\* Expected durability of LaserForm material



(a) Product Costs at Expected Durability of One Set Insert to Produce 1,000,000 product



(b) Product Costs at Assumed Inserts Durability to Produce Projected Number of Product

Figure 4-51. CS3 Product Cost Analysis

#### 4.5. Summary

This chapter has examined three major industrial case studies associated with the development of the new mould insert using a combination manufacturing

principles of indirect SLS and HSM, and with the application of the new insert in moulding process. Insert development for the three major case studies has able to indicate important benefits and improvements. The key advantages of employing the indirect SLS process are able not only to provide a freedom in design a complex geometry of the inserts but also able to potentially reduce the total amount of manufacturing time and cost required.

The freedom in design has provided benefit in merging several complex components that form the existing inserts into one solid material of new insert design. However, the limitation of the indirect SLS process have to be taken into account in considering suitable design of the inserts for manufacturing. The general accuracy and surface finish are two major limitations of the indirect SLS in producing a metal model concerning the preparation of a near-net shaped insert model for manufacturing. Therefore, providing appropriate machining allowances and designing suitable near-net shape for post-processing needs to be carefully considered.

The design freedom provides an opportunity to improve the moulding productivity by replacing the existing straight drilled cooling channels with the complex conformal cooling channels. Using indirect SLS process, the new designs of the conformal cooling channels for all case studies was able to utilise the available space to locate the channels closer to the moulding cavity. However, clearing the powder out from the channels was a major concern. Therefore, an effective and efficient approach is necessary. From all three case studies, it is evaluated that the length and path complexity of the channel as well as the weight of the inserts are important parameters.

Moulding trials for all three case studies has furthermore indicated that the new conformal cooling channels significantly reduce moulding cycle time as well as machine energy consumption. However, the durability of the new inserts is another concern. Based on the predicted durability of the insert material in CS1, the production/durability trial results have indicated its possibility of being competitive against the existing inserts if the inserts (single cavity) is run to produce up to 600,000 parts (CS1) and 350,000 parts (CS3).

## Chapter 5

# **Design Rules Application**

## Chapter 5. Design Rules Application

Three major industrial case studies for underpinning this research work have been described and discussed in the previous chapter. As mentioned, the selection of these case studies are related to the evaluation of the approach to develop plastic injection mould inserts using indirect SLS and HSM. Referring to the development procedure and methodology employed, this chapter summarises the significant findings from all case studies and then explains their utilisation as a set of rules to guide the development of the plastic injection mould inserts.

### 5.1. Issues Arising

#### 5.1.1. Design of the Inserts

The approach of combining indirect SLS-HSM to develop plastic injection moulding inserts requires special attention in understanding design considerations, especially in utilising and optimising the technological capability of the indirect SLS process to manufacture the near-net shape inserts. From all three case studies, it is indicated that the indirect SLS process allows complex inserts to be designed as well as the part number of the inserts to be reduced. Moreover, indirect SLS process also provides more ‘freedom’ in constructing conformal cooling channels into the inserts which potentially improves the efficiency of the inserts in removing heat from the mould cavity.

In designing and preparing the near net shape of the inserts for finishing, the first step is to design the finished (net) shape of the expected inserts. At this step, all potential capabilities of indirect SLS and HSM and/or other related post-processing capabilities are considered in order to achieve the required specifications. The next step is then to design and prepare the near-net shape of the inserts. Based on the case studies’ results, it is considered that there are three important issues that need to be addressed: geometry of the near-net shape inserts, additional material for machining/finishing, and ‘cut-out’ volumes for powder removal.

#### 5.1.1.1. Geometry

A first principle for creating a near-net shape insert is to generate inserts with a geometry as close as possible to the expected design of the net shape inserts. In order to minimise the machining/finishing time significantly, leaving as much geometry as possible in the SLS (infiltrated) state is recommended. However, the benchmarking results in Chapter 3 have identified that the indirect SLS process has limitations in building small/delicates features. Therefore, it is advised that any small/delicate features of the inserts which are less than 2mm in size are best produced by machining. Concerning infiltration process in the furnace, the features like holes for bolts and pin ejectors, and deep rib slots which can distort significantly should also be excluded in designing the near-net shape.

#### 5.1.1.2. Additional Material

Due to the level of dimensional accuracy and surface finish of the SLS inserts, the benchmarking results have clearly indicated that additional material for machining/finishing are required. This is to ensure sufficient stock material to work with, especially to all critical surfaces which require further machining/finishing processes. From the results of CS 2, additional material is also to be considered in terms of sufficient material for firmly holding the insert on machine fixtures.

#### 5.1.1.3. Powder Removal

The main benefit of the indirect SLS process is that cooling channels can be designed and constructed as close as possible to follow a contour of the mould cavity. However, special attention has to be taken to clearing loose powder from inside the channel. Clearing complex and winding cooling channels can be time consuming. In clearing the powder inside the cooling channels, the geometry and path complexity of the channels are two main parameters that need to be considered due to the flow-ability of the powder [Dalgarno, 2001]. Moreover, Dalgarno et. al. [Dalgarno, 2001] indicated that the weight of the insert is another parameter that need to be considered since the green-part is normally manipulated by hand.

To facilitate access and accelerate powder removal, an effective and efficient technique need to be considered when it is required. A 'cut-out' volume technique was used for clearing powder in the CS1. This technique is a recommended solution.

In the 'cut-out' volume technique, a basic idea is that a certain volume of the green part is cut out from the main body of the inserts in order to open and bisect the cooling channel at the most difficult/outreach location in clearing the powder. After the channel has been cleared, the cut-out volume is then assembled back to its main insert before the furnace infiltration step which joins it back to the main body of the insert. To remove any developed porosity, the insert is then infiltrated with a high-temperature resin.

### **5.1.2. Manufacturing the Net Shape Inserts**

Like cast parts, SLS near-net shape inserts are not equipped with a specific reference feature. As for machining/finishing, a surface or feature of the inserts therefore needs to be identified as a datum. For this purpose, the base plane of the inserts can be utilised and selected for machining primary reference. The surface of this specific plane is normally the most flat surface on the inserts.

In machining/finishing the near-net shape inserts, the major operations employed are HSM and EDM. HSM should be used for machining most designated freeform surfaces of the core and cavity inserts. EDM work is required for forming some special features such as deep rib slots, inaccessible and small shapes, undercuts in a hole, or sharp corners. To enhance final specifications, other standard machining operation such as milling, drilling, boring, turning and grinding are also included in shaping the inserts, whenever possible performed by the HSM machine. As required to fine finish critical surfaces, a polishing process will be employed after these machining operations.

## **5.2. Design Rules**

Based on the issues presented above, rules to guide design for manufacture of production quality injection moulding inserts using a combination of indirect SLS and HSM have been developed. The following sections discuss in detail the rules, starting from product design review up to tool insert design and manufacture.

### **5.2.1. Product Design Review**

The overall design of plastic injection moulding core and cavity set normally starts with an understanding of the plastic product to be moulded. Understanding the

product design can be carried out by studying and reviewing its important information through a drawing, a sample or a model of the products. Many product design guidelines for injection moulding, have been written. The following outlines standard and common information required in understanding the product before designing the mould inserts.

#### 5.2.1.1. Product Use/Function

Understanding the use/function of the product provides information about the importance of certain specifications and critical area of the product which directly or indirectly influence the design of the inserts. Furthermore, understanding the intended product function also provide an advanced indication toward a manufacturing plan which is appropriate to the inserts. Therefore, product material characteristics, tolerance, and surface finish need to be carefully studied and reviewed.

#### 5.2.1.2. Product Geometry

Product geometry represents the influence of several features constructed in the mould, including the core and cavity, parting lines, gating systems, and ejectors systems. The following are common elements of product geometry which need to be studied and reviewed.

##### 5.2.1.2.1. Parting Line

The *parting line* illustrates the plane that separates the core and cavity inserts. As the parting line forms the edge of the product, the factors that need to be considered are that parting lines are able to ensure that the product remains inside the mould cavity, the ease of product withdrawal from the mould cavity, ease of manufacturing, and to avoid plastic leaking from the mould cavity.

##### 5.2.1.2.2. Draft Angle

A *draft angle* should be applied on any vertical wall of a product in the direction of mould opening/closing for easy removal and to avoid product faults due to friction during ejection. The value of the draft angle varies depending on the depth of the product in the mould. The draft value has a significant impact on the surface finish and manufacturing method required. For standard practice, a draft angle greater than



1° is generally applicable for drawing the moulded product from the cavity.

#### 5.2.1.2.3. Wall Thickness and Ribs

In general, a uniform *wall thickness* should be maintained throughout the product in order to avoid distortion. In cases where a variable wall thickness is required, a smooth transition in thickness is required in order to avoid stress concentrations.

*Ribs* are essential reinforcement features to increase stiffness and structure integrity of the product, to support components, and to avoid thick sections. Ribs are generally designed by concerning any deformation possibility in products. A general rule is that thickness of the ribs is about 50% to 60% of the nominal wall thickness, and its maximum height is approximately three times of the nominal wall thickness. It is suggested that ribs should be positioned in line with the filling flow of the molten plastic

An appropriate minimum uniform wall thickness for the product should therefore be determined consistent with its function and process considerations because it not only minimises sinking, warping and residual stresses but also ensures shorter cooling/cycle times, and a minimum shot weight, which significantly affects product costs.

#### 5.2.1.2.4. Radii

*Radii* are normally applied to products to avoid high stress concentration that can often lead to failure of the products. Therefore, any sharp corners need to be radiused. The radius varies depending on wall thickness. In general, the radius is between 25% to 75% of the nominal wall thickness. In addition, it is important to notice that the radiuses provide a streamlined flow path for easier fill.

#### 5.2.1.2.5. Product Ejection

A general rule in designing the most suitable ejection mechanism is based on the important parameters of the product shape/geometry, material, wall thickness, and position relative to the parting line. Ejector pin is the most common method. A selection of ejector pin diameter should consider an ejection force distribution over the product. It is recommended that the ejector should be located and arranged at the strongest part of the product such as at the corners and ribs intersections. Since the

ejectors normally leave marks on the product, it is necessary not to locate the ejector in an area which will affect a function and appearance of the product.

### 5.2.2. Tool Insert Design and Manufacture

#### 5.2.2.1. Design of Net Shape Inserts

As design of the product studied and reviewed, the next step is to design a net shape of the core and cavity insert. There are several important constraints need to be considered in designing the both inserts. A shape/geometry of both core and cavity insert is normally determined by product position relative to the selected parting line. The orientation of the moulding also allow gate, runner, and ejection systems to be arranged. Furthermore, it is recommended that the shape/geometry of the insert must be suitable for available manufacturing methods. It is recommended also to have as small design of inserts as possible so that they can be handled easily.

Once the geometry of the inserts determined, product surface finish is one important design constraints to be considered. Beside parameters of the moulding process, the appearance of the product depend on the surface condition of the insert. Therefore, the quality of the surface finish needs to be clarified and an area where the surface finish will be applied on the product needs to be identified while designing the inserts. In general practice, a surface on the product which is visible to the end user requires fine finish quality. Also, a smoother mould cavity is required on order to allow moulded product to be ejected easily. However, a rougher surface finish is needed in some areas to ensure that the product remains in the place for proper ejection.

To overview common quality levels of surface finish which are usually applied to the inserts, Table 5-1 lists available ISO 1302:2002 standard finishes and shows common manufacturing methods that can be referred to [DSM, 2006].

Table 5-1. List of Standard Surface Finish ISO 1302:2002 [DSM, 2006]

Classes	Ra ( $\mu\text{m}$ )	Surface Requirements	Manufacturing Method
N0 – N2	$\leq 0.05$	High gloss, no visible scratches or flow line	Lapping; Polishing
N3	0.1	Glossy, small visible scratches acceptable	Polishing; Grinding; Honing; HSM
N4	0.2	“Technical” finish	Milling; Drilling EDM; SLS
N5	0.8	No aesthetical requirements	Sand blasting

As summarized in section 4.5, the indirect SLS process provides design ‘freedom’ due to its technical capability to form a one solid body of any geometrical complex inserts. However, feature detail and surface finish required for the insert mentioned above limit this kind of freedom, which needs to be considered as another important. Detail freeform surfaces, small/delicates features and deep rib slot on the inserts require an extra effort and time to finish. To achieve the required finish quality rapidly and ease the access for required operations, it is recommended that the inserts are designed with a number of parts that have opening surfaces. Concerning this, determining a required minimum number of part therefore becomes an important issue to be considered because it will be related to time and cost to manufacture the inserts.

Another important constraint in designing the inserts is related to the capability of indirect SLS in constructing and laying out cooling channels conformal to the mould cavity wall. The general rules which are recommended to locate and size the conformal cooling channels are based on the following considerations:

- *location*: as close to the mould cavity wall as possible, and kept at a minimum distance from other mould components.
- *Size*: allow a sufficient flow rate of coolant to produce turbulent flow ( $2300 < Re < 10^6$ ), and cover a maximum product surface area to achieve uniform cooling

From the case studies discussed on Chapter 4, the parameters used in designing the conformal cooling channels can be considered and referred to. As in CS3, a combination cross-sectional area between standard diameter of 6 mm to 8 mm (in CS1) and freeform shape (in CS2) cross section can be recommended. For laying out, it is also recommended that a constant distance from cavity and other mould components (i.e. ejector pins, bolts) should be maintained by at least a channel diameter. As noted in CS2, the channels actually could also be located closer to the mould cavity at a constant distance of 4mm as long as a sufficient high-load bearing cross-sectional area on the mould cavity can be maintained. A moulding analysis software is recommended to be a useable tool in simulating the cooling design for predicting filling/packing process of the product and the efficiency of the intended cooling system at different cooling time.

Concerning the layout of the conformal cooling channels, the placement and arrangement of the ejectors is another constraint to be considered because it can interfere with location of the channels. The ejector pins, strips, bushings, plates are some of the most common type used to remove the product from the mould cavity. Its selection mainly depends on the geometry/shape of the products as well as the rigidity and flexibility of the polymer. The most preferable location of the ejector at those spots around the expected shrinkage area and the strongest area of the product. The main concern in applying the ejectors is that their cross-sectional area as large as possible to distribute the ejection force without damaging the product.

Moreover, another important constraint which needs to be considered in designing the inserts is a gating system, which also has a significant impact on final quality of the product. To optimize the filling process, the gate type and location need to be selected properly. It is recommended that the gate is located where the thickest section of the product is. Any gate method selected in moulding always leaves a mark. Therefore, the gate location needs to be selected properly so that an unwanted mark that can obstruct product function and appearance can be avoided.

#### 5.2.2.2. Design of Near-Net Shape Inserts

The first principle here is that the generic shape must be determined and designed as close shape as possible to the intended net shape inserts. As an advantage of the process, indirect SLS allows complex (geometry) features on the inserts, conformal cooling channels, guides for ejectors, runner and gate to be included in the design simultaneously. However, there are important issues which are to be considered in designing near-net shape inserts.

In reference to the case study results, the main design considerations are that any small features that have a size smaller than 2 mm and/or delicate features that require special finish quality should be excluded from the design of the near-net shape inserts, including holes for ejector guides and bolts. It is recommended that these features should be added latter on using HSM machining and other finishing techniques. Moreover, additional material has to be added to all surfaces on the inserts at all building directions for machining/finishing allowance to achieve the required final quality. As evaluated from benchmark and applied in case studies, an average minimum machining allowance of 1 mm added to the 3D CAD model

surfaces is sufficient.

Another concern for additional material is that a 3D CAD model of the near-net shape inserts has sufficient stock for machine fixtures. In this case, the additional material ensure that the inserts can be held firmly by the machine fixture during machining/finishing. Then, a plan for manufacture of the near-net shape insert needs to be considered. Concerning this, it is recommended that the design of the near-net shape inserts comprises as many as possible features that can be left as its SLS/infiltrated state. This can be applied to the surfaces which are not dimensionally specific such as chamfers, vents, clearance holes/surfaces.

The basic process of indirect SLS is through the development of a green-part before manufacturing a dense metal part through bronze infiltration in the furnace cycle. Therefore, tabs for placing bronze ingots should be attached on as features in the near-net shape design. To achieve a fully dense metal part, the tabs are basically designed to accommodate and be able to handle a total weight of the bronze ingots which is about 72% of a total green-part weight. As the tabs will be cut off, it is important that their design should ease the cutting process. Moreover, the tabs should be attached to surfaces that do not require finishing, and constructed around the inserts to allow melting bronze infiltrate uniformly into the green-part.

A further important design consideration in the near-net shape design is in regard to a decision on whether it is necessary to have a plan and prepare a technique to resolve a problem in clearing un-sintered powder from inside the cooling channel at the green-part stage. Based on the case studies carried out (Chapter 4), this decision highly depends on the design complexity of the conformal cooling channels constructed inside the inserts. The following explains in detail the technical procedures and design guidelines recommended if a technique to resolve this powder removal problem is required. The technique is called 'cut-out volume', which basically leaves a certain volume from the main body of the inserts open to provide easy access in clearing the powder.

#### 5.2.2.2.1. Select 'Cut-Out' Location

A particular decision to apply this technique is based on a long winding/bending and/or circle/spiral/coil channel which normally increase a level of difficulty and minimise an access to reach loose powder inside the channel completely. Therefore,

length of the path and geometrical complexity of the channels are two important constraints that need to be considered. For winding/bending channels, a 'cut-out volume' technique is recommended to be applied whenever: (1) the channels are constructed with more than two corners (angle  $< 90^\circ$ ), and (2) the total length of the channels is more than 100 mm. In the case of circle/spiral/coil channel, the constraint are the radius and length of the circle/spiral/coil path. The technique will be very useful if the circle/spiral/coil channel has: (1) a radius less than 50 mm, and a length more than 100 mm.

#### 5.2.2.2.2. Select 'Cut-Out' Geometry

A geometry which is selected to be cut off from the main body of the inserts mainly depends on an arrangement/design of the cooling channel. For simple manufacturing process, it is recommended that a geometrical shape of the cut-out volume is design as close as possible to the primitive models (i.e. box, cylinder). In cutting out, it is important to notice that the cut-out volume is bisected exactly at the centre of the channel. The following Figure 5-1 shows a typical example of a cut-out volume selection.

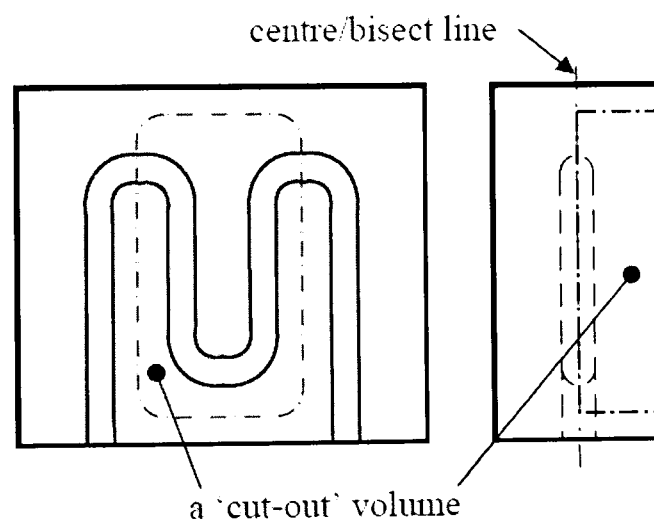


Figure 5-1. Cut-Out Volume Selection

#### 5.2.2.2.3. Design Considerations

After clearing the cooling channels, the cut-out volume is assembled back together to the main body before furnace cycle, which can bind them together. To facilitate an optimum assembly and binding, draft surfaces and guiding features are very crucial so that they must be considered and included in the cut-out volume design. The following Figure 5-2 shows the detail specification recommended in considering the design of the cut-out volume.

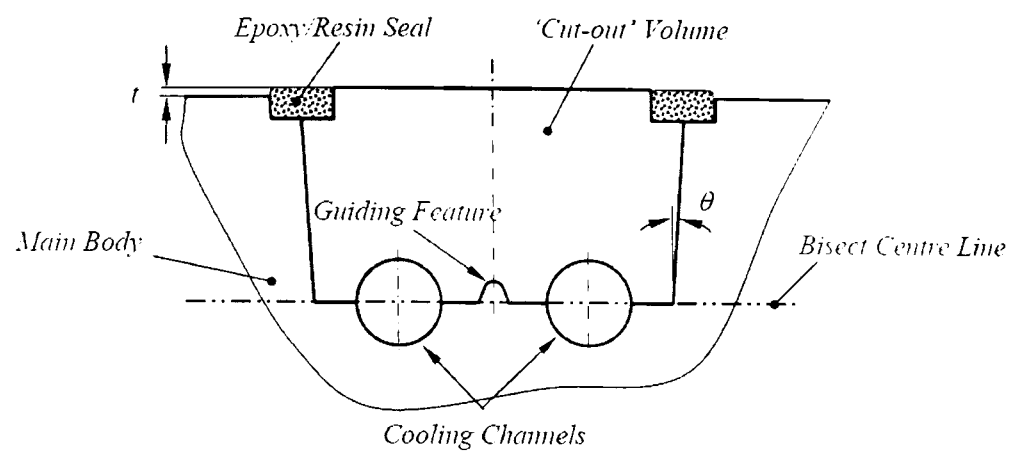


Figure 5-2. Design Specification of the Cut-Out Volume

All vertical surfaces on both cut-out volume and cut features of the main body which are perpendicular to the bisect/centre line need to be tapered or drafted. Depending on its thickness, typical draft angles of 3 to 5° per-side applied to the surfaces are recommended for a cut-out volume thickness up to 100 mm. In reference to the case study, dimensional changes at green-part stage is a further concern. To accommodate the changes, an extended ( $t$ ) between 0.5 to 1.0 mm is recommended to be added to the thickness of the cut-out volume.

Furthermore, special guide features also recommended to be created so that both part can be relocated and the bisect channels can aligned back properly. The geometry of these features should be designed with coned shape and located at any available space without obstructing any functional features on both parts. The following Figure 5-3 shows the recommended design and specification of a guiding feature. Concerning that the green-part is considerably fragile, it is recommended that a nominal diameter ( $\varnothing D$ ) is between 5 to 10 mm. For locating and guiding elements, a radius ( $R$ ) is 0.5  $D$  and an angle ( $\theta$ ) of cone is 10° are a reasonable amount.

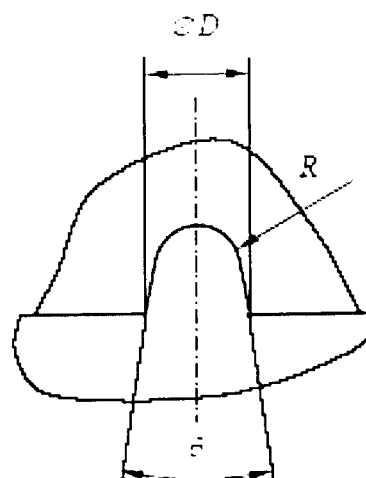


Figure 5-3. Design and Specifications of Guiding Features

To prevent any coolant leaking, the assembly is recommended to be sealed using a high temperature epoxy/resin after the furnace cycle. The following Figure 5-4 illustrates a construction of a groove which is prepared for sealing. A basic square cross-section groove is adequate for containing the required epoxy/resin. Geometrically, the groove can have a width ( $S$ ) between 4.0 to 8.0 mm and its depth is half of the width. Moreover, the characteristic of the epoxy/resin must have a good adhesion to metal, heat conductivity, and the most importantly suitable for operational temperature of at least 120°C.

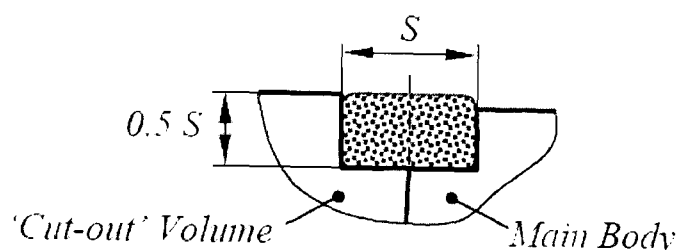


Figure 5-4. Groove Construction for Epoxy/Sealing Sealing

#### 5.2.2.3. Manufacture of Inserts

As clearly indicated in section 5.2.2.2. , available from indirect SLS is a near-net shape of the inserts that has been oversized by 1mm for machining allowance. For finishing the insert, it is first recommended to select the inserts base plane that can be utilised as a datum feature. This is normally the plane where the first layer is built up. The next step is then to 'block-out' the inserts by first cutting them to the approximate size, and then finishing them to true size. For accomplishing this, conventional machining such as milling, turning, drilling/boring, and grinding can be used. However, it is recommended that HSM is used whenever it is possible.

Once blocking-out completed, manufacturing of detailed features on the inserts is to be carried out using required methods. In general, HSM can be used as many as possible to machine and finish all the features. However, several important features such as deep rib slots with depth to width ratio of 4 to 1, mottled surface textures, and undercuts in a holes have to be manufactured by EDM. As mentioned in section 5.2.2.1. , special manufacturing attentions have to be considered for features that requires fine finish quality. Polishing work is required after HSM/EDM. As a condition of the cavity will effect the performance of the product, it is recommended the surfaces of mould cavity must be cleaned properly before

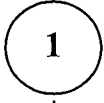
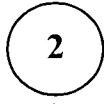
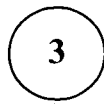



using.

### 5.3. Design Rules Application

This section discuss the application of the rules outlined in section 5.2. in designing a new core and cavity insert that will be used to mould the same related products selected in the previous case studies. The main objectives are to validate whether these developed rules can be applied to improve manufacturing lead-time and cost, cycle time and production performance. Table 5-2 shows the stages involved in developing the new inserts using the developed rules.

Table 5-2. Design Stages

No.	Stage Name	Stage Description
	<b>Product Review</b>	<ul style="list-style-type: none"> <li>• Part specifications (geometry/shape, dimensions, material, tolerance, and surface finish)</li> <li>• Product orientation relative to Parting line</li> <li>• Gate mark</li> <li>• Ejector marks</li> </ul>
	<b>Design of the Net Shape Insert</b>	<ul style="list-style-type: none"> <li>• General geometry of core and cavity insert based on product orientation</li> <li>• General dimensions of core and cavity insert</li> <li>• Detail geometry and layout of core and cavity insert</li> <li>• Selection of gate and ejector</li> <li>• Selection and layouting of cooling channels (dimension and location)</li> </ul>
	<b>Design of the Near-Net Shape Insert</b>	<ul style="list-style-type: none"> <li>• General near-net shape geometry of the inserts</li> <li>• General geometry &amp; layout of necessary 'cut-out volume'</li> <li>• General geometry of tabs for bronze ingots stand</li> </ul>
	<b>Manufacturing Plan</b>	<ul style="list-style-type: none"> <li>• Guidance for machining/finishing of near-net shape insert</li> </ul>

### 5.4. Case Study (CS) 1: 50 mm Snap-On Tube Top

#### 5.4.1. Product Review

A design process starts by reviewing the product design, including its technical specifications and detail features, product orientation, an marks that indicate parting line, gate and ejectors. This is carried out by reviewing the product and/or its drawing. The technical specifications required for CS1 closure product as



so that they can be finished with a fine polish quality. For undercut features of the retention beads and lid locks, their geometrical orientation on the product is a further constraint in providing access and handling for manufacturing process.

Figure 5-6 shows a sketch and cut sections of both core and cavity insert including main components which are required. As outlined in the figure, three main components that form the core (moving) inserts are main body, rib insert, and guide/pin insert. The rib insert is designed to be separated from the main body so that the surfaces to mould external and internal features of the product base can be polished. In the case of the guide/pin insert, it is designed to be separated due to the ejector system required, undercuts for retention beads, and surface finish required. Due to the undercuts, a bush type ejector is selected and located at the collar. Therefore, this core insert can then be utilised and function as an ejector guide simultaneously.

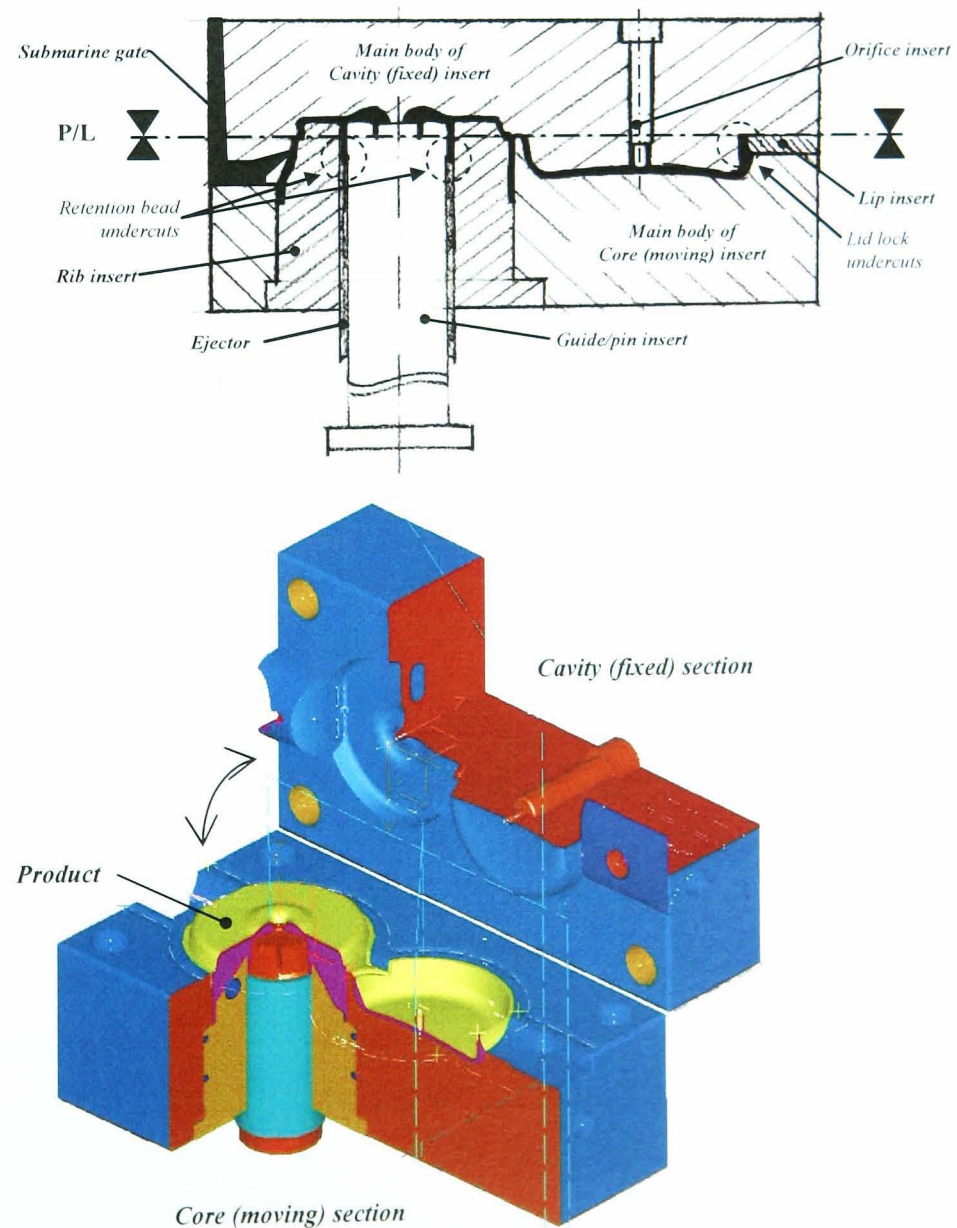


Figure 5-6. Sketch and Cut Section of a New CS1 Design

For the cavity (fixed) insert, it is also designed with three insert components: main body, lip, and orifice insert. The lip insert is designed to be separated from the main body is to provide machining access due to the undercuts required for lid lock features on the lid cap. To create an orifice feature on the lid cap, a separate orifice insert is required. Since a fine finish is required for the internal and external surface, an opening access is necessary. Therefore, a polish quality of a  $\varnothing$  2mm pin on one edge of the orifice insert is created.

As the main components of the inserts detailed, the next step is to design and layout conformal cooling channels for both core and cavity insert. Figure 5-7 shows a sketch of a new CS1 cooling system relative to core/cavity inserts. Considering a better cooling system, the conformal cooling channels are designed by combining standard diameter with freeform/irregular cross-sectional channels. These channels are outlined conformal to and separated from the cavity wall and other components at an average constant distance of 1 diameter.

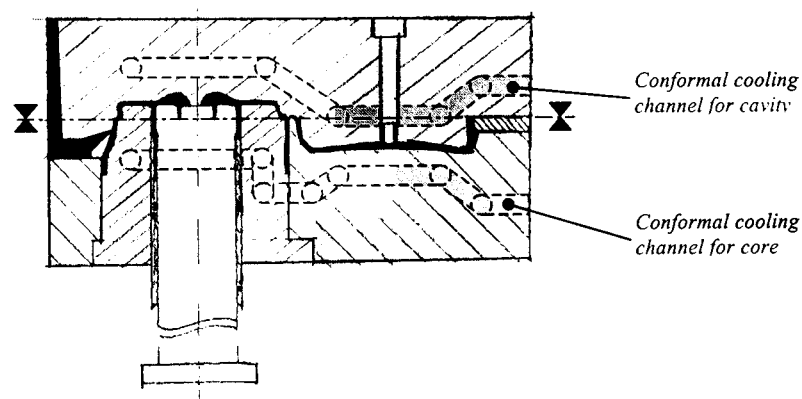


Figure 5-7. Conformal Cooling Channels Layout of a New CS1 Inserts

Furthermore, Figure 5-8 shows the layout of the conformal cooling channel. Figure 5-8a illustrates the geometrical shape of the channels for both core and cavity inserts. Whilst, Figure 5-8a and b shows the layout of each channel relative to the product, and indicates the sections where the standard/freeform channels constructed. A standard 8 mm diameter channels are constructed at the sections of the channel where the coolant enter to and exit from both inserts. These sections of the channels are constructed to interface them with the cooling channels which are constructed in the mould base. To provide more cooling onto the product, the flattened channels for both core and cavity are then located and constructed at the product lid cap and base. To interface these flattened sections, the transition channels with a standard 6 mm diameter are constructed between these product features.

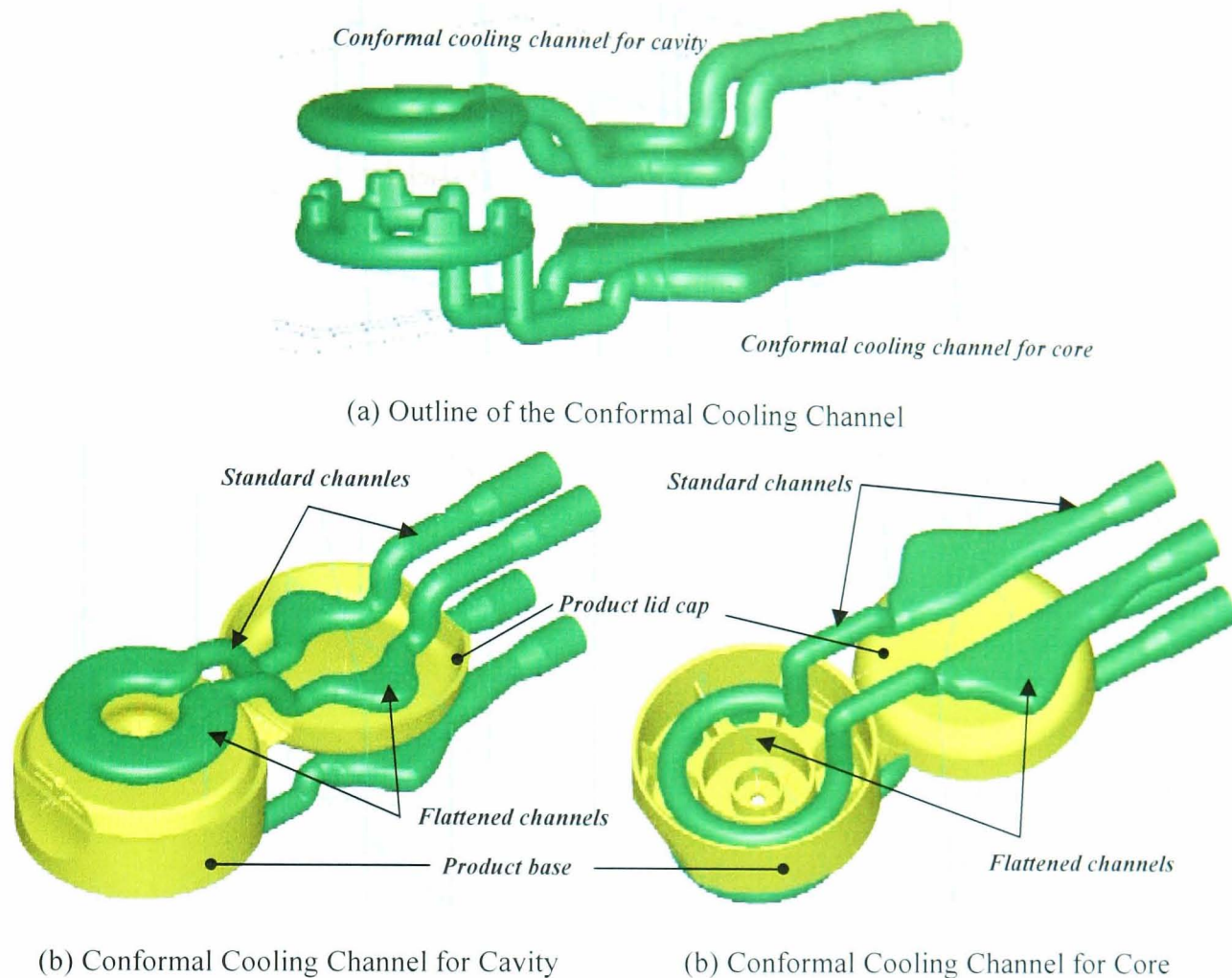


Figure 5-8. Design of New CS1 Conformal Cooling Channel

The cooling channel wall is averagely separated at a constant distance of 6 mm from the mould cavity surfaces. To evaluate the cooling channel design (location and uniformity surface temperature), the following calculations are carried out.

#### 5.4.2.1.1. Inputs:

As inputs in the evaluations, the following parameters which were using in for moulding trial are utilized in the calculation.

<b>Product</b>	Material	:	<b>Polypropylene (PP)</b>
	Density ( $\rho$ )	:	905 (kg/m <sup>3</sup> )
	Linear Shrinkage	:	0.006 (cm/cm)
	Melt Flow	:	13 (g/10 min)
	Melt Temperature ( $T_{melt}$ )	:	150 °C
	Mould Temperature ( $T_{mold}$ )	:	40 °C
	Ejection Temperature ( $T_{ejct}$ )	:	80 °C
	Specific Heat ( $C_p$ )	:	2000 (J/kg)
	Thermal Conductivity ( $\lambda$ )	:	0.1 – 0.13 (W/m K)
	Thermal Diffusivity ( $\alpha$ )	:	0.035 (mm <sup>2</sup> /s)

	Product Area	:	0.018 (m <sup>2</sup> )
<b><u>Insert</u></b>	Material	:	<b>LaserForm ST 100</b>
	Density (ρ)	:	7700 (kg/m <sup>3</sup> )
	Specific Heat (C <sub>p</sub> )	:	479 (J/kg)
	Thermal Conductivity (λ)	:	0.193 (W/m °C)
	Thermal Diffusivity (α)	:	0.065 (mm <sup>2</sup> /s)
<b><u>Coolant</u></b>	Material	:	<b>Water</b>
	Density (ρ)	:	997.6 (kg/m <sup>3</sup> )
	Specific Heat (C <sub>p</sub> )	:	4.18 (kJ/kg)
	Thermal Conductivity (λ)	:	0.58 (W/m °C)
	Temperature	:	20 (°C)
	Flow rate	:	2 (l/min)

#### 5.4.2.1.2. Calculations:

##### Cooling Time (t<sub>c</sub>):

A largest amount of heat needs to be exchanged during the cooling time. To ensure a dependable design, a selection of a critical cross-section (the thickest wall) of the part is considerably appropriate to become a basis of the cooling channel design because this part section required a longest time period required for the ejection temperature to be reached.

With assumptions that the melt temperature in the cavity is constant immediately after injection, the temperature of cavity wall rises rapidly and remains constant, the following equation 2-14 is used to evaluate the cooling time *t<sub>c</sub>* at the thickest wall (*s*) section on the part.

$$t_c = \frac{s^2}{\pi^2 \cdot a} \ln \left( \frac{4}{\pi} \cdot \frac{T_M - T_W}{T_E - T_W} \right)$$

$$t_c = \frac{(1.275)^2}{\pi^2 \cdot 0.065} \ln \left( \frac{4}{\pi} \cdot \frac{(150 - 40)}{(80 - 40)} \right)$$

$$t_c = 3.2s$$

A heat exchange from melting plastic to coolant takes place by thermal conduction through the cavity wall. As the thermal conduction described by Fourier differential equation, the calculated cooling time above was controlled using a Fourier number, as follow:

$$\frac{t_c \cdot \alpha}{s^2} > 0.1 \quad \text{or} \quad t_c > \frac{0.1 \cdot s^2}{\alpha}$$

$$t_c > \frac{0.1 \cdot (1.275)^2}{0.065}$$

$$t_c > 2.5s \rightarrow 3.2s > 2.5s$$

Estimated Cycle Time ( $t_{cyc}$ ):

To estimate a moulding cycle time, the following empirical ratio between cooling and cycle time was used [Rees, 1995].

$$t_c \cong 0.75t_{cyc} \text{ OR } t_{cyc} \cong 1.3t_c \cong 4.3s$$

Location

In practice, channel geometry and layout, thermal properties of insert material and coolant characteristics influence an effectiveness in transferring the heat from melted product to the coolant.

- Heat produced by melted product ( $Q_{mp}$ ) in the estimated cycle time  $t_{cyc}$  can be expressed as:

$$Q_{mp} = \frac{m \cdot \Delta h}{t_{cyc}} \quad \Delta h = \text{specific enthalpy different (see Figure 2-14)}$$

$$Q_{mp} = \frac{0.007 \cdot 166.7}{4.3} \rightarrow Q_{mp} = 0.27(\text{kJ/s})$$

- Heat transfer (conduction) in insert ( $Q_{mold}$ ) to the coolant can be express as:

$$Q_{mold} = \frac{K \cdot A \cdot t_{cyc} \cdot (T_{melt} - T_{cool})}{L}$$

From the heat balance  $Q_{mold} \cong Q_{mp}$ , the shortest distance of the cavity wall to the cooling channel and the position among them wall can be evaluated.

$$\frac{(0.193) \cdot (0.018) \cdot (4.3) \cdot (150 - 40)}{L} \cong 270 \text{ OR } \frac{(0.193) \cdot (0.018) \cdot (4.3) \cdot (150 - 40)}{270} \cong L$$

$$L \cong 0.0061m \cong 6mm$$

- Cooling error (j):

For uniform cooling distribution due to channel location/layout, a cooling error  $j$  was evaluated using equation 2-32 as follows:

$$j = 2.4 \cdot Bi^{0.22} \cdot (B/L)^{2.8 \ln(B/L)}$$

$$Bi = \frac{\alpha \cdot d_c}{k_M}$$

As noted in the rules, a distance between cavity wall and the channels as well

as between two adjacent channels (B) is equal to D or L. Therefore, the cooling error for this CS1 was calculated as follows:

$$j = 2.4 \cdot (1.43)^{0.22} \cdot (6/6)^{2.8 \ln(6/6)}$$

$$j = 2.6\%$$

For crystalline plastic material like polypropylene used for CS1 product cooling error (j) should not exceed 2.5-5.0% [Zollner, 1997].

As calculated cooling error within this range, the designed for the new conformal cooling channels at the thickest part section can be verified. Therefore, it was assumed that the whole dimensions set out in the cooling channel design can be implemented.

#### 5.4.2.1.3. Design Evaluation

To evaluate a performance of the cooling channel, heat balance between heat releases from product and heating efficiency by the coolant during the moulding process is furthermore examined to determine a process cycle time. In this evaluation, the following assumptions are then considered:

- The physical properties of the product is constant
- The heat released by product is completely absorbed by insert material and coolant
- The temperature of both mould cavity and cooling channel wall is constant
- The molten plastic is in steady state during cooling/solidification process
- An extreme/critical cooling condition is on the thickest part section of the product

#### Heat of Product

As equation 2-19, the heat transfer rate from the molten plastic into each mould per cycle is based on Fourier's law of heat conduction, which states:

$$\dot{Q}_M = \frac{\Delta h \cdot A_M \cdot s \cdot \rho}{t_{cyc}}$$

$\Delta h$  is calculated from the enthalpy different between injection and ejection for PP material (see Figure 2-14), which is 167 (kJ/kg). Therefore,

$$\dot{Q}_M = \frac{(167) \cdot (0.018) \cdot (1.275) \cdot (905)}{t_{cyc}}$$



$$\dot{Q}_M = \frac{3.5(\text{kJ})}{t_{\text{cyc}}(\text{s})}$$

### Heat Removal

Heat removal takes place in the cooling channels where the coolant flowing removes heat from the cavity wall. The quantity of heat transfer rate from insert to the coolant is:

$$\dot{Q}_C = V \cdot \rho_c \cdot c_{pc} \cdot \Delta T$$

where,

$V$  = Flow rate of coolant

$\rho_c$  = Density of coolant

$c_{pc}$  = Specific heat of coolant

$\Delta T$  = Temperature different (inlet vs. outlet), max 3 - 5°C [Menges, 2001]

Hence,

$$\dot{Q}_C = (3 \times 10^{-5}) \cdot 997.6 \cdot (4.18) \cdot (4)$$

$$\dot{Q}_C = 0.56(\text{kJ})$$

As assumed, the heat released by product is completely absorbed by insert material and coolant so that  $\dot{Q}_M \approx \dot{Q}_C$ . Utilising this heat balance, the cycle time  $t_{\text{cyc}}$  per shot using the new conformal cooling channels for CS1 can be obtained as follows:

$$\dot{Q}_M = \dot{Q}_C$$

$$\frac{3.5(\text{kJ})}{t_{\text{cyc}}(\text{s})} = 0.56(\text{kJ}) \quad \rightarrow \quad t_{\text{cyc}} = \frac{3.5}{0.5} = 7\text{s}$$

#### 5.4.2.2. Near-Net Shape Inserts

Considering a near-net shape design of the new CS1 inserts (see Figure 5-6), three components (cavity, core and rib) inserts are selected and decided to be manufactured using a combination of indirect SLS and HSM. The selection is mainly based on manufacturing constraints concerning both internal and external complex geometry of the inserts. For other components (guide/pin insert, orifice insert, lip insert, ejector), a decision is taken that these components will be manufactured using conventional materials and methods due to moving components, and manufacturing constraints for relatively small size components. Figure 5-9 shows the 3D CAD solid and wireframe models of the net-shape designs of the

selected inserts.

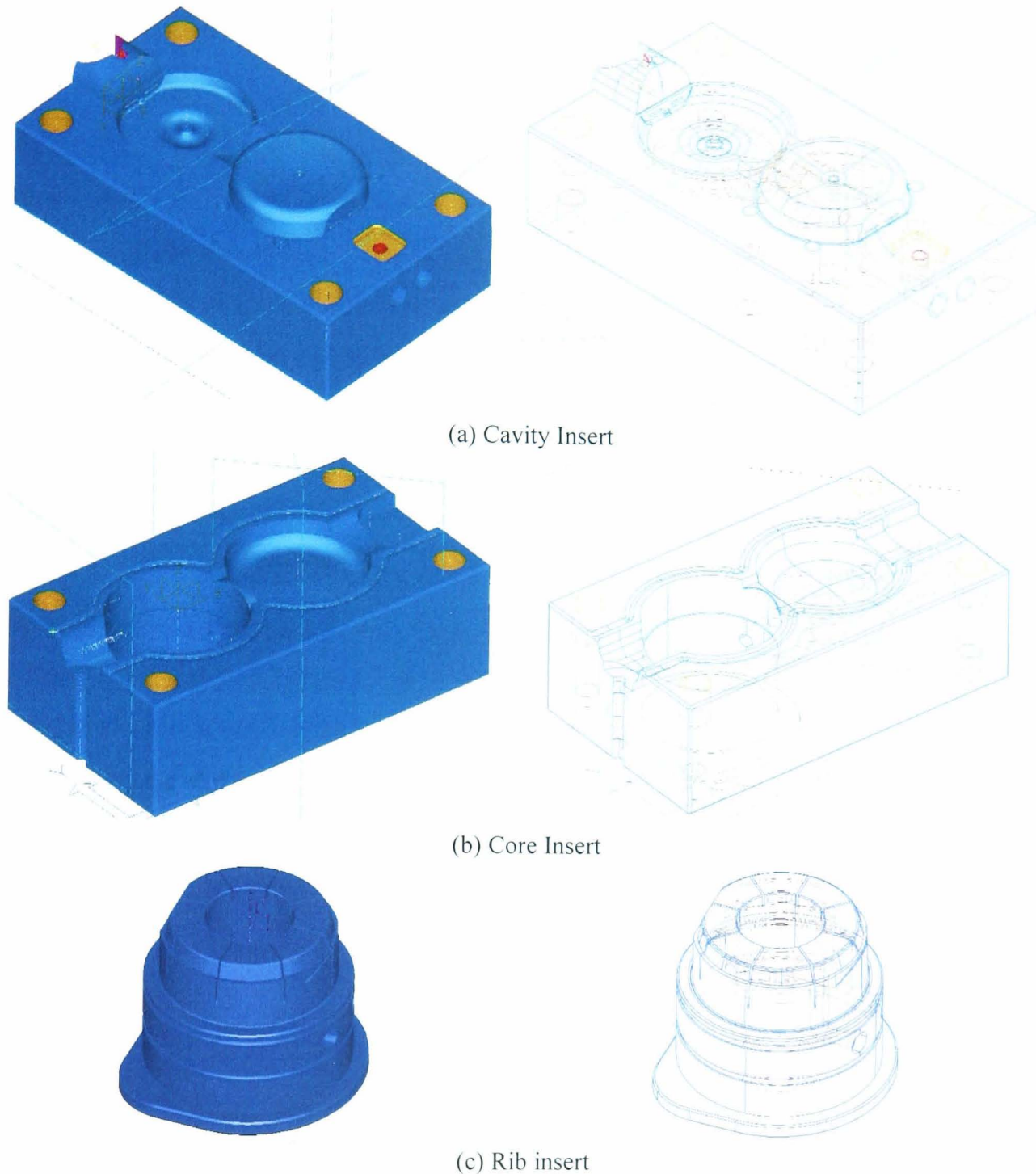


Figure 5-9. Net Shape Design of the New CSI Inserts

Based on the detail design of the net-shape inserts, a near-net shape design of each insert is generated. As in guidelines, the first principle in the near-net shape design is to consider generating the features which are as close shape/geometry as possible to the net shape inserts design in order to minimise its manufacturing operations. As the near-net shape inserts are developed using the indirect SLS process, its technical capability furthermore leads to the second principle that small/delicate features, deep narrow slots, and drilled holes on the inserts are to be added and finished later by the required post-processing. To anticipate dimensional changes during the process and to ensure sufficient material for finishing, additional

1 mm materials per-side for machining allowance are then considered in designing the near-net shape inserts.

Figure 5-10 shows the near-net shape models of the selected components. Referring to their net shape designs show in Figure 5-9, most detail features on the insert such as holes with specific tolerances, sprue, gate, hinge, and ribs are excluded from the design. For the cavity insert (Figure 5-10a), the features included in the near net shape design are: the core features to form the features of the hinge and the internal shape of the lid cap; the cavity feature to form the profile of a top base of products; the pocket for lip insert; the protrusion feature for generating runner and gate; the chamfers and the blind clearance holes which are not dimensionally specific for bolts, and orifice insert. In the case of the core insert (Figure 5-10b), the features included in the near-net shape design are: the cavity feature to form external shape of the lid cap, the initial hole where the rib insert is located, the channel prepared for vents, the chamfer and the blind clearance holes for bolts. A near-net shape of the rib insert (Figure 5-10c) is designed close to the basic external shape of its net shape design, solid cylinder with steps. Furthermore, an additional material of 4 mm is added to the base of the rib insert to provide a sufficient stock required for machine fixture.

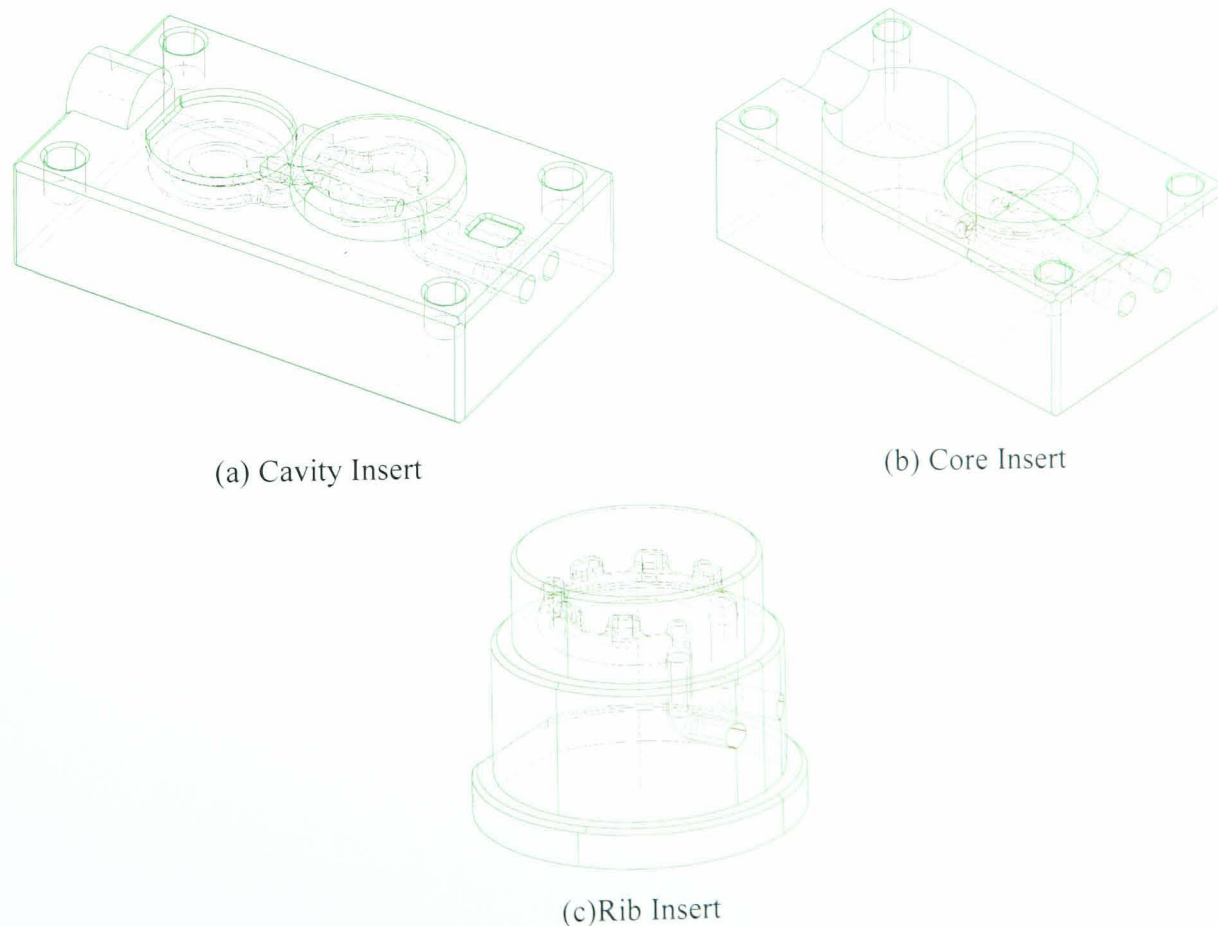
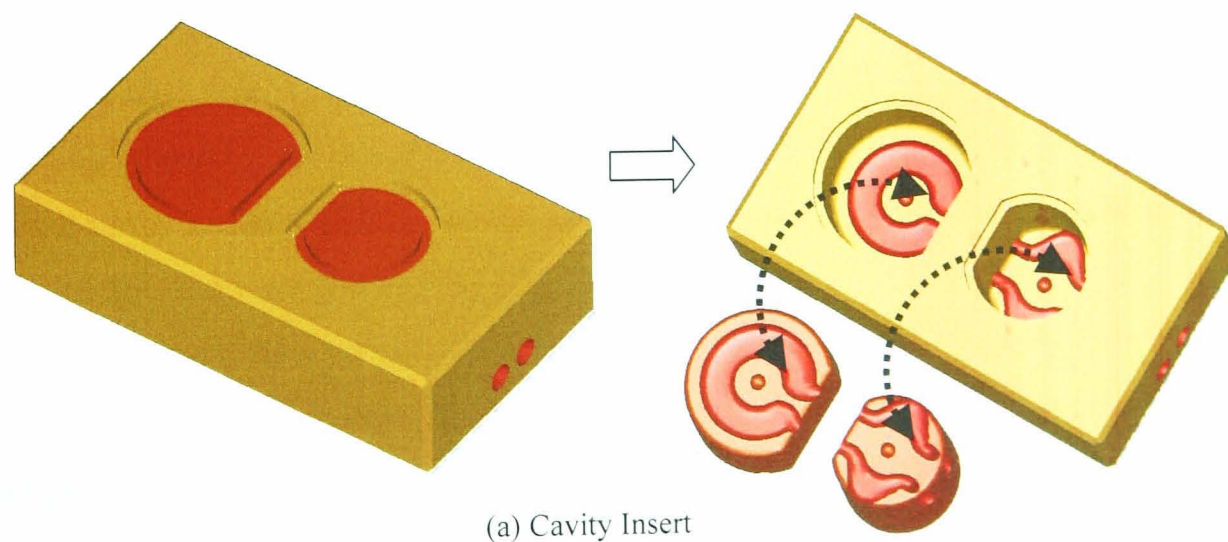


Figure 5-10. Near-Net Shape Design of CS1 Inserts

For these three main inserts, the conformal cooling channels are included inside their near-net shape design. This causes a careful consideration and decision whether a specific technique in clearing loose powder from the channel is required. From the wireframe models (Figure 5-10), the conformal cooling channels design inside cavity (Figure 5-10a) and rib insert (Figure 5-10c) definitely require a 'cut-off volume' technique to clear the powder. A long-winding and different level of channel inside cavity insert increases a difficulty level in clearing the powder. These decision also apply to clear the feature along the unique channel features inside the rib inserts. In the case of the core insert (Figure 5-10c), the channels basically have only two 90° bends and lay in a straight line. However, there are freeform/flattened sections which potentially causes a difficulty in clearing the powder completely.

To apply the technique, the location of the cut-off volume for all inserts are determined by considering the flattened sections of the channels where the powder is the most difficult to be cleared. Figure 5-11 shows the designs of the cut-off volumes which are taken off from its respective insert. The figure shows that the cut-off volumes bisect the channels and open the selected sections to provide an easy access for clearing the powder. To assemble back the cut-off volumes unique guiding features are included in the design. Moreover, the figure also shows the grooves on both cut-off volume and the main body are prepared for high temperature resin to avoid leaking.



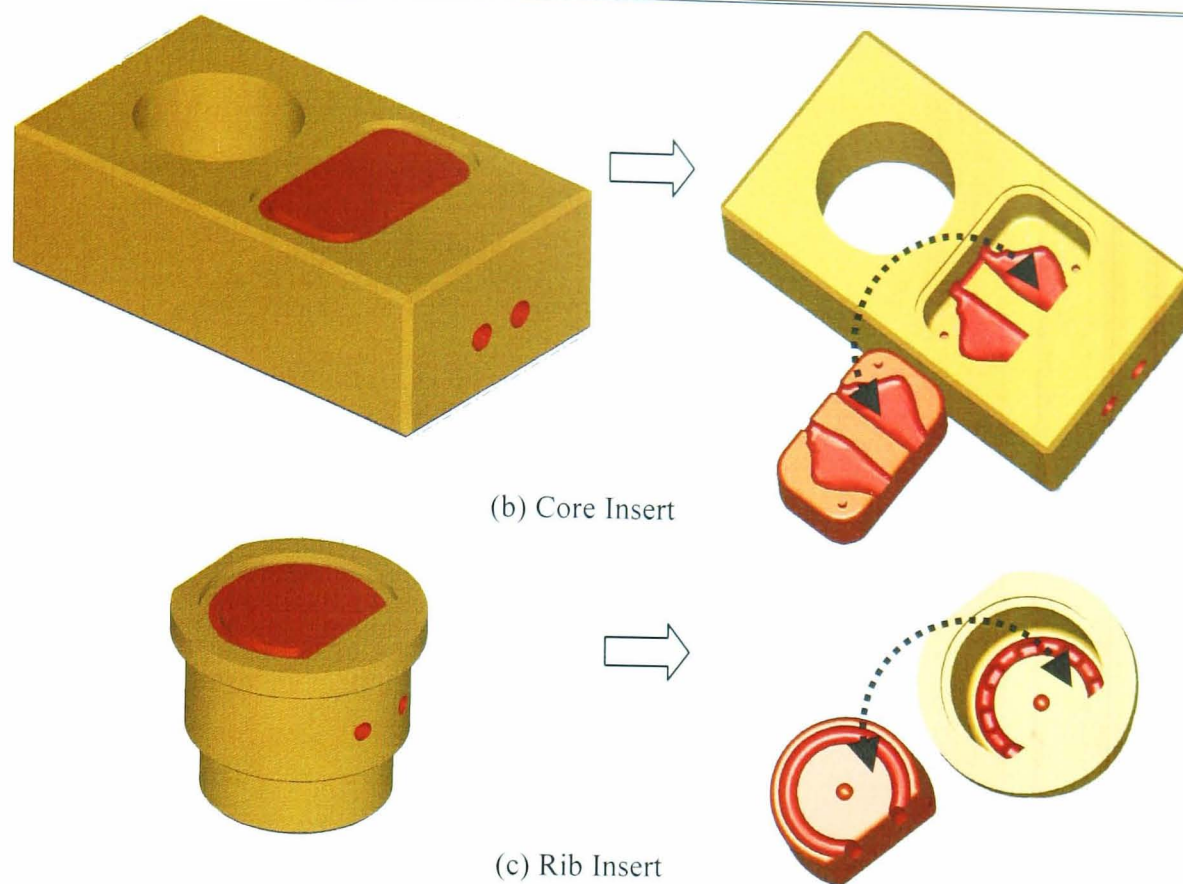


Figure 5-11. Cut-Out Volume of the CSI Inserts

### 5.4.3. Inserts Manufacture

In machining and finishing the inserts, a manufacturing operational plan is developed. All of the inserts are colour coded (blue, brown, red, green, pink, and yellow) in order to explain required machining and finishing processes that are required to form the respective features (Figure 5-12). A blue colour code indicates insert features which do not require further machining or finishing. Among them are the features that have been prepared for vents, chamfers, clearance holes, and cooling channels. As not dimensionally specific, their geometry are acceptable as a result of the indirect SLS. A brown colour represents the operations for blocking-out the inserts. For core and cavity, HSM is used for flat features to square and size the inserts. Whilst, turning and circular grinding are used to round and size the rib insert, including to flatten top and bottom face of the rib and to form two grooves prepared for o-rings. A red colour code represents the HSM operations that had been used to machine freeform surfaces of all the features that mostly form the mould cavity, including sprue/gate block and lip insert pocket. At this stage, the dimensions of any surface features that require fine finish quality are left with sufficient stock for polishing. Furthermore, a green code represents drilling, reaming, boring and tapping operations that had been used to add most features inside the holes for bolts, pushers, rib insert, orifice insert, guide/pin insert, and sprue channel. A pink colour

is for the features that require EDM operations due to recessed, inaccessible or sharp corners. Rib forming slots, gate channels, hinge freeform surfaces and slot, and lid lock undercuts are among them.

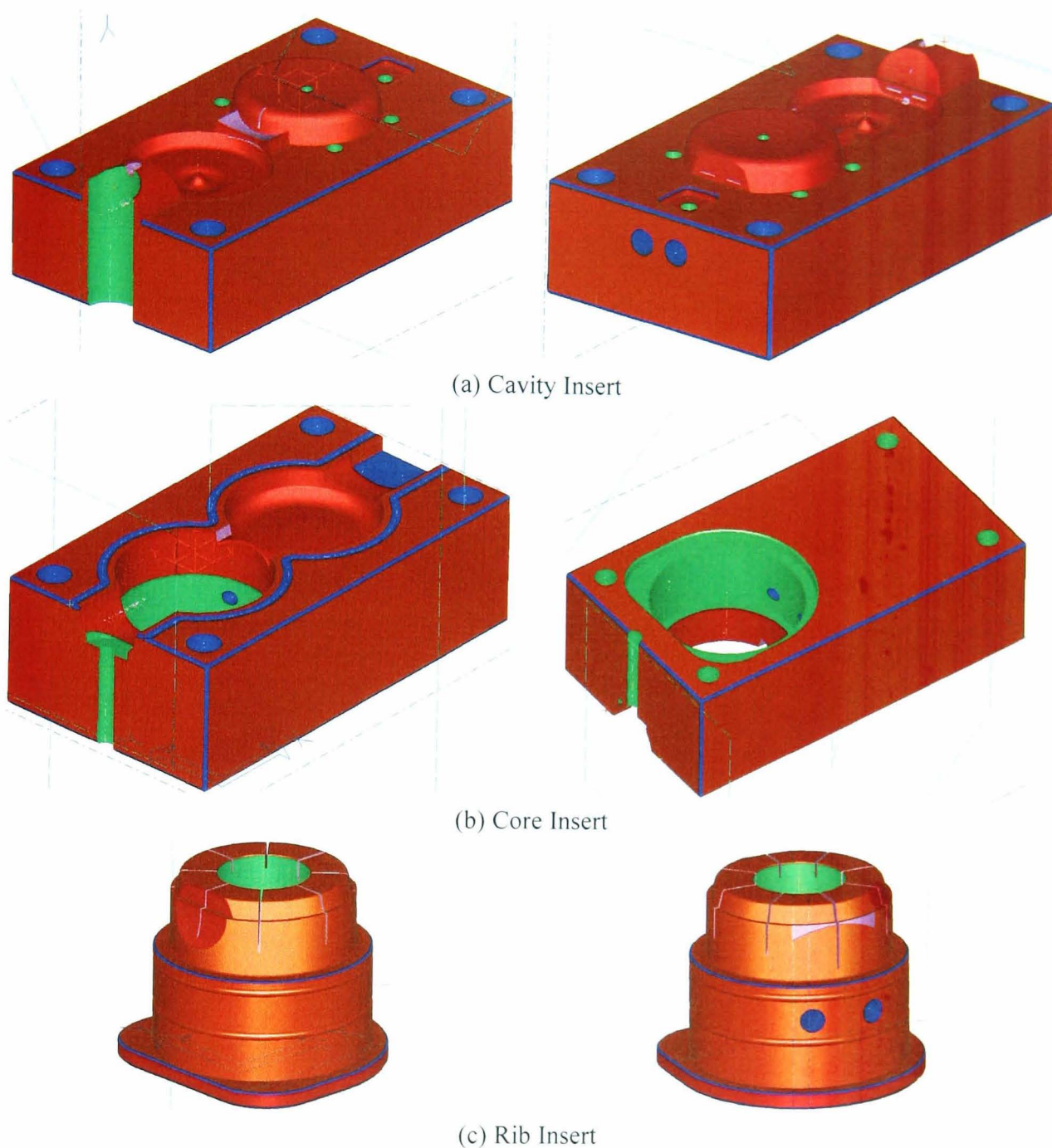


Figure 5-12. Manufacturing Colour Code of the CS1 Inserts

To enhance the insert final quality, Figure 5-13 furthermore shows a yellow colour code is used to indicate some surfaces of the inserts that require polished finish quality. For all inserts, required polishing is indicated on:

- the core insert: hole surface that form the side wall profile of the product base, mould cavity surface that form the external profile of the product lid cap, hinge channel.
- the cavity insert: mould cavity surfaces that form the internal profile of the product lid cap and the external (top) profile of the product base, hinge,

sprue/gate surface that form part of the external (top) profile of the product base

- the rib inserts: outer surfaces that form the internal profile of the product base

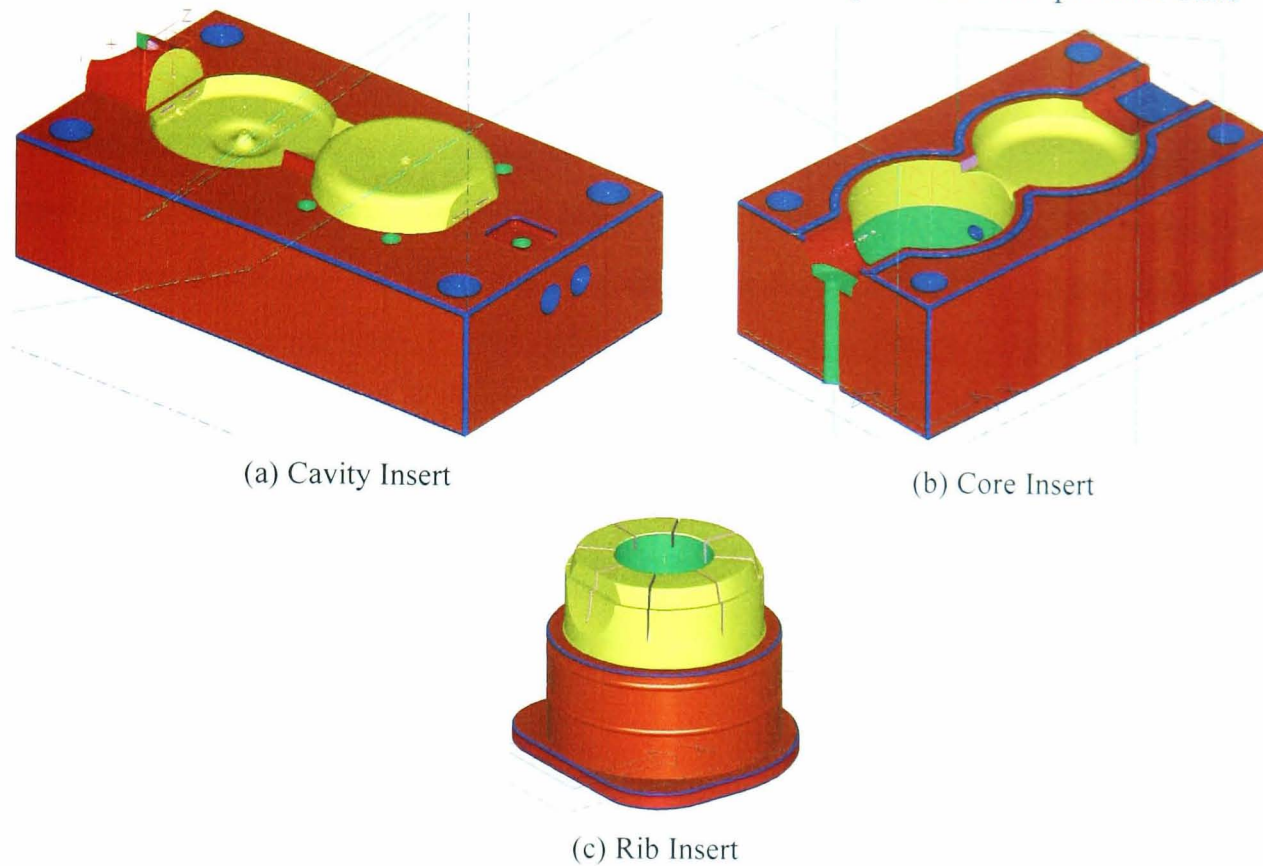


Figure 5-13. Polishing Colour Code of the CS1 Inserts

#### 5.4.4. Discussion

It can be seen that the design rules application in developing the new CS1 has combined the best design practices from both the original inserts and the conformal CS1 insert developed previously. Comparing with those two inserts, there are three important issues that need to be discussed in this design application. As constrained by product specification and manufacturing process, a minimum number of components required to form the CS1 core/cavity is similar to both designs. However, the general geometry of the new CS1 insert mostly adopts the basic design of the conventional insert rather than the conformal CS1 insert, especially the geometry of the rib inserts. Concerning manufacturing handling and process, the rib inserts of the new CS1 is designed to avoid a significant number of the surfaces to be machined (milling) as in the conformal CS1 insert.

The next issue is related to design of the cooling channel inside the insert. Significant changes have been made to the new cooling channel design for the new CS1. As in the conformal CS1 insert, the new cooling channels is also designed by utilizing the optimum capability of the indirect SLS process, which is able to

construct the cooling channel conformal to the mould cavity with a complex (freeform) cross-sectional area. As outlined (see Figure 5-8), the path of the new channels are brought closer to the cavity and the cross-sectional area are flattened at the selected sections to improve a heat transfer from the thicker wall and wider surface area of the product. As noted in the calculation (section 5.4.2.1.2. ), the new cooling channel location at 6mm from cavity wall is considerably appropriate to provide uniform cooling. The design evaluation (section 5.4.2.1.3. has furthermore indicated a better performance of the new cooling channel design. The new design is able to reduce the cycle time down to 7s compared to 12s of the conformal CS1 design and 14s of the conventional design and.

## 5.5. Case Study (CS) 2: Receptacle Spoke

### 5.5.1. Product Evaluation

The technical specifications for this CS2 product were reviewed as it was presented in Figure 4-25. For a new insert design, Figure 5-14 below indicates marks where the ejector, gate and parting-line (P/L) are located. As thread constructed, the product is ejected by retraction, unscrewing process, and ejector pin inside the thread. These information are referred to in designing the net shape of the new CS2 inserts.

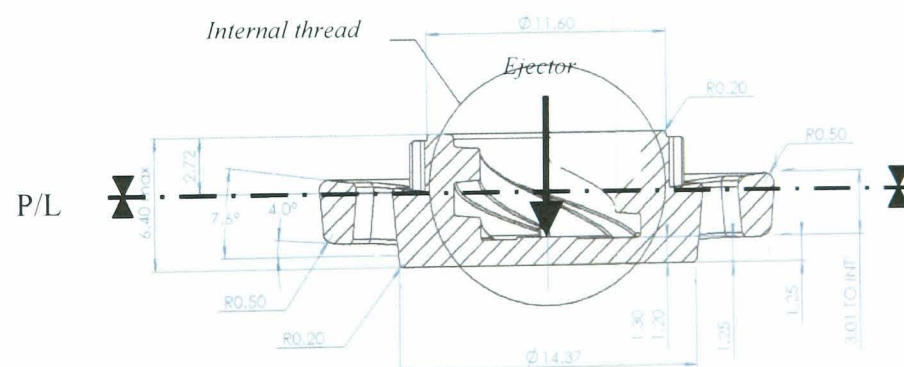


Figure 5-14. Receptacle Spoke [Trisport Ltd.]

### 5.5.2. Insert Design

#### 5.5.2.1. Net Shape Inserts

Based on the specified product design and defined P/L, three main components are designed to form a new CS2 insert: moving, fixed and thread inserts as outlined in Figure 5-15. The figure shows that a moving insert is designed to mould the bottom parts of the product. The fixed insert is to mould the top parts of



the product. And, the thread insert is used to form the internal thread. Moreover, the figure also indicates a hot manifold gate system located inside the fixed insert to inject melted plastic into the cavities, and an ejector pin inside the thread insert which is used to release the product from the mould cavity on the moving insert.

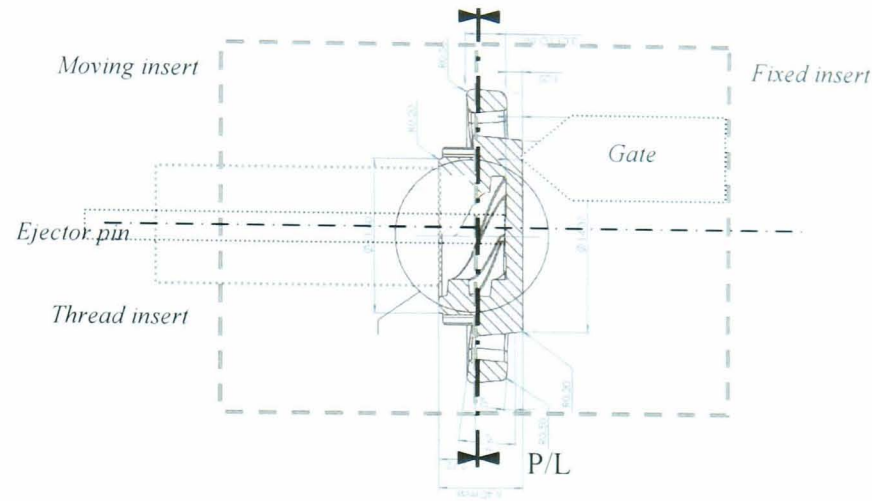


Figure 5-15. Outline of the New CS2 Inserts

Based on the above outline, both moving and fixed inserts are decided to be designed and manufactured using a selected approach of combining the indirect SLS and HSM process. Since the thread insert moves and relatively small in size for constructing cooling channel, it is decided this insert is to be conventionally manufactured using more conductive material to provide a better heat transfer. For the external geometry, both moving and fixed inserts are cylindrical in shape by referring to a basic shape of the product. To provide the way of coolant entering and exiting the insert, an external groove is then constructed on both inserts which also can be utilised as a cooling channel. To avoid coolant leaking from the groove, both inserts are equipped with o-rings. Figure 5-16 shows an assembly of the new CS2 insert and models the new moving and fixed inserts design.

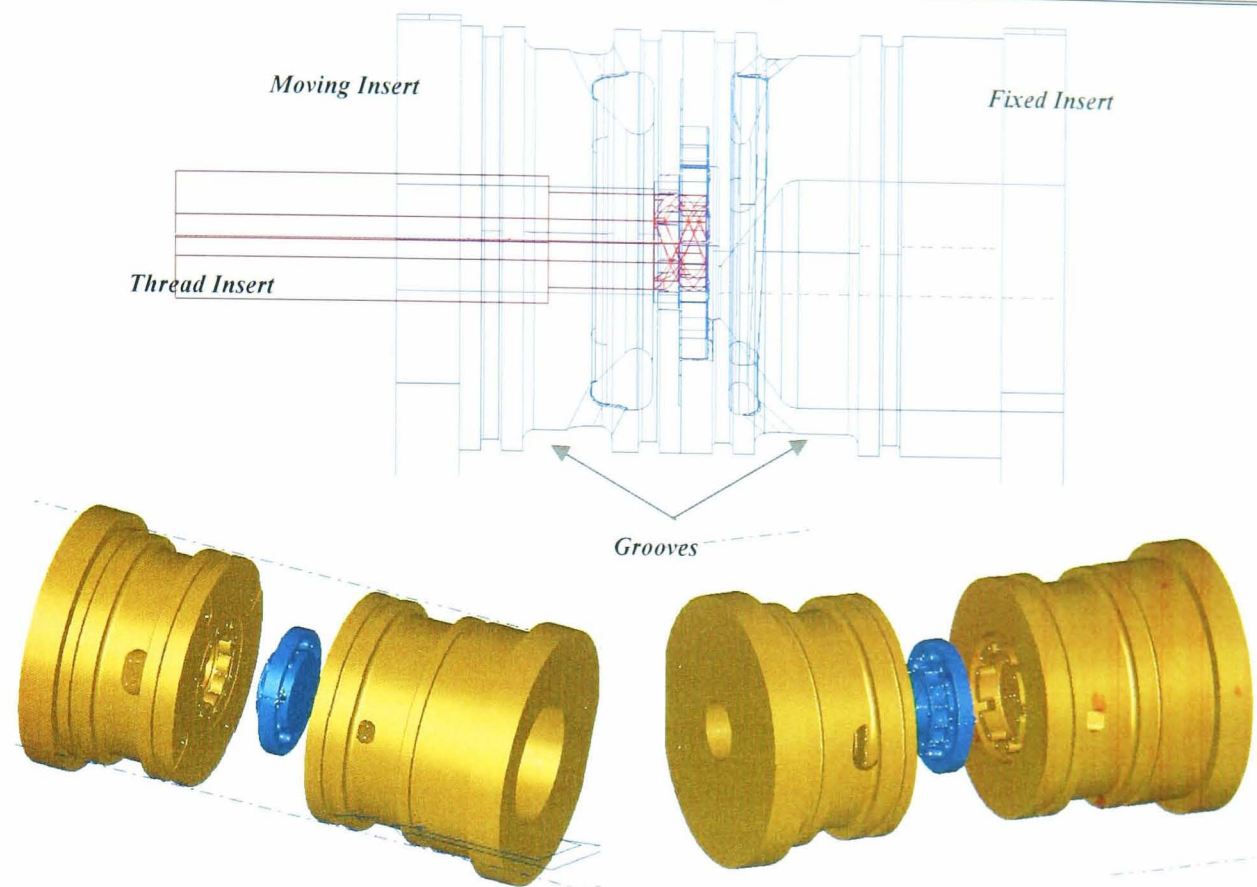


Figure 5-16. New CS2 Inserts

For cooling channels, several design constraints such as avoiding other features, maintaining insert strength, locating and dimensioning channels are considered. As in the new CS1 insert, freeform cooling channels are constructed conformal and brought closer to the mould cavity surface. However, a design of the cooling channel in the fixed insert requires a special attention due to an off-centre hole for hot manifold gate system which limits a space available around the mould cavity to construct the channel. Utilising the available spaces, the cooling channel is constructed in circular path with a various cross-sectional areas. In the case of the moving insert, there is no significant constraint in constructing and locating the channels. Therefore, the cooling channel is designed in similar shape of path with uniform cross-sectional areas. Figure 5-17 furthermore shows the design of the conformal cooling channels for both moving and fixed inserts which are located relative to the product.

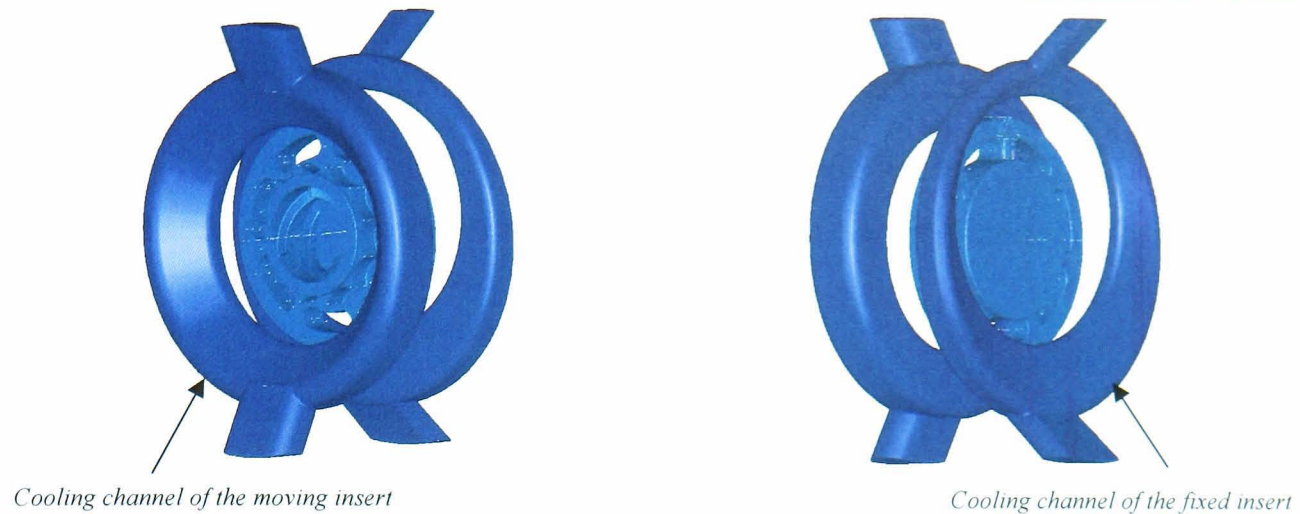


Figure 5-17. The New CS2 Cooling Channels Geometry

A unique freeform geometrical shape of the channels cross section for both inserts is selected in order to progress the channels as closer to the mould cavity surfaces as possible. Considering the strength of the insert, the channels are then located at constant distance of 4 mm between the mould cavity and the channel wall. As in CS1, the following steps and calculations are carried out as an approach to evaluate the new design of the new conformal cooling channel for CS2. The followings are the parameters that are utilized as inputs in the calculation and design evaluation.

<b>Product</b>	Material	:	<b>Stanyl TW341 Nylon 46</b>
	Density ( $\rho$ )	:	1.18 (g/cm <sup>3</sup> )
	Melt Temperature ( $T_{melt}$ )	:	295 °C
	Mould Temperature ( $T_{mold}$ )	:	80 °C
	Ejection Temperature ( $T_{eject}$ )	:	120 °C
	Specific Heat ( $C_p$ )	:	2.1 (J/g °C)
	Thermal Conductivity ( $\lambda$ )	:	0.3 (W/m.K)
	Thermal Diffusivity ( $\alpha$ )	:	0.12 (mm <sup>2</sup> /s)
	Product Area	:	0.0014 (m <sup>2</sup> )
	<b>Insert</b>	Material	:
Density ( $\rho$ )		:	7700 (kg/m <sup>3</sup> )
Specific Heat ( $C_p$ )		:	479 (J/kg)
Thermal Conductivity ( $\lambda$ )		:	0.193 (W/m °C)
Thermal Diffusivity ( $\alpha$ )		:	0.065 (mm <sup>2</sup> /s)
<b>Coolant</b>	Coolant	:	<b>Water</b>
	Density ( $\rho$ )	:	997.6 (kg/m <sup>3</sup> )
	Specific Heat ( $C_p$ )	:	4.18 (kJ/kg)
	Thermal Conductivity ( $\lambda$ )	:	0.58 (W/m °C)
	Temperature	:	20 (°C)
	Flow rate	:	2 (l/min)

Using similar approach and assumptions as in CS1, the following Table 5-3 show the results of estimated calculations and design evaluations

Table 5-3. Results of Design Estimations and Evaluations for CS2

No.	Descriptions	Results
<b>A.</b>	<b>Estimated Calculations</b>	
	1. Cooling time $t_c$ (s)	8.2
	2. Cycle time $t_{cyc}$ (s)	10.6
	3. Heat of Product $Q_{mp}$ (J/s)	120
	4. Shortest distance $L$ (mm)	4
	5. Cooling error $j$ (%)	2.8
<b>B.</b>	<b>Design Evaluation</b>	
	1. Heat removal by coolant $\dot{Q}_c$ (J)	834
	2. Cycle time $t_{cyc}$ (s)	6

#### 5.5.2.2. Near-Net Shape Inserts

Based on the detail design of the net-shape inserts (see Figure 5-16), a near-net shape design of each insert are generated. Excluding small features, the near-net shape of both the new CS2 moving and fixed inserts for indirect SLS process are designed as close to the basic external shape of its net shape design as possible with conformal cooling channels constructed inside them. A 1 mm machining allowance is added to all external dimensions as well as a 4 mm additional materials at the base of each insert for machine fixtures.

Figure 5-18 shows the near-net shape of both moving and fixed inserts. From the figure, it is shown that the grooves on both inserts for coolant enter and exit the cooling channels are prepared at the SLS process since they are not dimensionally specific. Also, an initial through hole for thread insert is prepared on moving insert. In this CS2, a circular design of the cooling channels with radius less than 50 mm allows powder removal process without ‘cut out volume’ technique. The geometry and path of the channels provide an easy access for powder removal inside the channels. This means that resin sealing are also not necessary.

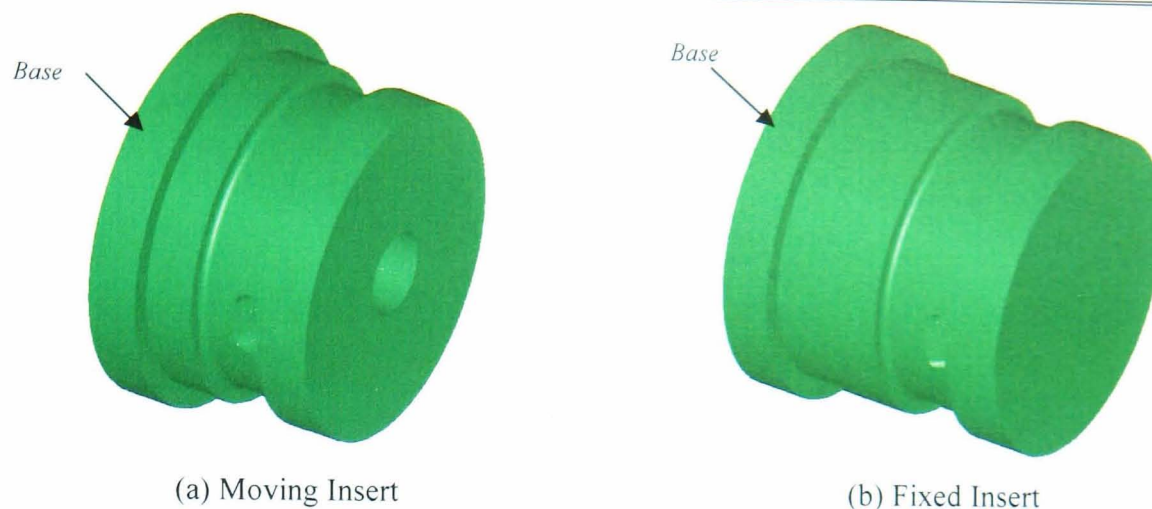
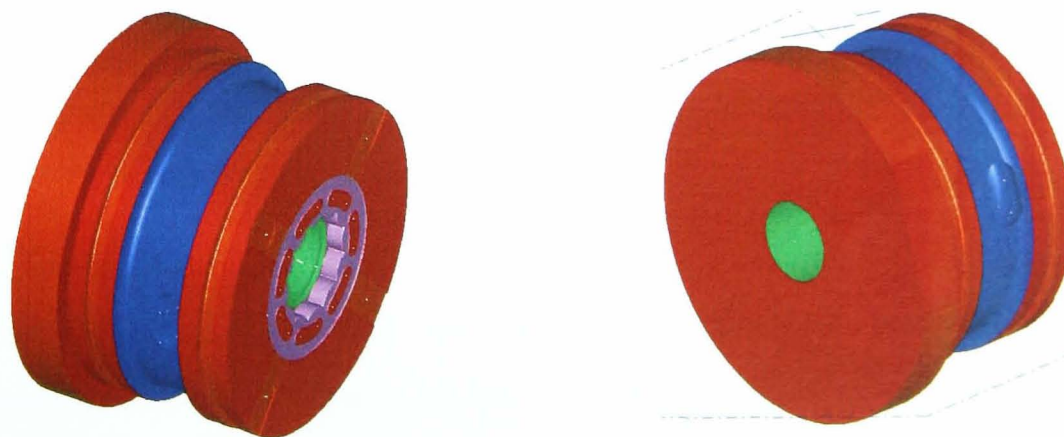
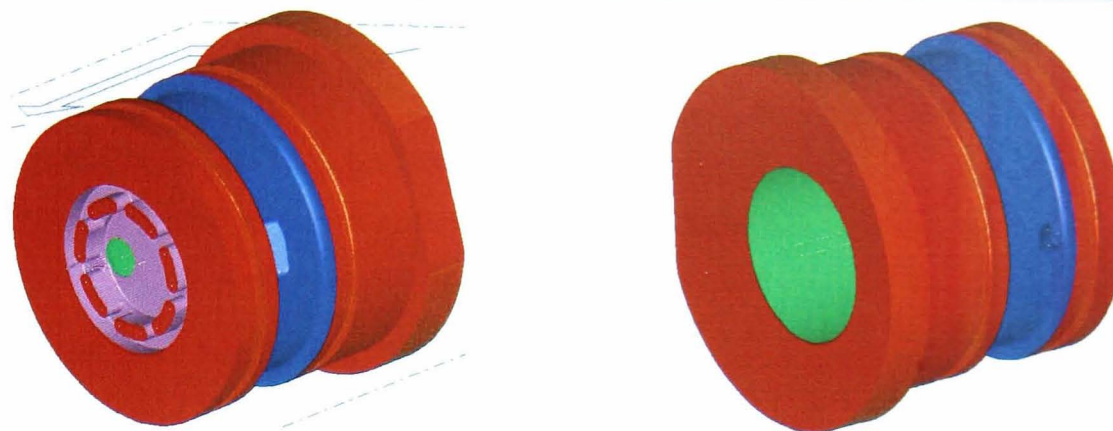


Figure 5-18. Near-Net Shape Design of the New CS2 Inserts

### 5.5.3. Insert Manufacture

In machining and finishing the inserts, a colour code for manufacturing operational plan is also prepared (Figure 5-19). As in CS1, a blue colour code is assigned for the coolant grooves which do not require further machining or finishing. A brown colour represents the turning operations for rounding-out the inserts, including o-ring grooves. A red colour code then represents turning and circular grinding which are used to round and size both insert, including. The red colour code also represents the HSM operations that had been used to machine freeform surfaces to flatten top and bottom face of the inserts as well as to flatten side on the base. Furthermore, a green code represents drilling and reaming operations to add a through hole for thread insert on the moving insert and a hot manifold system on the fixed insert. A pink colour is then coded for the mould cavity detail which require EDM operations. Rib forming slots, gate channels, hinge freeform surfaces and slot, and lid lock undercuts are among them.





(b) Fixed Inserts

Figure 5-19. Colour Code of Turning and Grinding Operation

#### 5.5.4. Discussion

It can be seen that there are no significant changes in the design of the new CS2 insert compared to its original (conventional) and the conformal CS2 insert. The minimum number of the insert components required and general geometry of the components are considered optimum for molding the selected product. However, the only changes are made to the design of the cooling channels. As noted in Chapter 4 (see section 4.3.4.2), both conventional and conformal CS2 inserts are able to be operated down to a limit of 6.5s cycle time from 7.7s with their respective cooling channel design. To have a better improvement, a cooling channel of the new CS2 insert is designed by adopting the design idea from both conventional (externally constructed) and conformal CS2 (internally constructed) inserts. By having and applying this design idea, the calculation in section 5.5.2.1. has predicted that the performance of the new CS2 insert can be improved with 6s operating cycle time.

### 5.6. Case Study (CS) 3: Cassio 200 ml Bottle Top

#### 5.6.1. Product Review

The technical specifications required for the CS3 closure product can be seen in Figure 4-37. The figure lists some important information regarding to a design consideration for a new insert. Figure 5-20 below indicates selected parting line (P/L), ejector and four pushers which are used to push the lid so that it remains its cavity as the mould opened.

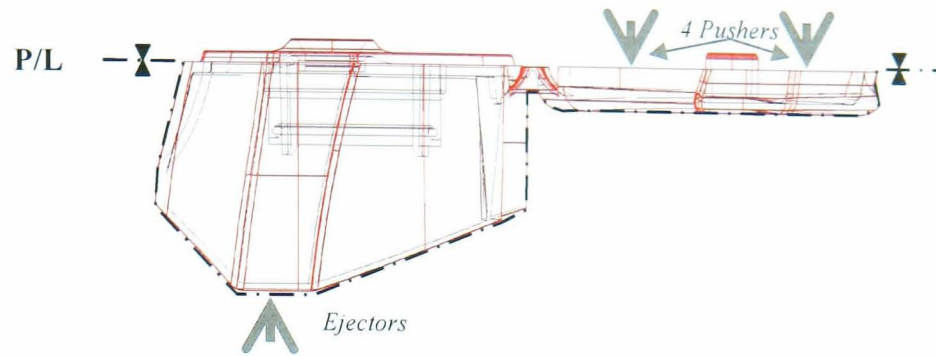


Figure 5-20. Product Orientation Relative to Parting Line

## 5.6.2. Inserts Design

### 5.6.2.1. Net shape Inserts

The final design of a new CS3 inserts is shown in Figure 5-21. In general, a closure product selected for the new CS3 insert has a similar function with the CS1 product. However, its unique geometry of the product base promotes different approach in designing the inserts. Due to its tapered geometry, a standard straight parting line (P/L) as in the CS1 cannot be employed. A wider size at the bottom of product base creates a difficulty for ejection process. Therefore, it is determined that a suitable P/L for this CS3 product is outlined by following the curves contour of the product base as indicated in the Figure 5-20 above.

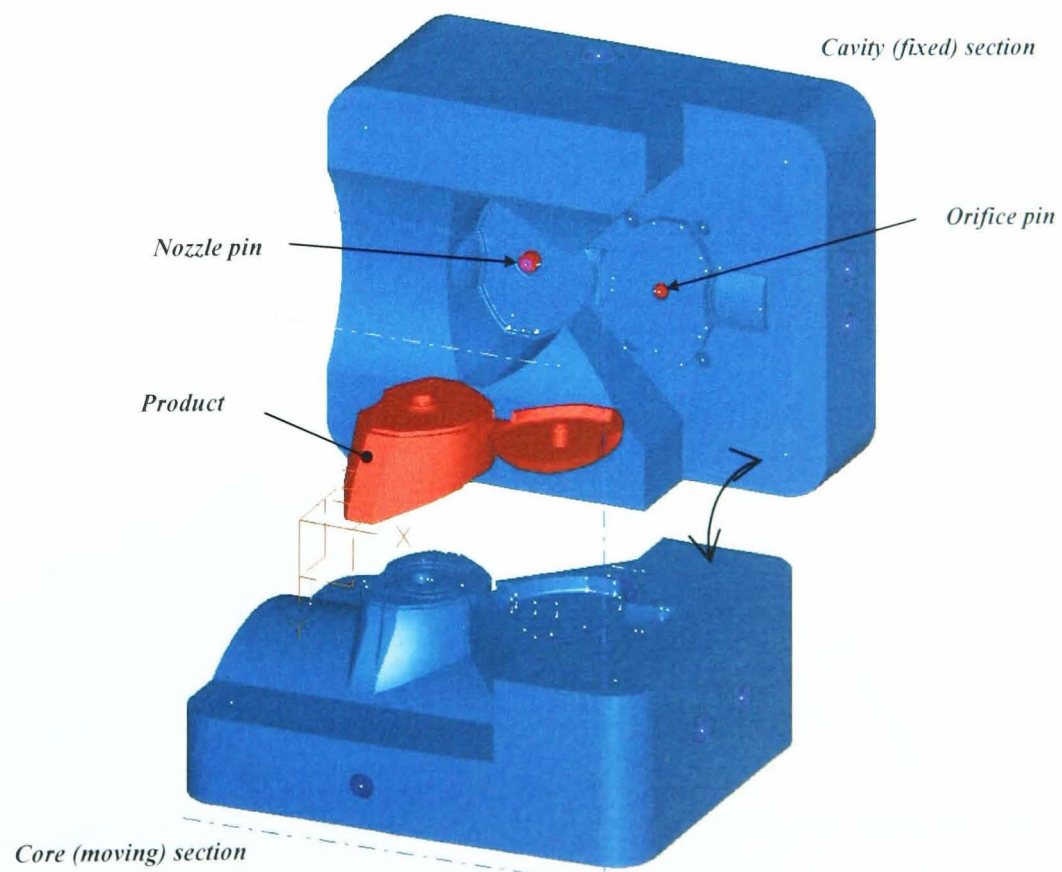


Figure 5-21. New CS3 Inserts

To utilise the selected P/L and to fulfil product requirements, a general geometry for both core and cavity inserts is then determined, and detailed. Similar to the previous two case studies, determining a minimum number required to form the core/cavity insert is based on the product requirements and the manufacturing constraints. As indicated in Figure 5-20 above, the feature surfaces which need to be polished are only on the top surface of the product base and the internal shape of the lid cap. In reference to the selected P/L, the mould cavity for these two features are geometrically opened and accessible on the cavity (fixed) inserts.

Moreover, the internal features (ribs and collar) on the product base are also another important issue that need to be considered in determining the minimum number of the insert. Like other features on the product, these features do not require polished finish quality. This promotes more freedom in designing the new core insert which allows a core to form internal feature of product base to be design as one main body of the core. For the cavity (fixed) insert, however, the existence of two inserts pins (nozzle and orifice pins) cannot be avoided due to a fine finish and opening access required on both pins.

By having the main components detailed, the design of the cooling channels are then generated. Figure 5-22 shows the new CS3 cooling channels for both cavity (a) and core (b) insert which is outlined relative to the product. As in the CS1, a combination of a standard 6 and 8 mm diameter with irregular cross-sectional are employed in constructing the channels. Considering for a better heat transfer, the irregular/flattened section of the channels are located and placed closer to thicker wall and wider surface area of the product. To evaluate the channel location and uniformity surface temperature for CS3, the following steps and calculations are carried out.

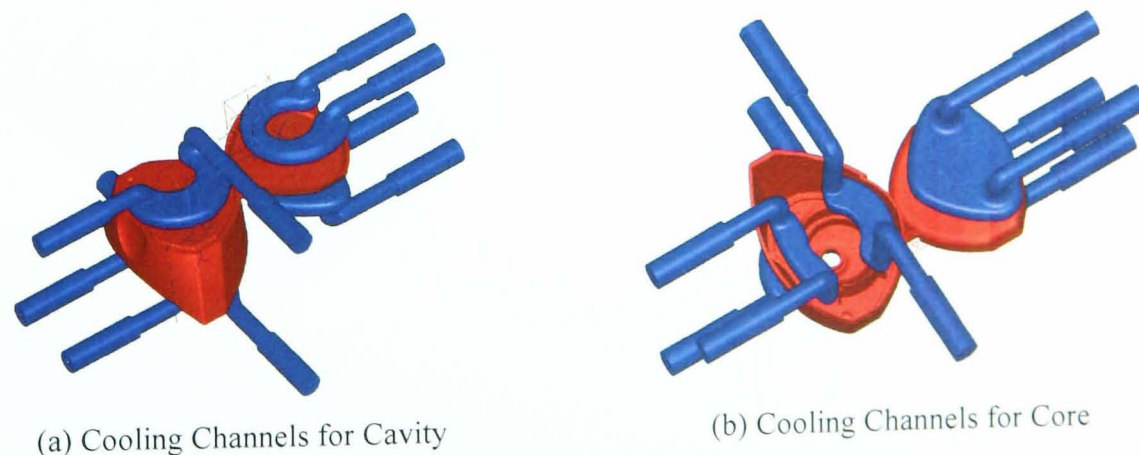


Figure 5-22. Design of New CS3 Conformal Cooling Channel



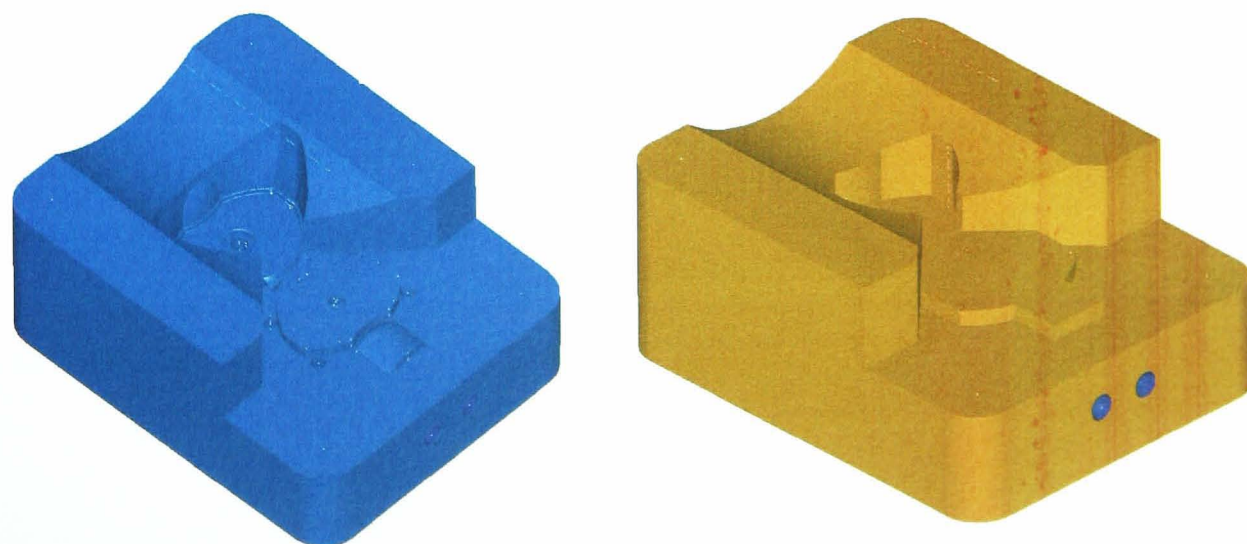
The product material for CS3 is PP similar to the product of CS1. Therefore, all material properties and parameter listed for the CS1 in section 5.4.2.1. were used as inputs in estimating and evaluating a new design of the CS3. Using the same approach as in CS1 and CS2, Table xx shows the results of the design estimation and evaluation for the new conformal cooling channel for new CS3.

Table 5-4. Results of Design Estimations and Evaluations for CS3

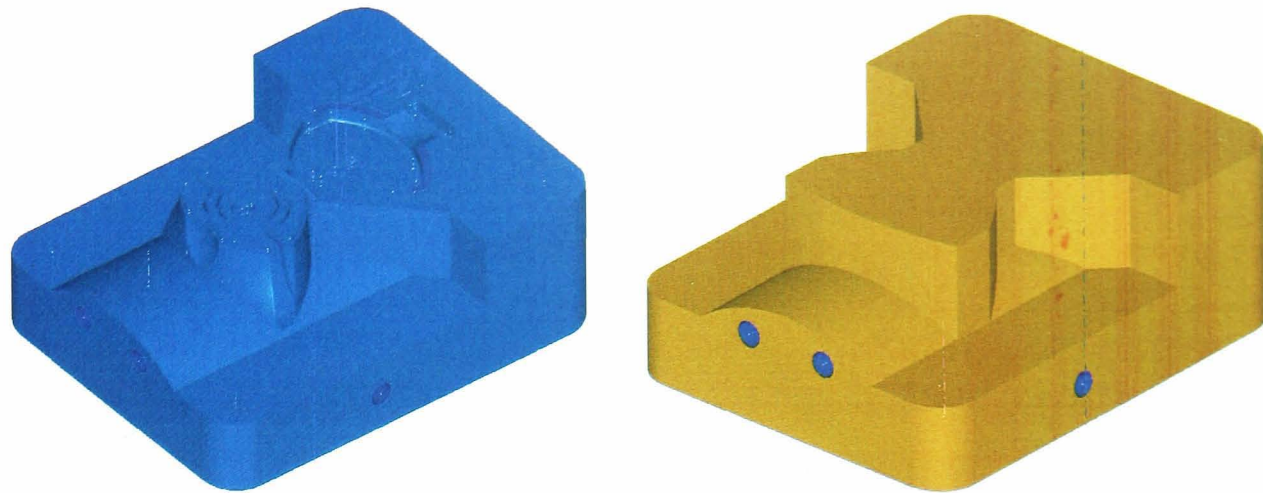
No.	Descriptions	Results
<b>Estimated Calculations</b>		
A.	1. Cooling time $t_c$ (s)	2.8
	2. Cycle time $t_{cyc}$ (s)	3.6
	3. Heat of Product $Q_{mp}$ (J/s)	300
	4. Shortest distance $L$ (mm)	4
	5. Cooling error $j$ (%)	2.6
<b>Design Evaluation</b>		
B.	1. Heat removal by coolant $\dot{Q}_c$ (J)	500
	2. Cycle time $t_{cyc}$ (s)	5

#### 5.6.2.2. Near-Net Shape Inserts

Referring to the net shape design, a near-net shape of the new CS3 insert are then generated. The near-net shape inserts are designed with a basic external geometry that as close as possible to the net-shape design, no small/delicate features, and conformal cooling channels constructed inside them. Figure 5-23 compares both net shape (left) and near-net shape (right) of the new CS3 inserts.



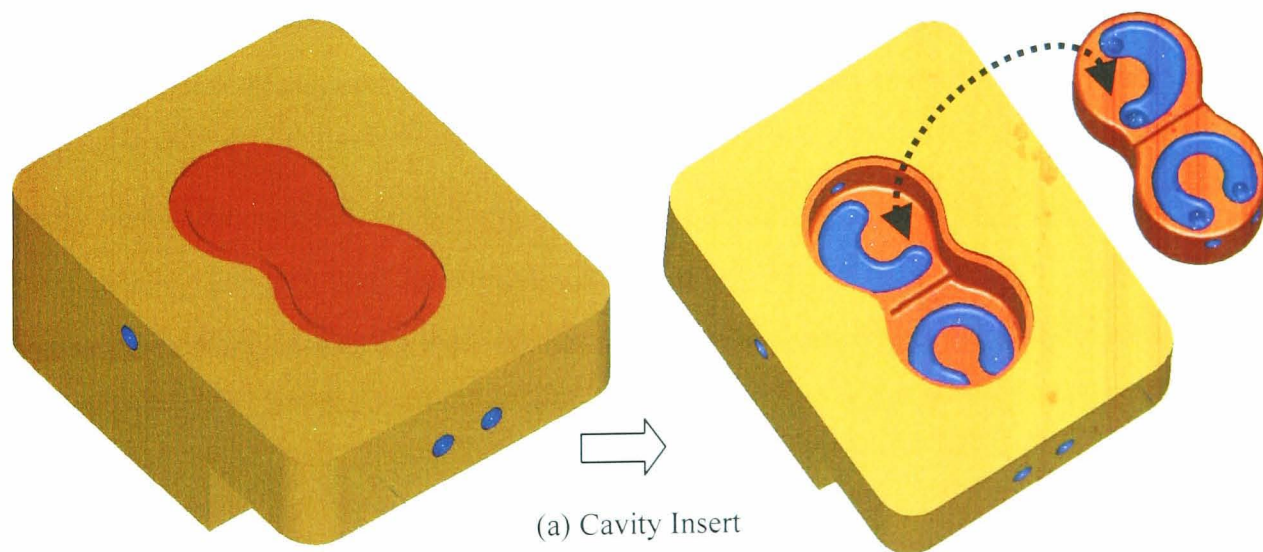
(a) Cavity Insert



(b) Core Insert

Figure 5-23. Net Shape vs. Near-Net Shape of the new CS3 Inserts

Due to a winding and different path level of the channels, the design of the cooling channels requires a 'cut-off volume' technique to clear loose powder inside the channels. Figure 5-24 shows the cut-off volumes which are designed and taken off from its respective insert. The figure shows that the cut-off volumes bisect the channels and open the selected sections to provide an easy access for clearing the powder. To assemble back the cut-off volumes unique guiding features are included in the design. Moreover, the figure also shows the grooves on both cut-off volume and the main body are prepared for high temperature resin to avoid leaking.



(a) Cavity Insert

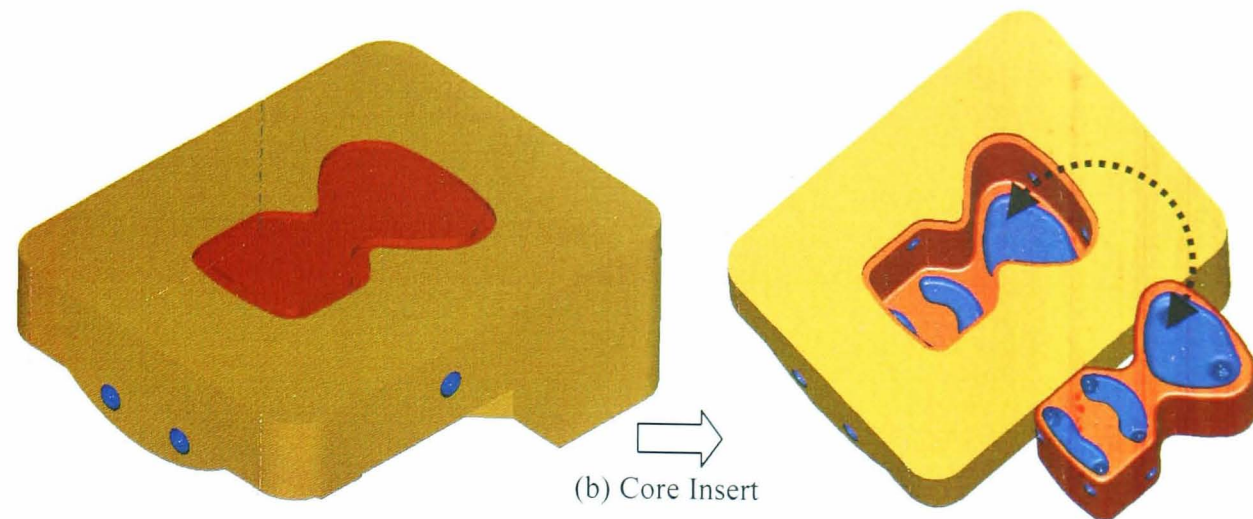
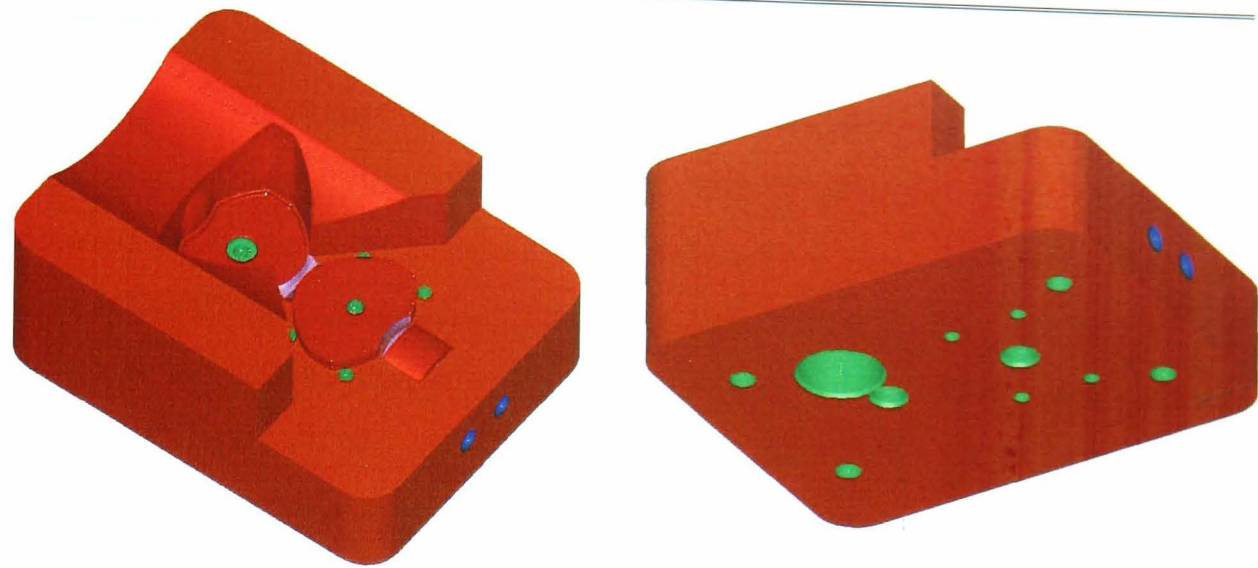


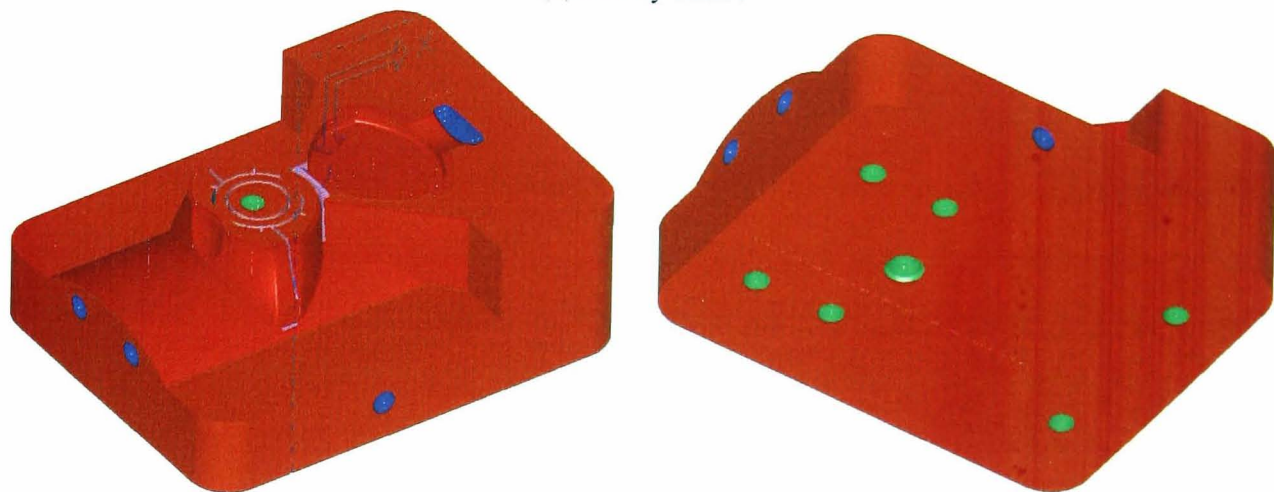
Figure 5-24. 'Cut-Off Volume' of the Inserts

### 5.6.3. Inserts Manufacture

As in the previous case studies, all of the inserts are colour coded (blue, brown, red, green, pink, and yellow) in order to explain required machining and finishing processes that are required to form the respective features (Figure 5-25) and to achieve the final quality. A blue colour code indicates insert features which do not require further machining or finishing, such as the conformal cooling channels and the clearance pocket for lip features on the cavity insert. A brown colour represents the operations for blocking-out the inserts. For core and cavity, HSM is used for flat features to square and size the inserts, including to flatten top core surface of the core insert to form ribs and collar. Whilst, a red colour code represents the HSM operations to machine freeform surfaces of all the features that mostly form the mould cavity. At this stage, the surface features that require fine finish quality are left with sufficient stock for polishing. Furthermore, a green code represents drilling, reaming, boring and tapping operations that had been used to add most features inside the holes for bolts, pushers, nozzle insert and orifice insert. A pink colour is for the features that require EDM operations due to recessed, inaccessible or sharp corners. Rib and collar slots, ejector slots, hinge freeform surfaces and slot, and lip feature are among them.



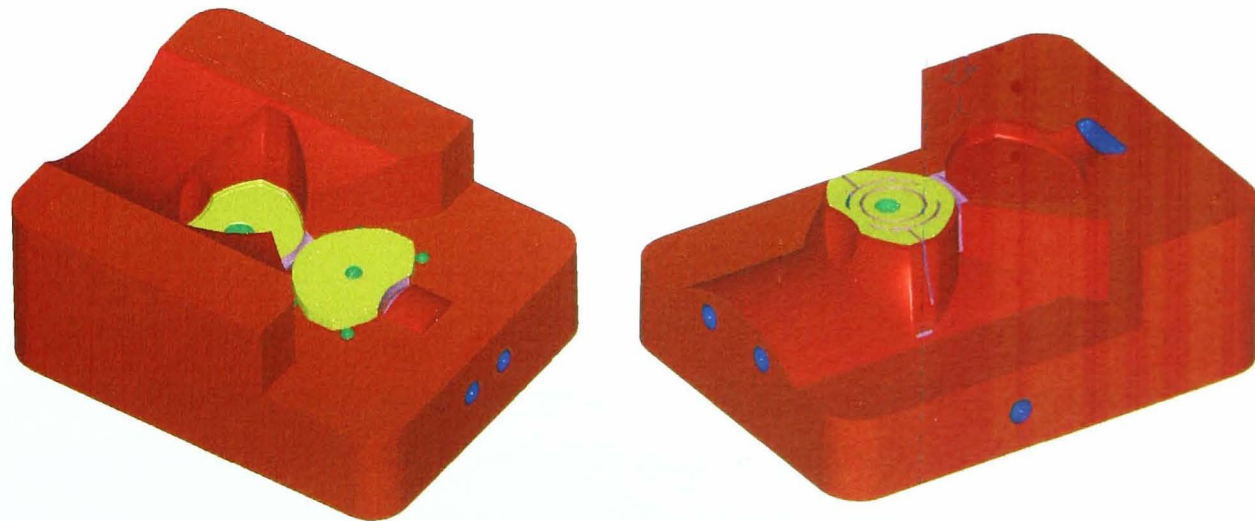
(a) Cavity Insert



(b) Core Insert

Figure 5-25. Manufacturing Colour Code of the new CS3 Inserts

To achieve a final quality specification, Figure 5-26 furthermore shows a yellow colour code is used to indicate mould cavity surfaces that require polished finish quality.



(a) Cavity Insert

(b) Core Insert

Figure 5-26. Polishing Colour Code of the new CS3 Inserts

#### 5.6.4. Discussion

A significant change made to the new CS3 inserts is that a number of the components to form the insert are reduced. Unlike in both original and conformal CS3 inserts, a rib core insert designed for the new CS3 is attached to the main body of the core insert which consequently reduce a significant number of the surfaces to be processed and fitted. However, it can be seen that the design rules application in developing the new CS3 has generally combined the best design practices from both inserts. Therefore, a general geometry of the new CS3 insert mostly adopts the basic design of both previous inserts.

Furthermore, significant changes have been made to the new cooling channel design for the new CS3. The new cooling channels for the CS3 inserts is designed with a freeform path and a combination of 6 and 8 mm standard diameter and freeform/irregular cross-sectional area. As outlined in Figure 5-22, the path of the new channels are brought closer to the cavity and the cross-sectional area are flattened at the thicker walls and wider surface areas of the product to improve the heat transfer. As noted in the results of design estimation and evaluation, the new cooling channel design for the new CS3 potentially provide benefits of being able to reduce the cycle time down to 5s from 9.9s using the original design and 6.2s using the conformal CS3 design.

#### 5.7. Summary

This chapter has examined the application of the design rules in developing three new inserts for the three major industrial case studies utilising a combination manufacturing principles of indirect SLS and HSM. In designing all new inserts for the three case studies, it has been indicated that design freedom as a main advantage of the indirect SLS process is constrained by parameters which are mostly associated with the requirements of the product design and the capability of the manufacturing process for finishing the inserts. The surface finish requirements of the product and the major limitations of the indirect SLS process in producing the insert are a combination of major parameters that significantly influence the process of determining a suitable parting line for the product, a minimum number of insert components required and design of the inserts.

However, the benefit of the indirect SLS process provide design freedom to

construct freeform conformal cooling channels as an opportunity to improve the heat transfers inside the insert which can reduce the cycle time of the moulding process. Utilising indirect SLS process, the new design of conformal cooling channels for all case studies has able to optimise the available space to construct the channels closer and conformal to the moulding cavity. Even though the design estimation and evaluation are carried out for the critical section (thickest wall), the results of this simple analytical approach are considerably appropriate for an initial prediction of a potential conformal cooling design which is able to reduce the moulding cycle time. The main limitation using this approach is that a selection of an optimum design can be determined.

Since the geometry of the new conformal cooling channel designs for all case studies is relatively complex, further accurate analysis using computer software is furthermore required. By means of finite element analysis, the calculation and evaluation of an optimum conformal cooling design can be obtained comprehensively. By introducing real operational parameter of the moulding process and providing allowance for the surrounding conditions, the finite element analysis approach are able: to provide solutions for complex geometries conformal cooling channel, to simulate more accurate cooling conditions, and to rapidly run a simulation of moulding process with various set up. Moreover, a 'cut-off volume' design has shown that the technique provides an effective and efficient approach in powder removal from the channels.

## Chapter 6

# **Conclusions and Recommendations**

## Chapter 6. Conclusions and Recommendations

Benchmark and case studies as well as design rules application have been carried out to support the main aim of this research: to develop a production injection mould (core/cavity) inserts using a combination approach of the indirect selective laser sintering (SLS) and high speed machining (HSM). The followings overview the overall conclusions of the works regarding to the knowledge and key benefits provided.

From the benchmark studies, the capabilities of the indirect SLS in developing metal inserts were characterized. Table 6-1 summarizes five important issues which were investigated as major constraints that need to be carefully considered in designing the near-net shape inserts, utilizing LaserForm ST-100 material. To anticipate dimensional changes and metal part deformation during the process, it was recommended that a minimum additional material of 0.5 mm in X, Y and Z building directions for features of up to 100 mm in size, and an oversize of 0.4% allowance in all directions for size above 100 mm can be applied to provide sufficient stock to work with. Concerning a fragile green part and a minimum feature size that can be built using indirect SLS process, small/delicates features that have dimensions of less 2 mm are recommended to be excluded from the SLS part and best produced by machining.

Table 6-1. Summary of Indirect SLS Capabilities

No	Descriptions	Unit	Value	Remarks
1	Dimensions relative error	(%)	1.0-1.20 0.0-0.4	<ul style="list-style-type: none"> <li>• between 5 to 25 mm (X,Y &amp; Z directions)</li> <li>• above 25 mm</li> <li>• <i>less than 5mm is uncontrollable</i></li> </ul>
2	Surface flatness	mm	0.1	<ul style="list-style-type: none"> <li>• part thickness <math>\geq</math> 10 mm</li> <li>• <i>less than 10mm cannot withstand warping)</i></li> </ul>
3	Surface roughness (Ra)	$\mu\text{m}$	2.0	<ul style="list-style-type: none"> <li>• <i>can be polished up to 0.08 <math>\mu\text{m}</math></i></li> </ul>
4	Surface hardness	HR <sub>B</sub>	82.4	<ul style="list-style-type: none"> <li>• <math>\approx</math> 2 to 3 HR<sub>C</sub></li> </ul>
5	Minimum feature size	mm	2.0	

In the case studies, the indirect SLS process has demonstrated its ability not only to provide a freedom in design a complex geometry of the inserts but also able to potentially reduce the total amount of manufacturing time and cost required. The



design freedom allows a number of complex components that form the inserts to be minimised and merged into one solid material. The freedom to design any complex geometry also has demonstrated an opportunity to improve the moulding cycle time and process control by replacing a conventional straight-drilled design of the cooling channels with the complex design of conformal cooling channels. To assess its performance, the inserts have been evaluated in the real industrial case studies. Table 6-2 furthermore summarises the performance differences of each case studies which were assessed against its original/existing inserts.

Table 6-2. Insert Performances

Case	Manufacturing Lead-Time	Cost Required	Cycle Time	Production Rate	Energy Consumption
CS1	- 44.3%	- 72.3%	- 11.3%	17.6%	- 13.0%
CS2	- 13.6%	72.7%	- 12.0%	13.2%	- 14.0%
CS3	51.0%	61.5%	- 37.0%	59.6%	- 20.0%

From this table, the developments of the new inserts using the approach have generally demonstrated significant benefits which could be valuable for the industry. However, as CS2 and CS3 demonstrated this new approach does not always translate to lead-time and cost benefits. The lead-time (CS3) and costs required (CS2 and CS3) in developing the insert were increased against their original inserts. These are considered due to the less geometrical complexity as well as the general size of the inserts to take best advantages of what indirect SLS has to offers. Therefore, it is clear that the injection moulding insert development using this approach needs further evaluations on a case by case basis.

Furthermore, extended moulding and production trials on each case studies have demonstrated the insert material durability in producing a quality product consistently, and have also indicated a clear economic (product cost) benefits in some cases. Utilising the performance data in Table 6-2 and calculated durability on CS1 after running 25,000,000 shots, there is a potential of these new inserts for being competitive against its existing/original inserts in the production volume less than 600,000 mouldings.

In the case of the design rules application, the developed rules have structured the design-to-manufacture procedure for the combination of indirect SLS and HSM, which may lead to important design rules that underpin future work in

this area. However, further detail studies in evaluating strategic design rules as well as manufacturing process are recommended so that the development of the insert can be more effective and efficient. Therefore, the utilisation of computer analysis software to strengthen the analysis results is recommended in designing the inserts so that the overall performance of the inserts can be accurately evaluated and predicted before manufacturing them. Finally, a further durability trial of the insert material is recommended to be carried out. A factual/reat data regarding to the maximum capability of the insert material (LaserForm ST-100) in producing plastic products need to be defined accurately.

# References

## References

- 3D SYSTEMS (2003). *Step-by Step Process, Products SLS systems* [online].  
[Accessed 19 Nov. 2003]. Available from world wide web:  
<[http://www.3dsystems.com/products/sls/stepbystep/proc\\_tour.asp](http://www.3dsystems.com/products/sls/stepbystep/proc_tour.asp)>
- AGARWALA, M., Bourell, D., Beaman, J., Marcus, H. and Barlow, J. (1995a).  
Post-Processing of Selective Laser Sintered Metal Parts. *Rapid Prototyping  
Journal*, 1 (2), pp. 26-36.
- AGARWALA, M., Bourell, D., Beaman, J., Marcus, H. and Barlow, J. (1995b).  
Direct Selective Laser Sintering of Metals. *Rapid Prototyping Journal*, 1 (1), pp.  
36–44.
- AMRCC (Advanced Manufacturing Research and Collaboration Cluster) (2004)  
*Product Development Tools and Technologies - Rapid Prototyping and  
Manufacturing* [online]. [Accessed 15 June 2004]. Available from world wide  
web: <http://www.amrcc.com/pdtt/rp.asp>
- AVERY, J. (1998). *Injection Molding Alternatives: A Guide for Designers and  
Product Engineer*. Munich, Germany: Hanser Publishers
- BARLOW, J. W., Beaman, J.J. and Balasubramanian, B. (1996). A Rapid Mould-  
Making System: Material Properties and Design Considerations. *Rapid  
Prototyping Journal*, 2 (3), pp. 4–15.
- BENHABIB, B. (2003). *Manufacturing: Design, Production, Automation and  
Integration*. New York, USA: Marcel Dekker.
- BOCKING, C. E. and Dover, S.J. (1996). Rapid Tooling Using Electroforming.  
*European Action on Rapid Prototyping (EARP)*, 6, pp. 8-9.
- BOOTHROYD, G., Dewhurst, P & Knight, W (2002). Design for Injection  
Molding. In *Product Design for Manufacture and Assembly*. New York, USA:  
Marcel Dekker, pp. 339-379.
- BRYCE, D. M. (1998). *Plastic Injection Molding: Mold Design and Construction  
Fundamentals*. Dearborn, Michigan, USA: Society of Manufacturing Engineers.

- BRYDEN, B. G., Wimpenny, D.I. and Pashby, I.R. (2001), Manufacturing Production Tooling using Metal Lamination, *Rapid Prototyping Journal*, Vol. 7, pp. 52-59.
- CHARMILLES (2004). *What is EDM?*. [online]. [Accessed 17 Sep. 2004]. Available from world wide web: <<http://www.charmillesus.com/products/whatsedm/whatedm.cfm>>
- CHEAH, C. M., Chua, C. K., Lee, C. W., Lim, S. T., Eu, K. H. and Lin, L. T. (2002). Rapid Sheet Metal Manufacturing. Part 2: Direct Rapid Tooling. *Int. J Adv Manufacturing Technology*, 19, pp. 510–515.
- CHEN, Y. M. a. L., J. J. (1999). Cost-Effective Design for Injection Molding. *Robotics and Computer-Integrated Manufacturing*, 15, pp. 1-21.
- CHUA, C. K., Hong, K. H. and Ho, S. L. (1999), Rapid Tooling Technology. Part 1. A Comparative Study, *Int. J Advanced Manufacturing Technology*, Vol. 15, pp. 604–608.
- CONNOLLY, J. (2004a), *Will RP Stand for Rapid Production Someday?* [online]. [Accessed 11 March 2004]. Available from world wide web: <[http://www.timecompress.com/magazine/magazin\\_articles.cfm](http://www.timecompress.com/magazine/magazin_articles.cfm)>
- CONNOLLY, J. (2004b), *RT Moves into a New Realm* [online]. [Accessed 11 March 2004]. Available from world wide web: <[http://www.timecompress.com/magazine/magazin\\_articles.cfm](http://www.timecompress.com/magazine/magazin_articles.cfm)>
- DALGARNO, K.W. and Stewart, T.D. (2001a). Manufacture of Production Injection Moulding Tooling Incorporating Conformal Cooling Channels via Indirect Selective Laser Sintering. *Proc. Instn Mech. Engrs. Part B*, 215.
- DALGARNO, K.W.(2001b). Production Grade Tooling via Layer Manufacture. *Rapid Prototyping Journal*, 7 (4), pp. 203-206.
- DALGARNO, K. W., Stewart, T.D and Allport, J.M. (2001c). Layer Manufactured Production Tooling Incorporating Conformal Heating Channels for Transfer Moulding of Elastomer Compounds. *Plastics, Rubber and Composites*, 30, pp. 384-388.

- DALGARNO, K. W. and Steward, T.D. (2001d). Production Tooling for Polymer Moulding Using the RapidSteel Process. *Rapid Prototyping Journal*, 7 (3), pp. 173-179.
- DALGARNO, K. W. and Wright, C.S (2003). Approaches to Processing Metals and Ceramics through the Laser Scanning of Powder Beds. *SME Technical Paper*.
- DAS, S., Beaman, J.J., Wohlert, M. and Bourel, D.L. (1998). Direct Laser Freeform Fabrication of High Performance Metal Components. *Rapid Prototyping Journal*, 4 (3), pp. 112-117.
- DEGASPARI, J. (2004). *Rapid Evolution* [online]. [Accessed 11 Marc 2004]. Available from world wide web: <<http://www.memagazine.org/backissues/mar02/features/rapidev/repidev.html>>
- DENTON, K. and Jacobs, P.. (1994), Quick Cast and rapid Tooling: A case history at Ford Motor Company. *Proc. of the 3rd European Conference on Rapid Prototyping and Manufacturing*, Nottingham, UK, pp. 53 - 72.
- DIMLA, D. E., Camilotto, M. and Miani, F. (2005). Design and Optimisation of Conformal Cooling Channels in Injection Moulding Tools. *Journal of Materials Processing Technology*, 164–165, pp. 1294–1300.
- DORMAL, T. (1999). New Rapid Tools for Injection Moulding. *Material Technology and Advanced Performance Material*,14, pp. 194-217.
- DUCK, J., Niebling, F., Neebe, T. and Otto, A. (2004). Infiltration as Post-Processing of Laser Sintered Metal Parts. *Powder Technology*, 145, pp. 62-68.
- EFUNDA (2002) *Design Guidelines: Injection Moulding Design Guidelines*. [online]. [Accessed 15 April 2004]. Available from world wide web: <[http://www.efunda.com/designstandards/plastic\\_design/plastic\\_intro.cfm](http://www.efunda.com/designstandards/plastic_design/plastic_intro.cfm)>
- ENGELMAN, P., Hayden, K., Guichelaar, P., Dealey, R. and Monfore, M. (2001). Injection Molding: Injection Mold Wear Mechanisms and Mold Design. *Plastic Engineering*, April, pp. 40-46.
- EOS (2004). *Application: Producing Metal Parts*. [online]. [Accessed 22 October 2004]. Available from world wide web: <<http://www.eos-gmbh.de/pag/file/found.htm>>

- FALLBOHMER, P., Altan, Y., Tonshoff, H.K. and Nakagawa, T. (1996). Survey of Die and Mould manufacturing - Practice in Germany, Japan and the United States. *Journal of Materials Processing Technology*, 59, pp. 158-168.
- FOLKESTAD, J.E. and Johnson, R.L (2001). Resolving the Conflict between Design and Manufacturing: Integrated Rapid Prototyping and Rapid Tooling. *Journal of Industrial Technology*, 17, pp. 1-7.
- FOLKESTAD, J.E. and Johnson, R.L (2002). Integrated Rapid Prototyping and Rapid Tooling. *Integrated Manufacturing Systems*, 13 (2), pp. 97.
- FRANCIS, E. H. and Tay, E.A., (2002). Laser Sintered Rapid Tools with Improved Surface Finish and Strength using Plating Technology. *Journal of Materials Processing Technology*, 121, pp. 318-322.
- FU, M. W., Fuh, J.Y.H. and Nee, A.Y.C. (2001). Core and Cavity Generation Method in Injection Mould Design. *International Journal of Production Research*, 39, pp. 121-138.
- GASTROW, H. (1993). *Injection Molds: 108 Proven Designs*. Munich, Germany: Hanser Publisher.
- GEIGER, M. and Coremans, A. (1997). Laser-Supported Rapid Tooling - Tools for the Manufacture of Functional Components with Net Shape properties, *International Conference on Industrial Tools (ICIT)*, , Maribor, Slovenia: TECOS - Slovenian Tool and Die Development Centre
- GIBSON, I. and Shi, D. (1997). Material Properties and Fabrication Parameters in Selective Laser Sintering Process. *Rapid Prototyping Journal*, 3 (4), pp. 129-136.
- GOSDEN, J. (1983), Polymer Engineering: 5 - Injection Mould Design, *Physics Technology*, 14, pp. 146-152.
- GREYDA, E. (2005). *Rapid Tooling Survey* [online]. [Accessed 5 February 2005]. Available from world wide web: <[http://home.att.net/~castleisland/tl\\_c.htm](http://home.att.net/~castleisland/tl_c.htm)>
- GREULICH, M. (1997). Rapid Prototyping and Fabrication of Tools and Metal Parts by Laser Sintering of Metal Powders. *Material Technologies*, 12 (5), pp. 155-157.

- GRIMM, T. (2004). *Rapid Tooling Is Not the Future; It is Today!* [online]. [Accessed 26 February 2004]. Available from world wide web: <[http://www.atirapid.com/news/ar\\_rt\\_today.html](http://www.atirapid.com/news/ar_rt_today.html)>
- GUANGCHUN, W., Huiping, L., Yanjin, G. and Guoqun, Z. (2004). A Rapid Design and Manufacturing System for Product Development Applications. *Rapid Prototyping Journal*, 10 (3), pp. 200-206.
- HAGUE, R., Campbell, I. and Dickens, P. (2003), Implications on Design of Rapid Manufacturing. *Proc. Instn. Mech. Engrs. Part C: J. Mechanical Engineering Science*, 217, pp. 25 - 30.
- HAGUE, R., Mansour, S. and Saleh, N. (2004). Material and Design Considerations for Rapid Manufacturing. *International Journal of Production Research*, 42 (22), pp. 4691-4708.
- HATCH, D., Kazmer, D. and Fan, B. (2001). *Dynamic Cooling Design for Injection Molding* [online]. [Accessed 3 June 2005]. Available from world wide web: <[http://kazmer.uml.edu/Staff/Archive/2001ANTEC\\_Dynamic\\_Cooling.pdf](http://kazmer.uml.edu/Staff/Archive/2001ANTEC_Dynamic_Cooling.pdf)>
- HILTON, P. and Jacobs, P.F. (2000). *Rapid Tooling: Technologies and Industrial Applications*, New York, USA: Mercel Dekker.
- HOPKINSON, N., Hague, R. and Dickens, P. (2006), Introduction to Rapid Manufacturing. In *Rapid Manufacturing: An Industrial Revolution for the Digital Age*, Chichester, West Sussex, UK: John Wiley and Sons, Ltd.
- HOPKINSON, N. and Dickens, P. (2001). Rapid Prototyping for Direct Manufacture. *Rapid Prototyping Journal*, 7 (4), pp. 197-202.
- HOPKINSON, N. and Dickens, P., (2003). Analysis of Rapid Manufacturing - Using Layer Manufacturing Processes for Production. *Proc. Instn Mech. Engrs Part C: J. Mechanical Engineering Science*, 217, pp. 31-39.
- ILLSTON, T. J. and Roberts, S.D. (2001). Direct Rapid Prototyping (RP) Tooling for Injection Moulds, In *Rapid Prototyping Casebook*, London, UK: Professional Engineering Publishing Ltd., pp. 151-156.
- JACK, H. (2001). *Injection Molding* [online], [Accessed 14 August 2006]. Available from world wide web: <<http://claymore.engineer.gvsu.edu/~jackh/eod/manufact/manufact-213.html>>
-



- JACOBS, P. (1996). *Stereolithography and other RP&M Technologies*, Dearborn, Michigan, USA: Society of Manufacturing Engineers - American Society of Mechanical Engineer.
- JACOBS, P. and Andre, L (2000). Rapid Production Tooling. in *Rapid Tooling: Technologies and Industrial Applications*, New York, USA: Mercel Dekker, pp. 95-120.
- JACOBS, P. F. (1999). New Frontiers in Mold Construction: High Conductivity Materials & Conformal Cooling Channels. *SME Technical Paper*.
- JENGA, J. Y. and Linb, M.C.. (2001), Mold Fabrication and Modification using Hybrid Process of Selective Laser Cladding and Milling. *Journal of Materials Processing Technology*. 10, pp. 98-103.
- KAMRANI, A. a. N., E.A. (2006) *Rapid Prototyping: Theory and Practice*, New York, USA: Springer.
- KARAPATIS, N. P., Griethuysen, J.-P.S and Glardon, R. (1998). Direct Rapid Tooling: a Review of Current Research. *Rapid Prototyping Journal*, 4 (2), pp. 77–89.
- KING, D. and Tansey, T. (2003). Rapid Tooling: Selective Laser Sintering Injection Tooling. *Journal of Materials Processing Technology*, 132, pp. 42-48.
- KLOCKE, F., Celiker, T. and Song, Y.A. (1995), Rapid Metal Tooling. *Rapid Prototyping Journal*, 1 (3), pp. 32–42.
- KLOCKE, F. a. W., C. (2003), Coalescence Behaviour of Two Metallic Particles as Base Mechanism of Selective Laser Sintering. In *Ann. of CIRP*, 52, pp. page 177-180.
- KNIGHTS, M. (2001), *Rapid Tooling is Ready for Prime Time* [online], [Accessed 14 January 2004]. Available from world wide web:  
<<http://www.plasticstechnology.com/articles/200101fa1.html>>
- KOCHAN, D., Kai, C.C. and Zhaohui, D. (1999). Rapid Prototyping Issues in 21st Century. *Computer in Industry*, 39, pp. 3-10.
- KRUTH, J. P., Leu, M.C. and Nakagawa, T. (1998), Progress in Additive Manufacturing and Rapid Prototyping. *Ann. CIRP Manufacturing Technology*, 47 (2), pp. 525-540.
-

- KRUTH, J. P., Vandenbroucke, B., Vaerenbergh, J.V. and Mercelis, P. (2005). Benchmarking of Different SLS/SLM Process as Rapid Manufacturing Techniques, In *International Conference Polymers and Moulds Innovations (PMI)*, Gent, Belgium.
- KULKARNI, P., Marsan, A. and Dutta, D. (2000). A Review of Process Planning Techniques in Layered Manufacturing. *Rapid Prototyping Journal*, 6 (1), pp. 18-35.
- LAMB, C. a. Z., M. (1999), *Wyko Surface Profilers Technical Reference Manual*, Tucson, Arizona, USA: Veeco Metrology Group,.
- LEVY, G. N., Schindel, R. and Kruth, J.P. (2003). Rapid Manufacturing and Rapid Tooling with Layer Manufacturing (LM) Technologies, State of the Art and Future Perspectives. *Ann. of the CIRP*, 52, pp. 589-609.
- LEVY, G. N. and Schindel, R. (2002). Overview of Layer Manufacturing Technologies, Opportunities, Options and Applications for Rapid Tooling. *Proc Instn Mech Engrs Part B: J Engineering Manufacture*, 216, pp. 1621-1634.
- LI, C. L. (2001). A Feature-Based Approach to Injection Mould Cooling System Design. *Computer -Aided Design*. 33, pp. 1073-1090.
- LIANG, J. Z. and Ness, J.N, (1996), The Calculation of Cooling Time in Injection Moulding. *Journal of Materials Processing Technology*, 57, pp. 62-64.
- LOU, Z., Jiang, H. and Ruan, X. (2004). Development on an Integrated Knowledge-Based System for Mold-Base Design. *Journal of Material Processing Technology*, 150, pp. 194-199.
- LU, L., Fuh, J.Y.H and Wong, Y.S. (2001). *Laser-Induced Materials and Process for Rapid Prototyping*, Boston, MA, USA: Kluwer Academic Publishers
- MA, Y. S. and Tong, T. (2004). An Object-Oriented Design Tool for Associative Cooling Channels in Plastic-Injection Moulds. *International Journal of Advanced Manufacturing Technology*, 23, pp. 79-86.
- MAGNOL, P., Jegou, L., Rivette, M. and Furet, B. (2006). High Speed Milling, Electro Discharge Machining and Direct Metal Laser Sintering: A Method To Optimize These Processes in Hybrid Rapid Tooling. *International Journal of Manufacturing Technology*, 29, pp. 35-40.

- MANSOUR, S. and Hague, R.. (2003). Impact of Rapid manufacturing on Design for Manufacture for Injection Moulding. *Proc. Instn Mech. Engrs Part B: J. Engineering Manufacture*, 217.
- MAS (2004). *Electric Discharge Machining*. [online]. [Accessed 20 September 2004]. Available from world wide web:  
<<http://cybercut.berkeley.edu/mas2/html/processes/edm/index.html>>
- MCP (2004). *Moulds and Dies* [online]. [Accessed 22 October 2004]. Available from world wide web: <[http://www.mcp-group.co.uk/alloys/lmpa\\_moulds.html](http://www.mcp-group.co.uk/alloys/lmpa_moulds.html)>
- MENGES, G., Michaeli, W and Mohren, P (2001). *How to Make Injection Molds*, Munich, Germany: Hanser Publisher.
- MOK, C. K., Chin, K.S. and Ho, J.K.L. (2001). An Interaktive Knowledge-Based CAD System for Mould Design in Injection Moulding Processes. *International Journal of Advanced Manufacturing Technology*, 17, pp. 27-38.
- NOORANI, R. (2006), *Rapid Prototyping: Principles and Applications*, New Jersey, USA: John Wiley and Sons, Inc.
- ODONNCHADHA, B. and Tansey, A. (2004). A Note on Rapid Metal Composite Tooling by Selective Laser Sintering. *Journal of Materials Processing Technology*, 153–154, pp. 28–34.
- OKI ELECTRIC, (1997). Applied Engineering of Rapid Prototyping. *Oki Technical Review*, 63 (159) [online]. [Accessed 17 August 2004]. Available from world wide web: <<http://www.oki.com/en/otr/html/nf/otr-159-12-1.html>>
- OTTO, K. and Wood, K. (2001) *Product Design: Techniques in Reverse Engineering and New Product Development*, Englewood Cliff, NJ, USA: Prentice-Hall.
- PALM, W. (2002). *Rapid Prototyping Primer* [online]. [Accessed 30 August 2004]. Available from world wide web:  
<<http://www.ne.psu.edu/lamancusa/rapidpro/primer/chapter2.htm>>
- PEREZ, C. J. L. (2002). Analysis of the Surface Roughness and Dimensional Accuracy Capability of Fused Deposition Modelling Processes. *International Journal of Production Research*, 40, pp. 2865-2881.

- PHAM, D. T., Dimov, S.S. and Lacan, F. (1997). Technique for Firm Tooling using Rapid Prototyping. *Proc Instn Mech Engrs Part B: J Engineering Manufacture*, 212, pp. 269-77.
- PHAM, D. T., Dimov, S.S. and Lacan, F. (1999). Selective Laser Sintering: Applications and Technological Capabilities. *Proc Instn Mech Engrs Part B: J Engineering Manufacture*, 213, pp. 435-449.
- PHAM, D. T., Dimov, S.S. and Lacan, F. (2000). The RapidTool Process: Technical Capabilities and Applications. *Proc Instn Mech Engrs Part B: J Engineering Manufacture*, 214, pp. 107-116.
- PHAM, D. T., Ji. C. and Dimov, S.S. (2004). Layered Manufacturing Technologies, *Proc. of the 1st Intl. Conference on New Forming Technology (ICNFT)*, Harbin, China., pp. 317-324.
- PHAM, D. T. a. D., S.S. (2001). *Rapid Manufacturing: the Technologies and Application of Rapid Prototyping and Rapid Tooling*, London, UK: Springer-Verlag,
- PHAM, D. T. and Dimov, S.S. (2003). Rapid Prototyping and Rapid Tooling, the Key Enablers for Rapid Manufacturing. *Proc Instn Mech Engrs Part C*, 217, pp. 1-23.
- RADSTOK, E. (1999). Rapid tooling. *Rapid Prototyping Journal*. 5 (4), pp. 164-168.
- RAHMATI, S. and Dickens, P. (1997). Stereolithography for Injection Mould Tooling. *Rapid Prototyping Journal*, 3 (2), pp. 53-60.
- RAO, N. S. (1991). *Design Formulas for Plastics Engineers*. New York, USA: Hanser Publisher.
- PROMETAL (2006). Rapid Production for Rapidly Changing Industries [online]. [Accessed 2 April 2006]. Available from world wide web: <<http://www.prometal.com/>
- PROTOMOLDS (2004). *Rapid Injection Mould: Design Tips* [online]. [14 April 2004]. Available from world wide web: <<http://www.protomold.com/news/designtips.asp>>
- REES, H. (1995). *Mold Engineering*. Munich, Germany: Hanser Publisher

- ROSATO, D.V., Rosato, D.V. and Rosato, M.G. (2000). *Injection Molding Handbook*, (3<sup>rd</sup> ed.), New York, Kluwer Academic Publishers
- ROSEN, D. W., Chen, Y., Sambu, S., Allen, J.K. and Mistree, F. (2003). The Rapid Tooling Test-bed: A Distributed Design for Manufacturing System. *Rapid Prototyping Journal*, 9 (3), pp. 122–132.
- ROSOCHOWSKI, A. and Matuszak, A., (2000). Rapid Tooling: the State of the Art, *Journal of Materials Processing Technology*, 106, pp. 191-198.
- ROWE, J. (2001). *Molding the Feature Advancements in Injection Mold Design and Processes* [online]. [Accessed 28 September 200]. Available from world wide web: <[http://mcadvision.ibsystems.com/October2001/feature\\_full.php](http://mcadvision.ibsystems.com/October2001/feature_full.php)>
- RUBIN, I. I. (1972). *Injection Moulding: Theory and Practice*, New York, USA: John Wiley & Sons.
- RUFFO, M., Tuck, C. and Hague, R. (2006). Cost Estimation for Rapid Manufacturing - Laser Sintering Production for Low to Medium Volumes. *Proc Instn Mech Engrs Part B: J Engineering Manufacture*, 220, pp. 1414-1427.
- SACHS, E., Wylonis, E., Allen, S., Cima, M. and Guo, H. (2000). Production of Injection Molding Tooling with Conformal Cooling Channels using the Three Dimensional Printing Process. *Polymer Engineering and Science*, 40 (5), pp. 1232-1247.
- SAMBU, S., Chen, Y. and Rosen, D.W. (2004). Geometric Tailoring: A Design for Manufacturing Method for Rapid Prototyping and Rapid Tooling. *Journal of Mechanical Design*, 126, pp. 571-580.
- SANDS, T. (2001). The Role of Rapid Immediate Production Tooling (IPT) in New Product Development, In *Rapid Prototyping Casebook*, London, UK: Professional Engineering Publishing Ltd., pp. 127-139.
- SANTOS, E. C., Shiomi, M., Osakada, K. and Laoui, T. (2006). Rapid Manufacturing of Metal Components by Laser Forming. *International Journal of Machine Tool and Manufacture*, 46, pp. 1459-1468.
- SANDVICK (2004). *High Speed Machining and Conventional Die and Mould Machining*. [online]. [Accessed 17 September 2004]. Available from world wide web:

<[www2.coromant.sandvik.com/coromant/products/die&mould/new\\_pdf\\_HSM.pdf](http://www2.coromant.sandvik.com/coromant/products/die&mould/new_pdf_HSM.pdf)>

SEAQUIST Closures (2004). *Personal Care Market: Form, Function, Style, Differentiation* [online]. [Accessed 25 October. 2004]. Available from world wide web:

<<http://www.seaquistclosures.com/@scwebsite/Europe/Markets/personal.asp>>

SHERMAN, L. M. (2004). *Rapid Prototyping: Pretty Soon, You Won't Be Able To Get Along Without It* [online], [Accessed 11 March 2004]. Available from world wide web: <<http://www.plasticstechnology.com/articles/200102fa2.html>>

STAUB, B. (2000). *Moldmaking Technology: Blending Rapid Tooling with Conventional Moldmaking* [online]. [Accessed 25 April 2005]. Available from world wide web:

<<http://www.moldmakingtechnology.com/articles/060006.html>>

STEWART, T. D., Dalgarno, K.W. and Childs, T.H.C. (1999). Strength of the DTM RapidSteel™ 1.0 Material. *Materials and Design*, 20 (2-3), pp. 133-138.

STUCKER, B. and Qu, X. (2003). A Finish Machining Strategy for Rapid Manufactured Parts and Tools. *Rapid Prototyping Journal*, 9 (4), pp. 194-200.

TAY, F. E. H. and Haider, E. A (2002). Laser Sintered Rapid Tools with Improved Surface Finish and Strength Using Plating Technology. *Journal of Materials Processing Technology*, 121, pp. 318–322.

TAYLOR, C.M. (2004a). *Innovative Injection Mould Tooling (IIMT) Project: Minute Meeting of the 1<sup>st</sup> Half-Year Review Meeting* [online] [Accessed 13 January 2004]. Available from world wide web: <<http://www.mech-eng.leeds.ac.uk/eet/Minutes.html>>

TAYLOR, C.M. (2004b), *Innovative Injection Mould Tooling (IIMT) Project, Presentation on the 2<sup>nd</sup> Half-Year Review Meeting* [online] [Accessed 1 July 2004]. Available from world wide web: <<http://www.mech-eng.leeds.ac.uk/eet/Comms.html>>

TAYLOR, C.M. (2004c), *Innovative Injection Mould Tooling (IIMT) Project, Minute Meeting of the 2<sup>nd</sup> Half-Year Review Meeting* [online] [Accessed 1 July

2004]. Available from world wide web: <<http://www.mech-eng.leeds.ac.uk/eet/Minutes.html>>

URBANSKI, J. P., Koshy, P Dewes, R.C. and Aspinwall, D.K (2000). High Speed Machining of Moulds and Dies for Net Shape Manufacture. *Material and Design*, 21, pp. 395-402.

VENUVINOD, P. K. and Ma, W. (2004). Selective Laser Sintering (SLS). In *Rapid Prototyping: Laser-based and Other Technologies*, London, UK: Kluwer Academic Publishers, pp. 245-275.

WEISSTEIN, E. W. (1999), *Relative Error* [online]. [Accessed 20 March 2004]. Available from world wide web: <<http://mathworld.wolfram.com/RelativeError.html>>

WOHLERS, T. T. (2002). *New Developments and Trends in Rapid and High-Performance Tooling* [online]. [Accessed 25 October 2006]. Available from world wide web: <<http://wohlersassociates.com/EuroMould-2002-paper.html>>

WOHLERS, T. T. (2006), *Wohlers Report 2006: Rapid Prototyping & Manufacturing State of the Industry*, Fort Collins, CO, USA: Wohlers Associates.

XU, X., Sachs, E. and Allen, S. (2001). The Design of Conformal Cooling Channels in Injection Molding Tooling. *Polymer Engineering and Science*, 14 (7).

YARLAGADDA, P. K. D. V. and Wee, L.K. (2006). Design, Development and Evaluation of 3D Mold Inserts using a Rapid Prototyping Technique and Powder Sintering Process. *International Journal of Production Research*, 44 (5), pp. 919-938.

ZHANG, H., Wanga, G., Luo, Y. and Nakagab, T (2001). Rapid Hard Tooling by Plasma Spraying for Injection Molding and Sheet Metal Forming. *Thin Solid Films*, 390, pp. 7-12.

ZOLLNER, O. (1997). Application Technology Information: Optimised Mould Temperature Control. Leverkusen, Germany: Bayer AG.